NASA CONTRACTOR REPORT

NASA CR-588

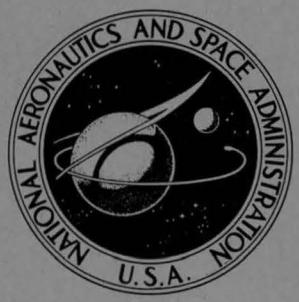

NASA CR-588

PEACEFUL USES OF EARTH-OBSERVATION SPACECRAFT

VOLUME III: SENSOR REQUIREMENTS AND EXPERIMENTS

Prepared by
UNIVERSITY OF MICHIGAN
Ann Arbor, Mich.
for

NATIONAL AERONAUTICS AND SPACE ADMINISTRATION • WASHINGTON, D. C. • SEPTEMBER 1966

NASA CR-588

PEACEFUL USES OF EARTH-OBSERVATION SPACECRAFT

VOLUME III: SENSOR REQUIREMENTS AND EXPERIMENTS

Prepared under Contract No. NASw-1084 by
UNIVERSITY OF MICHIGAN
Ann Arbor, Mich.

for

NATIONAL AERONAUTICS AND SPACE ADMINISTRATION

For sale by the Clearinghouse for Federal Scientific and Technical Information
Springfield, Virginia 22151 – Price $3.75

PREFACE

A major objective of programs of the National Aeronautics and Space Administration is to investigate and implement the adaptation of space technology for peaceful uses. As a part of one program, the Federal Systems Division of the International Business Machines Corporation has conducted a comprehensive study of the requirements for conducting an integrated set of experiments in a series of manned earth-orbiting laboratories which would lead to the realization of such peaceful uses of space. The Willow Run Laboratories of The University of Michigan's Institute of Science and Technology was asked to assist in this work and, as a subcontractor to IBM, has conducted a three-month study to survey potential applications of observation spacecraft in a number of important scientific and economic activities and to consider the program of ground-based and orbital experimentation required to develop this capability.

The results of the first phase of this investigation conducted by the Willow Run Laboratories are reported in this three-volume report. Volume I is an introduction and summary of the work performed. Volume II contains a comprehensive survey of potential applications of earth-observation spacecraft and the anticipated benefits. Volume III describes some of the requirements to be met by the orbital sensing devices and the manned earth-orbiting experiments proposed for developing the orbital sensing capability.

This investigation was conducted by the Infrared and Optical Sensor Laboratory under the supervision of Mr. M R. Holter, Head of the Laboratory, and Mr. D. S. Lowe, Principal Investigator. Staff members with major responsibility for the project were I. J. Sattinger, Research Engineer and Project Leader, and F. C. Polcyn, Associate Research Engineer and Project Leader for Experiment Definition Studies.

Since the material in this report was produced through the efforts of people in many disciplines with only a limited time available, the statements made herein are based on their judgments and do not necessarily reflect the endorsement of NASA, IBM, or The University of Michigan. Acknowledgment of the work of the many individuals who participated in or contributed to this study are included in the appendix to Volume I.

ABSTRACT

Earth-observation spacecraft have many potential applications in the fields of geography, agriculture, forestry, hydrology, wildlife management, oceanography, geology, air pollution, and archaeology. Substantial scientific and economic benefits could result from the use of sensors carried aboard earth-orbiting spacecraft for earth mapping, collection of agricultural census data, forest inventory, wildlife habitat assessment, detection of sea ice, measurement of sea surface temperatures, and many other uses.

Types of sensors to be considered for these purposes include photographic cameras with focal lengths ranging from 0.5 to 20 ft, infrared scanners, multispectral sensing systems, noncoherent and synthetic-aperture radar, microwave radiometers, and laser altimeters. The development of operational systems of observation spacecraft would require a research and development program which included preliminary ground-based and airborne experiments followed by a series of manned earth-orbiting experiments. The preliminary experiments would provide information on sensor characteristics and capabilities for observing natural and cultural phenomena on the earth's surface which would be necessary for design of experimental orbiting sensors and planning of orbital experiments. The objective of the manned earth-orbiting experiments would be to ascertain the optimum conditions for sensor operation and to demonstrate the feasibility of future operational systems. In the manned earth-orbiting experiments, predicted characteristics of the atmosphere would be checked, individual sensors calibrated, sensor performance measured, and imagery and other data collected over both land and water, which would be analyzed to determine the feasibility of detection and identification of earth-based objects and the best methods for employing future operational earth-observation spacecraft.

CONTENTS

FIGURES

TABLES

1
OBJECTIVES OF THE EXPERIMENTAL PROGRAMS

1.1. INTRODUCTION

The manned earth-orbiting laboratory should be the final platform for proving the feasibility of sensing from space. The overall experimental program should consist of an integrated, step-by-step approach beginning with preorbital experiments. Test sites will have been developed for sensor calibration to be used on a continuing basis as components and systems develop. The ground measurements and low altitude experiments will establish the detection mechanism for the particular application and will permit a general prototype sensor configuration to be determined. The objectives of the orbiting experiments will then be to identify what physical variables can still be reliably sensed (despite the change in altitude, environment, etc.) and what configuration of sensors is best suited to the task. The experiments will also identify the engineering and scientific advances needed in sensor design and components to insure operational feasibility.

The experiments discussed in the following sections are representative of the type of orbiting experiments to be conducted. As more information is collected through experiments conducted at or near the earth's surface, the details of a particular experiment can be defined accordingly. The areas of applications where sufficient information already exists to outline an experimental method have received more attention than those areas of applications where preliminary suborbital testing is needed to verify feasibility of remote detection of the phenomena.

1.2. PREORBITAL PROGRAM

As a means of making any program of orbital reconnaissance experimentation fully effective, a preliminary program of preorbital experimentation must be conducted to explore the use of new sensory capabilities from conventional aircraft and to establish the ground test sites, at which ground truth has been carefully measured and recorded, against which the orbital reconnaissance data may be checked.

The necessity for preorbital research programs is fully recognized. However, the primary purpose of the study reported herein is to delineate the ultimate uses of satellite reconnaissance systems and to define the orbital phase of the experimental program. The preorbital phase will therefore be discussed in this report only briefly to present the main outlines of this portion

of the program. Major emphasis is placed on defining the orbital phase of the experimental program, based on the assumption that the initial phases have been successfully performed.

1.2.1. GROUND TEST SITES. It is anticipated that ground sites will be selected by one or more of the NASA Technical Application Centers concerned with the orbiting remote sensing program. Each ground site selected to represent a particular area of technical or scientific interest will contain a series of objects or features typical of that interest, as a means of determining the capabilities of orbiting sensors to detect and identify such objects. Depending on the area of interest represented, such features might include a variety of geologic formations, types of soil and vegetation, and drainage systems. Test sites would also include urban communities and contain special man-made objects of interest, such as vehicles, roads, buildings and other structures. For oceanographic studies, a region of the ocean's surface should be used on which concentrated research has been performed and adequate information is available.

Special ground-based systems of meteorological instrumentation and sensor calibration will be installed. To measure sensor resolution, special test patterns will be used. The ground test site will be completely surveyed to provide photogrammetric control for analysis of the pictorial data obtained by airborne sensors.

If serious interference is expected with observations of a single ground test site because the site is covered by clouds for much of the time, two or three geographically separated sites of a single type may be justified.

1.2.2. PREORBITAL TESTING. A major function of the preorbital experimentation is to produce a detailed and accurate record of all conditions at each ground test site pertinent to the recording, analysis, and evaluation of pictorial data. This will be done both by observation from the ground and by overflights of the test site using each type of sensor with suitable combinations of spectral range, sensitivity, and resolution, and under various conditions of temperature, lighting, and weather.

Pictorial data produced during this preliminary test phase under favorable weather conditions and with good resolution will provide an idealized reference base against which to compare data produced by an orbiting vehicle. The preorbital experiments can also be extended to provide a realistic indication of the quality of imagery to be expected from orbiting sensors. This can be done by modifying the system performance to include a simulation of the additional effects caused by operating the sensors from a space platform. In particular, these effects could include the transmission and reflection characteristics of the intervening atmosphere,

the reduced resolution caused by the substantial distances covered, and the deterioration of image quality caused by transmission of the data over a space-to-earth data link. These simulated effects could be produced by the use of special devices which are operative during the airborne flight tests. Alternatively, realistic results could be obtained for some conditions by introducing the simulated effects in laboratory experiments using previously recorded data.

The preorbital testing will furnish practical experience with the types of sensing equipment which will later be used in the orbiting system. It will be possible to select the best operating parameters and modes of the equipment and to make any final adjustments and modifications in system design which appear to be necessary for the orbiting system. Investigations of proposed methods and equipment for data transmission, data processing, attitude control, or image motion compensation may also be conducted, if necessary.

1.3. ORBITAL EXPERIMENTATION

1.3.1. OBJECTIVES. The preorbital program of experimentation and site preparation just described will provide the necessary foundation for the interpretation of the data acquired during the subsequent program of orbital experimentation. The ultimate criteria for the evaluation of pictorial information gathered by observation satellite are the timeliness of the information and the quality of the imagery, particularly the ease with which photointerpretation processes can detect and identify objects of interest.

The data generated by the orbiting equipment in the ORL (Orbiting Research Laboratory) will be studied to achieve the following objectives:

a. Selection of the system design parameters and operating conditions producing the best system performance.
b. Evaluation of the usefulness of imagery obtained by the various sensors.
c. Collection of information on which to base the design of future operational systems for specific applications.

1.3.2. TEST PROCEDURES. During the ORL experimental program, each of the various sensors will be operated to acquire imagery as the ORL passes over each of the ground test sites. The sensor operating modes and parameters will be varied to determine the best operating conditions. Auxiliary data on communication, navigation, and image motion compensation equipment will also be recorded simultaneously to assist the analysis of system performance. Data measurement and recording activities will also take place at the ground site concurrently with periods of observation from the ORL. Information will be obtained concerning the type,

location, size, and emitting or reflecting conditions of natural and cultural features of the terrain, as well as specially-prepared targets. The test area should also be observed by airborne sensing systems similar to those used in the ORL, these observations being conducted concurrently with the passage of the ORL. This method of test operation will permit direct comparison of the ORL data with the airborne data. All data should be analyzed and interpreted with minimum delay, since this will make it possible to acquire missing data or check questionable conditions before significant changes occur.

The analysis and interpretation aboard the ORL will be confined primarily to quick looks at the data to ensure that the equipment is functioning as expected and to making decisions concerning conditions for subsequent experiments. More detailed analyses leading to extrapolations of the test results to other conditions and evaluation of specific configurations will be deferred for investigation by ground-based personnel.

Data-processing equipment performing several types of functions will be provided to assist ORL personnel in their operations. For data stored on photographic film or magnetic tape, film developing equipment and tape playback equipment can be provided to process the data so that it may be observed on board the ORL. Data-processing equipment will be provided for types of data requiring special processing. In particular, high resolution radar data as initially acquired must be processed in a specialized type of computing system.

1.3.3. DATA ANALYSIS. Imagery obtained during the ORL experiments will be studied intensively to provide information of several types. One type of information desired is concerned with the technical performance of the sensing equipment. The imagery returned to the ground will be studied to measure the ground resolution, tone gradations, and temperature sensitivity obtained, and to note the effects of atmospheric interference, system noise, and other disturbing influences.

In addition to pictorial data itself, information concerning system performance will be obtained from the recording and examination of auxiliary data. Records made of the performance of equipment used for position location, attitude stabilization and control, data storage, processing, and transmission can be analyzed to ascertain the effect which these auxiliary functions have on sensing system performance.

Since the performance characteristics of sensing and data-transmission equipment are already generally known, the primary emphasis in space experimentation will be to learn how the environment and operating conditions of space affect these characteristics. The effects of the individual design and operating features on image quality (resolution, dynamic range, sensitivity,

etc.) can be assessed by comparisons of imagery obtained under different system conditions and at different points along the data transmission chain. For example, a single ground test site can be observed under different sets of conditions and the sensor output, on film or tape, can be processed by alternative methods, to ascertain what combinations produce the best results. The effect on image quality of a link in the data transmission chain can be measured by comparing the quality of the image at each end of the link. Some of this experimentation with data acquired by sensors located in the ORL can be performed in ground-based laboratories.

1.3.4. USER EXPERIMENTS. In addition to the quantitative measures of system performance, the usefulness of the imagery for photointerpretation of test objects and conditions at each of the ground test sites will be investigated. The evaluation of image quality can be judged by personnel experienced not only in the interpretation of photography in the visible region but in the special problems of interpreting imagery in the infrared and microwave regions. A formal method of evaluation would be to provide such personnel with pictorial data, requiring them to detect and identify objects of interest without prior knowledge of ground truth data.

Once the capabilities of the sensing system for its various uses have been established, the experimental orbital sensing equipment will be used to acquire samples of imagery from other areas of the earth's surface as a means of extending our knowledge of system capabilities for observing unknown environments. In addition, this sample data along with a complete coverage of the earth's surface at small scale will provide the scientific community with a preliminary look at the earth which will be useful for planning the later acquisition of data in areas of special interest to be collected by future operational systems.

For this purpose, one early objective of the ORL experiments should be to produce a comprehensive set of imagery to give the various users an overall view of the earth's surface. This set of imagery should include a complete coverage of the earth's surface at a small scale (e.g., 1:800,000) in several spectral bands and under various conditions of season, weather, lighting, etc. In addition, coverage at larger scale should be provided (e.g., 1:60,000) of selected ground sites, urban areas, random samples, and areas of special interest as observed from orbit, amounting to perhaps 1% of the earth's surface.

The pictorial data or instrument records, after preliminary processing and storage will be used to provide a current map of the earth's surface and will be made available to the various types of scientists and engineers to permit them to study the results for planning modification or use of the techniques.

The ultimate objective of the ORL program is to perfect techniques for using the data for the scientific and economic applications discussed elsewhere in this report. Some of the scientific and economic objectives will be achieved during the ORL program itself, while others will require the initiation of operational systems.

In the case of pictorial data, initial interest of the scientific community will be centered on learning to identify objects or features of interest and relating them to ground truth data. It will be necessary to determine how closely observation from spacecraft corresponds with the equivalent observation from aircraft and to learn how to adapt to the differences in the appearance of the results. Special attention should be paid to observing unusual results which may reveal unexpected natural phenomena occurring at the earth's surface which are apparent only from the vantage point of a spacecraft. For certain types of applications, the required information is to be obtained by an indirect method, e.g., through interpretation of spectral signatures, automatic character recognition, or correlation of an observable physical quantity with a political or economic characteristic. For these cases, the ORL experiment will be designed to develop the method by providing imagery which can be analyzed and checked against ground truth data.

For the development of operational techniques, other experiments will be conducted aimed at establishing the requirements of operational systems with respect to repetition frequency, speed of data delivery, etc.

2
TYPES AND CAPABILITIES OF SENSORS REQUIRED

In this section the general characteristics of sensors which will have useful application from space platforms are outlined and specifications of prototype systems are given.

2.1. PHOTOGRAPHIC SYSTEMS

2.1.1. DESIGN CONSIDERATIONS. The photograph still remains one of the most compact information storage media so that camera systems have a major role to play in space reconnaissance for natural resources. Even so, the particular camera configuration best suited for space photography needs to be assessed. One can compare systems in three groups; the frame camera, the slit camera, and the panoramic camera (Ref. 1 through 4). The frame camera is best suited for mapping functions but requires accurate image motion compensation (IMC) to obtain the best resolution potential for the system at high orbital velocities. The slit camera, in which the film is moved past a narrow slit in the image plane, is automatically compensated for the image motion problem found with the frame camera, but is susceptible to distortion of the images when the v/h control of the film speed is misadjusted. In the panoramic system, the use of rotating mirrors, lenses, and/or prisms permit horizon-to-horizon photography, overcoming the limitations of wide angle refraction lens systems.

It can be argued that horizon-to-horizon photography from space may not be desirable because the long slant range path through the atmosphere reduces the contrast and decreases the ground resolution. Furthermore, the height advantage of orbital altitude geometrically permits wider coverage than one encounters with conventional aerial photography so that the need for horizon-to-horizon coverage is relaxed. For those applications where synoptic coverage of the earth is mandatory, increasing the number of satellites in orbit is the trade-off necessary when using limited FOV systems at 200 nautical mile altitudes. For special applications, one might use the panoramic system when mapping accuracy is relaxed and resolution for large slant ranges is adequate for the particular application.

It is not the purpose here to compare all types of photographic systems including the use of TV systems (see App. A.2) and systems using electrostatic or thermoplastic recording in place of film. Such alternatives to film, in combination with data transmission systems, represent a potential solution to the problem of getting information in real time to earth data centers for immediate analysis and dissemination. Nevertheless, the optical systems necessary to collect the reflected energy and focus this energy on a suitable transducer (film, photodetector, cathode

surface of orthicon or a treated electrostatic surface, etc.) will be a common subsystem and one of the limiting factors in the ability to photograph the earth at a particular ground resolution. Table I lists for comparison the theoretical resolution of a selection of camera objective diameters as limited by the Rayleigh diffraction principle $\left(\text{i.e., angular resolution } \frac{1.22 \text{ wavelength of light}}{\text{diameter of objective}}\right)$. The calculations are based on a wavelength of 1 micron partly for convenience and partly in recognition of the usefulness of the longer wavelengths for haze penetration. The table also shows the ground resolution corresponding to the nominal orbital altitude of 200 nautical miles or 1.2×10^6 ft. Thus, it is easily seen that 2 foot ground resolution capability requires at least a 36 inch diameter collector. For larger diameter systems, the resolution reaches an upper limit because of atmospheric turbulence: the minimum resolution (Ref. 5 and 6) appears to be limited to 1 to 2 ft under poor seeing conditions and to 2 to 3 inches under good seeing conditions. Thus very large diameter systems can be used to improve only signal/noise and not resolution.

Table II shows the expected angular coverage and scale which might be expected through a choice of focal length and size of film format. Thus for photography at 1:60,000 scale, a focal length of 240 in. is required, and with standard 9" × 9" film, an angular coverage of $2.1^o \times 2.1^o$ is obtained. This represents an area of approximately 8 miles on a side or 64 square miles. If the 36" diameter objective is used with a 240" focal length, an f/6.6 optical system is produced with a theoretical 2 ft ground resolution. The f/number is relatively slow, so that film with high ASA exposure index is required and/or longer exposure times must be used. But longer exposure time permits further degradation of resolution capability and increases the requirement for image motion compensation. The trade-off cycle begins. High speed films tend to be more grainy which may become the system limitation in resolution. So larger diameter optics are employed to gather more light and permit shorter exposure times. But eventually one is limited by size considerations and mechanical construction tolerance. Larger diameter objectives will probably have to be assembled in space.

2.1.2. EXPERIMENTAL CAMERA SYSTEMS. Experiments using three separate camera configurations are proposed, because of the range of applications encountered and because the space available in the ORL would probably vary from vehicle to vehicle and depend on joint requirements of other experimentors. The specifications for these systems are listed in Table III. The systems are considered to employ 9" × 9" film format and require about 50 lp/mm film resolution capability. The 12" diameter system has the capability to use film with up to 250 lp/mm before the system becomes diffraction-limited at 5 ft ground resolution.

TABLE I. THEORETICAL RESOLUTION OF SELECTED CAMERA OBJECTIVES

Diameter	Diffraction Limit in Radians for λ = 1 micron	Theoretical Ground Resolution from 200 n mi altitude
2" ~ 5 cm	24×10^{-6}	30 ft ~ 10 meters
6" ~ 15 cm	8×10^{-6}	10 ft ~ 3 meters
12" ~ 30 cm	4×10^{-6}	5 ft ~ 1.6 meters
18" ~ 50 cm	2.4×10^{-6}	3 ft ~ 1.0 meters
36" ~ 100 cm	1.2×10^{-6}	1.5 ft ~ .5 meters
72" ~ 200 cm	$.6 \times 10^{-6}$	.7 ft ~ .24 meters
120" ~ 300 cm	$.4 \times 10^{-6}$	.48 ft ~ .16 meters

TABLE II. ANGULAR FIELD OF VIEW FOR SELECTED FOCAL LENGTH SYSTEMS USING COMMON FILM SIZES

Image Size		35 mm	70 mm	5"	9"	18"	Scale at
Focal Length		.937" × 1.437"	2.25" sq	4" × 5"	9"	18"	200 n mi altitude
in.	cm						
6	15	$10.1^{o} \times 13.7^{o}$	21.3^{o}	$36.9^{o} \times 45.2^{o}$	73.7^{o}	112.6^{o}	1:2,400,000
12	30	$4.5^{o} \times 6.8^{o}$	10.7^{o}	$23.5^{o} \times 18.9^{o}$	41.1^{o}	73.7^{o}	1:1,200,000
18	50	$3.0^{o} \times 4.6^{o}$	7.7^{o}	$12.7^{o} \times 15.7^{o}$	28.1^{o}	53.1^{o}	1:800,000
36	100	$1.6^{o} \times 2.2^{o}$	3.7^{o}	$6.4^{o} \times 8.0^{o}$	14.2^{o}	28.1^{o}	1:400,000
120	300	$.47^{o} \times .67^{o}$	1.1^{o}	$1.9^{o} \times 2.4^{o}$	4.3^{o}	8.6^{o}	1:120,000
240	600	$.25^{o} \times .33^{o}$	$.53^{o}$	$.97^{o} \times 1.1^{o}$	2.1^{o}	4.3^{o}	1:60,000
600	1500	$.10^{o} \times .13^{o}$	$.23^{o}$	$.40^{o} \times .50^{o}$	$.87^{o}$	1.7^{o}	1:24,000
1200	3000	$.05^{o} \times .07^{o}$	$.10^{o}$	$.20^{o} \times .23^{o}$	$.45^{o}$	$.87^{o}$	1:12,000

NOTE: 1^{o} equals approximately 20400 ft at nadir of satellite at 200 n mi altitude.

TABLE III. COMPARATIVE SPECIFICATIONS OF THREE EXPERIMENTAL CAMERAS

Diameter of Objective	f/no	Focal Length	Scale	Ground Resolution at 200 n mi	FOV	Approximate Area Covered	Minimum Film Resolution Required
3"	f/2	6"	1:2,400,000	20-100 ft	74°	296 mi sq	33 lp/mm
12"	f/1.5	18"	1:800,000	5-25 ft	28°	112 mi sq	50 lp/mm
36"	f/6.6	240"	1:60,000	2-10 ft	2°	8 mi sq	45 lp/mm

As indicated earlier, the system giving a scale of 1:2,400,000 will be useful for geology, and for general orientation and reference. It would have a FOV of 74^{o}. The 1:800,000 scale system represents a useful compromise, i.e., 28^{o} for use in map making. The 1:60,000 scale system with a FOV of 2^{o} will be needed for the statistical sampling of area measurements of crops, and the identification of detail in all applications where ground resolution approaching 2 ft in required.

2.1.3. SYSTEM CALIBRATION. Calibration tests for photographic systems would include the following steps:

(1) Laboratory experiments, consisting of sine wave response tests.

(2) Field tests of resolution as a function of contrast (including black vs. white, and dark grey vs. light grey).

(3) Airborne tests:

(a) Preliminary test for general functioning (1,000 ft altitude).

(b) Test of detail at small scale (20,000 ft altitude).

(c) Test of contrast reduction by atmospheric absorption and scattering (100,000 to 200,000 ft altitude).

(4) Testing of operational feasibility at orbital altitudes.

Test patterns of moderate size could be prepared for resolution testing. For tests requiring extended patterns, existing man-made structures such as interstate highways would be used to test for resolution and contrast reduction effects. Alternate sections of straight runs could be painted black and white or shades of grey. These sites would be selected in areas where the air is clearest. Other possibilities are the regular undulation in sand dune areas, artificially produced patterns in water brought about by explosive charges, or parallel dense smoke trails laid down by low altitude aircraft and comparison between a satellite photograph and a high quality aerial photograph of the same area taken as the satellite passes.

2.2. MULTISPECTRAL SENSORS

2.2.1. SPECTRUM MATCHING CONCEPTS. While recognition or identification on the basis of shape information is relatively simple and straightforward, it requires prohibitive information rates when the object being sought is small in comparison with the area being searched. Therefore, in applications where one is searching for materials which have a characteristic spectral output, it may be considerably more convenient to identify the material by

virtue of its over-all spectral response rather than the shape of its components. The technique has potential in agricultural, geological, hydrological, and air pollution applications.

Color photography and multi-lens cameras represent techniques for identifying materials by discrimination of their spectral response. Color films merely display the reflectance of objects in three wavelength bands. The human observer then distinguishes the differences in spectral reflectance of objects in the scene as a difference in color. Multi-lens cameras record individual spectral bands as separate images on photographic film.

In a spectrum matching sensor, on the other hand, the spectral reflectance of each resolution element in a scene is observed by detectors which put this information in electrical form. Real time signal processing techniques can be used to determine how well the spectrum of the resolution element under observation correlates with the characteristic spectral reflectance of the material for which the sensor is searching. By using an optical-mechanical scanner, the spectrum matching need not be limited to the photographic region. Indeed, it need not be limited to the reflected signature and can include the thermal emission signature.

Such an operational sensor would consist of an optical-mechanical line scanner with a single scanning aperture, a dispersing system, and multiple detectors each observing at different wavelengths the radiation from a resolution element defined by the scanning aperture. The signals from the detectors are transferred into a signal processor which determines how well the spectrum correlates with the object being sought. Optical-mechanical scanners have the advantage that the output is in electrical form and can be processed and telemetered in real time.

Thus the potential for improvement in identification in real time appears to rest in the development of multispectral technology. Holter and Legault (Ref. 7) have given the motivation behind this scheme. Existing multispectral data provides considerable support for the hope that satellite reconnaissance using multispectral sensors will permit identification of a wide variety of terrain, particularly farm land, and observation of sea surface characteristics. Earlier work of Colwell (Ref. 8), although limited to visible and near infrared photography in two spectral regions, provides examples of identification of diseased crops and of coastline delineation. More recent results reported by Lowe, Shay, Legault and Polcyn (Ref. 9 and 10) using an airborne scanner operating in seven wavelength intervals from 0.4 to 14 microns also demonstrate the feasibility of distinguishing between several types of ground terrain.

2.2.2. EXPERIMENTAL MULTISPECTRAL SYSTEMS. We should not limit our attention to only those multispectral techniques which acquire simultaneous data with different sensors and require data processing by comparing several pictures with machine and image interpreters;

both methods add considerable time for extraction of information. What is needed is the development of sensors that combine the real time generation of electrical video analogs, such as with an optical mechanical scanner, with the simultaneous spread of spectral wavelengths, such as with a spectrometer. Individually filtered multi-element detectors or rotating filtering disks are only approximations to the ideal of acquiring spectral information instantaneously from the same resolution element. The approximate approaches will be useful mostly in the research phase for determining the classes of objects which have statistically different and identifiable spectral signatures.

With this qualification in mind, the multispectral instrumentation configurations recommended for ORL experiments would include the following:

(1) A 9 lens camera using cut film, to be hand held for initial experiments. A 9 lens camera has already been developed for airborne operations and could be adopted for space environment (Ref. 11). Experimental 9 lens cameras employing 4" × 5" film holders are relatively easy to construct and would be employed in early experimental flights where space and power demands might be critical.

(2) 9 lens camera with automatic film advancement for photography of extended test sites.

(3) 16 lens research camera combining polarization tests with multispectral experiments and having facility for automatic film advancement. The 16 lens camera could be adapted from conventional aerial cameras using 9" film. The scale would be 1:7,200,000 if one uses f/2, 50 mm lenses and ground resolution would be no less than 60 ft. The total FOV would be about 27^{o} by 40^{o}.

(4) 12" diameter optical-mechanical scanner with facility to interchange detector packages so that a variety of spectral bands can be sensed under selected conditions. This system may be the prototype for future multispectral sensors in operational satellites. The optical-mechanical scanner would have a ground resolution of 200 ft from the 200 n mi orbit, and in order to maintain the same S/N capability in space that has been found useful at lower altitudes, a total field of view of $1/25^{o}$ would be the limit for single element sensors. See Appendix B for more detailed calculations.

2.2.3. SENSOR CHECKOUT AND CALIBRATION EXPERIMENTS. In spite of recent advances, the limited multispectral data available do not yet provide sufficient information for the design of a satellite reconnaissance system. Such a design will require a considerable

amount of multispectral data obtained simultaneously from satellites and aircraft, also possibly correlated with ground-based measurements.

The design of data-gathering experiments will necessarily have to be based upon statistical considerations. The nature of the radiation received from the ground by a satellite sensor cannot be predicted exactly, even if the type of terrain is known. Thus, the signal of interest from the ground must be considered random. This signal is also contaminated by noise resulting from random variations in the atmospheric transmission of ground radiation and from radiation by the atmosphere itself. Thus, the signal from each spectral channel of an operational surveillance satellite will be random because of the unknown nature of the terrain and because of atmospheric noise.

For purposes of illustration, consider a system with only two spectral regions. Repeated passes by the satellite over a given type of terrain will not produce identical values of indicated radiance, but will produce a cluster of readings. Calculational procedures could be used, if necessary, to convert a scatter diagram into a joint probability density function. If a low-flying aircraft were used in place of the satellite, the cluster would likely be more compact because of the absence of random atmospheric effects. There are calculational procedures which could be used to obtain a probability density function representing atmospheric effects alone.

A different type of ground terrain would produce a different scatter diagram of radiance values which may or may not have some degree of overlap with the scatter diagrams of other types of terrain. The likelihood of overlap is increased as the number of types of terrain is increased, but is reduced as the number of spectral channels is increased. It is impossible to predict in advance whether there would be overlap of scatter diagrams for a general multispectral satellite surveillance system. If overlap did occur, then either more spectral channels would have to be added, or sophisticated statistical decision theory would have to be employed to effect a compromise. On the other hand, complete absence of overlap would permit considerable simplification of the decision process. The need for absolute radiance values would be eliminated, and discrimination could be based on relative differences of spectral shape, as discussed in Reference 10.

The general philosophy of experimentation should have as its goal the multispectral measurement of a wide variety of terrain from both satellites and low flying aircraft. Absolute radiance levels will be needed at first, so careful calibration procedures will be needed to minimize errors and correct for atmospheric variations. When the system can measure the spectral character of a test area at altitudes within an understood deviation of the spectral character as observed on the ground, the system will be ready for application experimentation.

2.3. INFRARED MAPPING

For experiments in the ORL, the infrared subsystems will consist of three different devices (see Table IV):

(a) Radiometer (temperature profiles)

(b) Low-Resolution Scanner (28^{O} FOV — 3600' Res. 4" D)

(c) High-Resolution Scanner (2.3^{O} FOV — 200' Res. 36" D)

Of the three devices, the radiometer is the only one which does not possess moving parts except possibly the chopper subassembly for calibration. The low-resolution scanner has two rotating prisms (axes perpendicular), whereas the high-resolution scanner has one prism and an oscillating flat. By judicious design, it should prove practical to minimize the inertial effects of the moving machinery. Otherwise, initial experiments may be carried forward with the radiometer only.

2.3.1. RADIOMETER. In the radiometer, an optical telescope, oriented toward the nadir, collects infrared radiation and focusses it upon the sensitive surfaces of the detectors. The detectors convert the radiation into electrical signals, which are then amplified and displayed (or recorded). A chopping device permits injection of blackbody calibration data into the profile information.

The infrared radiometer will serve two distinct purposes. The more important of the two is that of providing an absolute apparent temperature profile of the region directly beneath the spacecraft. In this manner, calibration points can be established and the stability of the scanning instruments can be checked.

The second purpose of the radiometer is its use in checking the feasibility of providing useful thermal maps from space with high sensitivity and fine resolution. In the initial experiments, it may be desirable not to utilize the scanners, concentrating instead upon the radiometer alone.

It is apparent that the radiometer must fulfill the following requirements in order to be useful:

(a) Resolution and sensitivity comparable to scanner performance capabilities.

(b) Absolute temperature measurement (i.e., stability) to $\pm 0.1^{O}K$.

The radiometer will occupy a space of 6" × 6" × 48", and weigh approximately 30 pounds. It will share a recording device with the other instruments. The radiometer should be inside

TABLE IV. INFRARED SENSOR PARAMETERS

	Radiometer	Low-Resolution Scanner	High-Resolution Scanner
Total Field of View (deg)	-	28 × 28	2.3 × 2.3
Angular Resolution (mrad)	1/6	3	1/6
Ground-Patch Dimension (ft)	200	3600	200
Absolute Temperature (^{o}K)	±.5	±.5	±.5
Temperature Sensitivity (^{o}K)	±.1	±.1	±.1
Data Rate (Elements/sec)	60	-	-
Telemetry Bandwidth (cps)	270	10^6	4×10^6
Pointing Accuracy Required (min)	±1	±60	±10
Orbit Altitude (n mi)	200 ± 30	200 ± 30	200 ± 30
Inclination of Orbit (deg)	90^{o}	90^{o}	90^{o}
Orbit Duration (da)	3-90	3-90	10-90
Operational Periods (min/orbit)	30-60	30-60	30-60
Crew Time Requirements (min/orbit)			
Set-up	-	-	-
Check-out	5-10	5-10	5-10
Standby	5-10	5-10	5-10
Experimentation	30-60	30-60	30-60

the spacecraft, with a 4" IR-window provided for viewing along the nadir. Although pressurization is not needed, an airlock should be provided for maintenance purposes.

2.3.2. LOW-RESOLUTION SCANNER. An optical object-plane scanner, consisting of two multi-faceted rotating prisms, can provide a TV-type scan of slightly overlapping $28^{o} \times 28^{o}$ frames. This would provide imagery with a high degree of geometric fidelity, with overlap for redundancy and improved contrast.

"Flying-spot" radiation would be collected by an optical telescope and focussed on a linear array of IR detectors. The detectors will convert the radiation into electrical signals, which will be amplified and displayed (or recorded). Calibration data would be recorded between frames.

The low-resolution scanner will produce low-resolution, high-sensitivity performance. The angular resolution would be 3 mrad (ground patch 3600 ft on a side), suitable for oceanographic observations. The output can be presented at a scale of 1:4,000,000 if 70 mm film is used or 1:1,000,000 with 9" film. A resolution element about 1 mm on a side will result, and the imagery at the smaller scale will tend to look quite coarse; however, for ocean surface observations, this should not be objectionable.

The scanner would occupy a volume of about 27 cubic feet, and would weigh approximately 60 pounds. It would share a recorder with the other equipment. The scanners could be mounted external to the spacecraft, in order to eliminate the need for large infrared windows.

2.3.3. HIGH-RESOLUTION SCANNER. An optical object-plane scanner, consisting of a nodding flat and rotating prism, would provide a TV-type scan of slightly overlapping $2.3^{o} \times 2.3^{o}$ frames. With the exception of the nodding flat, operation is identical with the low-resolution IR scanner.

The high-resolution scanner would produce high-resolution, high-sensitivity imagery. The angular resolution would be 1/6 mrad (ground patch 200 ft on a side), suitable for observation of sea-ice and coastal geography. Also, certain measurements may be made with accuracies on the order of a resolution element (i.e., one acre). The finished imagery can be displayed at a scale of 1:62,000 with a resolution element 1 mm on a side for 9" film. Again, as in 2.3.2, the imagery will tend to look quite coarse; this difficulty could be avoided by going to smaller scales of 1:250,000 with 70 mm film.

2.3.4. IR-SYSTEM CHECKOUT AND CALIBRATION EXPERIMENTS. Certain of the applications in which the infrared system will be used require absolute temperature measurements to within $\pm 0.5^{\circ}K$ and relative measurements to within $\pm 0.1^{\circ}K$. Such accuracies are unattainable with simple infrared scanning devices. Under any condition, signal amplification must be stable and calibration is required.

Absolute measurements of temperature will entail a stable level and gain contain. Stability is affected by variations in detector temperature (see App. B-3) and subsequent changes in detectivity and resistivity (c.f. Fig. 1).* Past experience has shown that a high degree of stability cannot be expected with infrared detectors, even over short periods of time.

Therefore, two types of calibration might prove feasible. The first involves including calibrated "blackbody" plates in the scanner, which would mix gain and level information in between successive scan lines. This would ensure a high degree of stability in the detection system.

The second involves the carrying out of "ground-truth" temperature measurements which could be utilized to provide reference points on the thermal maps. Areas of interest could include large inland bodies of water, desert areas, and selected stations on the major oceans. Criteria for selection might include areal extent, emissivity, temperature stability, and accessibility.

One important area of concern is emissivity. It is known that sea state tends to affect the apparent emissivity of the ocean surface. It is also reasonable to expect that cloud cover, humidity, wind velocity, etc., could influence the results to an unknown extent.

It is concluded that calibration sources will consist of: (a) internal "blackbody" references in the scanner, and (b) monitored terrain features in specific regions. It is desirable that the latter consist of at least one area per orbital passage, although economics may prevent the ideal from being reached.

In order to eliminate the effects of variable atmospheric transmission, it may prove desirable to station solar spectrographs at the calibration sites which would measure the atmospheric transmission via direct observation of the sun.

The tests will determine the experimental value of the minimum temperature difference detectable.

*As a rule of thumb, the variation in apparent target temperature is roughly equal to the variation in detector temperature for the case shown in Fig. 1.

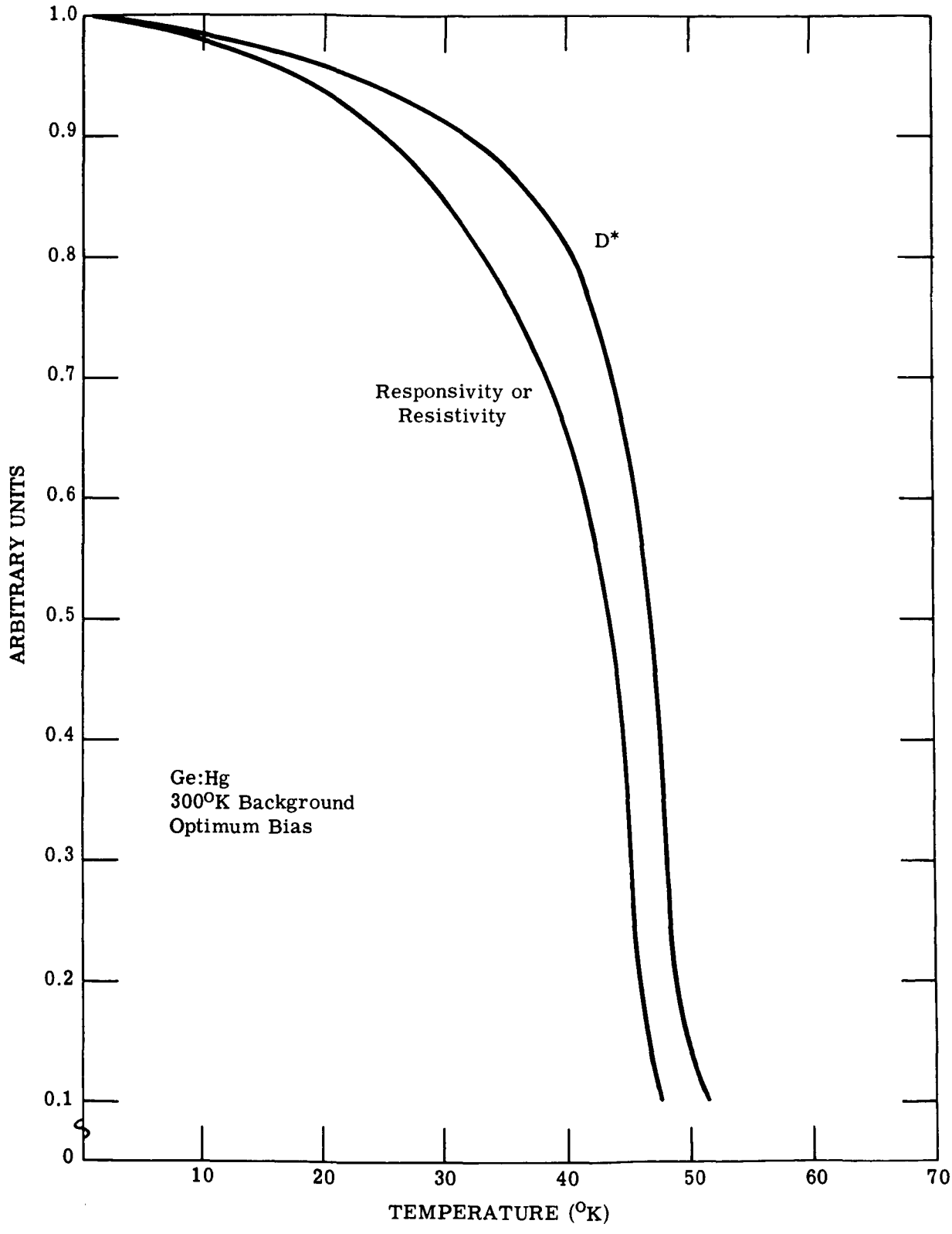

FIGURE 1. DETECTOR PERFORMANCE vs. CELL TEMPERATURE

2.4. PASSIVE MICROWAVE

2.4.1. GENERAL CONSIDERATIONS. The use of passive microwave techniques is extremely attractive for use in space programs for the several reasons enumerated below:

(1) Microwave systems have essentially an all weather capability when compared to IR and visible sensors.

(2) The use of passive rather than active systems greatly reduces primary power and space requirements.

(3) Many interesting effects and useful data appear to be available if and when passive measurement techniques are explored and developed.

The above arguments are general in nature and certainly not exhaustive for all applications. Also there are some inherent disadvantages which have curtailed the interest in passive systems. Such things as limited resolution capabilities, antenna structure size, and limited scanning techniques have all reduced interest in passive microwave devices, particularly since all of these limitations have been overcome by active systems.

For space applications there do appear, however, to be some applications where the use of passive systems can be utilized to advantage for radiometric measurements.

Microwave radiation to be detected originates from several sources, namely, the self emission of materials, sky reflections, and multiple reflections from other objects. Thus the radiation measured gives an effective temperature for the areas or objects being observed. Although the data obtained will be affected by several factors, useful information can be obtained, if measurements are carefully taken and properly interpreted.

The magnitude of the effective temperatures and the differentials which can be expected are shown in Figure 2 for a horizontally polarized system, which has been obtained with a Ku-band radiometer by several groups (Ref. 12) including Bell Telephone Laboratories, University of Texas, AFCRC, and Ohio State. Conway of Space General Corporation has shown that there is also a dependence of effective temperatures on the environmental conditions. This is illustrated in Figure 3 which was extracted from Conway's work presented at the 2nd Symposium on Remote Sensing of Environment in 1962 (Ref. 13).

Hodgin (Ref. 13) of Collins Radio has compared the work done by Collins at 4 cm with the work done by Straiton, Tolbert, and Britt at 4.3 mm. He has shown excellent agreement in the data. Therefore, the effective temperatures shown in Figure 1 are very good over a fairly wide spectral region indicating that emissivities do not vary extensively in the microwave regions.

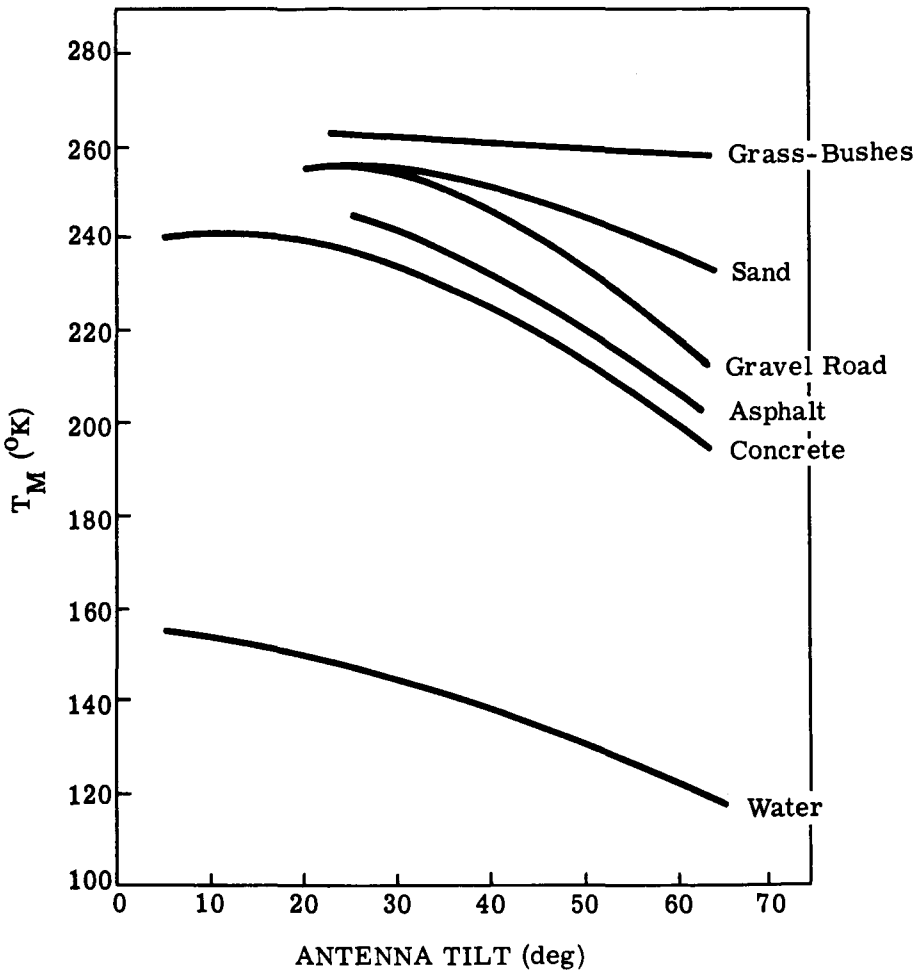

FIGURE 2. MEASURED TARGET TEMPERATURE vs. ANTENNA TILT (Ref. 12)

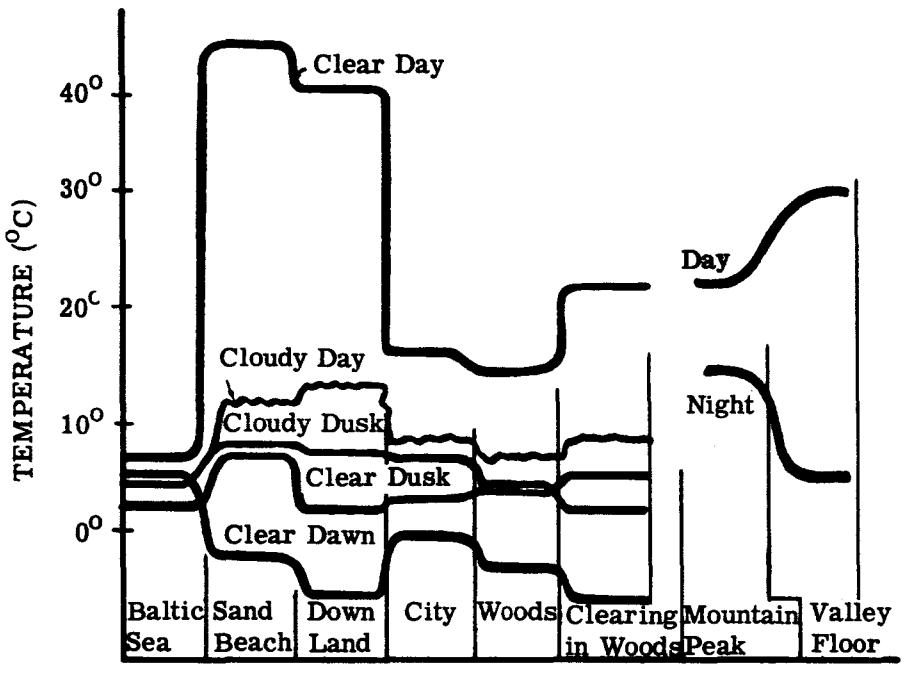

FIGURE 3. TYPICAL GROSS TEMPERATURE DIFFERENCES
(Ref. 12)

In reviewing this work it was also found that significant differences occur between the horizontally and vertically polarized data. In general the gradients are greater for the horizontal polarization.

From previous discussion it is evident that significant information is available by measuring radiation in the microwave regions if properly interpreted. In interpreting the data several problems arise; the more important ones are the losses encountered due to atmospheric transmission and the wide variations encountered in background temperatures over the earth's surface. For instance, water temperatures vary from approximately $-1.86^{\circ}C$ to perhaps $28^{\circ}C$ (Ref. 14). Such variations have to be carefully considered when making observations from a space platform. Also, the transmission varies as a function of wavelength (see Fig. 37, 38, and 39, App. C) and the type of weather encountered. The dependence on weather is shown in Figure 4 which was presented by Hodgin (Ref. 13) and which was extracted from work done by Gunn and East. It is generally concluded therefore that essentially all-weather devices are available if proper wavelengths are chosen.

2.4.2. EXPERIMENTAL SYSTEMS. Outlined here are the system requirements considered necessary to evaluate passive microwave systems for space applications. It is assumed that ground and airborne measurements are to be made prior to adaptation to a space application program.

(1) Measurements must be made simultaneously at wavelengths in the vicintiy of 10 cm, 3 cm, and 8 mm.
(2) Measurements must be made simultaneously at orthogonal polarizations.
(3) Data must be evaluated by comparing the orthogonal polarizations as well as determining the absolute values of each polarization by comparing with a known reference.
(4) Temperature sensitivities of 0.1 to $10^{\circ}K$ are necessary for these measurements.
(5) Resolution requires beam divergence values of 1 to 10 milliradians for acceptable operation at altitudes of ~200 nautical miles.

It appears that the receiver state of the art is adequate to make these measurements. This assumes that one dimensional scanning is used, namely, in the direction of flight path. It is generally recognized that further reductions in noise figures below those obtained by cooled ($77^{\circ}K$) parametric amplifiers in the S and X-bands would be of no significance since antenna background temperatures are already dominating the receiver temperature limitations. Therefore, increased performance can be accomplished only by increased bandwidth capabilities.

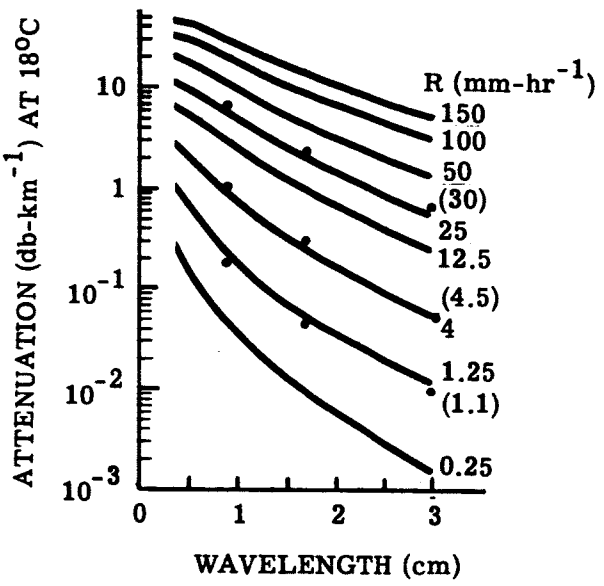

FIGURE 4. ATTENUATION vs. WAVELENGTH
FOR RAINFALL AT VARIOUS RATES
(Ref. 13, p. 134)

Operation of such a device to obtain coverage over large areas (two dimensional scan) is primarily limited by antenna scanning capabilities. In addition, receiver sensitivity will also be of importance.

In the 8 mm region, current receivers are adequate for one-dimensional scanning; however, for two-dimensional scanning, development work on receiver performance would be desirable. Some of this work is currently in progress and significant improvements should be available in about 2 or 3 years.

2.4.2.1. Microwave Radiometers. A function block diagram is shown in Fig. 5 which describes each system of the three wavelength regions to be considered. Each of the systems will be identical unless exceptions are noted. The systems will make use of pre-detection modulation in a "Dicke" type radiometer. It has been determined that a single antenna operating simultaneously at each of the three wavelengths desired can be developed. The unfurlable antenna would be 50 ft in diameter using a Cassegrainian system. Estimated feed movement capabilities for scanning purposes are 4^{o}, 3.5^{o}, and 3^{o}, with 2, 4, and 8 milliradian resolution capabilities for Ka, X, and S-band systems respectively (Ref. 15).

With an antenna having the complexities and unique requirements desired here, it is hardly reasonable to assume that it could be deployed entirely automatically. Man will be required to assist in deployment, in correction of feed location, and other adjustments.

The radiometer will sample each polarization and a reference load through use of ferrite switches, after which low noise amplifiers will be used which are followed by additional amplification. The output will then be detected and either transmitted by telemetry to the ground site or recorded on tape for delayed transmission. Also to be transmitted/recorded are the Ref. Generator signals as well as the sync and pointing information.

Data processing by synchronous detection will be performed at the ground site.

In Table V are listed the available values of system sensitivity (ΔT) as calculated from equations in Appendix C for one and two dimensional scanners based on the limits of state-of-the-art devices. The antenna limits used were those previously mentioned.

It should be noted that additional degradation of the signal will be caused by the fact that chopping is occurring during 1/3 less time and thus the values of ΔT in Table I will be increased by a factor of $\sim\sqrt{1.5}$.

In Table V the values assumed are for cooled parametric amplifiers for the S and X-band cases and are for TWT amplifiers in Ka-band. Watkins-Johnston expects improvements in noise

TABLE V. SPECIFICATIONS OF EXPERIMENTAL MICROWAVE SENSORS

FUNCTIONS	Ka-BAND	X-BAND	S-BAND
D	17 ft	34 ft	50 ft
λ	8 mm	3 cm	10 cm
R; α	2 mrad 68 mrad	4 mrad 55 mrad	8 mrad 51 mrad
v	4 n miles/sec	4 n miles/sec	4 n miles/sec
h	200 n miles	200 n miles	200 n miles
C	0.09	1.85×10^{-2}	2.4×10^{-2}
ΔT^* (one dimensional)	$0.45^{\circ}K$	$0.68^{\circ}K$	$0.05^{\circ}K$
ΔT^* (two dimensional)	$2.6^{\circ}K$	$2.55^{\circ}K$	$0.13^{\circ}K$

NOTE: An antenna temperature of $290^{\circ}K$ was assumed in the calculations. It may indeed be less than this.

*These figures would be increased if dual polarization done in single channel.

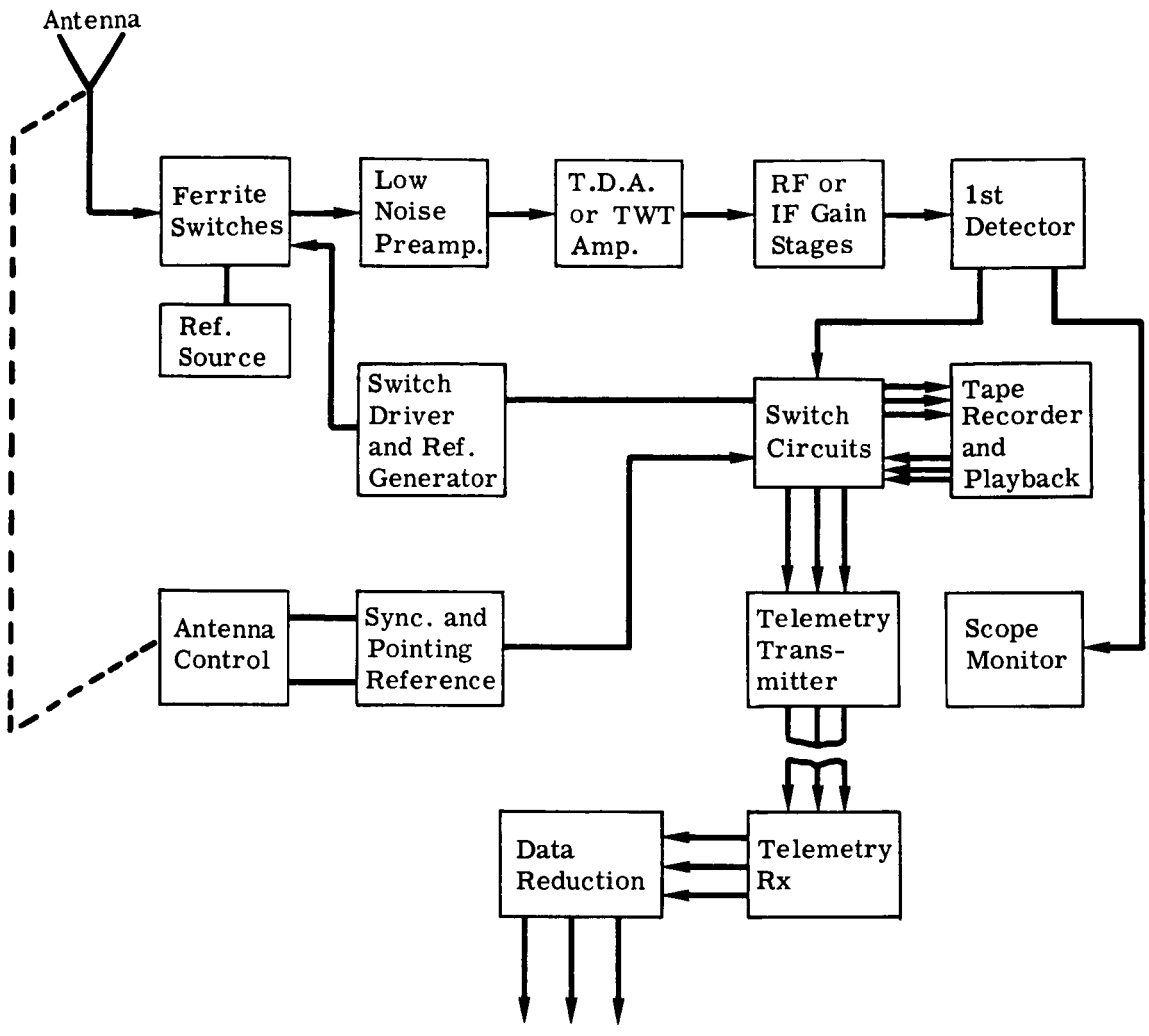

NOTE: This system will be duplicated for each wavelength being measured in the microwave region with exception of the antenna, antenna control, and the sync and pointing reference system.

FIGURE 5. MICROWAVE RADIOMETER BLOCK DIAGRAM

figures to ~6-8db in the next few years* and that advancements in low noise solid state preamps are quite probable.

Information bit rates required for information transmission can readily be determined from equation (4) and the modulation rate for each wavelength in question. If we assume a binary code and a 16 level resolution, the data rates required are 2×10^4 bits/sec/channel for Ka, X, and S-band.

Reference generator bit rates are determined by a 90% rise time requirement in a 50 microsec time period. The rate required here is 4×10^4 bits/sec for a 4 level system.

Pointing and sync references will also require a bit rate of $\sim 10^3$ bits/sec for antenna pointing information.

2.4.2.2. Conical Scanning Radiometer (X-Band). An X-band conical scanning radiometer could be employed to determine the wind direction at sea by measurement of the change in apparent temperature of the sea about the nadir of the space vehicle.

A block diagram of the wind direction detection system is given in Figure 6. The radiometer is of a "Dicke" type using predetection square wave modulation. The radiometer would be designed for the X-band region for which all of the components are readily available. The system will provide for data storage but would not provide for data reduction on-board the space vehicle. The information obtained would be telemetered to a ground site where the data would be reduced to a form to obtain wind directional information.

The antenna designed for X-band operation would be 1 meter in diameter and have the capability of scanning at rates up to 100 rpm through an azimuth angle of 360° and an elevation angle of 10° to 45°. Synchronizing and pointing reference signal will be generated which would correlate with the information being received.

The incoming signal would be chopped and compared to a standard. The receiver would consist of several Tunnel Diode Amplifiers in cascade. Output information is synchronously detected at the chopped rate and can be either recorded on tape for delayed transmission or directly telemetered to the ground station, at which site the data will be evaluated.

The system sensitivity can be expressed by the familiar signal to noise equation for radiometers which expresses the noise temperature of the system as

*Private communication with Watkins-Johnston.

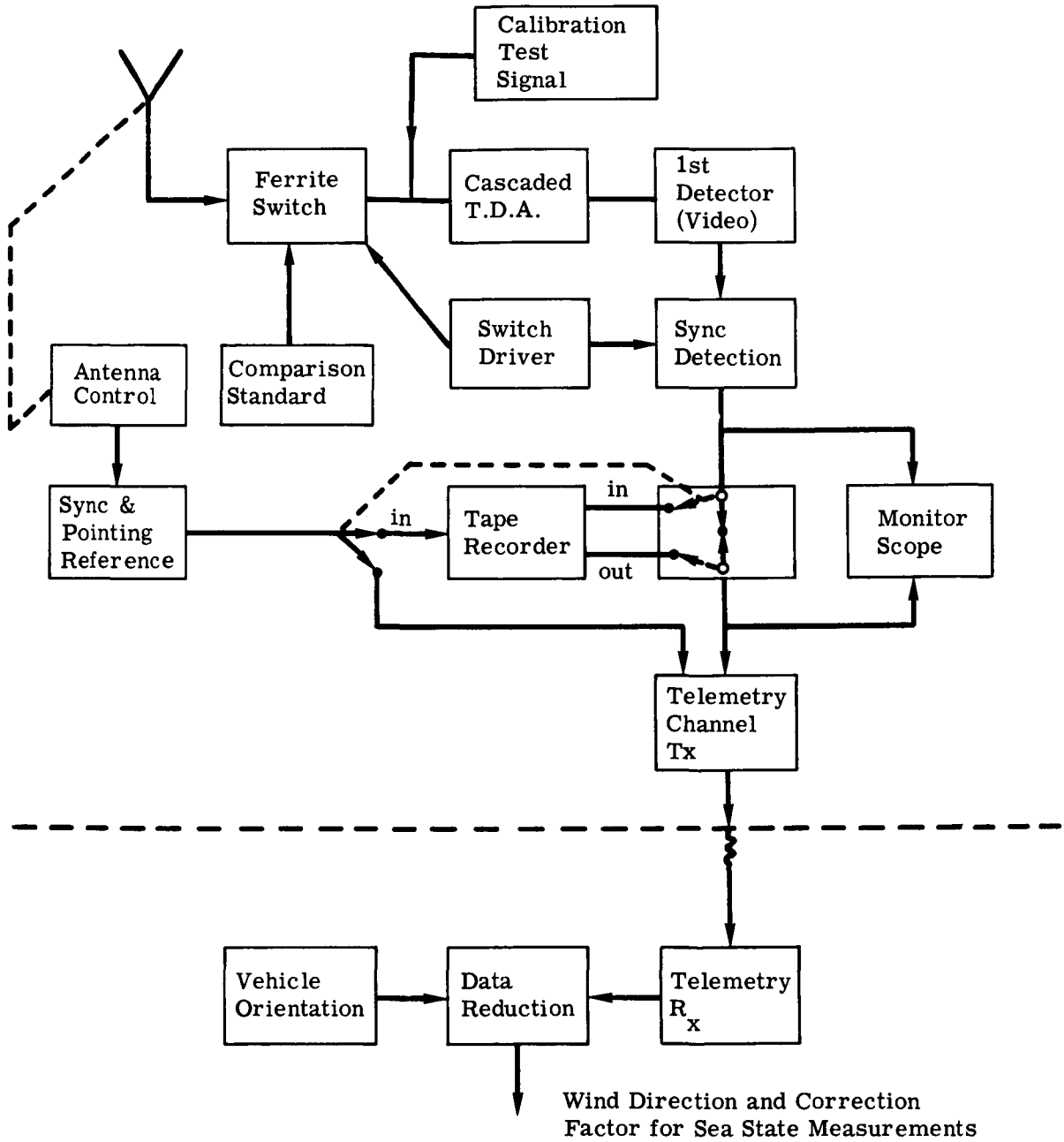

FIGURE 6. CONICAL-SCANNING RADIOMETER (X-BAND) BLOCK DIAGRAM

$$\Delta T_{RMS} = \frac{KT}{\sqrt{B\tau}} \tag{1}$$

where ΔT_{RMS} is the equivalent blackbody noise temperature required to give a $\frac{S}{N}$ of 1, K is a constant dependent upon the type of modulation, T is effective input temperature of the system, B is the pre-detection bandwidth, and τ is the post detection integration period.

All of the parameters for any given system are well known with the exception of τ which will be determined by the use to which the system is put and the information rate desired from it. The information rate will here be defined as the reciprocal of the time required for a point source to move through one beam width when the antenna is revolving at a given rate (A). The beam width (σ) is given as

$$\sigma = \frac{1.2\lambda}{D} \tag{2}$$

where λ is wavelength and D is the diameter of the reflector. The information rate (f_I) is therefore given by

$$f_I = \frac{2\pi A}{\sigma} \quad \text{or} \quad \frac{2\pi AD}{1.2\lambda} \tag{3}$$

For a point source passing through the beam, and allowing for a 90% rise time then

$$\tau = \frac{1}{2f_I}$$

or by substitution

$$\tau = \frac{1.2\lambda}{4\pi AD} \tag{4}$$

Substitution of Equation (4) into Equation (1) then gives the system sensitivity for a particular system. Therefore,

$$\Delta T_{RMS} = \frac{KT}{(B)^{1/2}} \left(\frac{4\pi AD}{1.2\lambda}\right)^{1/2} \tag{5}$$

By substitution of values into Equation (5) we find that system sensitivities (ΔT_{RMS}) of 0.1 to $1^{o}K$ are very realistic and can readily be achieved.

Values considered as SOA:

for λ = 3 cm	assumed values
$T = 1000^{o}$	A = 1 RPS
$B = 10^{9}$	D = 1 meter
K = 1.6	

This system should detect the expected temperature differentials (tens of degrees).

The determination of f_I from Equation (3) then gives us the bit rate of 800 bits/sec for a 16 level detection capability. To make use of this data an equivalent antenna position sync rate will also be necessary. Eight hundred bits/sec are therefore required in both channels of the tape recorder as well as the telemetry system.

2.4.3. CALIBRATION EXPERIMENTS. Various tasks have been assigned to the passive microwave systems. In each task calibration experiments are required to evaluate and optimize the various parameters. These calibration experiments fall into two categories; namely, ground-based (which includes airborne measurements) and space oriented. They will be discussed according to the task assigned.

2.4.3.1. Waves and Sea State. To justify the attempt to measure sea state from a space vehicle it is necessary to perform a series of preliminary experiments from naval vessels at sea as well as from low and high altitude aircraft. This is necessary since adequate experimental evidence is not available to predict precisely the results that will be obtained.

Initial measurements will examine the capability of simple passive radiometers to measure sea state at wavelengths of 8.6 mm, 3 cm, and 10 cm by absolute and differential polarization measurements. Sea state will be measured as a function of frequency, aspect angle, polarization, and wind direction over calibrated test sites. The ability to accurately measure and correct for wind direction will be determined. The data will then be evaluated and if feasibility is assured an optimum system can be designed for space by extrapolation. The space system must be evaluated over a calibration site and data corrections inserted. Space calibration will then provide the optimum parameters for future use.

Support information regarding wind direction must be available in the preliminary measurement program for a test site at sea being observed. This is for calibration and comparison purposes.

The ground site must have all spacecraft orientation and position information available to determine the wind direction from the data obtained on the space vehicles.

2.4.3.2. Sea Temperature. If the feasibility of sea state measurements is proven in Section 3.1.4.1, the sea temperature measurements can then proceed. Measurement of the absolute effective temperature will be extracted from the data obtained for sea state measurements and compared to the standard reference. The change in sea state can be subtracted from the absolute and compared to the actual measured sea temperature at the test site. From this the feasibility and accuracy can be determined. The optimum frequencies, aspect angles, and methods for extraction should be determined and used to design the space system. Space calibration would involve correcting for any transmission effects over the same calibrated site used for sea state measurements.

2.4.3.2. Area Measurements. Airborne measurements can be acquired over selected ground sites, whereby the optimum frequency, polarization, aspect angle, and resolution requirements can be assessed. A simple profiler on an airborne platform can be used. The optimized parameters would then be used to determine space feasibility and design. A calibrated site would be required to evaluate the data obtained.

2.5. LASER ALTIMETER PROFILERS

2.5.1. EXPERIMENTAL SYSTEMS. Appendix E describes two basic laser altimeters for determining the profile of objects on the earth's surface from an orbiting earth satellite at 200 nmi altitude. Section E.2 of this appendix discusses an advanced (1970) FM-CW laser altimeter having very high accuracies and continuous data output. Section E.3 of this appendix discusses a present state-of-the-art pulsed laser altimeter with less accuracy than the FM-CW altimeter and having slower output data (10 cps) than FM-CW altimeter. Continuous data are necessary for land surface profiles, but ocean wave height data are useful even for data points 100 miles apart.*

Both the FM-CW laser altimeter and the pulses laser altimeter can be operated only when there is no cloud occluding the propagation path in its narrow bandwidth. Cloud occlusions limit the probability for operating these altimeters to a value of 40 to 60 percent. Both laser altimeters have a field of view (beamwidth) of 10 seconds of arc and can measure surface profiles for a very small resolution area of 17.9 meters in diameter from a 200 nmi satellite. The diameter of the receiving aperture for these altimeters is 1.15 meters, but for an X-band system (10 Gcs) the equivalent antenna diameter would be 1070 meters (which is presently impractical for satellites).

*Private communication with Professor W. P. Pierson, New York University, 22 March 1965.

The present state-of-the-art pulsed laser altimeter system is shown in the block diagram of Figure 65, Section E.3, and is similar in the basic theory of design and operation to pulsed radar rangefinders or pulsed radar altimeters except that it operates at an optical wavelength of 1.064. It has maximum data rate of 10 cps or data points every 726.9 meters on the earth's surface and the data area is 17.96 meters in diameter. The pulsed laser altimeter has an accuracy error of ±.6 meters (see Sec. E.3.5). This pulsed laser altimeter has very high signal-to-noise ratio, calculated to be approximately 60 db for good pulse waveform fidelity (see Sec. E.3.4). It requires an input power of 285 watts, has an estimated weight of 128 lbs, and needs 9.8 cubic feet of volume (see Sec. E.3.6). The weight and volume can be reduced by decreasing the diameter of the primary receiving mirror to a diffraction limited size (from the present design of 1.13 meters to 8 centimeters).

The future FM-CW laser is shown in the block diagram of Figure 62, Section E.2, and is similar in the basic theory of design and operation to the FM radio altimeter except that it operates at an optical wavelength of 1.0610μ. It has a continuous data rate for a strip 17.96 meters below the satellite. The FM-CW laser altimeter has maximum accuracy ±.7569 millimeters but for larger ocean waves its accuracy is ±1.25 centimeters (see Secs. E.2.1 and E.2.4). This FM-CW laser altimeter requires the present highest power CW gas lasers of 3.55 watts (see Sec. E.2.3). But when injection lasers become more coherent, they should be used to replace the gas laser because they presently have efficiencies 10 times greater than gas lasers. This FM-CW laser altimeter cannot presently be constructed because CW lasers amplifiers having 30 db gain are not available. But with rapid progress in laser technology as in the past, this CW amplifier should be available within a few years at the most. The FM-CW laser altimeter requires an input power of 1200 watts, has estimated weight of 202 lbs and needs 15.3 cubic feet of volume (see Sec. E.2.5).

2.5.2. CALIBRATION EXPERIMENTS. The calibration of both the CW-FM laser altimeter systems described in App. E.2 and E.3 should be accomplished first with artificial targets of known height and then on natural objects, such as ocean waves, with known heights.

The calibration should first be made from high altitude aircraft on artificial targets having known reflectances. Such a target could be a series of rectangular up-down steps made out of concrete, like a "railroad tie" configuration, each tie 17 meters long with raised tie portion equal in width to the spacings. These could be constructed out of very smooth concrete and painted with highly reflective paint (and whose reflectance at 1.06μ is known). A number of these target strips would be necessary to check the height accuracy of these altimeters. The

height tracks of 1 mm, 1 cm, 10 cm, 1 meter and 10 meters would be desirable and could be used from both aircraft and satellites. Also, height of water could be measured from aircraft flying over canal locks in which the water is at different levels. The final calibration of the altimeters should be made on mid-ocean or mid-lake (i.e., Great Lakes) wind waves and having oceanographic ships determine wave heights.

Land profiles could be calibrated over desert regions where the height of sand waves was measured by surveying techniques.

2.6. RADAR*

2.6.1. GENERAL DISCUSSION. Radar appears to have many useful applications in space reconnaissance for peace time applications. Radar is particularly attractive for various reasons, some of the more important of which are discussed below.

First, radar which operates within the microwave spectrum, has essentially an all weather capability compared to the IR and visible spectrum. Its weather capability can be assessed by looking at the atmospheric characteristics shown in Appendix C, Figures 37-39 and by the scattering and absorption losses created by precipitation which is graphically illustrated in Figure 4, Section 2.4.1. It should be pointed out that the losses are a decreasing non-linear function rather than a linear function of altitude.

Second, the radar returns are generally less ambiguous than passive systems, since the signal return is a function primarily of the target reflectance. For passive systems the return is a function of both reflectance and emissivity variables. In general, the active systems can operate with higher S/N ratios this improving the detection capabilities.

Third, radar systems would not exhibit any diurnal variations as would most other sensors.

On the other hand, there are several disadvantages of using radars for space reconnaissance which must be considered. First, unlike passive sensors, all radar systems require transmitters of the space vehicle.

Second, relatively large antennas are required for good operation, which creates problems for space assembly. For the short wavelength sensors this is certainly no problem.

*Most of the information on the performance of radar systems is of a classified nature and is thus not presented in this report. The information given here is of a theoretical nature and does not necessarily indicate the present state-of-the-art. It does, however, indicate the performances which are required.

Considering the above factors, it is concluded that for some applications radar sensors do provide the best means of obtaining good data and thus should be considered for manned earth orbiting experimentation.

In general, there are two types of radar to consider for this purpose. It may be possible that both coherent and incoherent side looking radars can be used to advantage aboard the space platform. A discussion of each type, its attributes, and general theoretical design are discussed in the following paragraphs. Most of the side looking radar systems now in existence are classified and therefore only theoretical considerations can be discussed. However, it is believed that from these considerations, the value can be assessed.

The surveillance platform stability requirements for a radar system operating in a satellite are in general a function of the time it takes to measure the data associated with one resolution element. (To be specific the associated angle rates vary inversely with this time.) For noncoherent radar the tolerable pitch, yaw, and roll rates for the platform vary directly with the system pulse repetition rate; however, for a coherent radar system these rates vary inversely with transit time required for one resolution element to pass through the antenna beam. This time is much greater (by as much as 3 orders of magnitude) than that between adjacent transmitted pulses; thus, the requirements for platform stability for a coherent system can be as much as 3 orders of magnitude more stringent than for a noncoherent system. It appears that the stability requirements for coherent systems might be reduced if inertial information is available for data correction during processing.

It is also important to note that for active radar, as for passive microwave, added information can be gained to aid in identification of targets if orthogonal polarizations are used. This is due to the fact that the surface backscatter coefficient is a function of the polarization of the incident energy.

2.6.2. INCOHERENT RADARS (PROPOSED). Incoherent radar has its prime usage where gross mapping is desired and where fine resolution is not required. Such mapping interests include ice and snow area measurements, sea state measurements, and perhaps gross tectonic features.

In incoherent radar systems, the system azimuth resolution expressed as a distance varies directly with the system azimuth beamwidth and the range-to-the-target. Since a satellite based noncoherent radar will have to contend with target ranges of about an order of magnitude larger than an aircraft based system, a satellite-based system will have greatly reduced ground resolution capabilities over a comparable system operating from an aircraft-based surveillance

platform, unless the system azimuth beamwidth is reduced. The trade-offs between the power requirements for a satellite-based versus an aircraft-based system are not as easily ascertained, since the system power requirements are functions of many system parameters; however. in general it can be stated that the power requirement for the satellite borne system will be greater than that of an aircraft based system with comparable resolution. Where high resolution capabilities are not needed, a satellite system can be made to function with reasonable system constraints (in terms of peak and average power).

An incoherent system operating at the short wavelength end of the radar spectrum is optimized for some purposes, since such a system will provide the best system resolution for a given antenna aperture. The transmission characteristics must also be considered when the operational wavelengths are chosen. This information is given in other sections as stated above. For other purposes, where resolution requirements are lower and where wavelength dependent information is needed, longer wavelengths are required. The parameters of systems operating at wavelengths of 8.6 mm and 20 cm are shown in Tables VI and VII respectively. The data shown in these tables were computed using the equations and theory present in Appendix D of this report. A value of -40 db was used to calculate for the target backscatter coefficient, the peak, and average power requirements for this system; the system power requirements would have to be increased if it is desired to detect targets having lower back scatter coefficient values. Some vegetation (mainly grasses) have backscatter coefficients, which measure on the order of 20 db at a system wavelength of 8.6 mm. A better knowledge of the backscatter coefficients for targets of interest would make it possible to give a better estimate of required system power. It is felt that the values given in Tables VI and VII probably represent maximum system power requirements for the operating conditions.

The system parameter data shown in Table VI are those of a system operating at an elevation of 45^{o} (a typical value for side-looking radar applications) if better system resolution is desired, a decrease in elevation angle might be warranted. Decreasing the elevation angle to 10^{o} will improve the system resolution by 40% (resolution at 10^{o} would be on the order of 1000-2000 feet); however, if comparable swath widths are to be maintained, the power requirements of the system would have to be increased by a factor of as much as 6 to accommodate such an elevation angle change. The data rate will also increase slightly (on the order of 40%) since the illuminated area does not increase as rapidly as the resolvable area. A maximum of 16 gray level scales is assumed.

2.6.3. COHERENT RADAR (PROPOSED). Coherent or synthetic aperture radars show the most promise as remote sensors operating from an orbiting platform for certain agricultural

TABLE VI. OPERATIONAL PARAMETERS OF 35Gc INCOHERENT SIDE-LOOKING RADAR

Operating Frequency	35 Gc
Operating Wavelength	8.6 mm
Antenna Parameters	
a. Azimuth Aperture (beamwidth)	25 to 50 ft (0.08 to 0.04^{o})
b. Range Aperture (beamwidth)	0.5 to 1 ft (4 to 2^{o})
c. Elevation angle	45^{o}
d. Altitude	200 n mi
e. Velocity	2.4×10^{4} fps
Pulse Repetition Frequency	50 to 100 pps
Pulse Width	2 to 4 μs
System Predetection Bandwidth	(0.25 to 0.5) Mc
Nominal Ground Resolution	$(1.5 \text{ to } 3)10^{3}$ ft
Illuminated Ground Swath Width	14 to 30 n mi
Required Transmitted Peak Power	(30 to 800) kw (n_{min} = -40 db, S/N = 10)
Required Transmitted Average Power	(3 to 150) watts (η_{min} = -40 db, S/N = 10)
Maximum System Data Rate	$(1.2 \text{ to } 10)10^{3}$ $\frac{\text{resolution elements}}{\text{sec}}$ or $(5 \text{ to } 40)10^{3}$ bits/sec for a 16 level gray scale
Approximate System Volume	18 ft^{3} (including antenna)
Approximate System Weight	125 lbs

TABLE VII. S-BAND NONCOHERENT RADAR SYSTEM REQUIREMENTS

Operating Frequency	1.5 Gc
Operating Wavelength	20 cm
Antenna Parameters	
a. Azimuth Aperture (beamwidth)	25 to 50 ft (0.9 to 1.8^{o})
b. Range Aperture (beamwidth)	2 ft (20^{o})
c. Antenna Elevation Angle	45^{o}
d. Antenna Velocity	2.4×10^{4}
e. Antenna Altitude	200 n mi
Pulse Repetition Frequency	2 to 4 pps
Pulse Width	60 to 120 μsec
Predetection Bandwidth	10 to 20 kc
Nominal Ground Resolution	$(3 \text{ to } 10) \times 10^{4}$ ft (5 to 17 n mi)
Illuminated Swath Width	300 n mi
Required Transmitted Peak Power	50 to 350 watts (η = -40 db, S/N = 10)
Required Transmitted Average Power	10 to 70 milliwatts (η = -40 db, S/N = 10)
Data Rates	30 to 120 $\frac{\text{resolution elements}}{\text{sec}}$ or 120 to 480 bits/sec assuming a 16 level gray scale
System Volume	20 ft^{3}
System Weight	100 lbs

and oceanographic applications. This is due to the fact that the system resolution is not a function of range to the target or the portion of the microwave spectrum in which the system operates. Resolutions on the order of 25 feet are expected to be feasible by the early 1970's (Ref. 16).

For the first manned earth orbiting experimental program, it is proposed that a coherent system operating at X-band be incorporated; this is due to the simple fact that practically all synthetic aperture hardware which has been developed to date is designed to operate at X-band frequencies. Certainly systems operating in other portions of the frequency spectrum may prove to be useful; however, a great deal of experiment and development will have to be undertaken before such equipment becomes practical or its usefulness is ascertained.

For these reasons a system operating at long wavelengths is not proposed. Systems operating at long wavelengths are at present being considered for penetration experiments in connection with heavily infested forest areas; however, much experimentation in the area of ground truth information and equipment development is needed to prove the feasibility and practicality of such a scheme in early orbiting experiments. While the data that has been collected to date indicates that multispectral identification techniques may be possible, a great amount of further experimentation (both ground and aircraft based) and theoretical development is required before the practicality and feasibility of multispectral identification techniques for spacecraft applications, can be ascertained. Furthermore, there is a more academic question that needs to be answered before a full scale (multifrequency) coherent radar system can be incorporated into a space program; that is, can a coherent radar system operating from a satellite surveillance system do a better job with more system flexibility and less system cost than a comparable system operating from aircraft based platforms? There are certain applications where continuous surveillance of a large area is required. It can be pointed out, however, that the requirements of synoptic coverage and access to remote areas heavily support the use of satellite systems. Intuitively it seems that for these situations a satellite surveillance system would be ideal. For other short term or occasional look applications an aircraft system might prove to be more practical. However, detailed cost and systems analyses will have to be undertaken before a more definitive answer can be given to the satellite versus aircraft question.

The system parameters of a coherent or synthetic aperture radar operating in the 8 to 10 Gc frequency region is shown in Table VIII. The values shown there are those dictated by synthetic aperture theory (see App. D) for system resolution of 25 ft (the requirements shown are not necessarily obtainable). Published data indicates that for most targets of interest backscatter coefficients larger than -30 db have been measured; therefore the -30 db value was

TABLE VIII. COHERENT RADAR PARAMETERS

Operating Frequency	8-10 Gc
Operating Wavelength	3-3.75 cm
Antenna Parameters	
a. Azimuth Aperture (beamwidth)	50' (0.15^{o})
b. Range Aperture (beamwidth)	~5' (1.4^{o})
c. Antenna Elevation Angle	45^{o}
d. Antenna Velocity	2.4×10^{4}
e. Antenna Altitude	200 n mi
Pulse Repetition Frequency	1200 pps
Pulse Width	35 nano sec
Predetection Bandwidth	40 Mc
Nominal Ground Resolution	25 ft
Maximum Illuminated Swath Width	10 n mi
Required Transmitted Peak Power	(1.3 to 3.5) M watts (η_{min} = -30 db, S/N = 10)
Required Transmitted Average Power	(45 to 120) watts (η_{min} = -30 db, S/N = 10)
Maximum System Data Rate	$\sim 10^{9}$ $\frac{\text{resolution elements}}{\text{sec}}$
Approximate System Volume	30 ft^{3} (including antenna)
Approximate System Weight	< 200 lbs

used, and it is felt that the given peak and average transmitted power requirements are probably maximum. It might also be noted that the illuminated swath width listed in Table VIII is about an order of magnitude smaller than the maximum swath width that the system could handle if based only on system pulse repetition frequency constraints (see App. D); however, monitoring the maximum area as dictated by this constraint would increase the system power requirements by approximately 2 orders of magnitude and the system data rate requirements by an order of magnitude. It can therefore be seen that one advantage of a satellite surveillance platform (namely being able to monitor large surface areas) can not be used to full advantage by high resolution systems since system data handling and power requirements will ultimately set the limits on the size of the earth surface area that can be monitored.

For certain applications where the resolution capabilities need not be as fine as the 25 ft (for which the system parameters were computed), it can be shown that the system requirements can be reduced. For a nominal system resolution of 100 ft the system data rate requirements would be reduced by a factor of 16 (keeping other system parameters the same) and the power requirements can also be reduced by a factor of about 16 below those shown in Table VIII. The reduced resolution would not require the same amount of signal processing and probably would not require as complicated a system.

If a system capable of recording 16 gray levels is assumed, a data bit rate of 4×10^9 bits/sec is required of a telemetry system for a real time data link.

2.6.4. CALIBRATION EXPERIMENTS. The calibration experiments are discussed in connection with the various tasks that have been designated for the active radar systems, and these experiments can in general be subdivided into two categories: (1) those ground-based calibration experiments needed to optimize the system, and (2) those in the space calibration experiment needed for correct data reduction.

2.6.4.1. Woods vs. Low Cover. Preliminary calibration experiments will include airbased measurement programs to determine the frequency, polarization, and aspect angle dependence of contrast between the two classes of vegetation. These results can be used in the specification of an optimum system for space application. In space, calibration will involve the checking and setting of system dynamic range for the predicted contrast. Some in-space contrast measurements may also be required to determine the atmospheric effect.

2.6.4.2 Species Differentiation. Again airbased calibration experiments are needed to (1) measure the frequency, aspect angles, and polarization dependence of backscatter coefficients

for targets of interest, and (2) select the optimum system parameters for the space systems. In space calibration (if species differentiation proves feasible) will require calibrated earth surface areas for absolute signal calibration and dynamic range selection.

2.6.4.3. Area Measurement (Snow, Crops, Water, etc.). Again airbased calibration and measurement programs are required to select optimum system parameterization (frequency, system resolution, polarization, etc.). The in-space calibration will involve the setting up of earth based calibration areas (possibly with corner reflectors) so that the in-space system can be calibrated in terms of area and dynamic range requirements.

2.6.4.4. Sea State. Airborne calibration will involve the determination of required system resolution (which will determine whether coherent or noncoherent radar is needed) for adequate area averaging, and angle and polarization dependence of radar saturation effects as a function of sea state (sea state number and wind direction). In-space calibration will involve dynamic range selection for the various frequencies used.

3
SUMMARY OF EXPERIMENTS

3.1. INTRODUCTION

In this section, details are given of orbital experiments to be conducted for the development of earth sciences and resources applications of earth-orbital sensing systems. Special emphasis has been placed on experiments in the fields of agriculture (Sec. 3.2) and oceanography (Sec. 3.3). However, the experiments for these fields are also applicable in large measure to the development of techniques used in the other scientific/technical areas. Less detailed discussions of experiments in these other areas are also included in this section.

3.2. AGRICULTURE

The sensing instrumentation which appears to be most useful to agriculture includes:

(1) Multispectral sensors for crop identification.

(2) High resolution, large scale photographic camera for a statistical sample of crop area measurements and for a rapid assessment of flood damage and storage damage.

(3) Radar altimeter for snow depth measurements to estimate equivalent water volume.

(4) Infrared mapper or microwave mapper for snow area and stream delineation and possibly separation of woods from fields.

(5) Synthetic aperture radar for crop height discrimination, separation of woods from fields, and possibly all weather crop differentiation.

It is assumed that all sensors will have undergone extensive preorbital tests and calibration. The experiments performed on the manned earth orbital laboratory would consist of operating a prototype of each sensor to demonstrate feasibility of space sensing and of developing operational sensors through component evaluation. Before the species identification potential of the multispectral technique is proven in space, a series of preliminary orbital tests should be performed using a specific situation which is easily analyzed and verifiable, such as the mapping of all vegetated areas as opposed to non-vegetated areas. Other broad classes of objects for differentiation could be cultivated areas vs. uncultivated, and low cover crop fields vs. forests and orchards.

3.2.1. VEGETATION VS. NON-VEGETATION. The knowledge of the total area of vegetation on earth will be useful for energy budget calculations and land use analysis.

An experiment performed to separate green vegetation from non-vegetation areas would consist of operating the multispectral sensor adjusted to discriminate the characteristic spectral shape of the green foliage (see Fig. 7). The sharp rise in reflectance at .7μ appears to be the unique property of living vegetation. The experiment could consist of a two-channel sensor, one operating in the chlorophyll absorption band at .68μ and one operating in the high reflectance region between .7μ to .9μ. The two signals generated in real time would be compared either by subtraction or by ratio (to be determined during preorbital experiments). When a preset criteria for the magnitude difference between the two signals is observed, vegetation is identified. The expected results will be a good differentiation of green vegetation from all other objects. Diseased crops or trees wherein the chlorophyll absorption is decreasing or the structure of the leaf is such that the high reflectance in the .7 to .9μ band has been reduced will also be excluded in this mode of sensing.

A more general approach for this experiment would be to use the full potential of the multispectral technique by using enough channels to more reliably sense the shape of the spectral curve for green vegetation. Then multiple decision criteria would be used to separate categories of objects. This decision would be made on each resolution element with a probability of correctness based on the choice of decision criteria and uniqueness of signature. This general approach is precisely what will be needed to perform species differentiation. The astronaut operator will set the decision parameters in the sensor data processor and automatically the amplitude values of output will represent the probability that a given object was observed.

3.2.2. CULTIVATED VS. NONCULTIVATED AREAS. A knowledge of these classes is important for land use studies, and perhaps for detection of "intelligent life" on other planets. The detection of the two classes and measurement of their areas may be possible on the basis of the textural difference between the two areas. Cultivated areas are inherently more structured by man and thus should contain high spatial frequencies plus "characteristic harmonics." Noncultivated areas would tend to have random structure so that the spatial frequency content would characteristically be flat with less high frequency content.

An experiment consisting of the optical-mechanical scanner employing specially constructed IR detectors and used for day-night operation or a photomultiplier fitted with a spatial filter for daylight operation only would be conducted over a test site where large areas remain uncultivated but where regions of cultivation around towns and cities are widespread.

The first experiments would be conducted primarily to verify the high frequency content differences between cultivated land and uncultivated and would test the relationship between

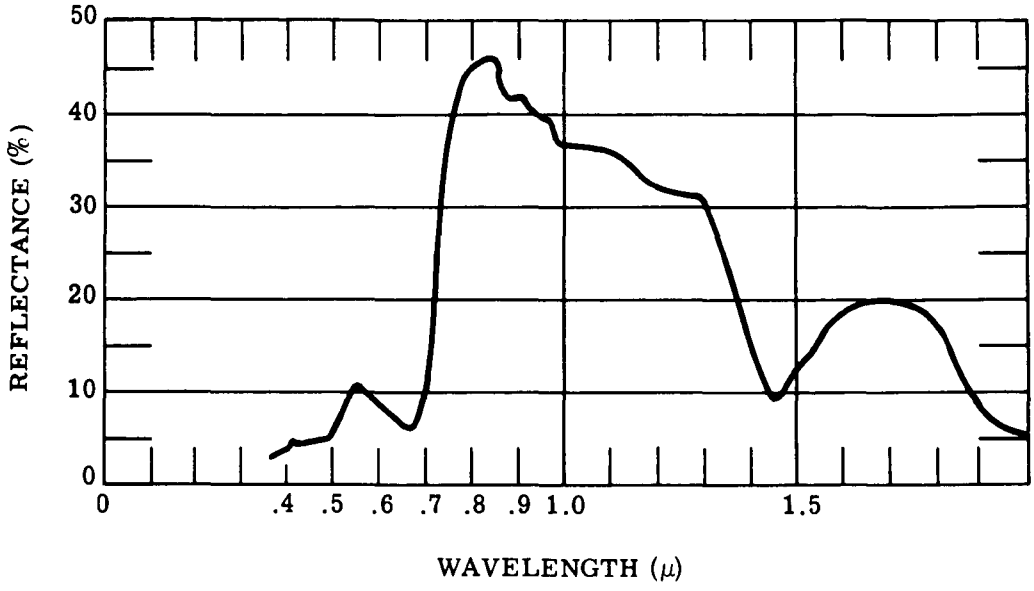

FIGURE 7. AVERAGE OF REFLECTANCE VALUES FROM GREEN FOLIAGE

altitude, the size of the instantaneous FOV of the sensor and the size of the patterns sensed. Later experiments would be operational feasibility tests for accuracy of area measurements.

3.2.3. WOODS VS. LOW COVER. As a subgroup for land use studies, the distinction between woods and low cover crops is necessary. From the first experiment (3.2.1) will come an area measurement of green vegetation. Then a map can be made with either a radar sensor where the brightest returns will be trees or a thermal map at night where the brightest returns are either trees or water areas, (or a thermal map during the day when trees will be darker than their surroundings) and correlated by a coordinate comparison with the vegetation map to identify those vegetated areas which are woods or orchards.

This experiment would be made to test the accuracy and reliability of distinguishing trees from all other objects with a radar sensor, or IR thermal mapper sensor from orbit in conjunction with a multispectral sensor. This experiment would be a prelude to the test for tree species differentiation.

If a synthetic antenna radar is employed in a satellite it can differentiate between woods and low cover and provide an area measure of the regions. The resolution of a noncoherent radar would be so poor that it would probably not be useful for this function. Synthetic antenna radar (operating at long wavelengths) may also prove to be useful in woods penetration experiments; however, a great deal of preliminary development will be required before such experiments will become practical. Both equipment and data analysis techniques will have to be developed and proved feasible.

3.2.4. SPECIES DIFFERENTIATION

3.2.4.1. Multispectral Sensing. For agricultural census, conservation and government support programs, the ability to identify crops, their state of maturity, vigor and the like is desirable. The space platform's advantage of wide coverage in short time needs to be exploited for the improvement of crop reporting and the assessment of a region's crop development.

Crops of major importance in the United States and the world include corn, wheat, rice, sugar cane, cotton, and soybeans. The orbital experiments would begin with a study of the feasibility of discriminating these crop types. The primary instrument for the experiments would be a multispectral scanner operating in several bands in the visible and infrared. Advantage would be taken of the growth cycle of each crop in a particular region of the country. Table IX shows a monthly growth cycle for several crops on a regional basis. It can be seen that one does not have to discriminate all crops at the same time in the green foliage conditions.

TABLE IX. GROUND CONDITIONS DURING THE YEAR

AREA: Ohio, Indiana and Illinois*

CROPS: MONTH	WINTER WHEAT	CORN	SOYBEANS
January	Frozen or snow Vegetation brown	Plowed, pasture or corn stalks	Plowed or stubble
February	Frozen or snow Vegetation brown	Plowed, pasture or corn stalks	Plowed or stubble
March	Ground with vegetation brown	Plowed, pasture or corn stalks	Plowed or stubble
April	Becoming green to short green	Plowed, pasture or disced stalks	Plowed or stubble
May	Green, Medium to Tall	Planting, May 5 to June 20	Planting, May 10 to 30 June
June	Yellow, Harvest, 20 June to 5 August	Short, green	Planting
July	Harvest or stubble	Green, ground covered	Dark ground, short green in rows
August	5 August—Stubble or plowed	Green, full height	Green, ground essentially covered
September	Planting, September 10 to 1 November	Drying starts Green to dry	Drying starts Harvest 10 September to 1 November
October	Planting, Dark soil and short green in drill rows	Harvest, 25 September to 5 December	Harvest
November	Dark soil and short green in drill rows	Harvest and/or corn stubble	Stubble or plowed
December	Frozen or snow Vegetation green to brown	Corn stubble Some fields cut for silo filling	Stubble or plowed

*Planting and harvesting dates are obtained from U. S. Department of Agriculture, "Usual Planting and Harvesting Dates," Agri. Handbook No. 283 (Field and Seed Crops), CRB, SRS, March 1965, Information for other months is filled in accordingly and some variations may be expected.

For example, fields where winter wheat is to be sown are bare in September at a time when corn is tall and yellow.

A similar state of affairs will occur at different times in different latitudes. This fact makes the discriminating job much easier. Also it will be noted that the average size of a crop field will have a bearing on the ability of the orbital sensor to discriminate crop types. The ground resolution for the first generation of multispectral sensors will be in the neighborhood of 200 ft, and since it is desirable to obtain about 10 resolution elements per object for reliable identification those fields of crops whose length is at least 600 ft on a side or about 9 acre blocks will be used for the first experiments.

Table X shows the distribution of corn field sizes in three Midwest states (Ref. 17). It can be seen that the percentage of total farms having a base acreage of 11 acres or more amount to 68% in Ohio, 76% in Indiana, and 83% in Illinois. The percentage of wheat farms exceeding 10 acres totals 47% in Ohio, 56% in Indiana, and 64% in Illinois. Cotton fields are extremely variable in size with the smallest fields in the Southeast, for example, Georgia (see Table XI). Soybeans are widely grown in Ohio, Indiana, and Illinois. Most fields would probably exceed 10 acres, and very few would be smaller than 5 acres. Most sugar cane fields are large, perhaps 20 acres or more. Rice is grown in concentrated areas, principally in Arkansas, Louisiana, California, and Texas. The percentage of farms which are at least 11 acres in size is more than 89% in Texas and California, 84% in Arkansas, and 81% in Louisiana.

Generally speaking, fields east of the Mississippi are smaller for most crops than those west of the Mississippi. In most parts of the world outside the United States, small fields prevail. Exceptions occur in developed countries having plains areas suitable for agriculture, for example, Canada, Australia, Argentina, and South Africa.

Thus the major experiment on the orbiting laboratory would consist of operating the multispectral scanner with the sensor decision parameter set to accept only those signatures whose spectral response matched the crop selected to be mapped. This will be a function of region selected and time of the year the orbital flight is made.

This experiment would be conducted after the multispectral optical mechanical scanner has been flown successfully in orbit. Prior to this time, it will be desirable to obtain multispectral data from orbit to determine which spectral bands are practical in the presence of haze, and atmospheric attenuation. One compact, relatively "simple" method is by multispectral photography. Multispectral photography properly performed can be considered an operation of a number of spectrometers viewing several objects simultaneously. The spectral scan is

TABLE X. DISTRIBUTION OF CORN FIELD SIZES

For the states of Ohio, Indiana and Illinois, the distribution of total base acreage for corn, sorghum, and barley appears in Table I ASCS-PPA-SSS, March 4, 1965. Barley and sorghum are minor crops, almost rare in these states so the data pertain essentially to corn.

STATE:	OHIO	INDIANA	ILLINOIS
TOTAL FARMS:	160,700	161,700	210,300
BASE ACREAGE:			
1-10	No. 56,600	No. 40,300	No. 34,000
	% 35	% 25	% 16
11-15	No. 22,000	No. 19,000	No. 15,400
	% 14	% 12	% 7
16-20	No. 17,700	No. 16,500	No. 14,400
	% 11	% 10	% 7
21-25	No. 13,542	No. 13,400	No. 12,400
	% 8	% 8	% 6
26 +	No. 51,000	No. 72,500	No. 134,100
	% 32	% 45	% 64

TABLE XI. DISTRIBUTION OF COTTON FIELD SIZES

STATE:		GEORGIA		ARKANSAS		TEXAS
COTTON ACRES, TOTAL:		900,000		1,355,000		6,500,000
NUMBER OF FARMS, TOTAL:		93,200		43,500		192,600
COTTON GROWING FARMS:		35,000		34,800		107,000
ALLOTMENT ACRES PER FARM:						
Less than 5	No.	6,300	No.	4,000	No.	8,500
	%	18	%	11	%	8
5.0-10.0	No.	9,500	No.	7,900	No.	8,000
	%	27	%	23	%	7
10.1-14.9	No.	5,200	No.	5,800	No.	6,600
	%	15	%	17	%	6
More than 14.9	No.	14,000	No.	17,100	No.	83,900
	%	40	%	49	%	79
AVERAGE FARM SIZE—ACRES		26		38		61

instantaneous and when the multiple lenses are bore sighted with each other, the data from each resolution element in view is recorded at the same time. The major drawback is the use of film for data storage. Image development can affect the range of densities on the film. The set of densities for a given point measured in each of the spectral channels represents the spectral signature. And for this set of densities we want to see the densities as a function of the object condition and how they may be affected by transmission through the atmosphere. Calibration of the camera exposures and control of the development process will be all important.

Filter selection and replacement should be programmed and analysis of data should determine which spectral ranges in the visible at least have the most potential for discrimination and which spectral ranges might be eliminated from further consideration.

Further experiments with spectrometers to measure angular dependence of the spectral signature as seen from orbit would be desirable. The spectrometer would be trained by the astronaut-operator at a specified test site and as the satellite passes over the site, a series of measurements at look angles forward, at the nadir and rearward could be carried out. Data would be analyzed to determine whether a constant angular relationship between sun, field of interest, and receiver must be maintained for consistent spectral signatures. If this proves to be the case, then choices of orbits for multispectral crop identification may be constrained.

3.2.4.2. Passive Microwaves. The use of passive microwave radiometers for crop identification, rate of growth, field size, etc. is improbable for several reasons. First, is the limited resolution attainable with current and projected systems. From the charts shown in Appendix C for resolution vs antenna size, it is shown that the maximum resolution attainable in the 1970 time frame is between 1 and 2 milliradians. This corresponds to an area measurement of approximately 40 to 140 acres which in many cases would be equivalent to or larger than many crop areas. Thus identification would be difficult and probably impossible in most cases. Second, sufficient measurements to demonstrate that identification is possible have not been made, although there is evidence that this may be possible.

It can be concluded that it is not presently feasible to use passive microwave systems for the above stated uses however a future potential does exist. It has also been ascertained that R/D programs as well as measurements must be performed before the ultimate potential can be assessed.

3.2.4.3. Active Microwaves (Radar). The use of active microwaves for remotely sensing crop type, growth, etc., appears to have great potential but has not yet been fully evaluated.

Figures 8 and 9 show some representative spectral differences in backscatter coefficients which have been measured for the indicated crops. Also shown in Figure 10 is some seasonal variations in backscatter coefficients for the various frequency spectra and crops. Except where the variation in coefficient is small, the information will probably be quite useful.

There are currently several programs getting under way or in progress which should eventually provide additional valuable target signature information for future use. The use of coherent rather than incoherent radar is presumed since the spatial resolution limitations of incoherent radar are the same as for passive systems. Coherent radar spatial resolutions of 25 ft are expected by the 1970 time frame as projected by Heavener in 1961. Presently, resolution capabilities of between 50 to 100 ft are within the present state-of-the-art which would be adequate for this purpose (Ref. 19).

In general, for most imagery the ground truth has not been collected, nor have extensive signature programs been undertaken until recently. Interpretation of the data (gray scale evaluation)thus remains as the prime hurdle to be achieved prior to use of such systems in satellites.

Another area for concern should be the development of methods whereby the dynamic range limitations of active systems can be improved. This could indeed be a serious limitation to any signature program using active radar techniques.

In addition, the use of radar techniques and/or active scanning techniques in the IR and visible regions should be examined as a means of obtaining signature data. Related research makes it appear quite probable that signature information could be obtained with these techniques. Theoretically, it is possible to instrument such devices, although little effort has gone into designing such units.

Experimental programs should be initiated to obtain the signatures suggested, but until this is done, signatures should not be considered as presently available for the ORL program.

3.2.5. AREA MEASUREMENT OF CROPS OR FOREST. As has been indicated earlier, accurate area measurement of crop acreage is required for most agricultural programs. For crop sizes of the order of one acre (209 ft on a side), a ground resolution of 2' would result in an error about 1/2 to 2% per side or 2 to 4% error in area. Better accuracy of area ground measurements can be obtained only for larger field sizes since resolution better than 2 ft cannot easily be achieved from 200 nmi altitude. If one knows the frequency distribution of field areas for a given species; then by a suitable sampling process, an estimate of crop acreage can be made by measuring the areas of selected sites with the high resolution sensor.

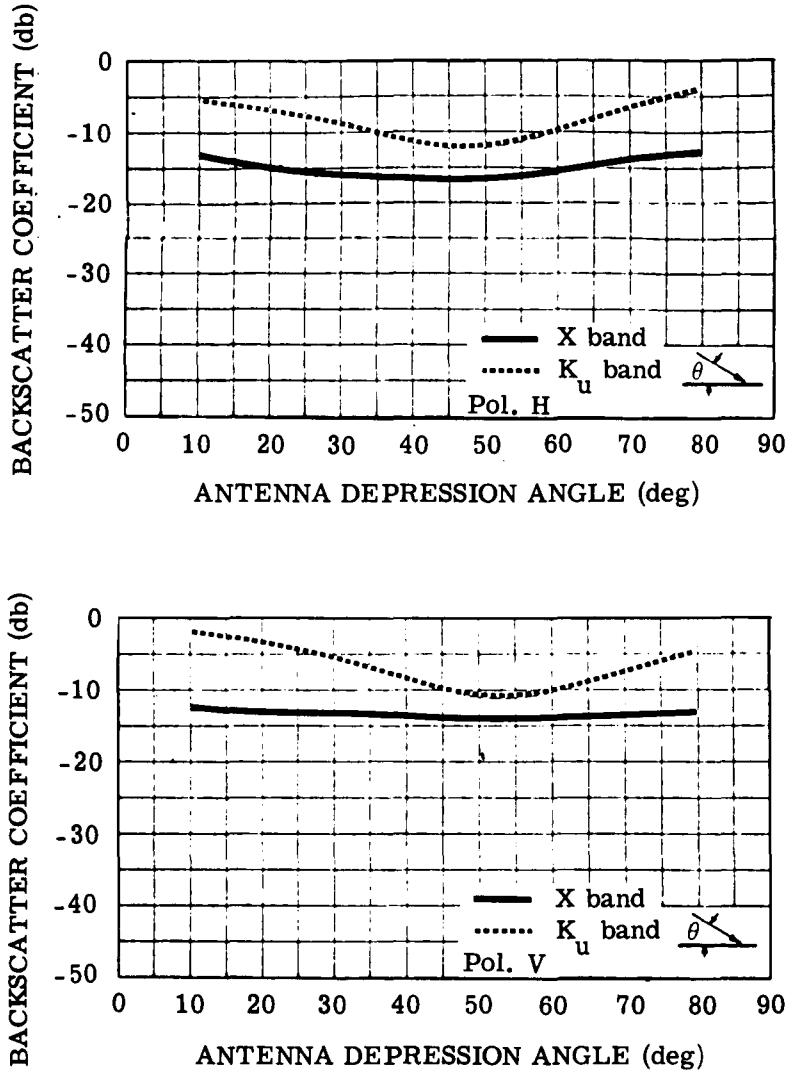

FIGURE 8. FOUR-FOOT OATS IN HEAD (JULY) (Reproduced from Ref. 18)

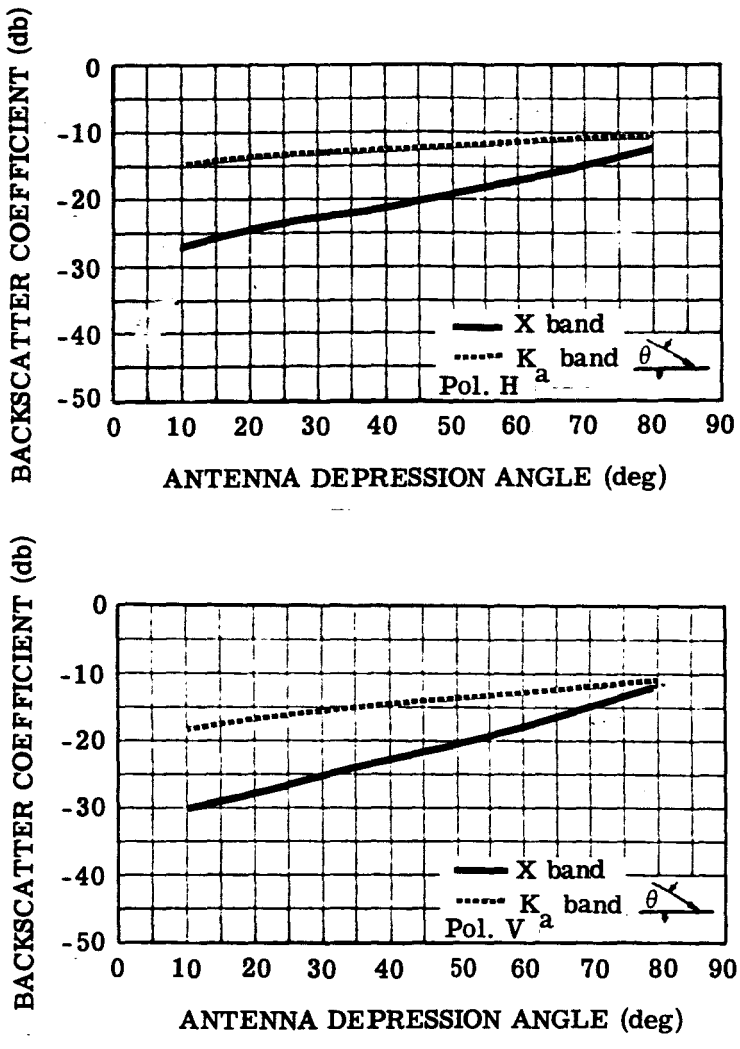

FIGURE 9. ONE-HALF-INCH GREEN WHEAT (Reproduced from Ref. 18)

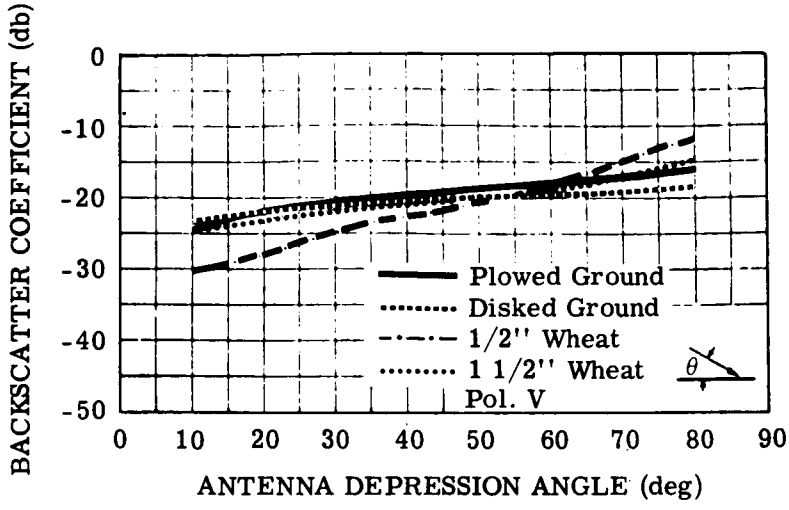

(a)

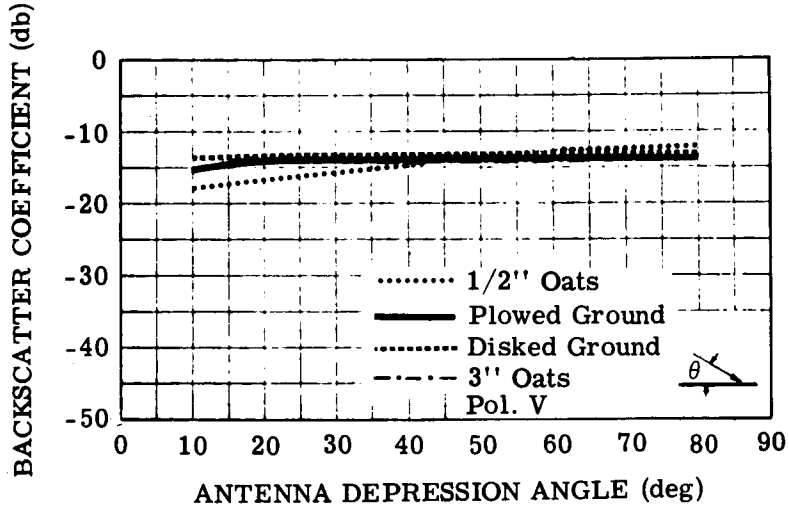

(b)

FIGURE 10. SEASONAL CHANGES. (a) Wheat field at X-band. (b) Oats field at K_a-band. (Reproduced from Ref. 18)

An experiment will be performed with the 1:60,000 scale photographic sensor described above. It will be used in conjunction with the multispectral scanner which will be obtaining information on crop identification. Both systems will have approximately the same total FOV (2^{o}) and if both data displays use 9" film, the scales will be nearly the same. The multispectral scanner will have coarser resolution and its output will not look like a true photo since the density will be determined by automatic decision circuitry indicating that a particular crop was observed. The patterns of density will be the pattern of that crop distribution and by overlay or by coordinate comparison the corresponding crop site on the high resolution photograph will be noted and that field will be measured by appropriate means. The measured values are then compared to the known field sizes at the test site. This experiment may also be used as a calibration procedure on resolution if a number of fields of different sizes are present at the test site.

Coherent radar techniques can be used extensively in agriculture surveys for area measurement purposes on relatively larger farms. Assuming the predicted 1970 resolution capabilities of 25' and assuming a minimum square area of 40 acres (1/16 section), the maximum error in measurement is approximately 1 acre or 2.5%. For all larger areas the percent error is of course less.

Area measurement with coherent radars is possible since fields are discernible due to the variance in reflectivities which produce gray level differences and with interpretation of the ordered shape recognition. However, as previously discussed in Section 3.2.4, the signatures are not well known and sufficient theory has not been developed to determine what crop is present (i.e., corn, oats, wheat, grass, etc.). At present then, it would be necessary that the crops be identified by some other remote sensor such as the multispectral sensors or by some other means. Of considerable importance is the recording mechanism. It must be adjusted or programmed to record within the dynamic range in which the gray scales or crop cross sections are available. We can plot only a portion of the total dynamic range available and therefore must pre-select or program for that portion of the dynamic range we wish to obtain.

Present instruments operate in the 3 cm wavelength region, which appears to be optimum for this work. There are several reasons why this is the optimum microwave region.

First, operation at long wavelengths would produce erroneous signatures because of the penetration capabilities in soils and vegetation. Thus, the signature and contrast obtained would change depending on soil type, etc. (Ref. 19).

Second, at shorter wavelengths the atmospheric absorption becomes pronounced, and depending on the weather conditions, would either reduce or obliterate the contrasts required for measurements. Thus, one concludes that the initial experiments should be performed in the spectral regions for which the variables and their effects are at a minimum.

Prior to placing such a radar instrument in the ORL, there should be a detailed investigation of the methods by which the data could be processed and used for area measurements. Proposed methods should be checked by use of data obtained from aircraft. It would be necessary to establish ground truth sites or perhaps use those sites presently available for the aircraft measurements. It is probable that once the methodology is established and proven adequate, new ground truth sites may be established for the ORL program.

3.2.6. MEASUREMENT OF SNOW COVER

3.2.6.1. Microwave Sensors. Snow coverage can be measured by passive or active microwave systems. The selection of passive or active would depend upon the resolution requirements and the ground patch size to be measured.

For extended areas and where coarse resolution can be accepted, the use of either non-coherent radar or passive microwaves will provide the extent of snow and ice coverage. The linear measurement accuracy will vary from approximately 0.4 to 1.6 n miles for the passive systems suggested or from 0.25 to 5 n miles for the non-coherent active. The variations are due to the frequency dependence or resolution. In the calibration experiments, the wavelength dependency will be evaluated.

When ground resolutions less than 0.25 n miles are required, then the coherent active systems must be used. Ground resolutions approaching 25 ft should be possible within the 1970 time frame if the prediction of Heavener is correct. The representative effects of snow cover for active systems are illustrated in Figures 11, 12, 13, 14 as a function of wavelength and polarization for various backgrounds.

Thus it is concluded that any one or all of the proposed microwave systems may be useful for snow and ice measurement capabilities.

3.2.6.2. Depth of Snow and Ice Penetrator with Radar Techniques. The depth of ice and snow can be measured within a resolution element by receiving the radar return from the surface of the snow and the radar return from the frozen ground beneath the snow and/or ice. Presently, there are experiments measuring snow and ice thicknesses by this method but most

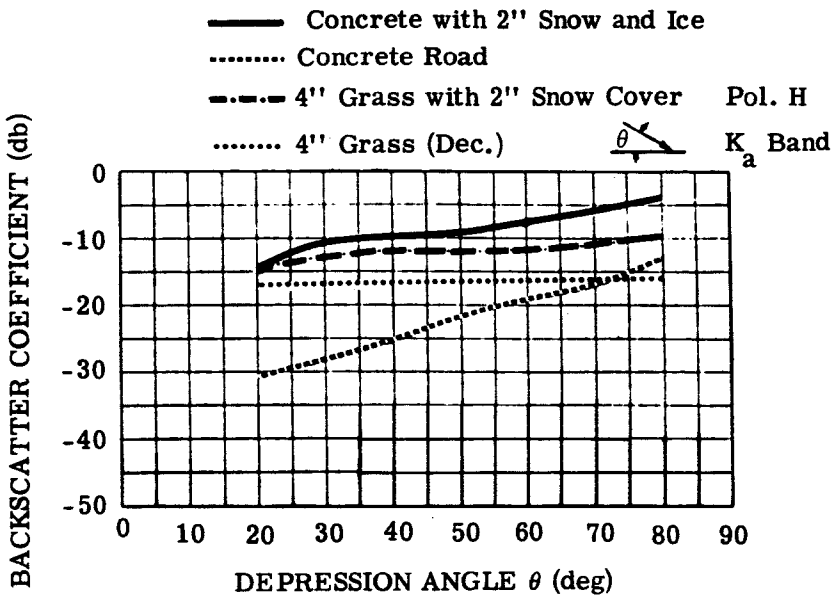

FIGURE 11. EFFECTS OF SNOW COVER UPON γ AT K_a-BAND, HORIZONTAL POLARIZATION
(Reproduced from Ref. 18)

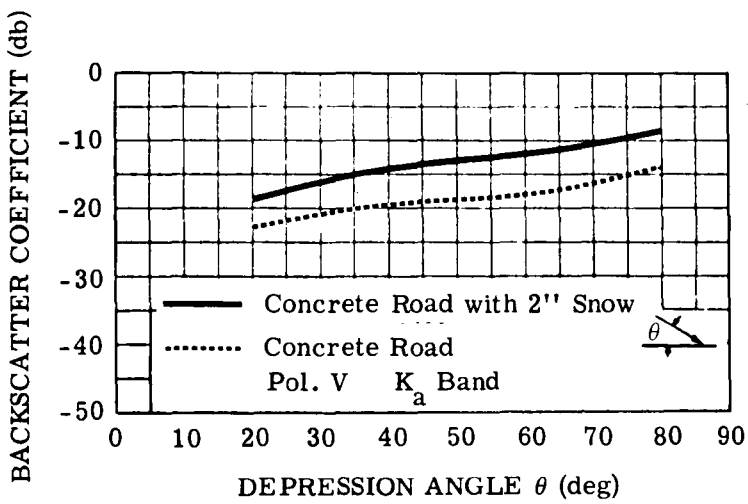

FIGURE 12. EFFECTS OF SNOW COVER UPON γ AT K_a-BAND, VERTICAL POLARIZATION
(Reproduced from Ref. 18)

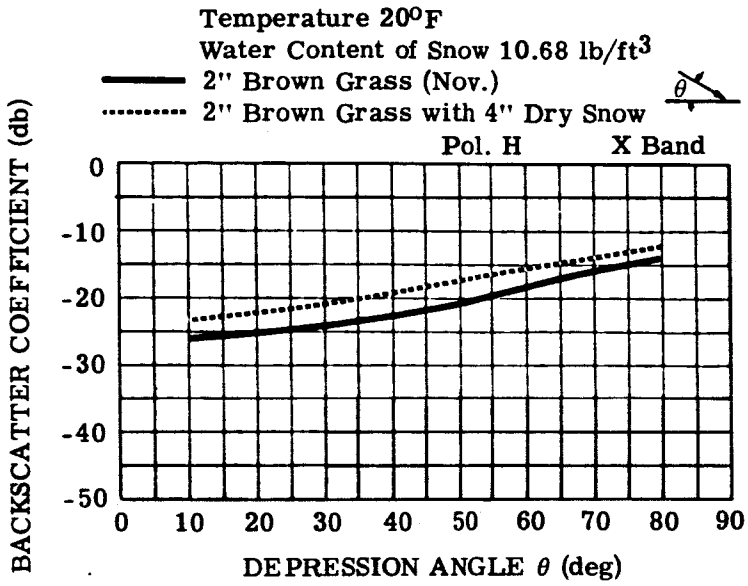

FIGURE 13. EFFECTS OF SNOW UPON γ AT X-BAND
(Reproduced from Ref. 18)

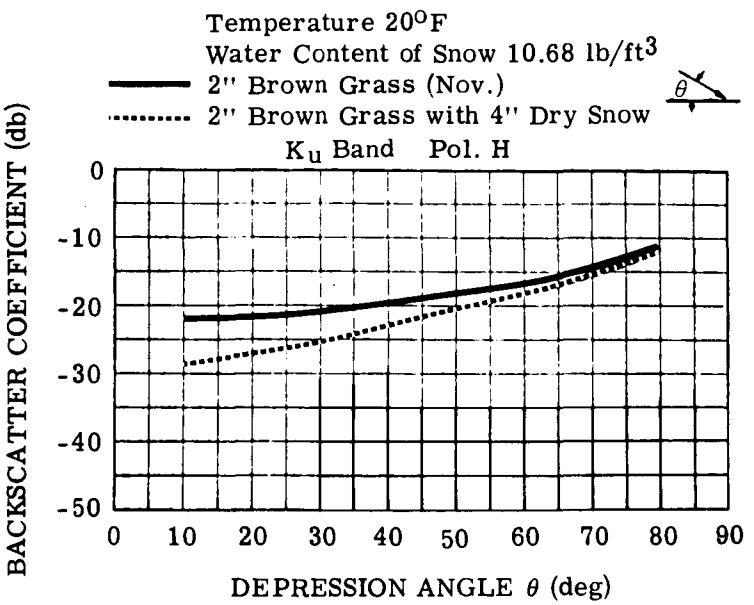

FIGURE 14. EFFECTS OF SNOW UPON γ AT K_u-BAND
(Reproduced from Ref. 18)

of these experiments use too low a frequency (110 to 440 mcs) to have an adequate resolution from a 200 n mile satellite (Ref. 20). The most applicable work was by Cummins who measured the permeativity, loss tangent and reflectivity of snow and ice at 9.375 Gcs, (Ref. 21). The penetration of snow or ice by electromagnetic waves can be calculated for a wide frequency by using the theory and data given by Von Hippel (Refs. 22 and 23). Table XII gives the attenuation for the frequency range of 10^3 to 10^{10} of three kinds of snow and ice. These calculations were made using Von Hippel's data on loss tangent and dielectric in the following equations

$$\alpha = \frac{8.686\pi \tan\delta}{\lambda} \cdot \sqrt{\frac{\epsilon'\mu'}{\epsilon_o\mu_o}}$$

for $\tan\delta = 0.0001$ to 0.05 (low-loss dielectrics)

$$\alpha = \frac{17.37\pi}{\lambda} \sqrt{\frac{\epsilon'\mu'}{\epsilon_o\mu_o} \frac{(1 + \tan^2\delta)^{-1/2} - 1}{2}}$$

for $\tan\delta = 0.05$ to 50 (medium-loss dielectrics) where α is the attenuation in db/meter and $\tan\delta$ is the dielectric loss tangent (in units), λ is the wavelength in meters, ϵ' is the permeativity of the media (i.e., snow or ice), ϵ_o is the permeativity of a vacuum, ϵ'/ϵ_o is the relative permeativity or dielectric constant (in units), μ' is the magnetic permeability of the media, μ_o is the magnetic permeability of a vacuum and μ'/μ_o is considered to be 1 for these calculations.

Figure 15 is a plot of the attenuation of freshly fallen snow, hardpacked snow, and ice vs frequency as calculated from the above equation and tabulated in Table XII. It can be observed from Figure 15 that the snow temperature has the greatest effect on the attenuation but the snow curve rises steeply in the 3 Gcs to 10 Gcs frequency spectrum as does the ice. It is also noted for the microwave region that the denser material is, the greater the attenuation.

Thus we have determined that using a frequency of 10 Gcs and an antenna diameter of 20 meters may be necessary for a sample calculation of radar penetration of low loss dielectrics. The well known radar equation is given by

$$\frac{S}{N} = \frac{P_t G_t A_r}{4\pi^2 r^4 K T_o \Delta f (NF - 1)} \qquad (1)$$

where S/N is the signal-to-noise ratio

P_t is the peak transmitter power in watts

G_t is the gain of transmitter antenna

A_r is the area of receiving antenna in sq meters

TABLE XII. ELECTROMAGNETIC WAVE ATTENUATION BY SNOW AND ICE

	Frequency (cps)	Dielectric-Loss Tangent	Relative Dielectric Constant (ϵ'/ϵ_0)	Attenuation (db/meter)
Freshly Fallen Snow (-20°C)	10^3	0.4920	3.33	$7.9414(10^{-5})$
	10^4	0.3420	1.82	$4.1378(10^{-4})$
	10^5	0.1400	1.24	$1.4144(10^{-3})$
	10^6	0.0215	1.20	$2.1422(10^{-3})$
	10^7	0.0040	1.20	$3.9856(10^{-3})$
	$3(10^8)$	0.0012	1.20	$3.5870(10^{-2})$
	$3(10^9)$	0.00029	1.20	$6.6688(10^{-2})$
	$*10^{10}$	0.00042	1.26	4.2882
Hard Packed Snow (-6°C)	10^5	1.5300	1.90	$1.6130(10^{-2})$
	10^6	0.2900	1.55	$3.2503(10^{-2})$
	$3(10^9)$	0.0009	1.50	$3.0078(10^{-1})$
	10^5	0.8000	4.80	$1.4927(10^{-2})$
	10^6	0.1200	4.15	$2.2193(10^{-2})$
Ice (-12°C)	10^8	0.0180	3.70	$3.1493(10^{-1})$
	$3(10^9)$	0.0009	3.20	$4.3932(10^{-1})$
	10^{10}	0.0007	3.17	1.1336

*At -6°C.

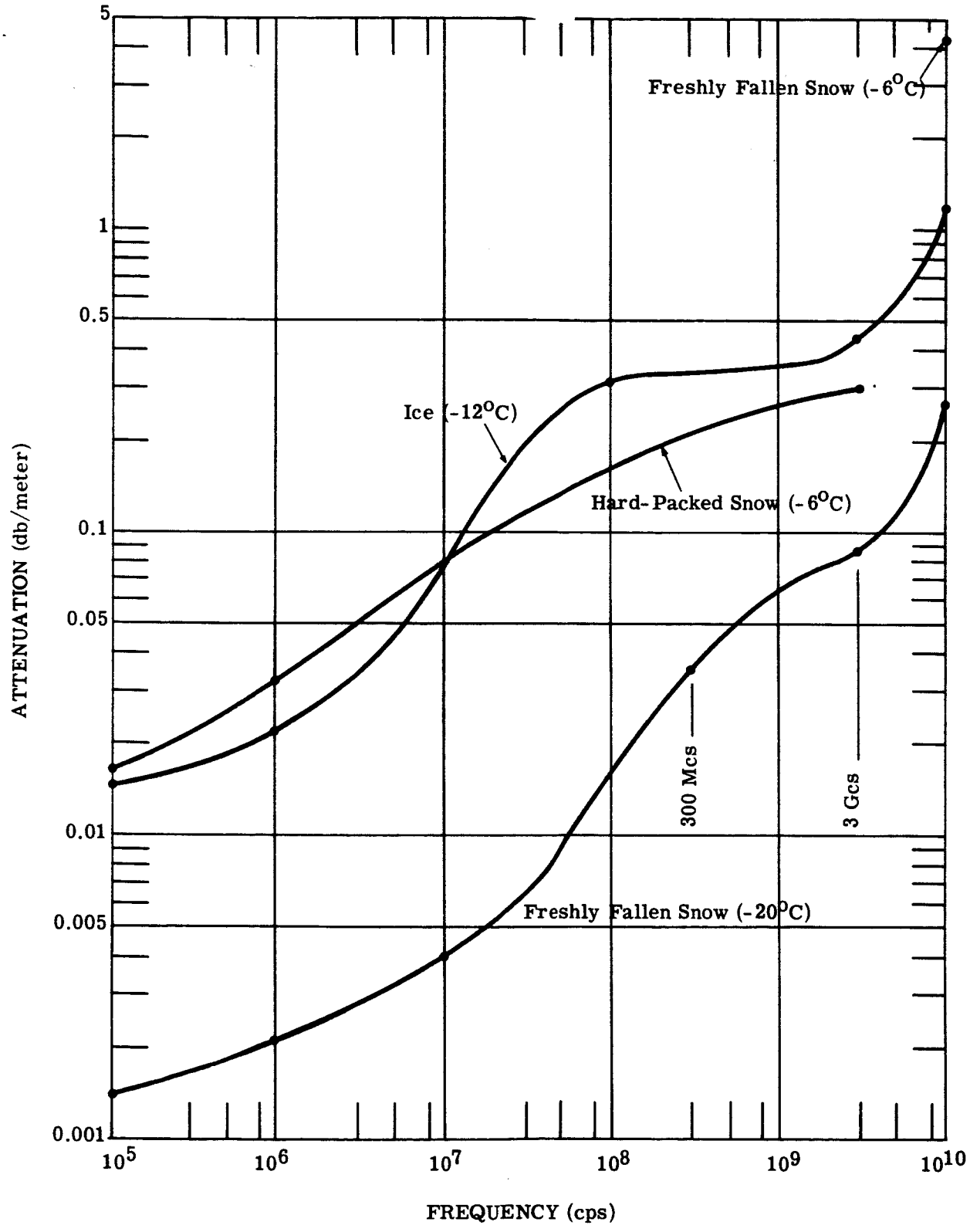

FIGURE 15. ATTENUATION OF ELECTROMAGNETIC WAVES BY ICE AND SNOW vs. FREQUENCY

r is the range in meters

K is Boltzman constant and equals $1.38(10^{-23})$ joules$^{o}C^{-1}$ cps^{-1}

T_o is the temperature and equals 290^{o}Kelvin

Δf is the bandwidth in cps

NF is the receiver preamplifier noise figure numerical ratio

Equation 1 can be used to determine the signal-to-noise ratio for a radar wave totally reflected from a flat surface. In the case of measuring snow depth, Equation 1 must be modified to measure the transmittance of the snow as follows:

$$\frac{S}{N} = \frac{P_t G_t A_r T_{A-S} \tau^2 \rho_{S-R} T_{S-A}}{4\pi^2 r^4 KT\Delta f(NF - 1)} \qquad (2)$$

where T_{A-S} is the transmittance of air to snow boundary and equal to 0.9 (Ref. 21)

τ is the transmittance of the total snow depth (one way)

ρ_{S-R} is the reflectance of the rock to snow boundary and equals 0.434 (Ref. 20)

T_{S-A} is the transmittance of the snow to air boundary and equals T_{A-S}

$P_t = 5(10^6)$ watts

$G_t = 4.09\ (10^6)$ for 50 percent antenna efficiency

$A_r = 400$ sq meters

S/N = 10 (assumed)

$r = 3.7\ (10^5)$ meters (200 n miles satellite altitude)

$\Delta f = 10^8$ cps for a 10 n sec pulse

NF = 2 for cooled parametric amplifier

Substituting these values in equation 2 gives $\tau = 10.3 = 11.07$ db

The transmission depth is

$$\alpha d = 11.07 \text{ db}$$

where d is depth in meters

α is the attenuation constant in db/m (snow at -20^{o}C α equals 0.25 db/m at 10 Gcs) (Fig. 15)

Thus the maximum snow depth measuring capability is 44.2 meters with this radar. But where ice (-12^{o}C) has an α of 1.1336 db/m, the maximum ice depth measuring capacity is 9.68 by this 10 Gcs radar system. Water snow (hard packed at 6^{o}C) has an α of 4.2882 db/m and the maximum measuring depth capacity of this 10 Gcs radar system is 2.58 meters.

The pulse resolution accuracy by received wave form spreading is 1 n sec or 0.3 meters using high precision dual beam oscilloscope indicator. The geometric resolution of a 20 meter antenna at 10 Gcs is about 0.15 meters as shown on Figure 16. The diameter of the resolution patch from a 200 n mile satellite is 531 meters.

It can be concluded that with large antennas freshly fallen snow depth can be measured but ice and packed snow had very limited depth measuring capabilities by radar. Radar antennas of 20 meters in diameter are practical according to radio astronomers (Ref. 24). Radar could be used to measure snow depth for flat terrain on the order of the large resolution patch diameter of over 500 meters.

3.2.7. AREA MEASUREMENT OF OPEN WATER ON LAND. The mapping of streams, rivers, lakes, etc., appears to be an application for ORL experimentation on the basis that there is a seasonal variation in open water area and that in underdeveloped areas of the world, a detail geography of the stream, rivers, etc., may not exist.

The detection of these areas may be accomplished in each of several ways. The ORL experiments would be performed with the goal of assessing which method proved to be the most feasible technically, economically and accurately.

The first method is the use of infrared photography taking advantage of the 0.7 to 0.9μ band with its high absorption characteristic for water and maximum reflectance of vegetation. The darkest areas on a print would be classed as water surfaces. Resolution would be the best of the three methods and scale would depend on which camera system is used.

The second method is the use of a thermal mapper operated at night when significant thermal differences exist because of the heat capacity differences between land and water. The water areas will be the brightest tone on a print. Resolution would be about 200 ft for the first experiment.

The third method is the use of microwave or radar systems. In all probability, the only useful microwave sensor for area water table measurement would be the coherent radar since good resolution would be required for evaluation purposes, particularly for small rivers and lakes. All of the microwave sensors can readily distinguish between water and land areas but there remains the question of resolution required. The presence of small streams can usually be detected by radar by observing the foliage surrounding the streams. The foliage exhibits different cross section characteristics than the foliage tens of feet from the stream. Thus indirect measurements may be possible. Assessment of these properties would be necessary in the experiment calibration program.

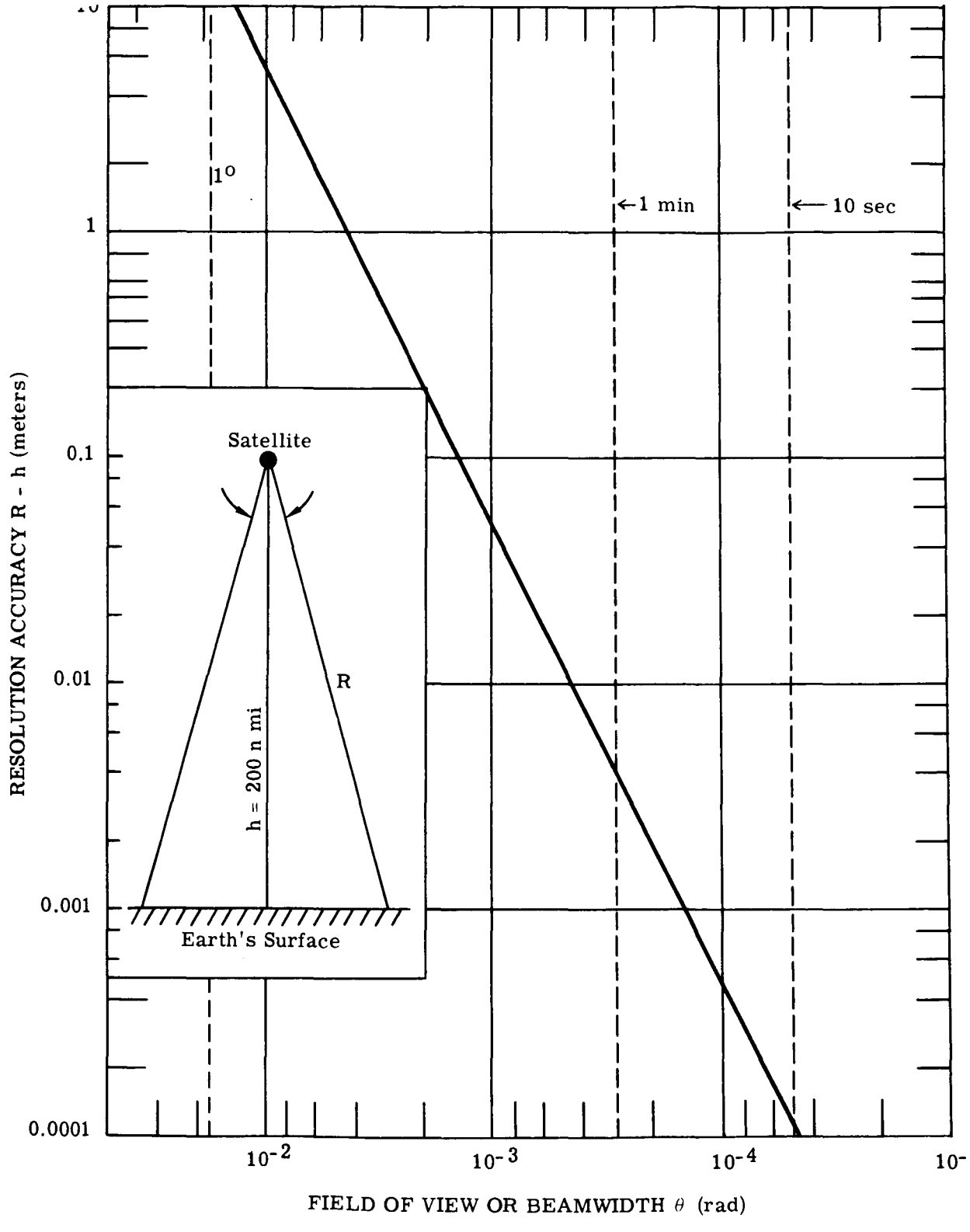

FIGURE 16. GEOMETRICAL RESOLUTION ACCURACY vs. FIELD OF VIEW FROM A 200-n mi SATELLITE

3.2.8. AREA MEASUREMENT OF DAMAGE. Since damage assessment of floods, earthquakes, etc., is not frequently required, no long range specific experiment can be planned other than the specification that high resolution photography would be most preferred and that a comparison be made of the "before" and "after" condition. This may not always be possible unless reasonably up-to-date photography is available for those areas most susceptible to earthquake, flood and storm damage. Preliminary comparative experiments should be conducted at altitudes such as 1000 ft, 20,000 ft, and 100,000 ft to assess the loss of information about damaged areas as a function of altitude.

As in Section 3.2.7 the only sensor which may have adequate resolution for all weather damage assessment would be the coherent radar system. Here the assessment would again be made by comparing the before and after maps. In the case of flooding, the extent of water coverage could be readily detected and the presence or absence of particular features of a map would provide one with an indirect measurement.

Radar would be most useful only when the use of IR and visible reconnaissance techniques are not possible due to adverse cloud cover and/or weather conditions. Both the IR and visible photographic techniques have better resolution capabilities.

The recommendation of using coherent radar for damage assessment is made only because other uses of this radar are anticipated. If this were its only use then damage assessment could be made from high or low altitude aircraft having the same coverage and resolution capabilities at much lower expense.

3.3. OCEANOGRAPHY

3.3.1. SEA SURFACE TEMPERATURE MEASUREMENTS. At the present time, sea surface temperature measurements are made by surface vessels and by anchored or drifting weather/oceanographic buoys. All of these techniques present technical and financial limitations which make high-resolution, daily measurements impractical.

When one considers the total surface area of the ocean in relationship to its mean depth, surface measurements become highly significant. In particular, studies of currents, ice fields, and coastal geography can be made quite easily with infrared reconnaissance mapping equipment.

For a 200 n mi earth orbit, each consecutive orbit crosses the equator at a distance of about 1400 n mi from the preceding crossing. With a 28^{o} total field of view, complete coverage of the earth's surface(with 20% overlap) would be obtained daily with 18 satellites. With a 2.3^{o}

T.F.V.. the scanner would require "pointing," and total coverage of the earth's surface would be obtained in 10 days (assuming weather and cloud cover conditions to be favorable) with 18 satellites.

In all cases, it is expected that temperature difference sensitivities on the order of $\pm 0.1^{\circ}K$ will be achieved. The atmospheric effects on this figure have not been assessed, and a certain amount of caution is urged when one seeks to assess how well the temperature can be measured. Certainly, atmospheric disturbances, emissivity fluctuations, sea-state, etc., will produce effects which will influence the radiometric measurements. Therefore, proper choice of wavelength (Ref. 25) and experiments on atmospheric transmission in conjunction with ground-based measurements will assist in assessment of the data.

The 2.3° FOV scanner will have a ground resolution of 200 feet. This should make it useful in observations of sea ice, small upwellings, and coastal geography. It may prove desirable to construct this device such that the astronaut-scientist can point it at regions of interest.

The 28° FOV scanner will have a ground resolution of 3600 ft or 1 km. This should make it useful in observations of sea surface temperature, ocean currents, and large ice fields.

Phenomena which require resolutions finer than 200 ft cannot be measured in detail with the infrared devices which are proposed herein, although it should be possible to measure averaged effects over areas comparable to resolution-element dimensions. For instance, a very small iceberg ($-20^{\circ}F$) which fills 1% of the field-of-view (the rest being filled with $32^{\circ}F$ water) will cause a depression in signal level equal to a Δt of $0.3^{\circ}K$ (which should be observable with a $0.1^{\circ}K$ sensitivity). In fact, if the temperature of the ice is known and a Δt is measured, it should be possible to relate the signal output to the percentage of ice in the region under observation (within a certain confidence level).

The data could be presented on 9" × 9" photographs with a spot-size of 1 mm, at scales of 1:62,500* and 1:1,000,000 (high and low-resolution imagery, respectively). Although this is fairly coarse, it should prove practical for some of the desired observations. However, as indicated earlier, a smaller scale data format on 70 mm would not appear objectionable at normal viewing distances.

Experiments should be conducted to measure absolute apparent temperatures from orbit at the same time that surface vessels measure both bucket temperatures and radiometric

*Figure 17 . shows an aerial photograph of an airport at a scale of 1:29,060 and with a spot-size of 1 mm (square aperture). Aperture-shaping could enhance the appearance of the imagery considerably.

FIGURE 17. AERIAL PHOTOGRAPH OF AIRPORT AT SCALE OF 1:20000
WITH 1-mm SPOT SIZE

temperatures. Every attempt should be made to determine the necessary correction factor to convert apparent temperatures to so-called "contact" temperatures if oceanographers require these values for studies of energy exchanges and air-sea interactions. This is one of the areas in which measurements may be made by sensors housed in a system of buoys and later temperature readings are transmitted to the satellite. This may be the only acceptable method of providing synoptic readings of ocean temperatures.

Microwave radiometers may have potential for making sea temperature measurements. Radiometers measure the total effective temperature which originates from several sources. Over the surface of the sea these sources include the atmospheric absorption, emissivity of the sea, sea temperature, and the sky noise reflected from the surface, all of which contribute to the effective measured temperature. Temperature sensitivities of 0.1 to 1^{o} can readily be obtained for these devices (see Appendix C); thus, it remains necessary to measure the variables and subtract them from the measured temperature.

In Section 3.3.3 a scheme for measuring sea state has been suggested and if it proves feasible then one of the largest variables can be measured, namely, the change in emissivity which has resulted from varying sea states. Depending on the accuracy with which the sea state can be measured, one can thus correct the temperature and improve the accuracy of the sea temperature readings.

It is recognized that a great deal of experimentation must be performed prior to evaluating this technique, and therefore this is a second order experiment in terms of importance, particularly since fairly accurate IR measurements are probable.

3.3.2. MARINE BIOLOGY

3.3.2.1. Photography and Multi-Spectral Sensors. The primary instruments to be used to conduct feasibility experiments for the detection of chlorophyll, plankton, fish, etc., on or near the surface of oceans will be the multispectral sensors. The spectrometer and multi-lens photography will be used initially and later optical-mechanical scanners with real time processing for mapping a particular distribution to establish the character and statistical reliability of a spectral signature for the plankton, chlorophyll, etc. A multi-lens camera with 25 ft ground resolution is already under study by NASA planners and could be used for the application from an ORL. Pre-orbital experiments conducted with multispectral cameras in areas known to contain concentrations of the plankton, clupeoid fish and chlorophyll would be necessary to study the effects of sun angle, sea state, weather conditions, and areal extent of the phenomena. Color photography will also be used and may be considered a relatively simple compact version of

multispectral photography in which data processing has already been performed and the image presents a color coded profile of light reflected from the ocean. The chlorophyll absorption band in the red is precisely where one of the color dyes response peak occurs. Sunlight reflected from a chlorophyll surface will be filtered in this red band at about .68μ and the color image will be affected accordingly. In addition, a potential means of detecting living organisms is by detecting the presence of trace elements of iodine, etc. as suggested by Barringer (Ref. 30). The method should receive further study and experimentation.

3.3.2.2. Radar. The experiments which can be envisioned for an ORL type of system in connection with marine biology are at this time thought to be marginal. This is due in part to the lack of evidence to support the likelihood of success of such experiments and the need for preliminary experimentation to determine the practicality of such experiments. This is not to say that information which might be obtainable by an ORL, would not be useful to the fishing industry. Certainly sea-state, sea chlorophyll concentrations, sea-climatical conditions, and sea-temperature condition which are thought to be monitorable from an ORL would be invaluable, when used in conjunction with fish behavioral patterns, to predict likely fishing areas.

It has been noted by some observers that some surface fishes exhibit visible scintillation. The likelihood of observing this phenomena with a sensor from an ORL is low; however, it should not be discounted until checked. Of course, it is obvious that a visible sensor would have only clear weather capabilities (no cloud cover). The resolution capabilities of such systems would also require that the school of surface fish be large. It has been suggested that it may be possible to detect schools of surface fish using active radar systems; however, the likelihood of success of such a system is marginal since active radar systems can observe only surface phenomena over water (microwave penetration of only a few millimeters being possible). Therefore, only those fish on the surface (provided they have sufficient radar cross section) or the surface disturbance associated with the fish would be observable and only then if the surface disturbance was distinguishable. Aircraft or other preliminary experimentation should be undertaken to prove the feasibility and practicality of such a scheme.

The area of fisheries applications for which the ORL shows the most promise is the monitoring of the fishing fleet movement; here again, preliminary investigations are required to determine the feasibility of such a program. Since the size of sea going fishing vessels of primary concern is on the order of 40 feet or greater, only high resolution photography and synthetic aperture radar have the resolution (theoretical) capabilities to do the job from an ORL.

To determine specific power requirements, radar cross sections typical of such vessels would have to be evaluated, possibly from an aircraft platform.

3.3.3. WAVES AND SEA STATE*

3.3.3.1. General. The techniques presently used for measuring sea state are inadequate for obtaining measurements over extended areas. These techniques include the use of accelerometers, pressure sensors suspended in quiet waters below the sea surface, and other similar devices (Ref. 26).

Several spectral regions have been considered for making sea state measurements and th most promising appears to be the microwave spectrum. Techniques for measuring sea state have been suggested and discussed by others (Ref. 27 and 28) but have not been implemented. A survey of the literature indicates that measurements have been made which partia ly support some of the techniques. The measurement in the microwave spectrum of active, passiv and bistatic scattering coefficients from various terrain types and from water surfaces establish the feasibility of these techniques.

Microwave techniques are of particular interest because a system operating in this area of the spectrum would have essentially an all weather capability as compared to IR or visible sensors.

3.3.3.2. Passive. Microwave radiation to be detected originates from several sources, namely, the self-emission of water, sky reflections, and multiple reflections from other nearby objects. In the case of sea state measurements, the self-emission and sky noise reflections constitute the radiation available which determines the apparent temperature to be measured.

It has been observed by many researches that the apparent temperature of the sea varies considerably depending on the wind conditions, angles of look, global location, and the polarization at which the information is obtained. By careful measurements and the proper interpretation of the data obtained one should be able to measure sea state remotely.

Two methods have been suggested for possible passive microwave sea state measurement. They are dependent upon the polarization effects observable from water and upon the water vapor absorption/emissivity characteristics (Ref. 28). It is suggested here that the polarization technique appears to hold the greatest promise.

*Much of this material was previously evaluated for another program and is presented with only **minor** modifications. (See Ref. 29).

The effects of polarization can be shown by first looking at the emissivity of smooth calm water as a function of incidence angle with polarization as a parameter (see Fig. 18). At or near the Brewster angle, a maximum temperature difference occurs. As the sea approaches a rough state, then it becomes a diffused emitter/reflector and the polarization difference becomes negligible as is shown at 90^{o} incidence.

The apparent sky temperature increases as the look angle approaches the horizon resulting in an apparent temperature variation as shown in Figure 19.

The final apparent temperature measured then is a combination of both sky reflections and water emission characteristics. The variations in apparent temperature between orthogonal polarization therefore appear to be as great as 30-50^{o}K at particular incidence angles.

We must consider the effects of wavelength upon these temperature differentials. As was shown above the polarization differentials approach zero as the sea becomes rough, and the absolute radiometric temperature approaches the ambient conditions. It should be obvious that the sea is rough only on the basis of the wavelengths by which comparisons are being made. It can be seen then that at short wavelengths saturation occurs and polarization discrimination is lost as sea state values increase. Longer wavelengths saturate at higher values of sea state. Thus a dependence of measurement on wavelength has been established. Therefore it is necessary to make measurements at three wavelengths to produce what may be considered the optimum in sea state measurement. The choice of wavelength to be used was made by considering other additional parameters (see section on wavelength selection) as well, and thus 3 cm, 10 cm, and 8 mm were chosen.

Absolute measurements of orthogonal polarizations will be taken simultaneously and will give pertinent information within a given test site where measured data will be related to that obtained from the radiometers. However, the absolute data will be of little value when measuring over large areas, as absolute sea temperatures are known to vary by as much as 30^{o}K. Variances of this magnitude could easily be mistaken for sea state changes.

The advantage to the differential measurements are therefore now quite clear as these changes will affect the differential measurements only to a very small extent.

Other researchers making bistatic and reflection measurements have found considerable variations in sea cross sections depending on the direction in which they were measuring with respect to the wind (Ref. 31, 32, and 33). When looking downwind the cross section was greater than upwind by factors exceeding 5 db. Cross wind measurements differed by smaller amounts but were readily detectable. It has been shown by researchers at Ohio State University

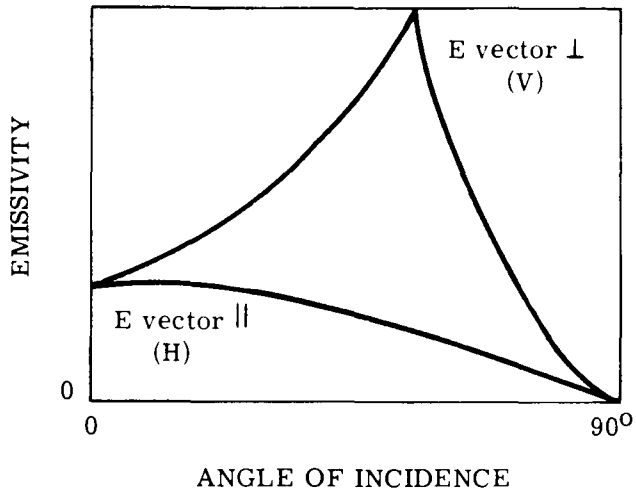

FIGURE 18. EMISSIVITY OF WATER vs. ANGLE OF INCIDENCE AND POLARIZATION (Ref. 29)

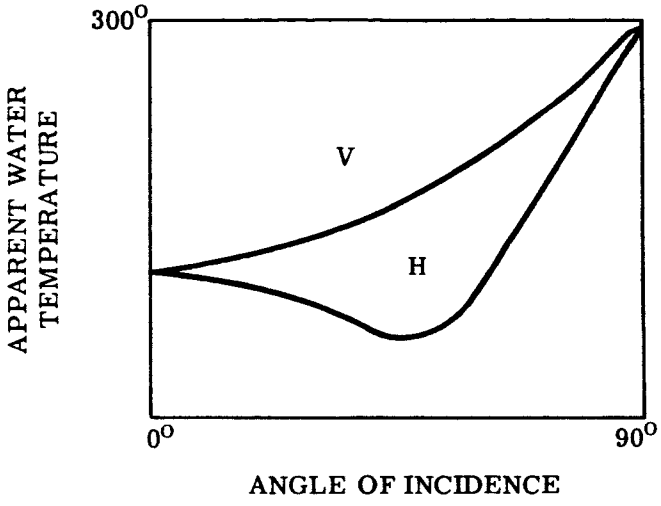

FIGURE 19. APPARENT WATER TEMPERATURE vs. ANGLE OF INCIDENCE AND POLARIZATION (Ref. 29)

Antenna Laboratories in terrain measurements (Ref. 34, 35), that there is a direct correlation between bistatic and passive measurements. It is not expected that this would differ greatly in measurements over the sea. Thus, it is expected that errors in measurements of sea state will exist depending upon the wind direction. It, therefore, is considered necessary to measure wind direction and determine the dependence of sea state measurements on wind directions.

Resolution Determination

It has been noted on very special occasions that sea state has varied significantly within a 1/4 mile path. It would be desirable to resolve an area 1/4 mile across, and therefore, this was considered when the preliminary resolution criterion was established.

Wavelength Selection

The wavelengths at which maximum information can be obtained are defined by several parameters. They include antenna size requirements, system sensitivity required, current receiver and antenna state of the art and all weather operation.

Loss measurements as a function of weather conditions and wavelength to 35 Gc are shown in Figure 20 from a 12 mile altitude above which little loss would exist. The maximum losses indicated are 8 db in the worst condition cited.

From Figure 37 (Appendix C) it can be seen that at 40 Kmc losses increase and good low noise receivers are not available. Also in this region tropospheric scattering is beginning to be a problem. Therefore, 40 Kmc is considered an upper limit on radiometer frequencies to be considered.

At the longer wavelengths galactic noise increases rapidly. Therefore, the best frequency range is in the decimeter to 8 mm region. Since it is desirable to avoid the water band at 22 Kmc, the wavelengths chosen are at 10 cm, 3 cm and 8 mm for which optimum performance can be obtained.

For the initial experiments aboard the ORL, it is not necessary to use a scanning radiometer. A simple profiling device should be adequate to establish the operational criteria necessary for future use.

3.3.3.3. Active Radar. Much of the incentive used to develop the passive technique described in Section 3.3.3.2 came from bistatic and active measurements which have been made. In the active case, the noise (i.e., signal in sea state) or clutter has been a problem for most radars used at sea. A review of the technical literature indicates that the clutter varies as a

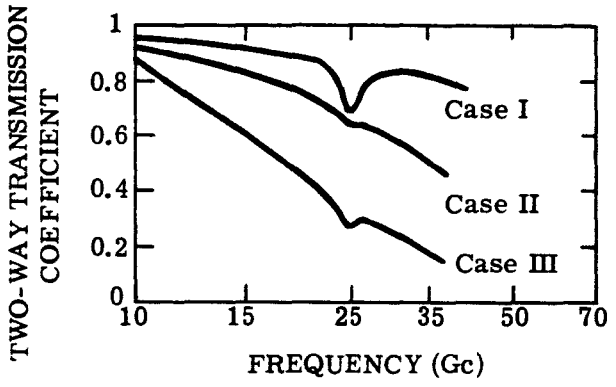

FIGURE 20. TWO-WAY ATMOSPHERIC TRANSMISSION COEFFICIENT vs. OPERATING FREQUENCY FOR A 12-mi ALTITUDE (Ref. 36). Case I: maritime tropical atmosphere containing water vapor but no clouds. Case II: heavy snow falling from a dense mixed water-ice cloud to an altitude of 5 mi. Case III: heavy snow turning to rain falling through a dense water cloud. Heavy weather extends to an altitude of 4 mi.

function of sea state, aspect angle, wind direction, polarization, and wavelength of operation. (The investigations were usually being made to find ways to reduce clutter.)

The literature search has revealed that many researchers have attempted to analytically describe the surface of the sea, from which the theoretical feasibility of the measurement could be established. Thus far, these efforts have not succeeded in modelling the sea. There is, however, sufficient evidence in the literature to allow some conclusion to be drawn and warrant a laboratory investigation.

The arguments for using active radars would thus be similar to those for use of the passive systems. From these general considerations, it is concluded that the use of radar for sea state is feasible.

The wavelength selection criteria would be similar to that of passive; however, a single operating frequency is recommended for initial ORL experiments, namely, an incoherent system operating in the S-band spectrum. This region is chosen as it has been observed that some saturation effects take place at the shorter wavelength at intermediate sea states. Also, the storm penetration capabilities would be near optimum at this wavelength. Additional measurements can be made with the X-band coherent and K_a band incoherent radars to establish their usefulness to limitations for sea state measurements. The use of the X-band coherent will help to further establish the minimum resolution requirements for sea state measurements from space.

Before any program for space applications is commenced, some simple airborne experimentation will be required to establish the feasibility of the measurements proposed. This is discussed in Section 3.1.

3.3.3.4. Determination of Waves and Sea State by Laser Altimeters. For beams not occluded by cloud cover, the pulsed laser altimeter can measure from a 200 n mile satellite wind wave heights from .6 meters to greater than 100 meters directly below the satellite and with a data rate as high as 10 cps (see App. Sec. E.3.5). The future FM-CW laser altimeter can determine and measure from a 200 n mile satellite wind wave heights from .7 millimeters to greater than 100 meters directly below the satellite and with a continuous data rate (see App. Sec. E.2.2 and E.2.4). Because of this continuous data profile, swells and tsunamis waves might be detected because high resolution of the area observed by the laser altimeter (17.9 meters in diameter). Also by observing the waves at an angle from the nadir direction, the direction in which the waves are moving might be determined. From the wind wave height profile data and wave direction, surface winds for oceans could be determined.

3.3.4. SEA ICE. There are several sensors which may be used from a satellite platform that can contribute to the knowledge and to the mapping of ice distribution in the North Atlantic, at the Poles, and elsewhere. Instrumentation recommended for use in the other application areas will serve the purpose readily. Experiments on ice distribution should be carried out with both high and low resolution photography, with the multispectral sensors, with low and high resolution infrared mappers, with the X-band passive microwave sensor as well as the high resolution synthetic aperture radar. The tests will determine the efficiency of each sensor for this application, and will indicate to what extent each sensor provides unique information.

3.3.5. COASTAL GEOGRAPHY. Color photography combined with infrared and conventional photography has proven of value in work of the U. S. Coast and Geodetic Survey (Ref. 37). The use of low and high altitude photography taken on regular flights along the coasts would appear to be satisfactory. Satellite studies of coastal phenomena would appear to be necessary only for coastal regions when normal aircraft facilities are unavailable, where knowledge of coastal phenomena are important for geography, geology and other scientific and engineering studies and where repeated coverage is desired. An experiment to test the feasibility of space sensing of coastal areas that provide information similar to what is presently available would be in order. Each of the three camera systems described earlier as well as the multispectral camera and scanner instrument would be operated over a test site and a comparison made of the information content degradation because of atmospheric attenuation and orbital environment.

3.3.6. ATMOSPHERIC CONSTITUENTS. The entire field of remote sensing of the earth's surface is dependent on the absorption characteristic of the earth's atmosphere. For observing the ground one selects the atmospheric windows. For observing the distribution of H_2O, CO_2, Ozone, and other atmospheric constituents, one naturally selects a wavelength interval characteristic for the constituent. Some of the characteristic wavelengths for H_2O, CO_2, and O_3 occur in the infrared, and by appropriate filtering infrared radiometers may be used to detect their distribution and amount.

In general however, suitable instrumentation needs to be developed and tested at suborbital altitudes to verify the feasibility of detection of a given constituent before ORL experiments are defined. Background radiation may interfere, the proper wavelengths need to be selected and special detection schemes need to be invented in some cases.

3.4. EXPERIMENTS FOR OTHER APPLICATION AREAS

Experiments described in the previous sections for agriculture and oceanography will have direct application to many other disciplines. Techniques of crop identification and area measurement, for example, can be adapted to the problems of forest inventory, and estimates of biomass. This section will not repeat the coverage of fundamental types of experiments already discussed, but will indicate some additional areas for experimentation in other subject areas.

3.4.1. GEOGRAPHY. In early experiments, coverage of test sites and other special areas of interest should be obtained with the various types of sensors and for different conditions of time of day, season, cloud cover, local weather, etc. This imagery can be studied to select the best conditions for cartographic and other purposes. In order to expedite the process of experiment and evaluation, much of the preliminary interpretation of developed film should be performed aboard the ORL to guide the planning of individual steps in the experimental program.

Once optimum conditions for acquiring imagery are decided on, at least one set of pictures should be obtained of the entire land surface of the earth in the useful spectral ranges. Complete photographic coverage at a scale of 1:800,000 could be accomplished without excessive cost or effort. This preliminary coverage of the earth will supply the scientific community with useful data so that members of the various disciplines can make preliminary studies of the earth's surface which are of special interest to them and can select areas to be observed at increased scale during the ORL experiments.

Cartographers will use this first coverage to establish a data bank, learn how best to store, retrieve, and distribute the imagery, and how to apply it to the updating and improvement of existing maps. They will be particularly concerned with accurately identifying the region covered by individual photographs, relating the imagery to a geodetic control network on the ground, providing geometric rectification, and interpreting natural and cultural features.

In addition to the study of rural land use patterns, which is related to the agricultural experiments, geographers will study imagery of urban areas and transportation networks. They will want to establish the resolution and other viewing conditions necessary for reliable detection and identification of items of interest to them. The use of regions of the spectrum other than than the visible should be thoroughly explored. Particular interest will center on the possibility of deriving indirect indications of levels of urban and industrial activity through measurement of man-induced energy. Archaeologists will have interests similar to geographers, and multispectral sensing capabilities may enable them to spot ancient settlements which could not be seen in the visible. It will be of particular interest to obtain some large-scale imagery of

remote and inaccessible regions in developing areas. For all of these purposes, it would be highly desirable for the ORL experimental team to perform direct reconnaissance of the earth and pick out likely areas of interest for remote sensing coverage.

3.4.1.1. Determination of the Earth's Profile by Laser Altimeters. Elevation data useful for topographic mapping could be obtained by laser altimeters. The height variations along a continuous strip 17.9 meters in width can be determined to an accuracy of centimeters by the future FW-CW laser altimeter (see App. Sec. E.2.2 and E.2.4). To get these high resolution strips from a 200 n mile satellite of the total earth's surface will require a polar orbit. If the probability of cloud cover is 40-60 percent for the earth's total surface, the number of orbits required to profile the earth would be $1.425(10^{13})$, but this figure could be decreased to practical limits by sampling procedures.

As indicated in Appendix Section E.1.4, the reflectance of natural land objects is higher than for ocean water. Thus the FM-CW laser altimeter will require less source power than was calculated in Section E.2.3.5.

3.4.2. FORESTRY. The forest inventory application requires two distinct processes, forest mapping and determination of tree size. The mapping of forest areas, involving both area measurement and species identification, is similar to the processes of crop identification and measurement of farm areas; hence, the proposed experiments are extensions of those suggested for agricultural applications. However, because of nonuniform forest stands and the relatively small size of individual trees, a higher resolution capability is expected to be required. Experiments to determine the effectiveness of measuring tree size will use high resolution photography of forest test sites. Tree size will be estimated from measurements of average crown diameter and checked against ground truth.

To establish the feasibility of forest fire detection techniques, a series of experiments is suggested. A simple but highly useful beginning would be for the ORL experimenters to make direct observations by telescope of areas in which forest fires are burning, in order to find out how much can be seen visually from orbital altitude and how accurately position can be determined. These observations should be checked against ground truth data on location, size, and character of the fire. Additional experiments should be conducted with radiometric equipment trained on a test site area where a simulated fire has been prepared or on actual forest fires with known characteristics, as reported from the ground. Assuming favorable results on detection capability are obtained, tests with infrared scanners and possibly passive microwave

equipment would be conducted to check the capabilities of automatic methods of fire detection, discrimination and position location.

The development of measurement methods for energy balance in forested areas will require experiments with multispectral data collected in the ultraviolet, visible and infrared regions with ground resolutions ranging from 200-400 ft up to 1000 ft, depending on the purpose of the measurement. Within the infrared region, a temperature sensitivity of $1^{o}K$ or less will probably be required. Basic data are required on total insolation, energy reradiated from the earth, surface temperatures, and vegetative characteristics of the area scanned. Experiments leading to definition of vegetative characteristics have already been discussed. The other items can be obtained by measurements made over specific test sites with varying types of vegetative cover. These must be coordinated with ground-based and airborne tests made simultaneously with the orbital passage.

3.4.3. WATER RESOURCES. Much of the value of orbital sensing for water resources applications depends on the development of techniques for measuring the quantity and distribution of water in various forms, including snow, ice, and soil moisture, and the corresponding temperatures. Thus, the initial emphasis of the experimental program must be on perfecting the equipment and measurement techniques needed for accurate determination of these quantities. Hydrologic studies also depend to an important extent on the characteristics of vegetative cover; the ORL experiments related to this subject have already been discussed in previous sections.

Experiments should be conducted to determine the accuracy and resolution with which measurements can be made of snow depth, equivalent water content of the snow, areal cover of snow, and its spectral reflectance characteristics. Development of measurement techniques for river and lake ice and surface temperatures of rivers and lakes should benefit from similar experimentation as discussed under oceanography. The problem is somewhat different, however, primarily because the smaller extent of the lake and river surfaces will demand better resolution. Delineation of flooded areas by radar sensors will require experiments to determine the resolution required to give usable definition of areas covered by water, and the swath width to which effective coverage can be extended.

Radar and visible photography should be used to obtain imagery for the study of basin geomorphology and to develop methods of using quantitative geomorphic data for hydrologic studies. As a means of developing correlation methods initial studies should be devoted to a river basin whose characteristics are already well known.

Once the techniques for measuring individual physical quantities have been developed, attempts should be made to use them for estimating total snow volume, equivalent water content, and rate of snowmelt for sizable areas. The accuracy of the data estimated from orbital measurements can be checked against ground measurements. Also, some concept can be gained of the operational problems of providing the necessary information for a given area on a short time scale.

3.4.4. WILDLIFE AND FISHERIES RESOURCES. High resolution photography and multispectral sensing should be obtained for selected areas used as wildlife refuges and waterfowl breeding and wintering grounds for study by specialists in wildlife management. The assessment of wildlife habitats with respect to water and vegetative cover will rely on techniques already discussed for agriculture and hydrology. The small size of lakes and ponds and other features which must be observed may exceed available limits of resolution of multispectral sensing devices; hence, this factor will require special investigation.

Detection of large flocks of waterfowl or herds of caribou could first be accomplished by visual observation, with direction from the ground. At a later stage, infrared equipment might be used for detecting sizable groups of wildlife on the basis of thermal discrimination. During the initial tests, the sensor would be trained manually on the known position of the group of animals, the main objective of the tests being to determine the thermal sensitivity required for detection.

3.4.5. GEOLOGY. There is much preliminary work to be done in the laboratory and in the field before ORL experiments are conducted. Laboratory research should include use of all sensing devices on representative samples of rocks and minerals in an attempt to establish their spectral characteristics. The effects of vegetative cover over certain rock types should also be studied in detail.

Field investigations would then be conducted. These field studies would be concentrated in several large areas of the earth's crust whose geology has been mapped in detail. These studies would be used to confirm any parameters established in the laboratory.

A number of field areas are suggested below for both preorbital and ORL investigation:

(1) Porphyry Coppers and Molybdenite deposits—of the Western United States. These are arid areas with little vegetative cover.

(2) Comstock Lode—Thermal (ΔT) contrasts due to hot mine waters issuing out of the mine.

(3) Gossan zones — Coppermine River area, and the Giant Quartz Veins, in the Northwest Territories, and the huge sedimentary iron deposits formed by selective leaching of silica during weathering processes in the Labrador Trough.

(4) Rocky Mtn. Front Range and Texas-Louisiana Gulf Coast — to detect faults, folds, and hydrocarbon haloes (vegetation affected due to escaping gases with trace elements, and their distribution along faults). These are areas of contrasting geologic settings. Complex folding and thrust faults due to compressive stresses in the Rocky Mountains and gravity faults due to tension stresses along the Gulf Coast.

(5) Pacific Coast — an area of active earthquakes and an active geosynclinal basin. Continuing studies would be required to make any evaluations.

(6) Sudbury Basin — rock contrasts and sulphide zones associated with a large norite intrusive and the subsequent basin development due to regional collapse.

(7) Lac La Ronge and Beaverlodge, Saskatchewan, and Blind River, Ontario — Uranium rich areas to test gamma and x-ray sensors in addition to the other spectral ranges.

(8) Bushveld Igneous Complex — a huge differentiated igneous mass with bands of gabbro, norite, and granodiorite, and associated iron and titanium oxides, and sulphide deposits also in regional bands. Gravitational settling of constituents can be related to ionic radii and geochemical principles.

(9) Duluth-Gabbro — differentiated igneous mass — not as well developed as the Bushveld Complex, but has certain similarities.

(10) Mexico — areas of active volcanoes, silver rich mineral belts, and petroleum accumulations, has been probably poorly exploited since nationalization of that country's industry. A regional geologic survey of Mexico and the relationship of any economic deposits would be of great value to the Mexican Government.

The size of any geologic features could be grouped as follows:

(1) Regional (R). Readily detected from an ORL. These would be all features greater than one mile in size.

(2) Intermediate (I) features are less than one mile in size, and would be readily visible from an aircraft.

(3) Small (S) features would be less than one quarter mile in size and would be further subdivided with appropriate subscripts as follows:

1. S1 -- 500' wide × 1000' long
2. S2 -- 100-500' wide × 1000' long
3. S3 -- 40-100' wide × 500' long
4. S4 -- 10-40' wide × 250' long
5. S5 -- 10' wide × 50-100' long

3.4.6. AIR POLLUTION. Assuming that preliminary experiments establish that the ozone bands can be utilized for monitoring air pollution areas, the following program could be adopted for making specific observations on the earth's surface. Selected regions for testing would be established over known areas of air pollution. For example, let us pick the Los Angeles area as being one of these test sites. The ozone distribution over the Los Angeles basin would be determined at the time of a given satellite pass. However, because there are general variations in the lateral distribution of ozone the emission should be compared with a region somewhat near the test site. For example, the satellite might monitor an area over the Pacific Ocean a hundred miles west of the Los Angeles basin. The emission characteristics would then be compared over these two test sites. If this experiment is done in a period of high smog in Los Angeles there should be a significant increase in the 9.6 μ emission in the Los Angeles area as compared with the reference site over the ocean. Parameters which might influence pollution measurements should be examined in such an experiment; for example, some of these parameters are:

(a) Comparison of cloud layers vs. clear areas

(b) Diurnal variations in the transmission characteristics over pollution areas

(c) The lateral distribution of smog, that is, the area covered on a particular day

(d) Variations of the ozone content vs. the characteristics of the aerosol (k_C/k_W) ratio, or a ratio of two other spectral regions

The use of a nonpollution reference site preceding measurements over a given test region may provide a method of comparative measurements which is not restricted to cloudless areas. In general, clouds are somewhat transparent at the 9.6 μ region and providing both the reference and test areas are covered with a similar cloud pattern, measurements might still be continued. It would be expected, however, that the resolution would be somewhat reduced as compared with cloudless areas. The comparison of proximal sites also reduces the effect of localized variations in barometric pressure which could affect the transmission characteristics.

4
MAN'S FUNCTION IN EXPERIMENTAL PROGRAM

There can be no doubt that man has a role in the experimental program in orbit. His unique ability for reasoning, planning, observing, judging, analyzing, correcting, adjusting, etc., are precisely what is required for the types of feasibility demonstration envisioned in an ORL program. Specifically, each sensor type requires his general attention in addition to some specialized function characteristic of the particular sensor configuration.

4.1. PHOTOGRAPHIC SYSTEMS

The space experiment must prepare system for observation, select target, will have to load and reload film, record data, inspect rapid processed film and select data for telemetry. He may have to erase or discard data to reduce storage requirements or data rates. He may have to provide fine tracking of selected test sites. His role will evolve from operator of instruments during initial flight to maintenance and eventually to experimenter-manipulator of more sophisticated sensors.

4.2. MULTISPECTRAL SENSORS

Besides the routine performance of maintenance and alignment tasks, he will be required to select filters for a specific experiment and to set the parametric variables to process for a specific crop type or condition. Alternately, he will be required to monitor recording of a set of spectral channels and later to replay data with different settings of decision variables to determine optimum recognition probabilities.

4.3. INFRARED SENSORS

There are a number of tasks to be performed by a scientist-astronaut in the actual conduct and calibration of the experiments and maintenance of cooler and other critical subsystems. Section 6.4 discusses the extremely wide range of temperatures likely to be encountered along the ground path of a polar orbit. Some regions of this ground path have local variations of $50^{o}C$, while others are considerably less. For example, a task involving the mapping of polar ice fields would have different gain and calibration requirements than would the mapping of ocean currents, coastlines, or various types of vegetation. The temperature variation of the ocean surface may be only 2^{o} and the absolute temperature will change for each change of latitude. For 90 minute orbits the astronaut may be required to adjust level and gain settings every 2.5 minutes until he passes over land where temperature excursion will become variable over

many degrees centigrade. An automatic system would tend to give average data from portions of the track and degrade other portions.

4.4. PASSIVE MICROWAVE

Man's presence aboard the ORL allows the use of advanced sensor equipment and thus enhances system performance. Man's function in terms of a passive microwave sensing experiment would include the assembly, installation, and evaluation of the system antenna(s) once the space station was in orbit. (To obtain reasonable resolution capabilities, large antennas are required.) Calibrating the instrumentation once the microwave system is in its space environment, maintenace of the system detection equipment (which probably requires cooling), and on board data selection are important functions of man in space. The data selection is accomplished by monitoring incoming data and introducing selectivity into the data acquisition. Of course, the maintenance of the equipment should not be minimized because the ultimate success of the experimental program fails if the electronics that are involved fails.

4.5. RADAR

As was mentioned in the passive microwave case, man's primary function on board an ORL in connection with the radar equipment will probably be to reduce data storage requirements of the system. It has been estimated that the on-board operator could reduce the data rate requirements at least an order of magnitude (Ref. 19). Initially, the system antenna will have to be assembled in space. The system will then have to be maintained and calibrated. Probably a greater portion of the operator's time will be spent on these functions as compared to the passive microwave systems because the radar systems are inherently more complex.

The operator of the equipment would be responsible for:

1. Equipment turn-on and check for proper operation.
2. Checking the radar returns to be sure antenna pointing is correct, correcting if necessary.
3. Setting proper signal level for recording.
4. Operating recording equipment, reloading film as necessary.
5. Making sure film is properly developed if it is to be scanned for data link transmission.
6. Provide maintenance whenever possible.
7. Perform data processing for synthetic antenna radar on board if necessary.

As was mentioned in the passive case, man's presence will allow the use of advanced equipment for system improvement and component evaluation.

4.6. LASER ALTIMETERS

Man's function in the operation of laser altimeter require that:

(a) The equipment is turned on when data are desired over cloudless or partially clouded surface areas beneath the satellite

(b) The equipment is turned off when the earth's surface is occluded by large area cloud cover.

(c) The operator must set the yaw angle of the stabilized platform to coincide with ground track beneath the satellite. For a polar orbit this yaw angle is greatest at the equator $\left(\tan \theta_{yaw} = \frac{464}{7255}\right)$ and zero at the poles due to the satellite velocity of 7255 m/sec and equator velocity of 463.5 m/sec (also see Sections E.2.6 and E.3.5.4).

(d) The operator can adjust the fine pointing of the receiver aperture so as to view the irradiated area on the water and tune for maximum returned signal on the indicator CRT. As indicated in Section E.2.5.4 for a 200 n. mile satellite, the transmitter optical axis must lead the receiver optical axis by 10.57 second of arc. (For changing satellite altitude this lead angle will need changing.)

(e) The operator must record the height data with time marks so as to determine the point on the earth's surface where the profile data was determined.

(f) The height data must be determined manually by the operator for the pulsed laser altimeter. The comparison and estimation of the received stretched pulse waveform is compared to transmitted pulse waveform (see Appendix Section E.3.1).

(g) The operator must set the range gate adjustment containing the expanded sweep portion on the indicator for the pulsed laser altimeter.

(h) The height data can be taken either manually (reading a scope or meter) by the operato or automatically recorded with time marks.

(i) Recorded data need to be returned to earth by retrieving the data from an electronic storage device and telemetering the data to a ground station.

(j) The operator must monitor the laser altimeter systems (and adjust voltage when necessary) to make sure that laser altimeters are operating correctly and up to their maximum performance.

5
ENGINEERING AND SCIENTIFIC ADVANCES NEEDED

In the following sections, some of the important areas are discussed in which advances will be needed to make space reconnaissance feasible.

5.1. CONTRAST IMPROVEMENT

One of the factors limiting photography of the earth is the contrast reduction of objects because of atmospheric scattering and attenuation. The reduction in contrast is a function of wavelength so that, in general, sensing at longer wavelengths is recommended. However, some of the application areas where real time multispectral sensing techniques will be needed may have to use wavelengths affected by varying percentages of attenuation and scattering. These systems will not focus the energy directly on photographic emulsion but rather on semiconductor transducers to obtain an electrical analog signal directly thereby permitting electronic gain to provide a more acceptable contrast in the data display. Such systems should be built large enough to operate at sufficient S/N ratios.

5.2. POINTING ACCURACY FOR SELECTED TARGETS

While the use of star photography can be used to establish the location of a given photograph taken from orbit, the need for insuring beforehand that a predetermined point on the surface of the earth will be photographed or scanned will become commonplace especially with the use of high resolution sensors with only 2^{o} FOV. Horizon sensor accuracy in roll and pitch axis will have to be improved. Many application areas will require a capability to map a specified point: damage assessment of flooded areas, mapping thermal anomalies around volcanoes, detection of fires and knowledge of their location, mapping of test sites for calibration and check of sensor performance, etc. Man in the ORL experimental phase should be able to perform the necessary object selection and pointing direction. But before the sensory system becomes operational, automatic means of control from ground stations for accurate sensor look angles will have to be developed.

5.3. DATA PROCESSING AND ANALYSIS PROCEDURES

Suppose it were decided that synoptic coverage of the Continental United States is desirable and that the coverage is to be carried out in 1 week time. (For example, the Department of Agriculture wants to know the total area of wheat to be harvested).

To obtain data on area measurements with a 2 ft. resolution, 2^{o} FOV camera system, it will take 30 satellites, 1 week (see Section 3.6.3). Each satellite will have traversed the United States twice a day during daylight hours. Each traverse would be about 1500 miles apart for the 200 mile orbit. A total of 210 transects of data across the United States would be generated. The data would be taken at the same local sun time by proper choice of orbit and launch time which would be chosen to minimize cloud interference. However, it may be necessary to require multiple looks over each transect to guarantee clear coverage of the ground. Thus, 1260 transects may be necessary if a factor of 6 is assumed satisfactory to increase the probability of observing all the area free from clouds at one time or another. A cloud-free mosaic of the United States would then be made from selected portions of the data. For accurate area measurements, enlargements of a statistical sample of the high resolution photograph would be made. This sample would have been chosen after a correlation had been made with the data from a multispectral sensor providing crop identification. Timing signals and position information would have been required to match coordinates between the two sets of data.

After area measurements of sample points were conducted, appropriate conversion to total acreage would be made and results disseminated to proper local agencies.

It is abvious that a new era of data processing, analysis and handling will have arrived with the use of multiple satellite reconnaissance of the earth. If the full potential of the technique is to be derived, then the advances in techniques of analysis, in the development of data processing machinery, and in training of personnel will have to be made as soon as possible in relation to the development of the space sensors. Data generated during the ORL experiments should be the input to begin the development of this capability. New data about new phenomena will be generated as well as new data forms of more familiar events; both will have to be assimilated and diseminated.

5.4. IMPROVEMENT IN COMPONENT PERFORMANCE

5.4.1. OPTICAL SYSTEMS. There is a definite need for wide angle optical systems of large diameter and long focal length. Improvements of spectral transmission properties of materials will be required and upgrading of television reconnaissance systems in comparison to the theoretical limitation of films may be necessary. See Appendix A-1 and A-2 for discussion of current state-of-the-art for films and television reconnaissance capabilities.

5.4.2. INFRARED DETECTORS. The current state-of-the-art of infrared detectors indicates that they are not operating at their natural physical performance peak. For example, although Ge:Hg detectors are very close to being "background-noise-limited," there is yet much room for improvement.

For the initial experiments of the ORL, it is not deemed necessary that extensive improvements in detector size, sensitivity, or stability be made. However, one area of possible concern is that of extension of the shelf-life and useful operational life of the detectors. Otherwise, performance of the system will be limited by calibration complexities and possible loss of sensitivity.

5.4.3. COOLERS. Infrared coolers are a vital part of any high-resolution, high-sensitivity infrared sensing system. As shown in Figure 1, the detectivity and resistivity of a typical detector cell depend rather strongly upon the cell temperature. Appendix B-2 contains a calculation which indicates that the cooler must maintain a temperature stability up to 4 times better than the required temperature sensitivity of the system for cell temperatures less than $25^{o}K$.

Figure 21 shows the typical performance capability of state-of-the-art "sublimation" IR-coolers.

5.4.4. ROTATING PRISMS IN VACUUM. As indicated elsewhere, some of the rotating members of the infrared scanning systems will be subjected to a vacuum environment. This could entail some difficult design problems, especiallv with respect to bearings and seals. Much work has been done in this area (Ref. 39, 40, 41) but details will have to be worked out in order to meet the specific needs of this application. Non-lubricated designs should be investigated.

5.4.5. INFORMATION HANDLING RATES. Based on a $2.3^{o} \times 2.3^{o}$ field of coverage, a 1/6 mr resolution element, a 7 bit temperature resolution (see Section 6.5), and an estimated frame rate of 10 frames per second, the most stringent information handling capacity would be approximately 4×10^{6} bits per second for each spectral channel. The corresponding telemetry bandwidths would depend upon the type of modulation employed. For purposes of magnetic analog recording, the approximate bandwidth would be about 6×10^{5} cps. multielement-multispectral sensors will require improvement in tape recording capabilities in that there will be a need for more channels at wider bandwidths as resolution capability increases. Figure 22 shows the expected tape consumption per orbit for a given tape speed (frequency requirement)

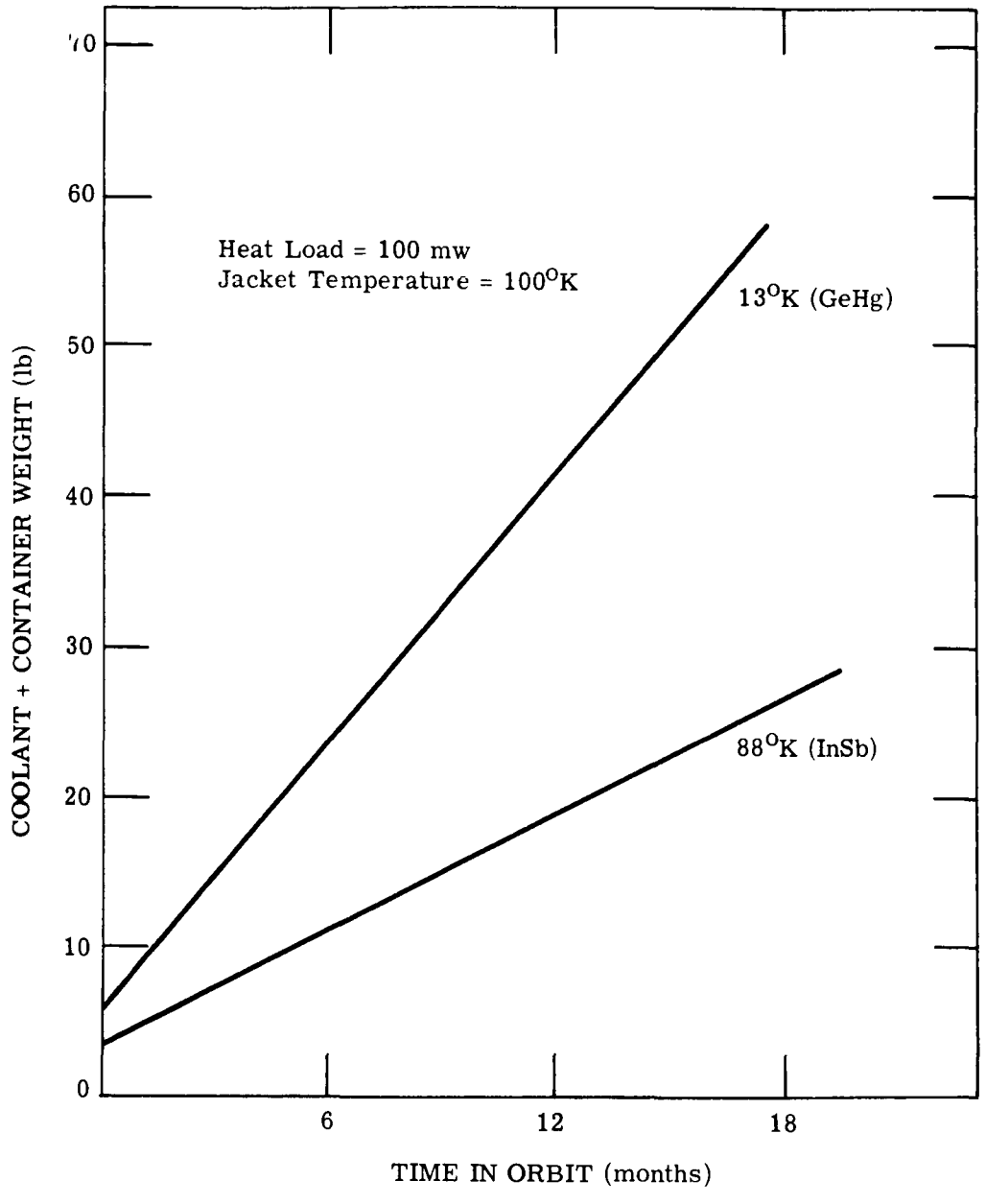

FIGURE 21. COOLANT + CONTAINER WEIGHT vs. TIME IN ORBIT.
Reproduced from Ref. 38.

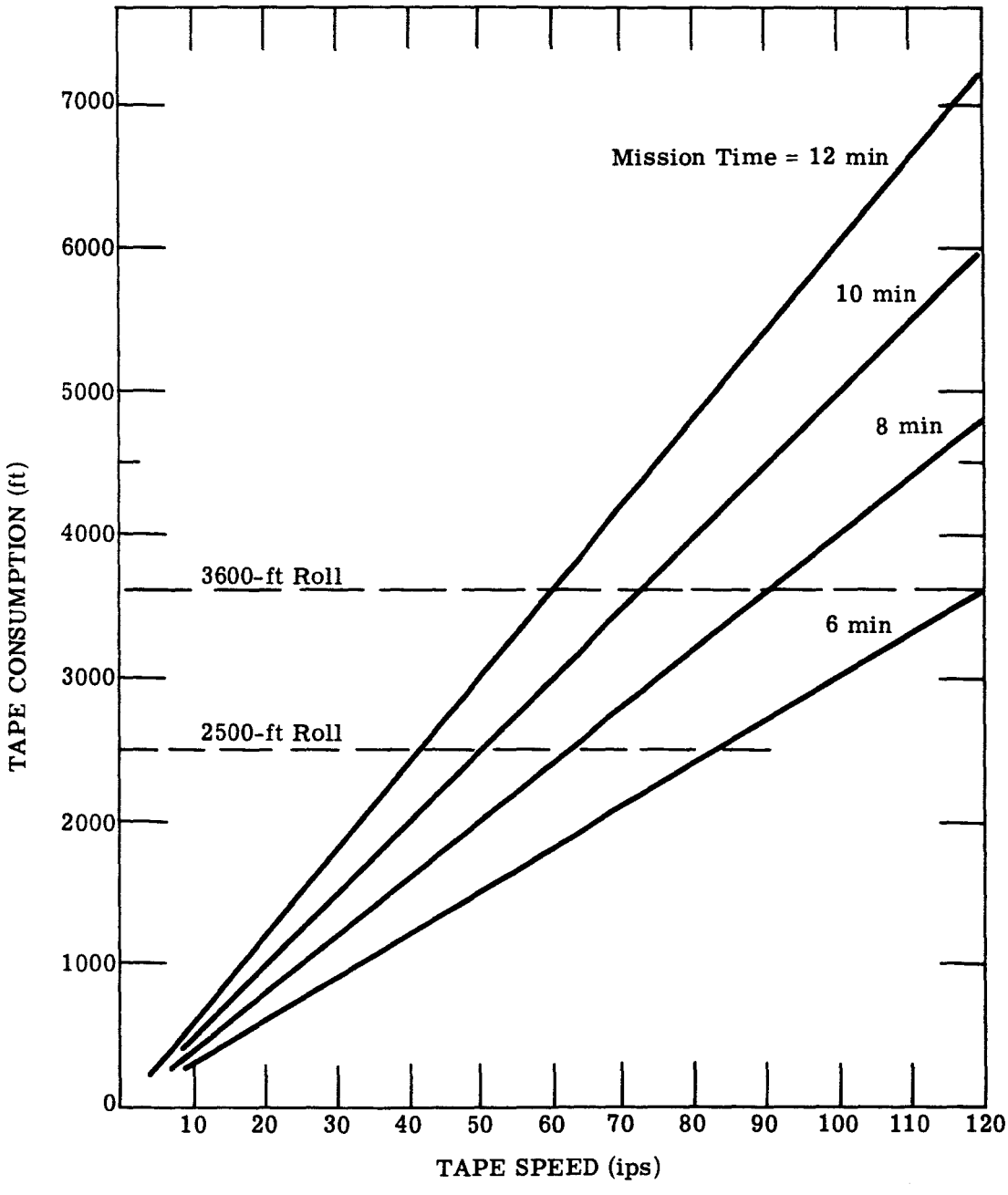

FIGURE 22. TAPE CONSUMPTION PER ORBIT vs. TAPE SPEED AND MISSION TIME

and length of experiment duration. If recording of multiple-channel data in operational systems proves necessary, then storage or resupply problems will become critical. A similar problem with film consumption is shown in Figure 23. Wide band telemetry links for future operational systems appears to be a prime requirement.

5.4.6. MICROWAVE. Advances in the state-of-the-art of some of the basic radar components (both active and passive) would aid in reducing the system requirements and improve their capabilities for application in an ORL program. The required improvements and their implications are discussed in the following sections.

5.4.6.1. Antenna Improvement and Development. The two most urgent needs for development of antennas to be used in an ORL program are: 1) the development of an unfurlable 50 foot antenna with the accuracy required of the various systems, which can be fabricated in space automatically or manually, and 2) the development and improvement of scanning techniques for the passive microwave system. These improvements would have direct bearing on the system capabilities in the space environment.

5.4.6.2. Development of Cooled Parametric Amplifiers for Short Wavelength Operation. The development of cooled parametric amplifiers for short wavelengths would aid in reducing the system power requirements for active system since it is expected that these systems would have lower receiver noise figure than systems currently in use, and would increase the temperature sensitivity of passive systems since greater bandwidth and lower noise figures would be obtainable. However, such amplifiers would require the use of some form of refrigeration. For space applications this would possibly mean the developments of some new techniques such as the use of solid refrigerants (nitrogen, etc.) or a radiation scheme employing the space environment.

5.4.6.3. Detectivity Improvement at Millimeter Wavelengths. Detectivity improvements and developments of some solid state materials which are sensitive in the millimeter wavelength region would make feasible the use of multiple-element passive scan devices for space application.

5.4.7. LASER ALTIMETERS. As it was discussed in Appendix E.2, the future (1970) FM-CW laser altimeter requires the development of a 30 db light amplifier between the optical system and photodetector. This light amplifier could be a neodymium $CaWO_4$ solid-state laser

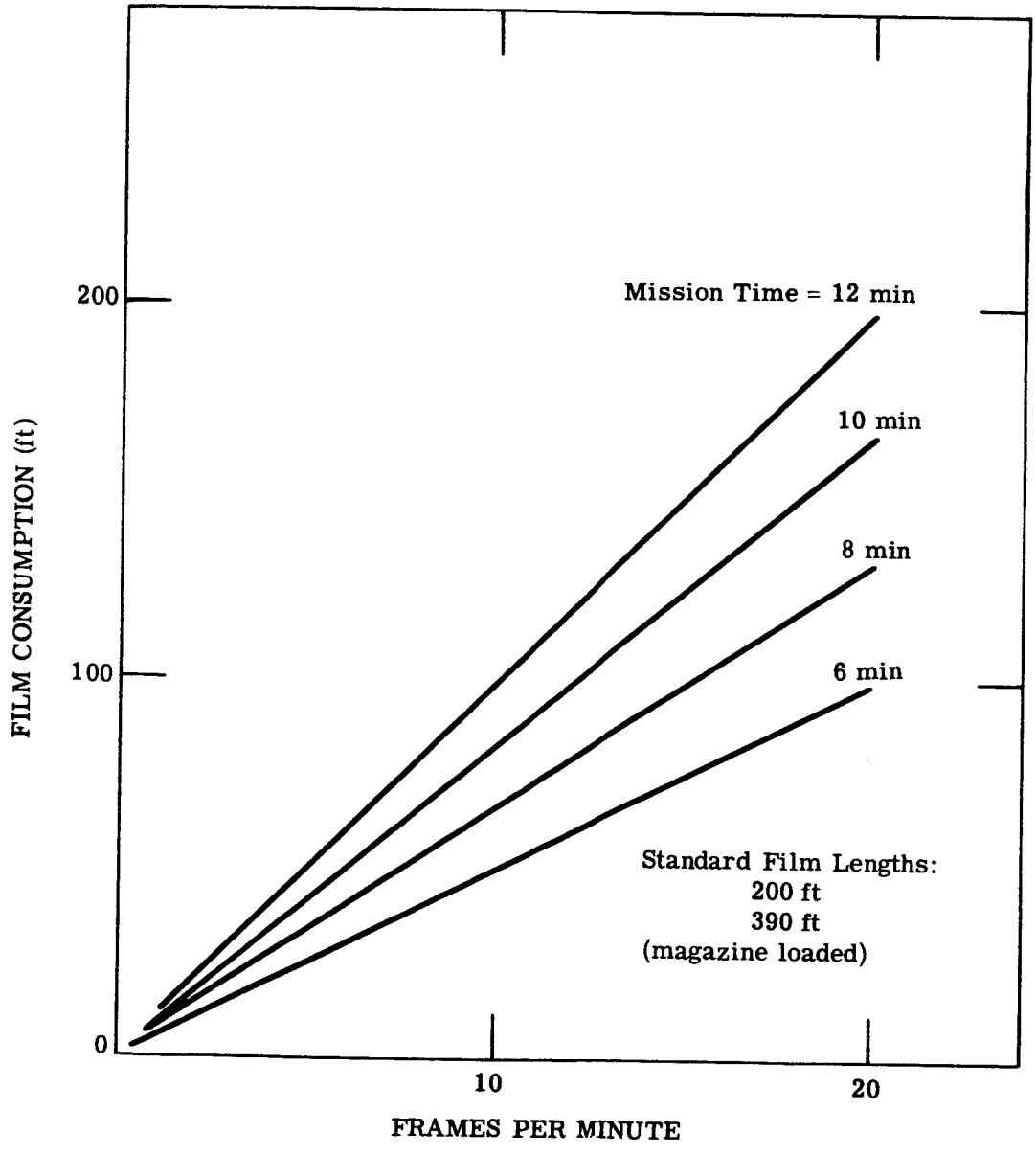

FIGURE 23. FILM CONSUMPTION PER ORBIT vs. FRAMES PER MINUTE AND MISSION TIME. 9- by 9-inch camera.

amplifier operating at 1.0610 μ. Present laser technology has developed two types of pulse laser optical amplifiers, the straight-through type and the feed-back type (Ref. 42 and 43). The most powerful of these laser amplifiers has given gains up to 22 db but for pulse amplification only. It is felt that a CW laser amplifier having a gain of 30 db could be developed within 1/2 to 2 years.

5.5. PRIMARY ELECTRICAL POWER SOURCES

A prime power source is necessary input for the various equipments in the orbiting research laboratory (ORL). Table XIII is a summary of data for solar, chemical, radioisotope and reactor prime power sources for satellites and/or space vehicles (Ref. 44 through 48). Power output, weight, energy conversion method, operating life and operational data are given. Note that power sources vary widely as to power produced (a few watts to 1 megawatt), operating lifetime (up to 10 years) and weight (a few pounds to 6,000 pounds). The radioisotope types have the most danger to man because radiation may be excessive for safe operation in or near the ORL and may therefore require additional shielding weight. The heavier shield weight is particularly required for the Sr^{90} beta particle emitter power supplies.

TABLE XIII. SATELLITE AND SPACE VEHICLE PRIME ELECTRIC POWER SYSTEMS

System	Power Output	Weight Unshielded	Energy Conversion**	Design Life	(Estimated) Operational Date
SOLAR					
1. Solar Cells (N-P)	0-4 kw	~4 w/lb (max)	PV	10-20 yr	1957
2. Solar Cells (Thin film)	0-200 w	1-2 w/lb	PV	10 yr	1965
3. Solar Collector	100-500 w	5 w/lb	TI	1 yr	--
4. Solar Collector	1.5-15 kw	5 w/lb	TbE	1-2 yr	1963
5. Solar Collector	34 kw	2800 lb	TbE	10,000 hr	--
6. Sunflower I	3 kw	700 lb	TbE	1 yr	--
7. Solar Binary	70 kw	1800 lb	TbE	1 yr	--
CHEMICAL					
1. H_2O_2 Fuel Cell	900 w	83 lb	TE	1000 hr	1964
2. LI-H_2 Fuel Cell	.5-4 kw	127 lb	TE	1 yr	--
3. Vortex MHD (Chem. Fuel)	50 kw	293 (incl. fuel)	MHD	60 min	--
4. Battery	0-2 kw	1.5-100 w/lb	EC	1 day	--
RADIOISOTOPE					
1. SNAP 3 (Po^{210})	3 w	4 lb	TE	3 mo	1960
2. Transit IV A and B (Pu^{238})	2.7 w	4.6 lb	TE	5 yr	1961
3. SNAP 13 (Cm^{242})	12.5 w	4 lb	TI	3 mo	1965
4. SNAP 9A (Pu^{238})	25 w	27 lb	TE	5 yr	1963
5. SNAP 11 (Cm^{242})	25 w	30 lb	TE	3 mo	1965
6. SNAP 17 (Sr^{90})*	25 w	28 lb	TE	5 yr	Study
7. SNAP 19 (Pu^{238})	50 w	48 lb	TE	5 yr	1965
8. COMSAT (Sr^{90})*	150-250 w	1+ w/lb	TE	20 yr	1965
9. Radioisotope (Ce^{144})	500 w	<300 lb	TI	1 yr	Study
(Cm^{244})	500 w	<200 lb	TI	>1 yr	1967
REACTOR					
1. SNAP 10A	550 w	935 lb	TE	8750 hr	1964
2. SNAP 2	3 kw	1470 lb	TbE	8750 hr	1966
3. SNAP 8	35 kw	6125 lb (35 lb/kw)	TbE	10,000 hr	1966
4. SNAP 8A	60 kw	2700 lb	TbE	5-10 yr	1967-68
5. STAR-R	70 kw	1400 lb	TI	1 yr	Study
6. START	60 kw	1000 lb	TI	1 yr	Study
7. SPUR (LMCM-2)	300 kw	2800 lb	TbE	10,000 hr	Study
8. TI REACTOR	300 kw	1200 lb	TI	1 yr	Study
9. DCR-300	300 kw	1900 lb	TI	1 yr	Study
10. SNAP 50	300 kw-1Mw	6000 lb (20 lb/kw)	TbE	5-10 yr	1970

*This is a beta emitter and requires the greatest shielding (a 160-w energy converter needs 80 lb of uranium for shielding).

** PV = Photovoltaic
TI = Thermionic (11-15% efficient)
TE = Thermoelectric (4-6% efficient)
TbE = Turboelectric
MHD = Magnetohydrodynamic
EC = Electrochemical
w = watts
kw = kilowatts
SNAP = Systems for Nuclear Auxiliary Power
LMCM = Liquid Metal Cooled Demonstration

6
LIMITATIONS IN SPACE RECONNAISSANCE OF EARTH

6.1. LIMITATIONS ON FOV, CONTRAST AND RESOLUTION BECAUSE OF ATMOSPHERE

Contrast and resolution of a photographic image are closely related — resolution has no meaning without contrast but contrast is present with low resolution.

The principle contrast degrading factors of the optical path between the source and the sensor in satellite photography of the earth are atmospheric scattering, turbulence, and bending of the light rays due to the non-uniformity of the index of refraction of the atmosphere. The cause of these factors cannot be removed; the only way to reduce the limitations or contrast is to reduce the effect of these limitations on the photographic image. The two types of scattering, Rayleigh and Mie, due to air constituents and particles in the air, can be minimized by selecting certain wavelength regions where the effects are less or by operating sensors with small total angular FOV. The variation of atmospheric transmission attenuation with propagation angle and wavelength may not allow wide-angle multispectral sensing because the effect of this variation of transmission would be the same as color-sensitive lens vignetting. Monochromatic vignetting could be corrected but panchromatic vignetting would be difficult to correct.

Concerning turbulence affecting resolution or the "shimmer" of an object viewed through the atmosphere, most researchers discuss the effect visible by the eye or recorded with time exposures as used in astronomy. If short exposures on fast film were used, the effect of turbulence may be minimized. More investigation is needed here. Of course, with existing film, graininess becomes a problem. It is known that films have higher resolving powers at lesser exposure which is in the proper direction for lessening the effect of turbulence. Another consideration here, though, is that the net exposure due to an image formed through haze may be treated as the superposition of two images, one of only target image forming light plus a uniform "haze" image. This "haze" image increases the fog level on film and makes low exposures impractical.

The bending of light rays due to the variations of the index of refraction of the atmosphere cannot be avoided. It is a static property of the atmosphere. If all rays that entered the camera objective were bent equally, no difficulty would result. To decrease the effect of atmospheric bending, narrow field of view cameras would be best since there would be more chance of the index of refraction being constant over the small angle. However, one reference (49) states that this static bending of light rays due to differences in the index of refraction is negligible.

6.2. CLOUD COVER

The objective of photographing large areas of the earth's land surface from an orbiting space vehicle raises the problem of obscuration of targets by overlying clouds. What are the probabilities that terrain targets will be visible to cameras on board an orbiting vehicle? How frequently do clouds obscure the earth's surface? What can be done in the space vehicle to enhance the camera's chances of photographing terrain in spite of the presence of clouds?

Certain general knowledge can be drawn on which relates cloud cover to visibility of the earth's surface. It has frequently been estimated that somewhere between 1/2 and 2/3 of the earth's surface is obscured by clouds at any time. The fraction is variable, depending upon the observer, the season, etc. Lt. Cooper, for example, observed that clouds obscured all of the earth's surface as he passed over northern Africa and Pakistan on the Mercury IX flight (Ref. 50).

Cloud frequency maps such as those in Reference 51 show by means of cloud-cover isopleths that cloud cover is not very uniform over the earth's surface. It is least over deserts and high arid regions. It is greatest generally over the North Atlantic and North Pacific Oceans, and typically low near the equator belw 10^{o} and 20^{o} latitude. The east coasts of continents are generally the most densely clouded, and coastal lines are generally cloudier than other areas. The air masses over the Gulf Stream and the Japanese Current are generally cloud-laden. A small region of clouds is also expected wherever air moves regularly off water onto land and again when this air moves onto high land or over mountains. Cloud cover over the oceans is rather consistent through the year, and is somewhat greater in winter than is summer. Cold air masses traveling out of the arctic areas onto the warm oceans become quite laden with clouds. Cloud cover over land masses is generally least in the winter, since land masses do not stay warm as do the oceans, hence do not furnish the air with water vapor.

The cloud cover over most land masses is typically cumulus, with mixtures of towering cumulus and cumulonimbus. Three classes are defined in the International definition of clouds, and a total of 4 conditions result:

0 - Clear - no clouds present.

CL1 - Cumulus with little vertical extent, or ragged cumulus other than of bad weather.

CL2 - Cumulus with moderate or great vertical extent are present. Length and width of cloud elements is similar to CL1.

CL3 - Cumulonimbus or thunderstorms are present. These may be mature thunderstorms or not yet fully developed ones.

It should be noted that CL2 and CL3 require only that these clouds be present among the smaller cumulus clouds which have not developed vertically. All three classes may be present in a region of CL3, for instance. The development of a CL1 region of clouds to a class CL2 involves the vertical development of some small cumulus into towering cumulus, without much increase in their length or width. As the CL2 region develops further into a class CL3 region, the towering cumulus develop in horizontal dimensions quite markedly. Therefore, there is not a simple relationship between area and thickness in the growth of a cloud. It will be seen later that the International cloud description can be used as a basis for predicting the size of clear intercloud spaces available for photographing terrain of a region.

A pronounced diurnal variation in amount and in class of cloud cover exists over all the United States, and presumably over most of the earth's land area. The morning sky, shortly after sunrise, has a strong probability of being clear. This condition is surprisingly stable and normally persists until after mid-morning or almost until noon. Typically, cloud cover of class CL1 appears in later morning, develops gradually to CL2 by an hour or so after noon, and proceeds to develop during the remainder of the afternoon to class CL3 cover containing thunderstorm clouds. This type of cloud cover prevails during the later afternoon and evening gradually clearing away during the night (See Ref. 52 and 53).

The above observations are only generalizations on the clouds vs. visibility problem. Two general approaches can be taken toward a solution of the problem: 1) Attempts can be made to avoid the presence of clouds. 2) Techniques can be sought to look through, or around the clouds, or to process the data to fill in gaps brought about by obscuration. From the above information it would appear that for land area targets, the first approach of avoiding the clouds can be applied in a limited way. The desired area can be overpassed shortly after sunrise. This utilizes the tendency toward clear air of this time of day. It is recognized, however, that too soon after sunrise may be unsatisfactory because of early haze in many areas. Photography, however, should be easier through haze than through clouds. Multiple orbits should be possible between sunrise and late morning, and at this time the clouds present should have their minimum horizontal extent.

The second approach, that of photographing terrain through or around clouds, can also find limited application. Photography, using visible or infrared energy, through cloud cover has no present hope of success, due mainly to the nearly perfect scattering of light of these wavelengths by water particles of clouds. However, by viewing at an angle from the vertical, it is possible to see under and around clouds, which leads to some gain in area visible under partial cloud conditions. The cameras described in Section 3 to obtain photography at scale of

1:800,000 and 1:2,400,000 would have a field of view of 28.1° and 73.7° respectively. These would be large enough to permit an appreciable gain in area covered if several photographs are taken of a general area to obtain different angles of view for every terrain element in the area.

The problem here is, how small must a cloud element be for this procedure to be successful? The width, length and thickness of clouds, their height above the terrain, as well as the length and width of intercloud spaces all are involved in determining whether or not the entire underlying terrain can be seen or photographed. The altitude of the space platform does not have much influence in this consideration, because it is so much greater than the height of the cloud tops, and because the average open intercloud space subtends such a small angle at the camera (1 mi. at 200 mi. subtends an angle less than 1/3 degree. One condition for visibility of terrain under clouds is that the width of a cloud should not be greater than the length of the space between two clouds. A second condition is that the ratio of cloud width to cloud altitude be less than the tangent of half the camera's field of view. Figure 24 illustrates these requirements. A third condition is that the terrain be outside of the shadow of a cloud cast by the sun. The blue sky light which illuminates such shadowed areas is so strongly scattered and attenuated by atmosphere that it may be useless for photography from satellite altitudes (Ref. 52, 53, and 54).

Blackmer, Serebreny and Alder photographed a strip 200 mi wide between Cocoa Beach, Florida and Edwards AFB, California on three occasions. June, July, and August 1962, from a U-2 aircraft flying at 50,000 ft. They divided these strips into regions of CL1, CL2, or CL3 or clear cloud cover, and for each class they found the range of cloud lengths, widths, thicknesses, and cloud spacings. These are considered quite typical for cloud cover over most land areas of earth. This information can be combined with Weather Bureau estimates of percent cloud cover, and cloud type, to yield the size of the average clear area between clouds for this type, and degree of cover. A further analysis allows us to estimate the probable maximum angle of view at which all terrain can be seen underneath a given type and degree of cloud cover.

This analysis leads to the conclusion that even with 3/10 cloud cover, all terrain can be photographed in a strip 50 miles wide on each side of the satellite's trace. A 4/10 cloud cover allows 93% of the terrain to be photographed in a strip 30 miles wide each side of the satellite's trace. A 6/10 cloud cover (class CL2) allows 80% of a strip 16 miles wide each side of the satellite to be photographed. These percentages assume a very large number of photographs (many viewing angles). In the practical case where the camera takes, say, only 3 photographs

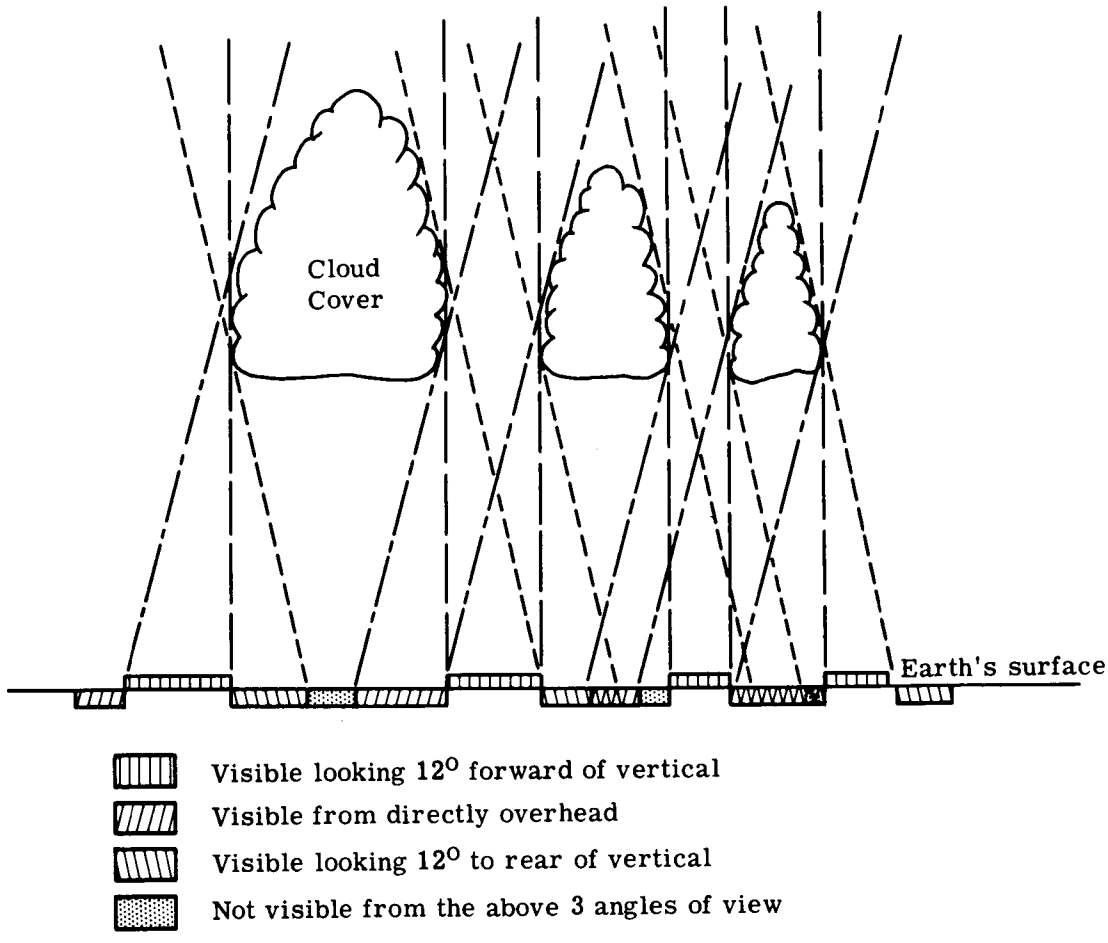

FIGURE 24. EFFECT OF CLOUD COVER ON TERRAIN VISIBILITY

of any given area on a single pass, these percentages are slightly too high, but still represent the situation reasonably well. Of course, the low visibility of details in shadows may reduce the above percentages appreciably. More intensive cloud cover would allow considerably poorer results because of the much greater probability of thunderstorms being present (CL3) whose tops are often found at 50,000 feet of more, and which would permit only viewing angles near 90^{o}.

In summary, it has been shown that the chances of satellite-based photography of all terrain in a given region of interest can be enhanced by correct timing of the flight over the area, and by viewing the area from several different angles to view around obstructing patterns of small clouds.

6.3. NEED FOR MULTIPLE SATELLITES

One of the future considerations for space reconnaissance of the earth is the optimum trade-off among number of satellites, length of time allowed for mapping of the area of interest, frequency of repetition, scale, and resolution.

In practice, many of the application areas will not require operational systems that provide total-earth's-surface coverage on a daily basis. Crop types and area determinations will entail weekly and seasonal coverage, while geographical and geological observations needed to be covered only once or at long intervals.

Meteorological observations, on the other hand, bring about a need for daily coverage. Sea surface temperature, damage surveillance, and other dynamic-process observations must be carried out in a rapid sequence in order to be meaningful.

Fortunately, the high-resolution applications require the most infrequent coverage, whereas the low-resolution situations require the most frequent observations. This means that satisfactory results in some areas of concern can be obtained with a minimum number of satellites.

The following equations are needed for analyzing the coverage requirements:

$$\alpha \leq \beta \ell w$$

$$\alpha \leq \frac{w}{12hS}$$

where $\alpha \equiv$ Total Scan Angle (Radians)

$\beta \equiv$ Resolution Angle (Radians)

$h \equiv$ Orbital Altitude (Ft.)

$\ell \equiv$ Film Resolution (Lines/inch)

$S \equiv$ Photographic Scale (=Magnification)

and

$w \equiv$ Film Width (Inches).

It is apparent that both inequalities must be satisfied—the first because the film resolution must not limit the systems and the second because the scale must be suitable for photographic interpretation.

Limiting the film width to 9 inches, and selecting ℓ = 2500 lines/inch as a typical case, the equations yield (with $\beta \geq 0.1$ mrad):

$$\alpha \leq 2.25 \text{ rad } (\simeq 130^{\circ})$$

$$\alpha \leq \begin{matrix} 0.04 \text{ rad. } (\simeq 2.1^{\circ}) \ (S = 1 \div 60{,}000)^{*} \\ 0.5 \text{ rad } (\simeq 28^{\circ}) \ (S = 1 \div 800{,}000)^{**} \end{matrix}$$

Therefore, the limitation on the coverage will be the scale. At a scale of 1 ÷ 800,000, 14 satellites could provide daily coverage of the entire continental U. S. At the higher scales, however, total coverage would be limited to weekly and even monthly intervals. For example, the time required for mapping the continental United States is shown in Figure 25 with the angle of coverage as a parameter.

It is first assumed that a satellite is in a polar orbit with a nominal altitude of 200 nautical miles and period of 90 minutes. The exact period and hence altitude must be adjusted to meet track-to-track displacement requirements, which will depend on the field of view, desired overlap, etc., as well as the satellite life requirement. Thus the exact period and altitude will differ from those given above, but the answers obtained using these values will still be reasonable approximations.

The entire continental United States is contained within the bounds of longitudes 67° and 127°W. and latitudes 25° to 49°N. In order to map this area with the minimum possible overlap, the ground swaths will be just contiguous at the widest point, namely at 25°N. latitude with overlap occurring and increasing north from that line. If the field of view of the mapping instrument is W miles wide at the ground normal to the satellite ground track, the minimum number of passes required for complete coverage will be

---

*Corresponds to high-resolution case.

**Corresponds to low-resolution case.

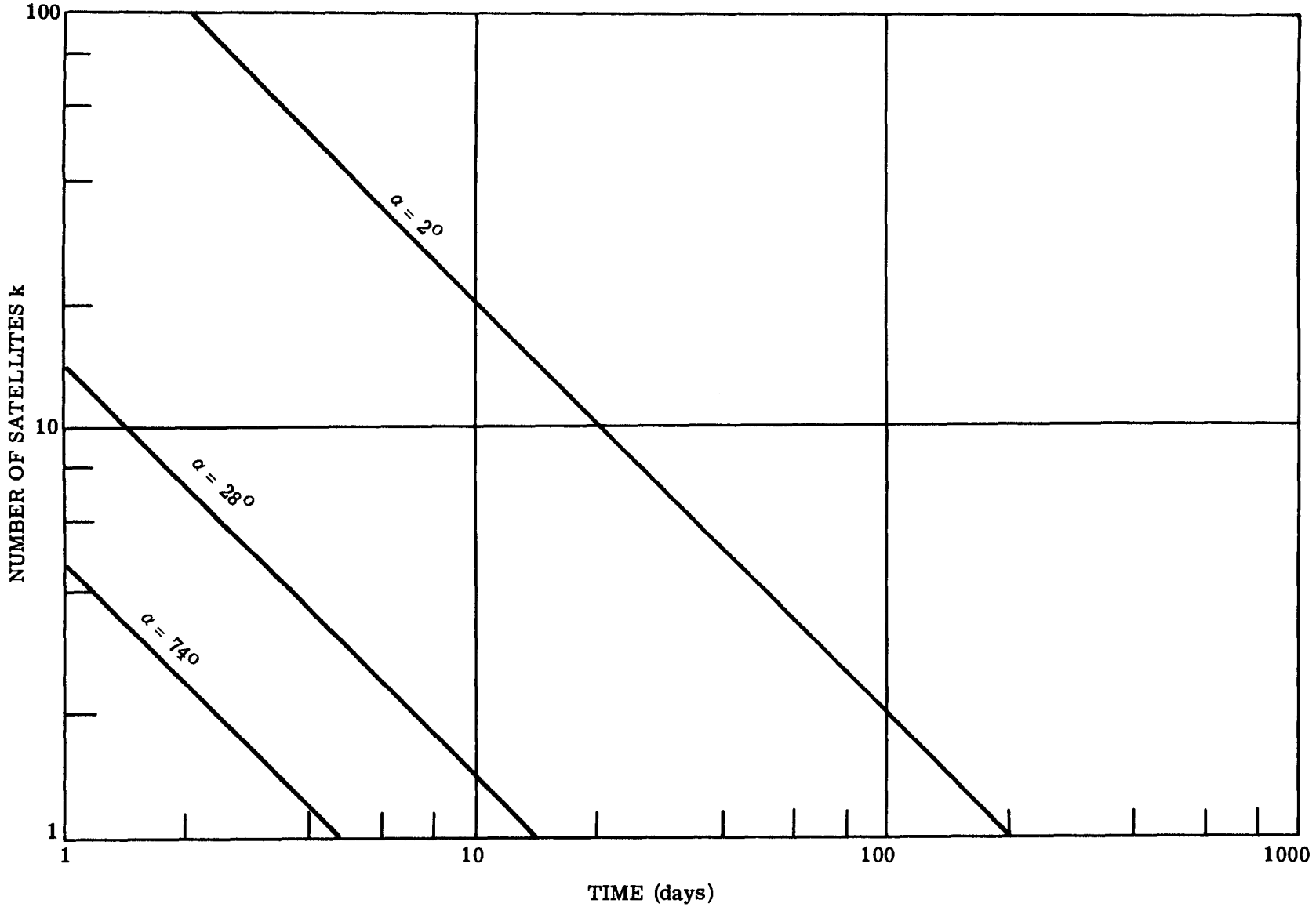

FIGURE 25. TIME REQUIRED FOR SINGLE COVERAGE OF CONTINENTAL UNITED STATES

$$N = \frac{1}{W} \frac{125 - 67}{360} \times 25{,}000 \times \cos 25^{o} = \frac{3650}{W}$$

If a single satellite is used and its period adjusted so that its track is displaced exactly W miles at 25°N. latitude every day, then over the period of time required to completely cover the area given above, the number of passes per day which the satellite will make over this area will vary between two and three. In order to determine the number of days required to complete the coverage, it should be first noted that for a 90 minute period, the displacement between successive tracks will be

$$D = \frac{90/60}{24} 360^{o} = 22.5^{o}$$

in longitude. At 25°N. latitude this corresponds to a distance

$$d = \frac{22.5}{360} \times 25{,}000 \times \cos 25^{o} = 1{,}416 \text{ miles}$$

It may be seen that if the ground track is displaced W miles every day, then in

$$n = \frac{1416}{W}$$

days, the entire distance between successive orbits will have been covered for all latitudes above 25°N. Thus, after n days, and not before then, the entire area of interest, namely the continent of the United States, will have been completely covered. Other satellite tracks where the day-to-day displacement is greater than W may also be used to cover the same area in the same time, but these displacements must be carefully chosen to obtain complete coverage in n days. If more than one satellite is used, n becomes the minimum number of satellite-days. That is, for k satellites, the minimum number of days is

$$n' = \frac{n}{k} \text{ days}$$

For a field of coverage of α degrees normal to the ground track,

$$W = 2 \times 200 \times \tan \frac{\alpha}{2} \text{ miles}$$

Thus the minimum time required for complete coverage of the continental United States will be

$$n' = \frac{1416}{400 \tan \frac{\alpha}{2} k} = \frac{3.54}{k \tan \frac{\alpha}{2}} \text{ days}$$

Where redundancy by a factor of m is desired to increase the probability of viewing a given point on ground uncovered by clouds, then the number of days required becomes mn'.

6.4. DYNAMIC RANGE OF SIGNALS

6.4.1. INFRARED. Experiments conducted by the U. S. Air Force (using bar-patterns near threshold of modulation) have demonstrated that, under suitable conditions, the human eye is capable of distinguishing among 128 different density levels in the linear range of ordinary photographic films. Although the figure cited may differ from the results obtained by other researchers, it corresponds quite closely with the 7-bit signals* utilized in the monitor systems at commercial television stations.

If the sensing device has a noise-equivalent-temperature sensitivity of $0.1^{o}K$, then a 7-bit range will handle $12.8^{o}K$. Similarly, if the NET is $0.5^{o}K$ or $1.0^{o}K$, the range will be $64^{o}K$ or $128^{o}K$.

Utilizing only 5 bits of information per resolution element, the corresponding dynamic ranges are $3.2^{o}K$, $16^{o}K$, and $32^{o}K$ respectively.

Figure 26 illustrates the relationship between NET, the number of bits per element, and the dynamic temperature range.

Unfortunately, an extremely wide range of temperatures can be expected along the ground path of a polar orbit. An example of this variation is shown in Figure 27 for an orbit along the Greenwich meridian and the international date line. Temperatures from $-50^{o}C$ to $+70^{o}C$ are possible. Naturally, such a wide variation could not be expected within a single frame. However, cracking ice in polar regions could easily produce local variations of 50^{o}. If temperature readings to the nearest 0.5^{o} are required for such tasks as ice thickness mapping, then 100 temperature levels, or a 7 bit range would be needed. Possibly 6 or 5 bit capacities could be used for regions with smaller local variations, such as those shown (for a typical June day) in Figure 28.

6.4.2. RADAR. The dynamic range of the return signals of the various radar system that have been discussed depends on the system resolution, the expected spatial extent of the various targets, and the backscatter coefficients of the targets of interest. Shown in Figure 29 is the

*i.e., $2^{7} = 128$ signal levels.

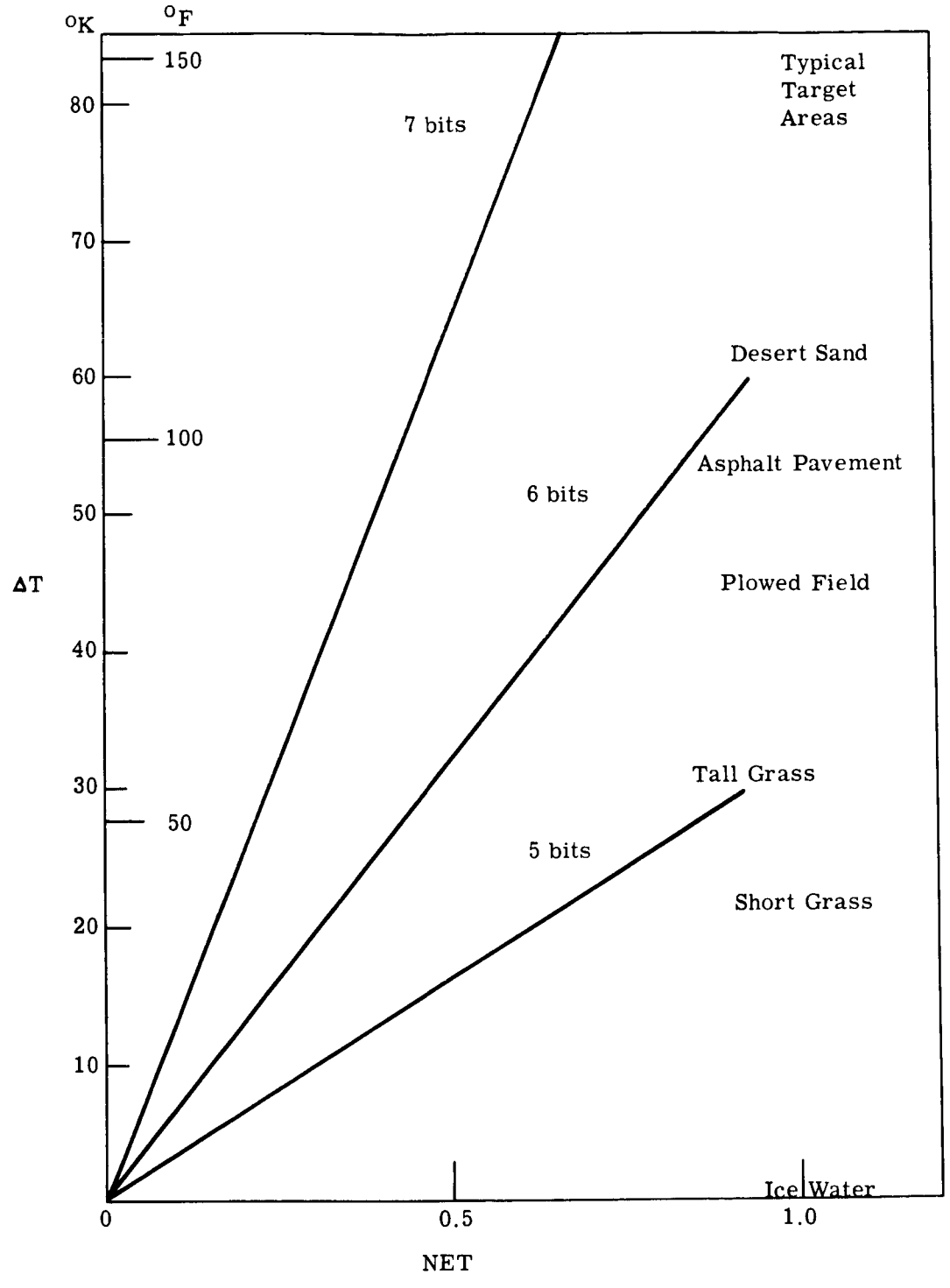

FIGURE 26. RELATIONSHIP BETWEEN NET, BITS/ELEMENT, AND TEMPERATURE

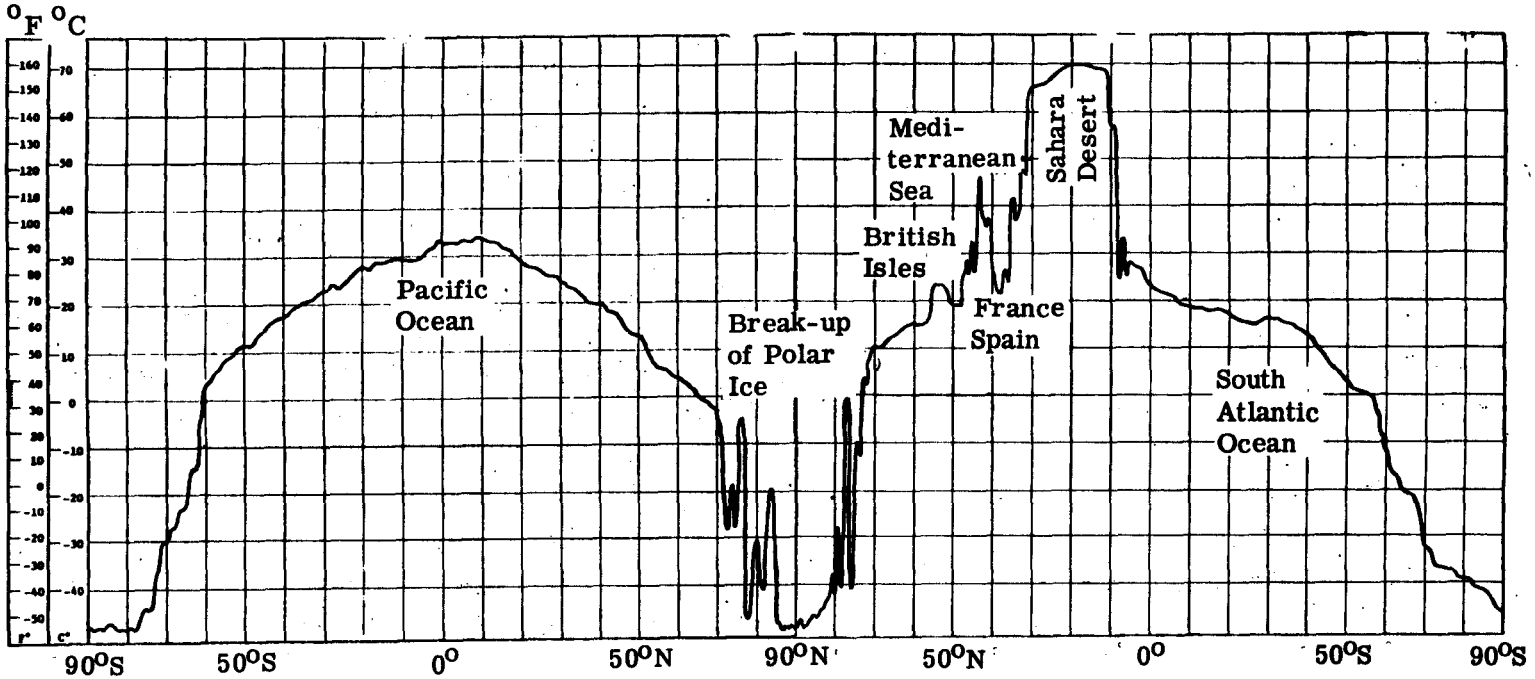

FIGURE 27. EXAMPLE OF A TEMPERATURE PROFILE FOR ONE EARTH ORBIT

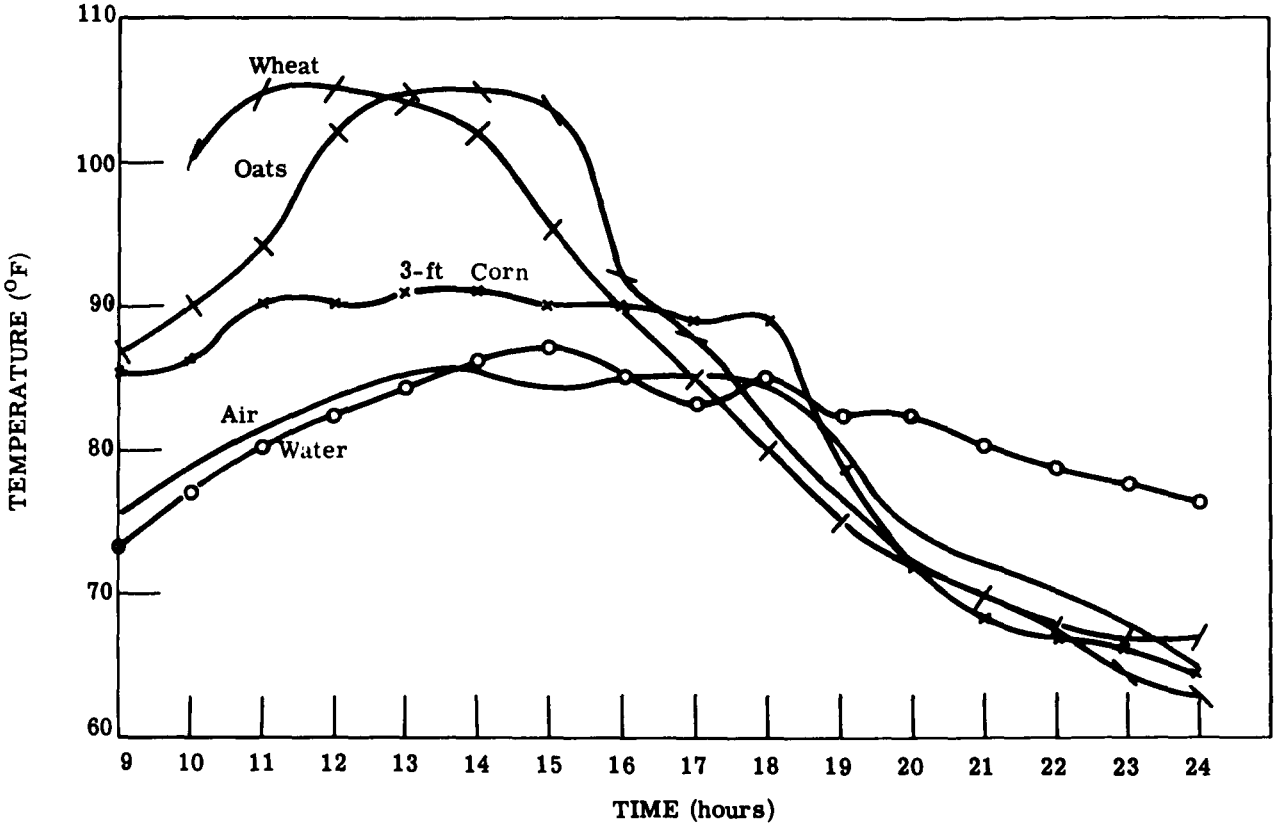

FIGURE 28. TEMPERATURE VARIATIONS OF CROPS

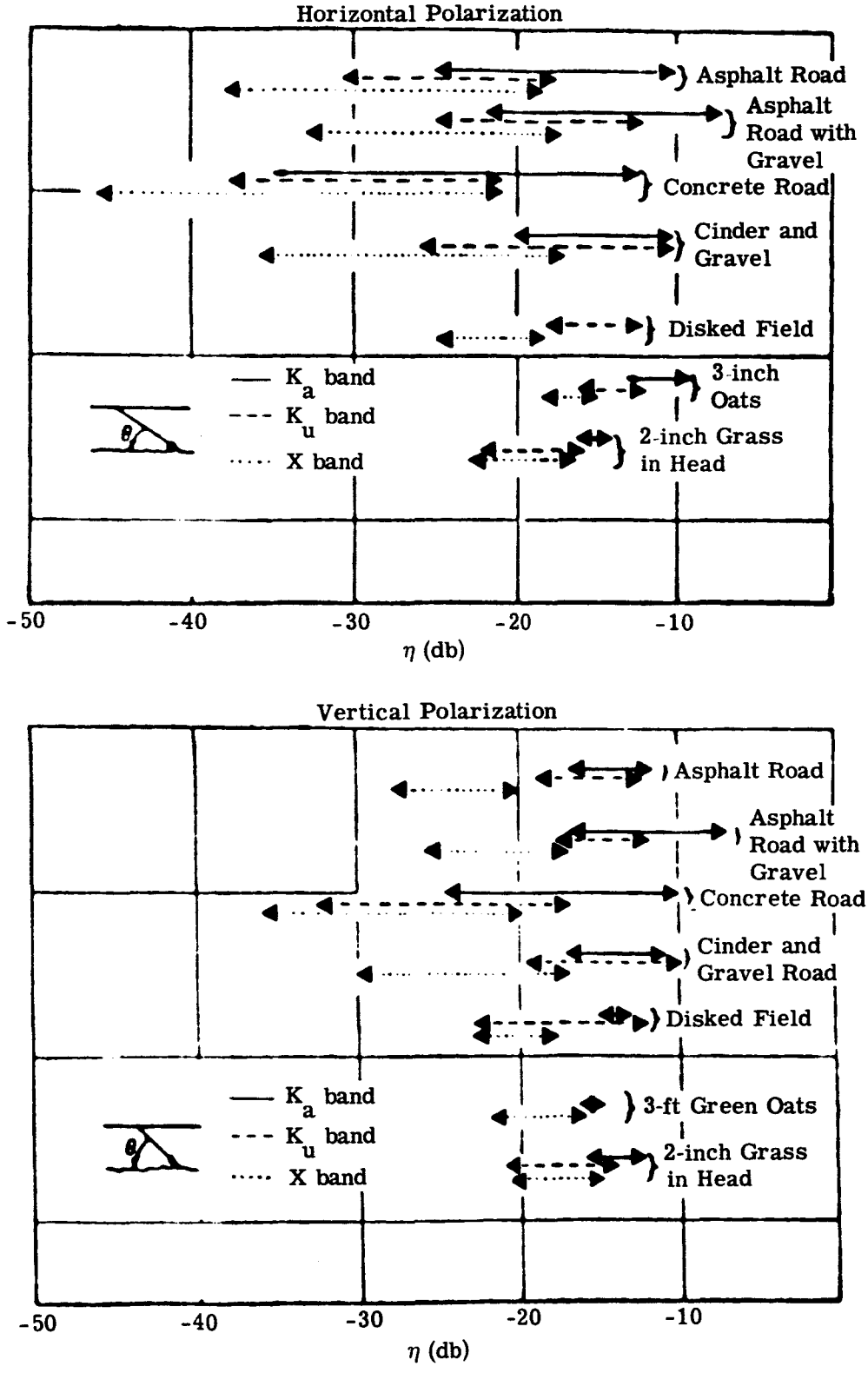

FIGURE 29. DYNAMIC RANGE OF η FOR VARIOUS TYPES OF TERRAIN (Reproduced from Ref. 18)

dynamic range in backscatter coefficients for a few targets that may be of interest. For a high resolution system such as the proposed coherent or synthetic aperture radar whose resolvable element size is on the same order as that of the smallest targets (i.e., roads for the targets shown) then the signal dynamic range will be on the same order as the dynamic range of the target backscatter coefficients (in this case of the targets shown in Figure 29 the signal dynamic range would be on the order of 30 db). It appears that the dynamic range requirements of the system can be made smaller than this if the area to be monitored does not include targets which have backscatter coefficients representative of the extremes. If this is the case, the dynamic range of the equipment may be set by an on-board observer to meet the requirements of the targets to be monitored.

The dynamic range requirements for the noncoherent radar system, because of its poorer resolution capabilities, will in general be less than that for the coherent radar system. Only in those areas such as large cities where the presence of road like surfaces predominate does it seem likely that the dynamic range requirements for the noncoherent system will have to be greater than 15 to 20 db.

Appendix A.1
PHOTOGRAPHIC EMULSION AND PHOTOCATHODE RESOLUTION VS. SENSITIVITY

A.1.1. INTRODUCTION

An attempt was made to determine the limits on sensitivity and resolution for various photographic materials. One conclusion becomes immediately apparent; the resolving power varies at least as much with the method of measurement as it does with the choice of material. The same emulsion may vary by a factor of 2 or 3 according to what measurement method was used. For this reason a theoretical approach was employed for this investigation which attempts to establish ultimate limits on the resolving power of photographic emulsions.

A.1.2. GENERAL

Present high-speed emulsions require approximately 10 to 20 photons to make a silver halide crystal developable, a few crystals might require as low as 4 photons (Ref. 55). For exposure to fast electron beams up to approximately 100 silver halide crystals can be made developable for each primary incident electron, depending on its incident energy. On a macroscopic level this corresponds to approximately 10^8 photons/cm^2 or some 10^6 electrons/cm^2 (in the 10 to 100 kV range) in order to obtain a visible record on high speed film. There is little hope that these figures can be changed drastically for both photon and electron exposures of silver halide systems. Other photographic systems now under investigation do not give much promise of extending these limitations.

A.1.3. FACTORS DETERMINING RESOLUTION IN PHOTOGRAPHIC FILMS

In instances where small scale or microdetails are of interest, the standard characteristic curves for photographic films are of little help since they are determined by measuring the densities of large, uniformly exposed areas. When a point of light is imaged on a film, the intensity extends over a finite area, called the spread function, and causes a contrast reduction. An increasing loss of contrast is experienced as an image becomes smaller.

Another factor influencing the quality of detail rendition is the glanular structure of the developed image. The photographic image is made up of silver grains which are somewhat randomly distributed over the image area. The granular structure results in density fluctuations about a normal value. The resolving power of a film is inversely related to its granularity.

A third cause of image degradation is revealed when we examine the statistical nature of incident photons. It can be assumed that the number of photons incident on a given subject area

in a fixed time follows a Poisson distribution. If μ_1 photons are incident on one subject area μ_2 photons are incident on an equivalent area then there must exist a minimum $\Delta\mu = \mu_2 - \mu_1$ such that a contrast difference is just detectable. The ratio $\Delta\mu/\mu$, where μ is the variance of the Poisson distribution, is termed the "signal contrast."

A.1.3.1. LIMITATIONS IMPOSED BY QUANTUM EFFICIENCIES. If $\gamma = \mu/a$ where γ is the number of photons per unit area for a small square area a of side length s, the resolving power can be expressed as

$$1/S = \frac{(\gamma\eta^2)^{1/2}}{K} \frac{\Delta\mu}{\mu}$$

where η^2 is the "detective quantum efficiency" (Ref. 56 of the film relative to an ideal film whose only source of noise is the statistical nature of the incident photons. The peak value of η^2 which can only be reached if no exposure latitude is permitted is $\eta^2 = 0.01$. Allowing an exposure latitude of 100:1 lowers the quantum efficiency to $\eta^2 = 0.004$. A quantum efficiency of 10% has been assumed for photocathodes.

The ASA exposure index S_x is related to the number of photons by the conversion

$$\gamma = \frac{5 \times 10''}{S_x} \text{ (photons/mm)}$$

This formula gives the number of photons γ having a wavelength $\lambda = 555$ mμ for an equal energy spectrum of the illuminant. A film latitude of 100:1 has been assumed.

The theoretical limits shown in Fig. 30 represent only that limitation imposed on the resolving power of detectors by the quantum-statistical nature of the impinging illumination. The actual figures for high-speed films are lower because of the spread function and the granularity. Image spread and granularity will be more prevalent as limiting factors of resolution as the film sensitivity is lowered and the quantum-statistical nature of the incident photons becomes less significant.

A.1.3.2. DERIVATION OF CURVE. Data for the curves relating resolution to ASA exposure index for the image orthicons and Royal X Pan film was obtained from Ref. 57 and 58. It was necessary to convert the authors' abscissa, film illumination foot candles, to an equivalent ASA number. An equal energy spectrum was assumed and the ASA index was determined by solving for the number of incident photons/mm at a wavelength $\lambda = 556$ mμ.

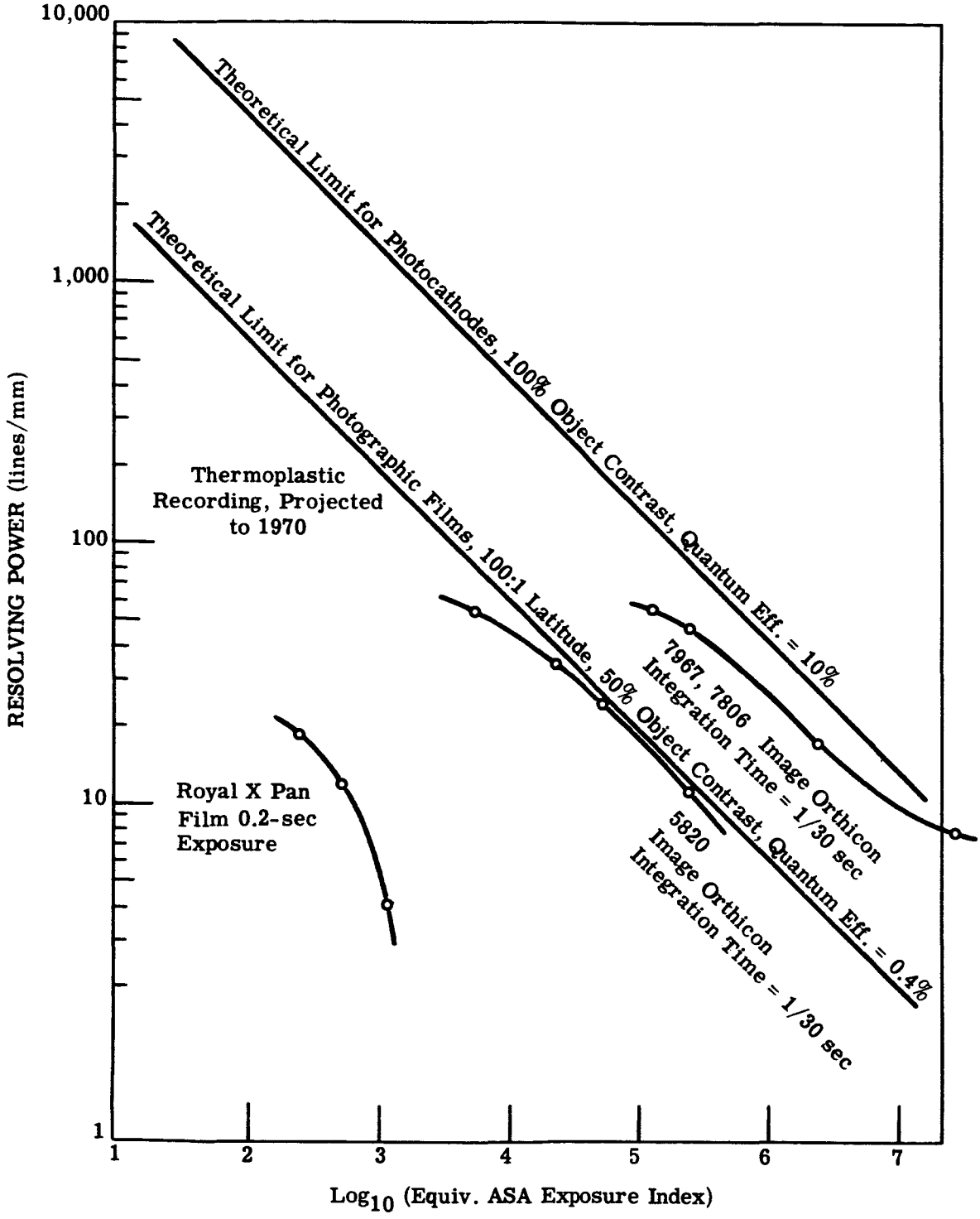

FIGURE 30. THEORETICAL PERFORMANCE FOR PHOTOGRAPHIC FILMS AND PHOTOCATHODES

Appendix A.2
TELEVISION SYSTEMS FOR RECONNAISSANCE

The most critical limitation of television systems used in aerial reconnaissance is the limited resolution they provide. The standard TV system resolution is about 340 lines vertical and 600 lines horizontal in the center of the picture, decreasing to 400 in the corners. Efforts to improve system resolution are usually directed at improving the camera tube resolution since other technical difficulties can usually be overcome if one is willing to accept increases in power and bandwidth requirements.

The resolution performance of a television camera tube is determined by the cascaded performance of a number of stages, each of which can be considered as an optical low-pass filter. One limiting component which is common to both orthicon and vidicon camera tubes is the aperture presented by the scanning electron beam. Broad electron velocity distribution impairs resolution. RCA Astro-Electronics Division has experimented with the smoothing of the oxide cathode layer (Ref. 59). This smoothing produces a more uniform electron emission density. This process has doubled the intrinsic resolution capability of standard image orthicons. RCA has measured the equivalent passband for the modified electron guns at 2,200 TV lines/inch.

Livingston (Ref. 60) has performed investigations to determine what the system specifications should be in order to obtain the highest possible resolution from an image orthicon. The TV camera was not studied alone but only as one link in the complete camera-recording chain. However, his results indicate that when all system parameters were optimized the limiting resolution was determined primarily by the interelement capacitive coupling at the target of the image orthicon. A resolution of 900 TV lines at 50% amplitude response was obtained for a 3 inch tube while the limiting resolution was 3000 lines.

The image orthicon, although capable of somewhat higher resolution than the vidicon under normal operation, is bulky, complex, and high in cost. The 1 inch vidicon, however, is capable of a limiting resolution of only about 700 lines in the center decreasing to 400 lines at the corners. Pourciau, Altman, and Washburn (Ref. 61) have improved the vidicon resolution considerably by doubling the magnetic deflection field. A limiting resolution of better than 1200 lines has been achieved.

A 1 1/2 in. diameter vidicon designed specifically for high resolution television systems by RCA Electron Tube Division has a claimed limiting resolution of 1200 lines or better at the picture center (Ref. 62). The resolution at 50% amplitude response for this tube, the 8051, is 500 TV lines. Sensitivity is 1 footcandle of illumination at the tube face for a signal current of .8 μ amps.

The more sensitive pickup tubes are the image orthicons and image-intensifier orthicons. Because of their high sensitivity they can frequently be used to provide brightness amplification in low-light-level photographic recording. Below levels of illumination of 0.001 foot-candles, television systems show definite advantages in resolution capability compared with photographic films. Above 0.01 foot-candles, films are definitely superior. Neuhauser (Ref. 63) has rated the Z5294 tube with an ASA exposure index of approximately 160,000. This same tube is capable of resolving 700 lines with the illumination supplied by a half moon zenith (Ref. 58) assuming a 10% object reflectance and an f 1.0 lens.

An image orthicon operating at low levels of illumination has an effective shutter speed of 1/30 sec when operated as an electronic shutter.

One of the most promising directions for the improvement of sensitivity of image converter tubes is the incorporation of fiber optic windows at one or both ends of the tube (Ref. 64). When a copying camera employing a photographic emulsion is used to photograph an electron image on a fluorescent screen, the light transmitted to the image is only about 1% of the light leaving the screen. If an electron tube is fitted with a fiber optics window to support the phosphor, about 50% of the light from the phosphor is transmitted to the image. Fiber bundles made with .0006 in. fibers have a resolving power of about 600 TV lines which is about the same as that of a standard TV system (Ref. 65).

The best limiting resolution one can expect from conventional television reconnaissance systems today is about 1000 TV lines. The information capacity of the conventional system is limited because the optical system images an entire scene on the orthicon tube face at one time. Fiber optics may be employed as a shape transducer to divide a single long scanning line into many TV scanning lines on the photocathode. This effectively lengthens the scan line for the image orthicon. The fiber optics, for example, might scramble one long scan line of the image into 40 scan lines on the camera, the camera thus imaging 25 long scan lines of the scene at one exposure. Assuming a frame rate of 30 frames/sec, a rectangular picture 40,000 × 40,000 elements could be completely imaged in 1.3 sec.

Appendix B
OPTICAL-MECHANICAL SCANNERS

A comprehensive discussion of the design and performance characteristics of optical-mechanical scanner systems is given in Ref. 66. In Section B.1 of this appendix, an analysis is given leading to the development of curves showing the relationship between noise-equivalent temperature differences of infraed sensors and the instantaneous field of view or ground resolution. These trade-off curves permit the study of system trade-off relationships between desired temperature sensitivity and acceptable ground resolution. The effects on system performance of changes in detector temperatures and variation in v/h are discussed in Sections B.2 and B.3, respectively. Finally, general specifications of an infrared or similarly a multispectral scanner to be used in space experiments are discussed in Section B.4.

B.1. INFRARED SENSOR CAPABILITY

The infrared detector is, as a general rule, situated near the focal point of an imaging-type optical system. Infrared radiation captured by the detector is contained within an angle, β, as follows:

$$\beta = d/F \tag{1}$$

where d is a linear dimension of the detector and F is the focal length* of the collecting optics.

The instantaneous field of view, G, of the detector system will be:

$$G = h\beta \tag{2}$$

where h is the distance to the object being viewed by the system. In terms of the magnification, M, of the system, the instantaneous field of view is:

$$G = d/M = d(h/F) \tag{3}$$

(The quantity M is also known as the "scale" in photographic work.)

In a scanning system, one may consider the image of the target as being swept across an aperture (the detector sensitive area). The information which is contained in the image is filtered spatially by this aperture. Considering the detector as a spatial filter, the "first zero" of the filter, f_0, may be taken as indicative of the required frequency bandpass for the system. This is given by:

*Actually, this is only an approximation. In the usual optical terms, F would be called the "image distance" of the object. In general, however, the image distance is very nearly equal to the focal length in infrared systems.

Nomenclature

β = Angular Resolution

ϵ = Emissivity

ϕ = Frame-Rate

τ = Time-Constant (or Transmissivity)

ω = Angular Velocity

A_d = Area of Detector

C_1, C_2 = Constants

D = Collecting Aperture Diameter

D^* = Detectivity of Detector

d = Detector Diameter (or width)

E = Blackbody Function

f = Frequency

F = Focal Length of Detector Optics

G = Instantaneous Field of View (Ground Patch)

h = Distance to Target

m = No. of Detector Elements, Linearly Arrayed

M = Optical Magnification (image distance ÷ object distance)

n = Scans/Revolution

r = Rotation Rate

S/N = Signal-to-Noise Ratio

T = Target (or background) Temperature

v = Velocity of Vehicle

W = Radiative Flux Density

$$f_0 \equiv \frac{\omega}{2\beta} \tag{4}$$

where ω is the rate of rotation of the image plane about the center of the optical system.

The rotation rate ω is related linearly to the scanning mirror rotation rate, r, as follows:

a) If the rotation axis is along the optical axis:

$$\omega = 2\pi r$$

b) If the rotation axis is normal to the optical axis:

$$\omega = 4\pi r$$

Both of these conditions can be expressed by the single equation:

$$\omega = 2\pi r\left[1 + \frac{|\vec{r} \times \vec{F}|}{rF}\right] \tag{5}$$

Thus, f_0 becomes:

$$f_0 = \frac{\pi r}{\beta}\left[1 + \frac{|\vec{r} \times \vec{F}|}{rF}\right] \tag{6}$$

If no processing is to be done on the resultant signal, the maximum frequency which must be passed by the system usually can be chosen as f_0. This places limitations on the time-constant, τ, of the detector. From basic Fourier analysis, this relationship is:

$$\tau \leq \frac{1}{2\pi f_0} = \frac{\beta}{2\pi^2 r\left[1 + \frac{|\vec{r} \times \vec{F}|}{rF}\right]} \tag{7}$$

The limitations on r are set by the requirement for complete coverage of the target (i.e., contiguity of adjacent scan-lines). If the scanner is carried in a vehicle moving at a velocity v and at a distance h from the target, the apparent angular rotation rate of the target with respect to the vehicle is v/h. If the scanner provides n scans per revolution, and if there are m lines of information per scan (e.g., because of an m-element linear array of detectors), then the following relationship must hold for contiguity:

$$\beta mnr = v/h \tag{8}$$

Often, through the use of nodding mirrors or slowly rotating auxiliary prisms, it is possible to modify the apparent angular motion of the target as follows:

$$\beta mnr = v/h + 4\pi r_A \tag{9}$$

where r_A is the rotation rate of the auxiliary mirror. If the auxiliary mirror is an n_A-sided prism, the frame-rate will be:

$$\phi = n_A r_A$$

One of the primary performance criteria is the sensitivity of the system to small changes in target temperature. The signal-to-noise ratio produced by a temperature difference ΔT is:

$$S/N \equiv \int_{\lambda_1}^{\lambda_2} \frac{D^*_\lambda}{\sqrt{A_d \Delta f}} [\tilde{W}_\lambda(\lambda, T + \Delta T) - \tilde{W}_\lambda(\lambda, T)]\, d\lambda \tag{10}$$

where

$$\tilde{W}_\lambda = \frac{\tau_\lambda d^2}{4(F/D)^2} \epsilon_\lambda E_\lambda(\lambda, T) \tag{11}$$

For the typical quantum detector (cut-off wavelength λ_c), D^*_λ is proportional to λ up to λ_c and zero for $\lambda > \lambda_c$:

$$D^*_\lambda = \frac{D^*_{\lambda c} \lambda}{\lambda_c}; \quad (\lambda < \lambda c) \tag{12}$$

The blackbody function of equation (11) may be approximated by Wien's law for $\lambda < 14\ \mu$, $T < 300^{o}K$:

$$E_\lambda(\lambda, T) = \frac{C_1 e^{-C_2/\lambda T}}{\lambda^5} \tag{13}$$

For $\Delta T << T$, the Taylor's expansion of (13) gives:

$$E_\lambda(\lambda, T + \Delta T) - E_\lambda(\lambda, T) \cong \left(\frac{C_2}{\lambda T}\right)\left(\frac{\Delta T}{T}\right) E_\lambda(\lambda, T) \tag{14}$$

Substituting (11), (12), and (14) into (10), the signal-to-noise equation becomes:

$$S/N = D^*_{\lambda_c}\left(\frac{C_2}{\lambda_c T}\right)\left(\frac{\Delta T}{T}\right) \frac{d^2}{4(F/D)^2 \sqrt{A_d \Delta f}} \int_{\lambda_1}^{\lambda_2} \tau_\lambda \epsilon_\lambda E_\lambda(\lambda, T)\, d\lambda \tag{15}$$

If the wavelength region is one in which $\tau_\lambda \epsilon_\lambda$ does not vary significantly, the integral in Equation (15) may be written as:

$$\overline{\tau\epsilon}[E(\lambda_2, T) - E(\lambda_1, T)] \tag{16}$$

where

$$E(\lambda, T) \equiv \int_0^{\lambda} E_{\lambda}(\lambda, T)\, d\lambda \tag{17}$$

Considering $A_d = d^2$ and $\Delta f = f_0$, with S/N = 1, the "noise-equivalent temperature difference" is:

$$\text{N.E.T.} = \frac{4F\sqrt{\pi r}\, Th^{3/2} G^{-3/2}}{D^*_{\lambda_c}\left(\frac{c_2}{\lambda_c T}\right) D^2 \overline{\tau\epsilon}[E(\lambda_2, T) - E(\lambda_1, T)]} \tag{18}$$

Note that (dh/F) = G, which is the instantaneous field of view (sometimes called the "ground patch") for the system. Using equation (18), it is possible to plot N.E.T. vs. G, with

$$K \equiv \left(\frac{D^*_{\lambda_c}}{\lambda_c}\right) D^2 [E(\lambda_2, T) - E(\lambda_1, T)] \tag{19}$$

as a parameter, and the fixed quantity

$$k \equiv \frac{4\sqrt{\pi r}\, T^2 h^{3/2}}{C_2 \overline{\tau\epsilon}} \tag{20}$$

(c.f. Figure 31.)

B.2. APPARENT SIGNAL CHANGE DUE TO CHANGE IN DETECTOR TEMPERATURE

In an infrared sensing device, the fractional change in signal level due to a change in target temperature is given by:

$$\frac{\Delta S}{S} = \frac{\Delta \tilde{W}}{\tilde{W}} = \left(\frac{c_2}{\lambda T}\right)\left(\frac{\Delta T}{T}\right)$$

A similar change in signal level may be produced by varying D^*:

$$\frac{\Delta S}{S} = \frac{\Delta D^*}{D^*}$$

With a detector which behaves differently at different cell temperatures, D^* may vary as follows:

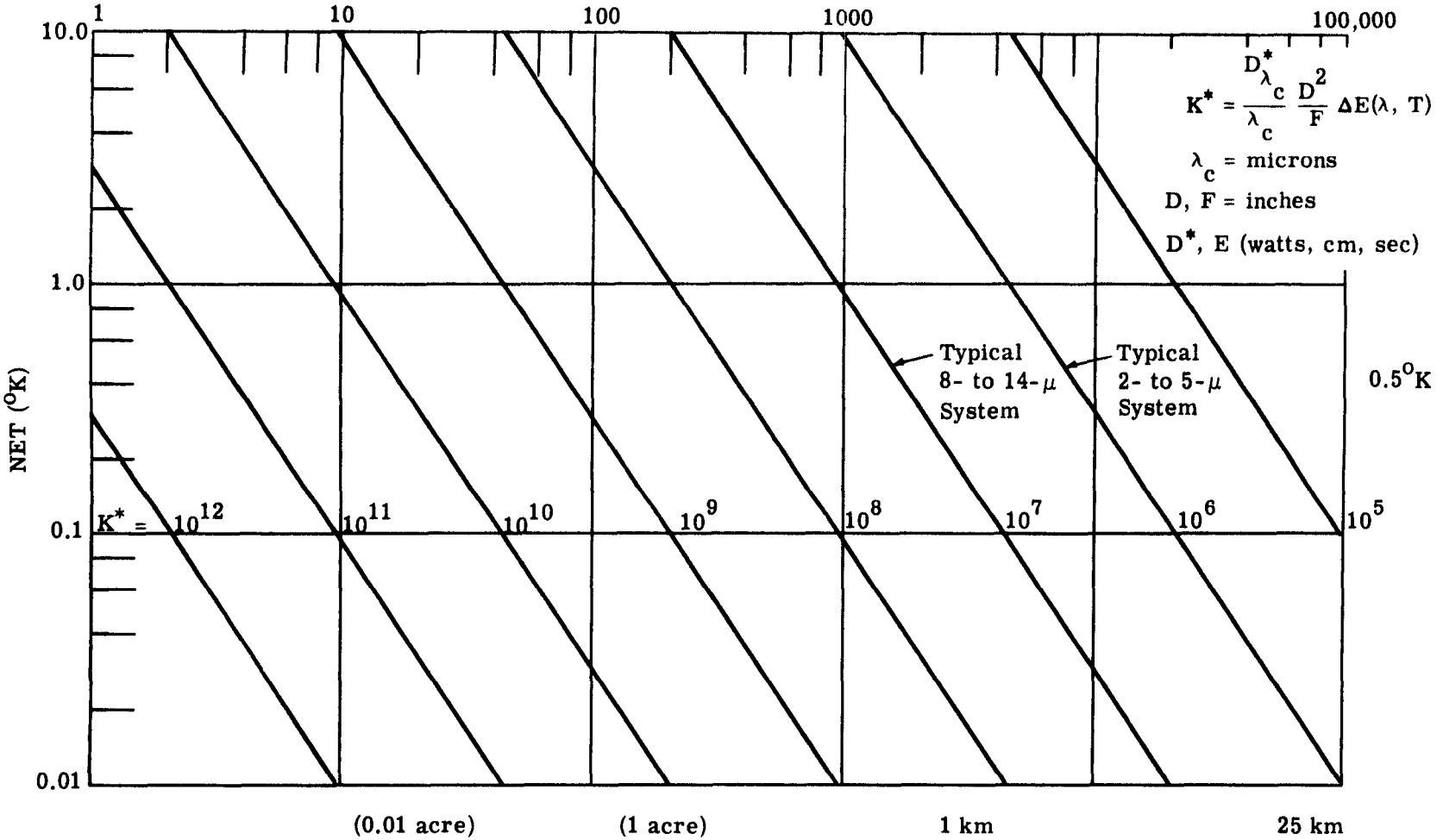

FIGURE 31. NOISE EQUIVALENT TEMPERATURE DIFFERENCE AS FUNCTION OF INSTANTANEOUS FIELD OF VIEW

$$\Delta D^* = \frac{\partial D^*}{\partial T_c} \Delta T_c$$

where T_c is the cell temperature.

Combining the above relationships, it is possible to ascertain the signal-level stability as a function of cell temperature as follows:

$$\frac{\Delta T}{\Delta T_c} = \frac{\lambda T}{c_2} \frac{T}{D^*} \frac{\partial D^*}{\partial T}$$

This function is plotted in Figure 32 for the detector which behaves as that in Figure 1.

At a cell temperature of 25°K, it is seen from the figure that the variation in signal level will look the same as that for a variation in target temperature equal to 4 times the variation in cell temperature. Thus, the cell temperature must be maintained to within ±0.025°K between calibrations to maintain a ±0.1°K temperature level stability.

B.3. VARIABILITY OF v/h

One of the important parameters in any aerial reconnaissance mission is the apparent angular rotation rate of the target area with respect to the surveillance instrument (camera or scanner). This rate is equal to the ratio of the relative normal velocity to the distance between target and instrument (i.e., v/h).

In the case of a satellite-borne device, the ratio of v to h will depend upon the orbit eccentricity and upon the decay of the orbit as a function of time. For nearly circular orbits, v/h does not change significantly. However, as the orbit decays, the altitude decreases and the velocity increases, thus causing v/h to grow quite rapidly. For the predicted orbit (i.e., Figure 33 the variation of v/h is shown in Figure 34 For a circular orbit at 200 n. mis. altitude, v/h is equal to 0.021.

B.4. GENERAL SPECIFICATION OF AN INFRARED OR MULTISPECTRAL SCANNER FOR SPACE APPLICATION

The trade off between two systems, one airborne and one spaceborne will be outlined in this section. It is assumed that the spaceborne system will require a S/N ratio as good as, if not better than, a scanner system operated at, for example, 1000 ft. It is further assumed that detectors of the same size are employed in both systems, (If it is postulated that smaller detectors could be used in space, then we could also use them at lower altitudes to obtain correspondingly better performance). Then based on the S/N relationship for scanners and v/h requirements derived in Ref. 66, a ratio of trade-off parameters of the space system (sym-

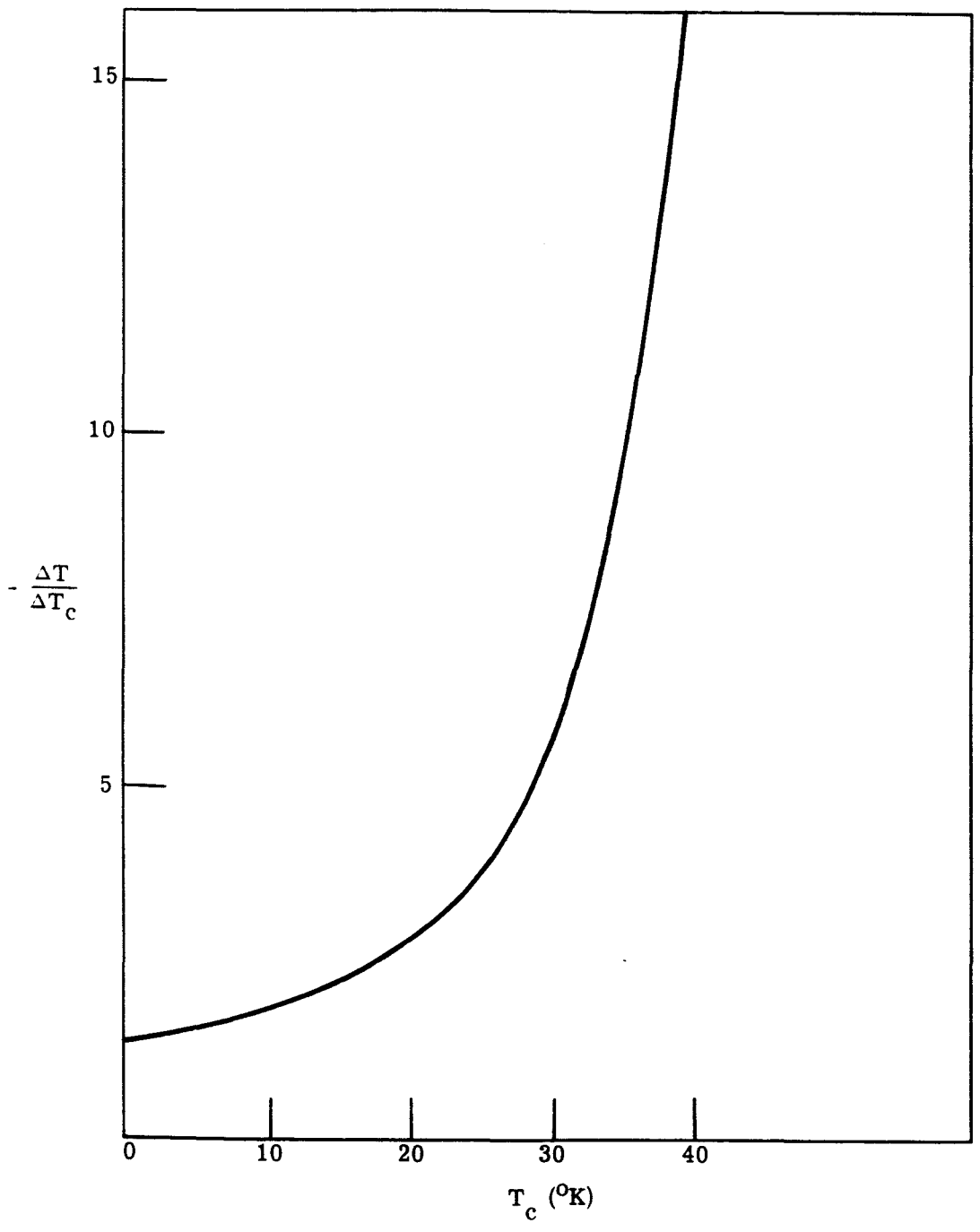

FIGURE 32. SIGNAL-LEVEL STABILITY AS A FUNCTION OF CELL TEMPERATURE

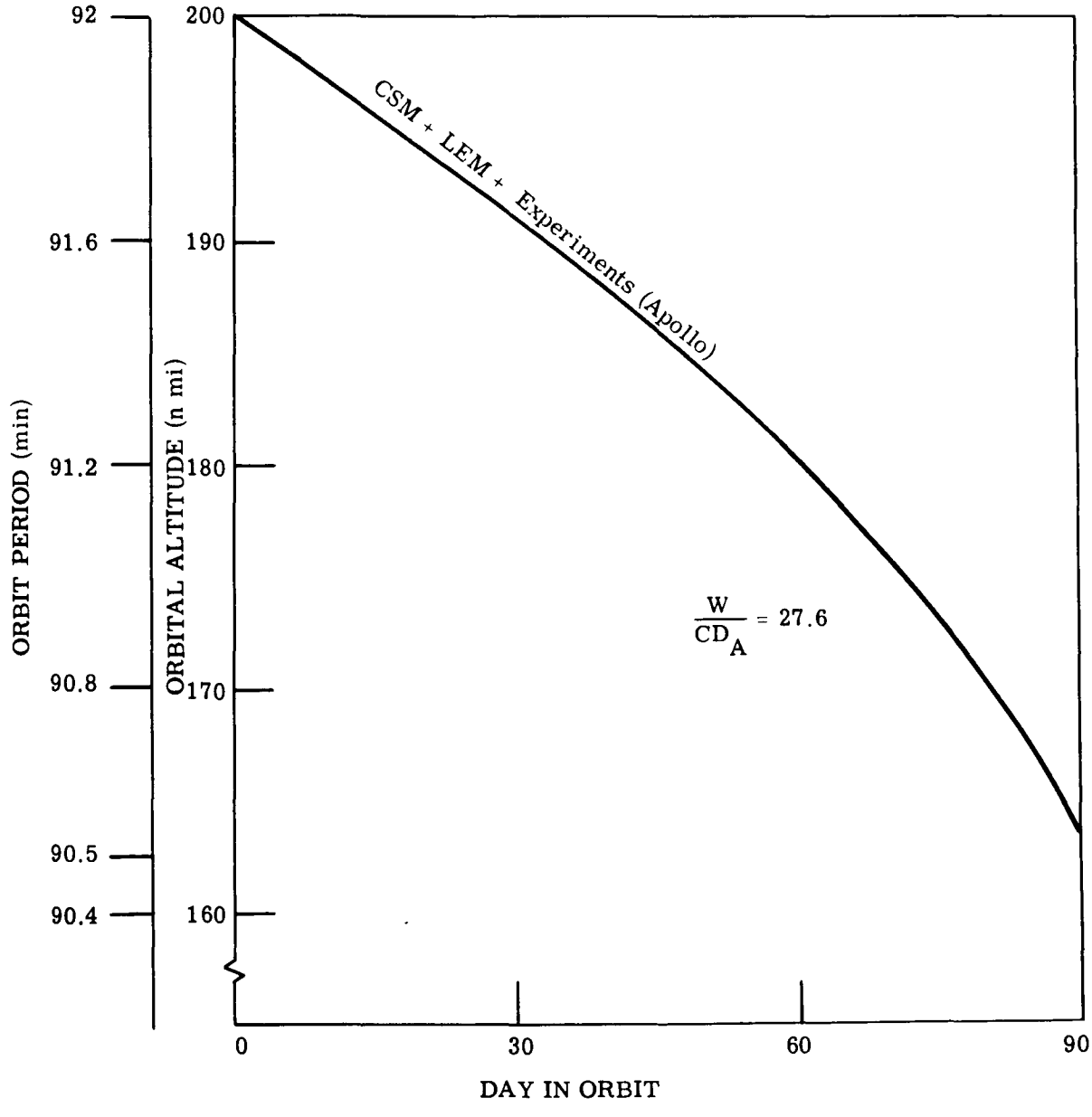

FIGURE 33. APPROXIMATE ORBIT DECAY

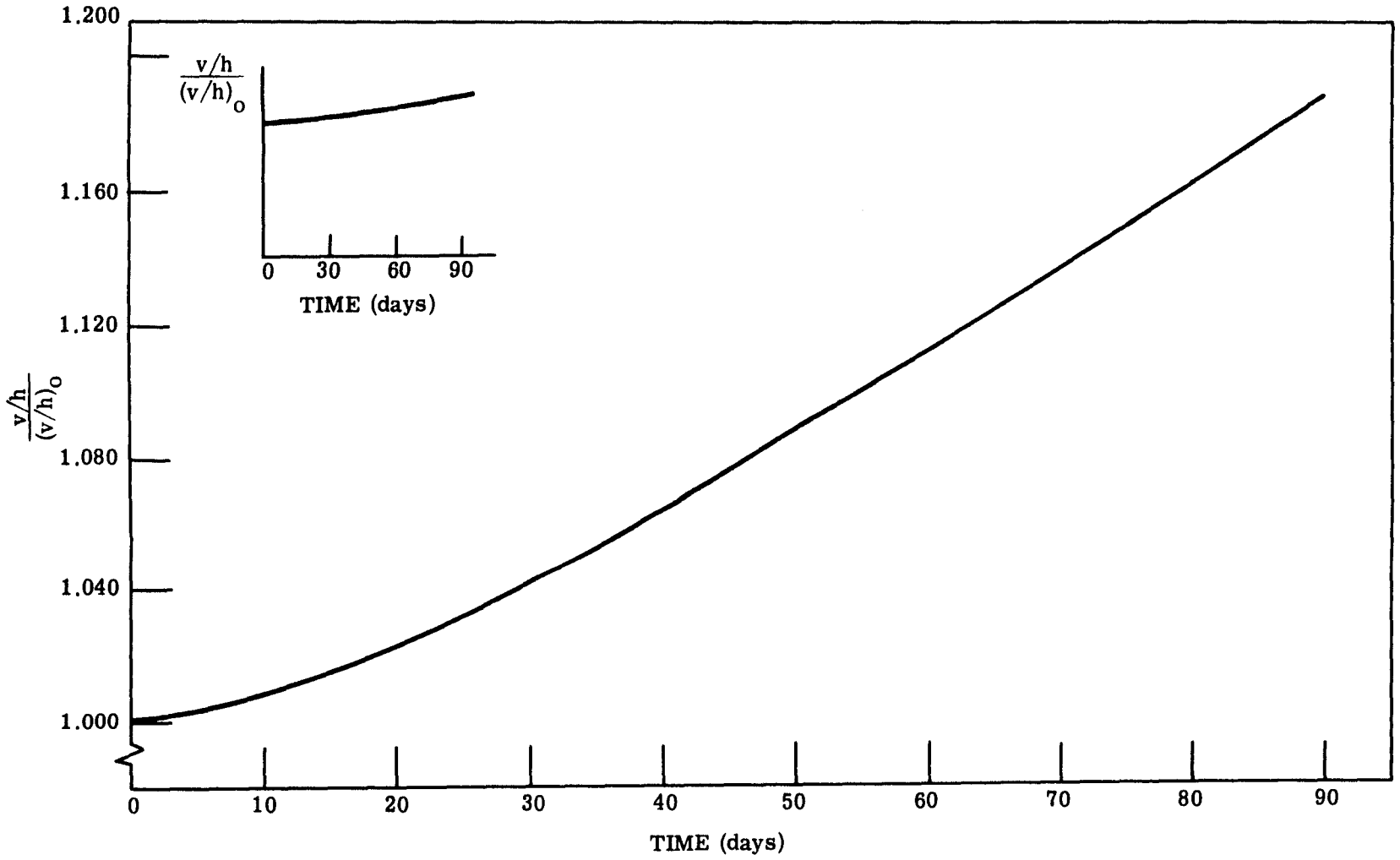

FIGURE 34. VARIATION OF v/h

bols labeled with suffix two) to the airborne system (symbols labeled with suffix one) is given below

$$\text{Equation (1)} \quad \frac{\sigma_2^6}{\sigma_1^6} \cdot \frac{A_2^2}{A_1^2} \cdot \frac{(v/h)_1}{(v/h)_2} \cdot \left(\frac{\theta_1}{\theta_2}\right) \cdot \frac{\ell_2}{\ell_1} = 1$$

where σ = instantaneous angular field of view

A = area of the collecting aperture

v/h = velocity to height ratio

θ = total angular field of view

ℓ = number of detectors in a linear array oriented in the direction of flight.

This equation holds only for extended objects which fill the instantaneous field of view. For our purposes here the same detectors are used in both systems and the choice of wavelength intervals is adjusted so that the loss due to increased path length for the space system is accommodated by sensing in a wider spectral band. This loss of signal could also be adjusted for by an increase in collecting diameter, thereby leaving the spectral intervals the same. However, the comparison between the two systems becomes unnecessarily complicated by employing the second scheme, since only general trade-offs are to be investigated here.

Case I. Space borne system to retain same instantaneous angular field of view: $\sigma_2 = \sigma_1$ (a 2 mr IFOV would give 2400 ft. ground resolution at 200 nm). Other characteristics postulated for the airborne system to obtain usable S/N ratio would be such that

$$(v/h)_1 = 6(v/h)_2$$

and we will also assume that

$$\ell_1 = 1$$

$$\theta_1 = 180^\circ$$

$$A_1 = \frac{\pi}{36} \text{ sq. ft.}$$

Therefore, by substitution into Equation 1

$$\frac{A_2^2 \ell_2}{\theta_2} = \frac{+A_1^2}{6\theta_1}$$

But if

$$\theta_1 = \theta_2 \text{ and } \ell_2 = 1$$

Then

$$A_2 = \frac{1}{\sqrt{6}} A_1 = \sim .4 A_1$$

Thus, for the assumption of equal angular resolution, the space borne system requires a smaller collection diameter. This is possible because of the smaller v/h ratio in space.

Case II. Space-borne system to retain same ground resolution: Then $\sigma_1 h_1 = \sigma_2 h_2$, $h_1 = 1000$ ft., $h_2 = 1.2 \times 10^6$ ft. and with same assumptions for system 1 as in Case 1 the following relationship holds:

$$\frac{A_2^2}{\theta_2} \ell_2 = \frac{(1.2)^6}{6} \cdot 10^{18} \frac{A_1^2}{\theta_1}$$

Consider trade off (1), if $\theta_1 = \theta_2$ then,

$$A_2 = 7.2 \times 10^8 \frac{A_1}{\sqrt{\ell_2}}$$

Consider trade off (2), if $\theta_1 = 180\, \theta_2$ then,

$$A_2 = 5.4 \times 10^7 \frac{A_1}{\sqrt{\ell_2}}$$

Thus, we immediately see impractically large collecting diameters and/or very large numbers of detectors would be required.

Case III. Space-borne system to provide reasonable compromise e.g., $\sigma_2 h_2 = 100 \sigma_1 h_1$. Then under the same assumption for v/h, θ, and A as in Case I for system 1 we have:

$$\frac{A_2^2}{\theta_2} \ell_2 = \frac{(1.2)^6}{6} \cdot \cdot 10^6 \frac{A_1^2}{\theta_1}$$

Consider trade off (1), if $A_2 = 10 A_1$ then,

$$\theta_2 = \frac{\theta_1}{5000} \ell_2$$

Consider trade off (2), if $A_2 = 100A_1$ then,

$$\theta_2 = \frac{\theta_1}{50}\ell_2$$

Under the assumption 2, the total field of view of the spaceborne system would be 3.6^o for a single element system. The elemental ground resolution from 200 n miles would be 200 ft. The collecting diameter would be 3.3 ft. Thus systems with collecting aperture diameters of 3 ft. or better may be needed to provide systems with about 40^o total angular field of view that operate with 10 element detector arrays giving 200 ft. ground resolution each. If systems with collecting aperture diameter of 1 ft. are used, then for single element sensors only a small total angular FOV of about 1/25 degree is feasible.

The system trade-off to obtain larger total fields of view, with a collecting diameter on the order of 1 ft. and single detector sensors is to coarsen the resolution. For example, a 600 ft. ground resolution from 200 n miles would permit a total field of view of 26 degrees.

Appendix C

CAPABILITIES OF A PASSIVE MICROWAVE RADIOMETER AND SCANNER

C.1. GENERAL CONSIDERATIONS

To establish the general system criteria for passive microwave systems, the important parameters must be evaluated. Those parameters which govern the system performance include the operational wavelength, the receiving aperture size, the spatial resolution and scan width, and the temperature resolution; each of these is discussed and evaluated.

In any system, trade-offs in performance are available. These trade-offs are evaluated and the results are shown graphically with state-of-the-art limits indicated or assumed. Some projections into the 1970 time period are made. Representative system calculations were made to illustrate the performance which can be expected.

C.1.1. TEMPERATURE RESOLUTION. The receiver's minimum detectable temperature difference is generally expressed as

$$\Delta T = \frac{KT}{\sqrt{B\tau}} \tag{1}$$

where ΔT = rms noise temperature in ^{o}K

K = constant of system, dependent upon the type of modulation used

T = effective system noise temperature

B = equivalent-square pre-detection bandwidth

τ = post-detection integration time

In general, once the wavelength of the system has been established, the value of $\frac{KT}{\sqrt{B}}$ can be readily obtained; thus a figure of merit for the system can be given as

$$\Delta T(\tau)^{1/2} = C \tag{2}$$

Since ΔT is the term desired, we must evaluate it in terms of the integration time (τ) which is dependent upon the following: the number of resolution elements per scan, the instantaneous system field of view, the scanning rate, and the velocity-to-height ratios involved.

For a Rayleigh limited system, ΔT can be expressed as

$$\Delta T \simeq \frac{CD}{1.2\lambda}\left(\frac{2\alpha v}{h}\right)^{1/2} \tag{3}$$

where ΔT is now the system sensitivity (thermal resolution) for a S/N ratio of 1. D is the diameter of the collecting aperture, λ the wavelength of operation, α is the scanning angle, and v/h is the velocity-to-height ratio of the space vehicle from which the measurements are being taken.

The values of v, h, and α are fixed by the space vehicle and the area to be scanned, and thus would be relatively constant. By assignment of values, then, a parametric plot of $\frac{\Delta T}{C}$ vs. D with the wavelength as a parameter can be established; see Figure 35, where the values assigned were v/h = 0.02 and $\alpha = 10^{\circ}$; $\alpha = 10^{\circ}$ gives a path ~40 miles wide from an altitude of 200 nautical miles. (Note: this figure neglects the "fly-back" time of the scanning system.)*

C.1.2. OPERATIONAL WAVELENGTH AND SPATIAL RESOLUTION REQUIREMENTS. To obtain good spatial resolution, it is desirable to use large collecting apertures at very short wavelengths within the limits of receivers and physical limitations of aperture size; however, Eq. 3 implies that system spatial resolution (proportional to $1.2\lambda/D$) and temperature resolution are inverse functions, and, therefore, a compromise is necessary. The selection will be governed by both the resolution and the minimum detectable temperature difference desired as well as other physical limitations. Thus, 6 for a given figure of merit and a given v/h, the temperature-detection ability of a system can be improved only by making the spatial resolution more coarse or by reducing the scan angle.

Microwave receivers with small figures of merit do not currently exist for operation at wavelengths of ~6 or 7 mm or shorter; therefore, there is a lower limit on the wavelengths to be considered here. A plot of the figures of merit vs wavelength is shown in Figure 36. These are given for existing state-of-the-art receivers with an assumed background of 300°K. Bandwidths could be increased to give lower figures of merit, but in many cases the antenna feed's bandwidth limits were approached to attain the values cited. In the region below 10 gc, the systems are generally background limited and thus improvements in the receiver figures of merit would be of little value. Thus, one can conclude that, below 10 gc, single-channel receivers are nearly optimized.

Also to be considered are the atmospheric losses encountered as a function of wavelength. In general, the losses are low at wavelengths longer than 2 cm and are relatively low in a

*Errors in ΔT due to neglect of "fly-back" time could increase ΔT in the worst case by the $\sqrt{2}$ since inclusion would effectively increase α by a factor of 2. It should be possible to keep this factor below 10% of α.

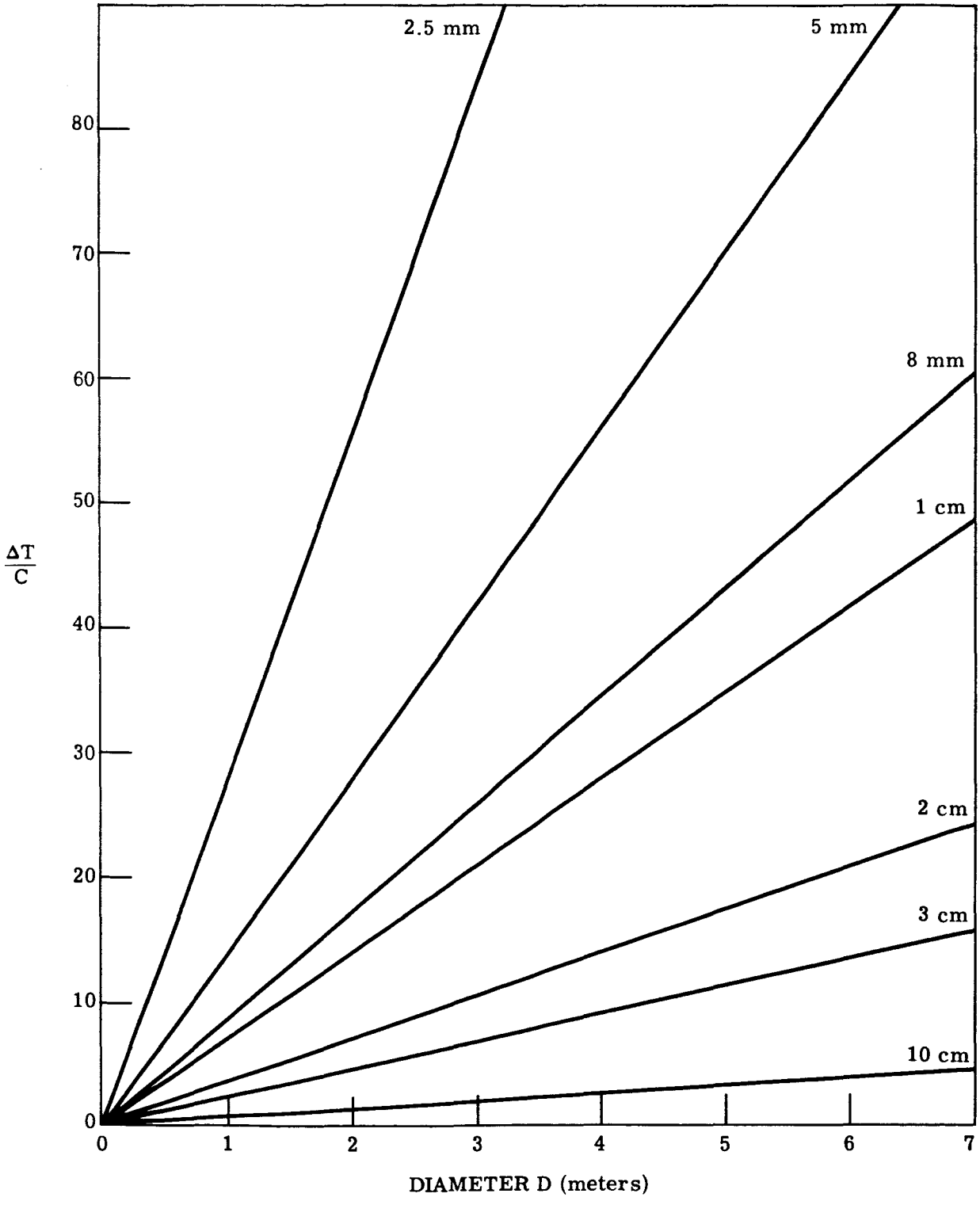

FIGURE 35. $\frac{\Delta T}{C}$ vs. APERTURE DIAMETER. This represents the operation which can be expected for a system at an altitude of 200 n miles, v/h = 0.02, and a scan angle $\alpha = 10^{o}$.

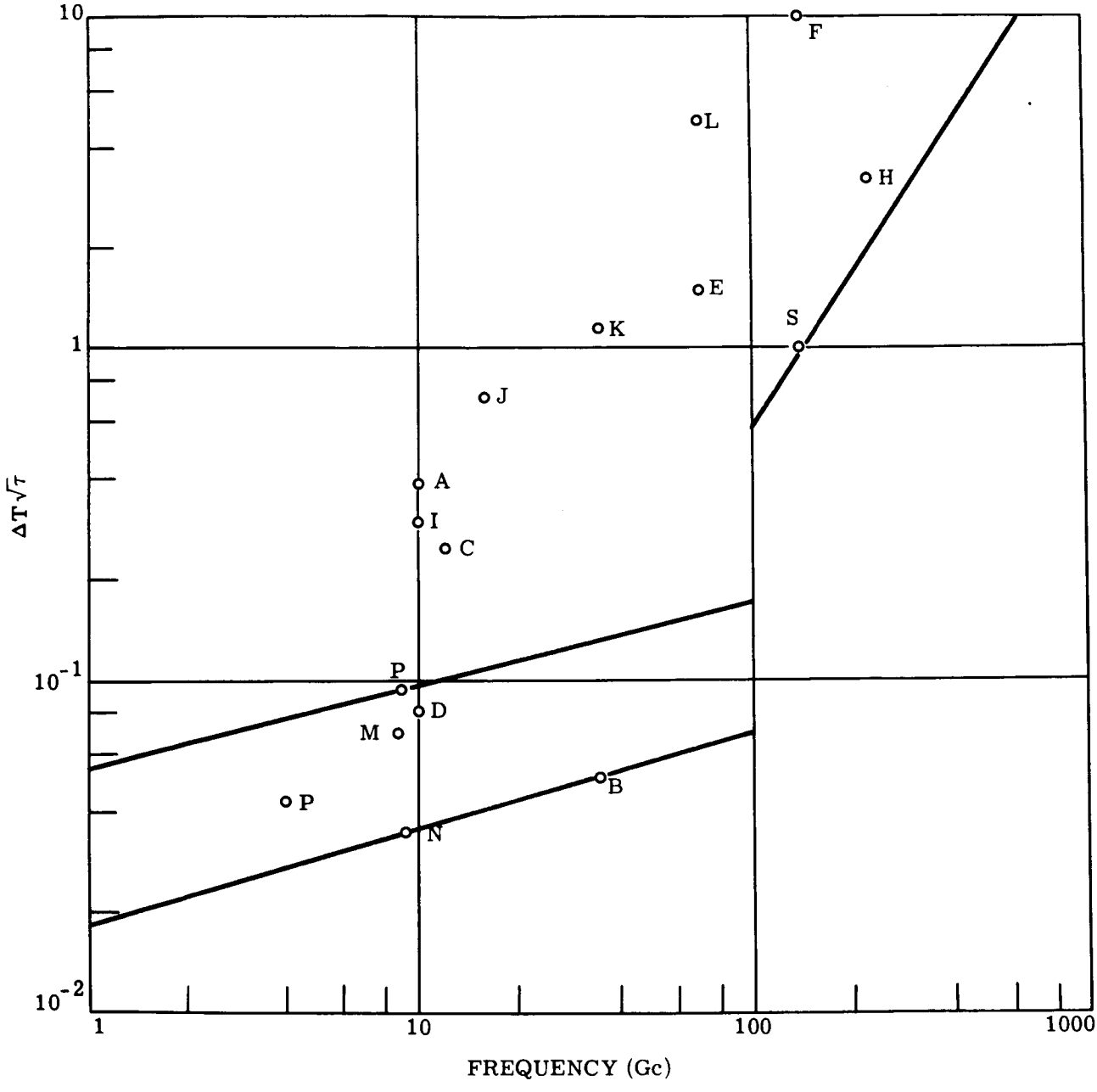

FIGURE 36. RECEIVER FIGURE OF MERIT vs. FREQUENCY
(for state-of-the-art devices)

window occuring at ~8 mm. However, operation in the band between 8 mm and 2 cm is not advisable because higher atmospheric losses occur in this region than on either side of it as seen in Figures 37, 38 and 39.

Several possibilities exist for the antenna structure. It may be designed into the surface of the vehicle, it may be assembled outside the vehicle by a man, or it may be an unfurlable or inflatable type. It is generally believed that the physical size of the collecting aperture should be limited to a diameter of 20 meters or less, which even then would probably necessitate a assembly, inflation, or unfurling of the unit outside the space vehicle. In general, the achievable size of the antenna is a function of its wavelength; until 1970, practically achievable antenna diameters are expected to be as shown in Figure 40. The size limits of the antennas are imposed by the surface tolerances which can be maintained. A dish diameter of 1 meter would give (from 200 n mi altitude) a ground resolution of 2 miles at the shortest wavelength available (8.6 mm). This value is considered to be an upper limit of acceptability on the resolution requirements for most cases.

The angular resolution vs. diameter of an antenna is plotted in Figure 41 with wavelength as a parameter. Also shown are the practical limits which can be assumed for the 1970 time frame.

Selections of the wavelength for operation and the aperture size would be determined primarily by the resolution required to map particular sources. Thus, if one assumes the use of the maximum aperture attainable at each wavelength, the wavelength to be used is determined by the resolution requirements. Then the system temperature resolution capabilities can be established, and the value of the system will thus be determined for each particular usage according to the trade-offs already established.

It should be pointed out that the transmission losses have not been considered in the equations and will degrade the operation to a varying extent. The degree of degradation will depend on the operating wavelengths chosen. Since the best detectivity as well as a minimum physical aperture size is required, this requires that λ be chosen for optimum operation. Therefore, the selection would generally be the 8-mm region at a sacrifice of slightly increased atmospheric losses.

With the selection of λ and the maximum and minimum limits on the aperture size, the minimum values of detectable signals can be determined. For example:

$$\Delta T = 0.43^{\circ}K$$

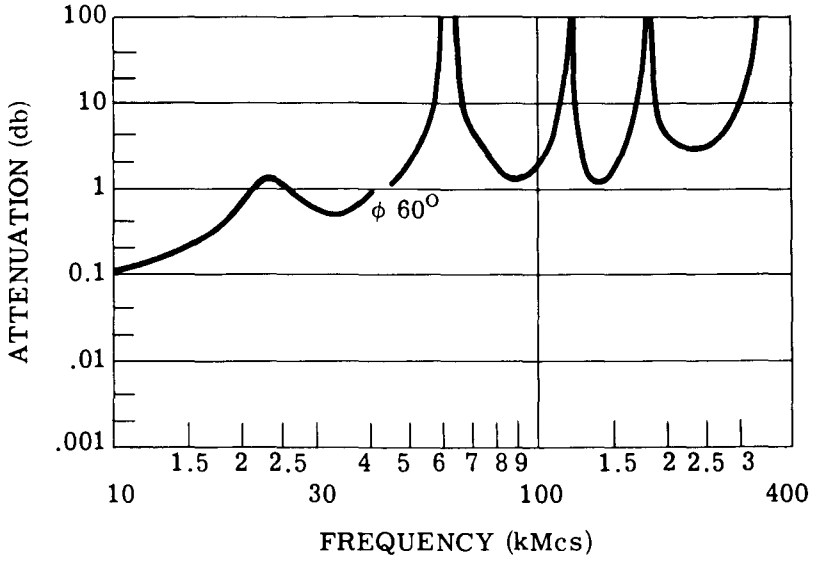

FIGURE 37. TOTAL ATMOSPHERIC ABSORPTION
(Extracted from Ref. 12)

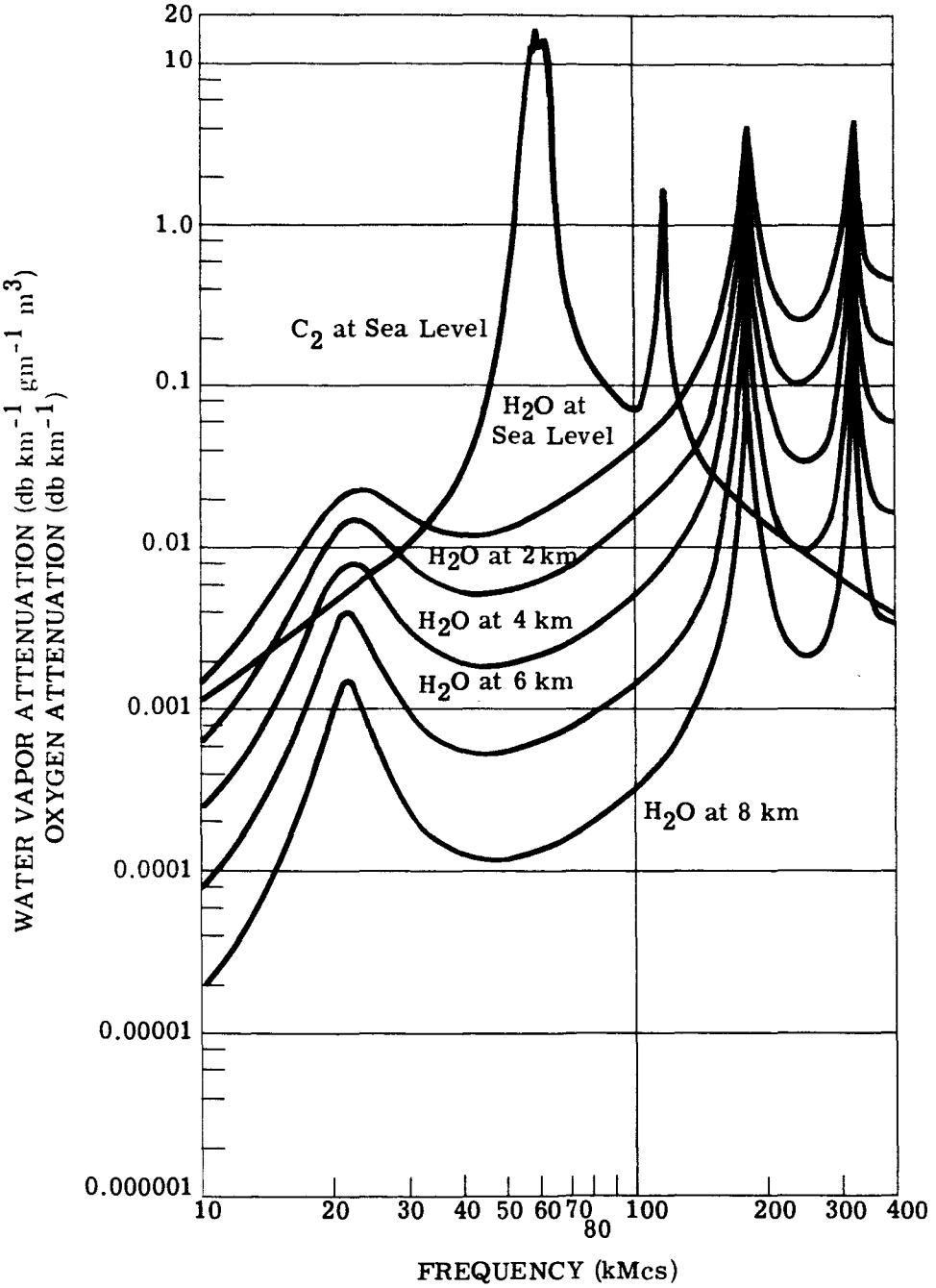

FIGURE 38. OXYGEN AND WATER VAPOR ATTENUATION FOR VARIOUS ELEVATIONS IN THE EARTH'S ATMOSPHERE

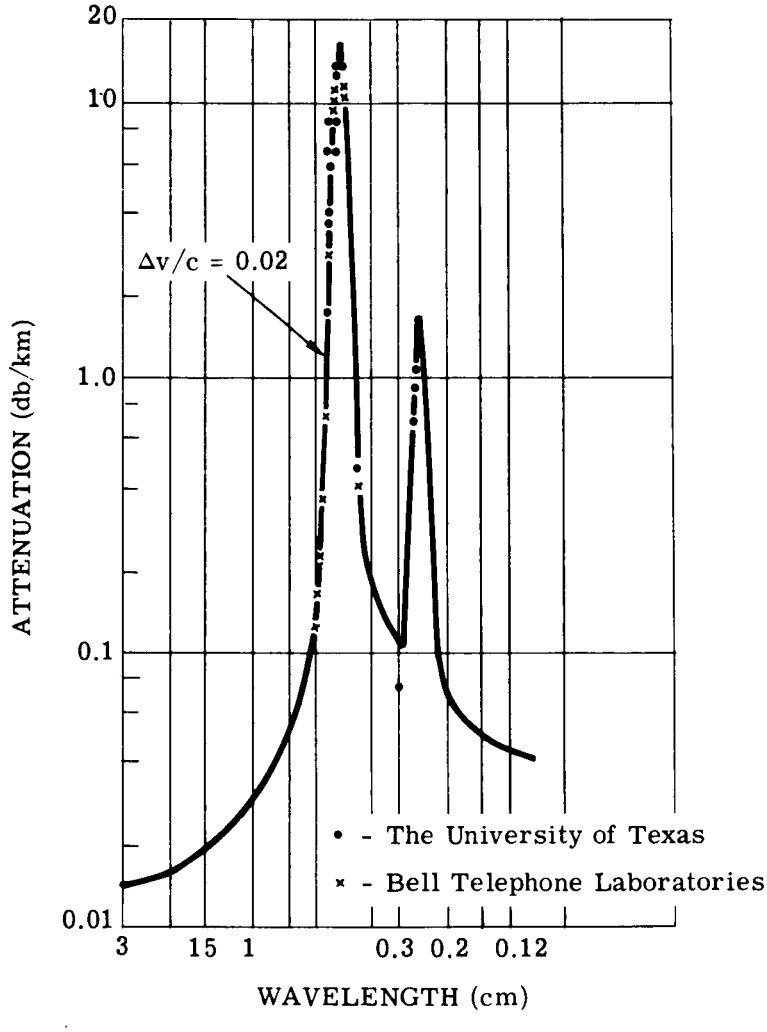

FIGURE 39. ATTENUATION OF OXYGEN vs. WAVELENGTH
(Reprint from Ref. 13, p. 135)

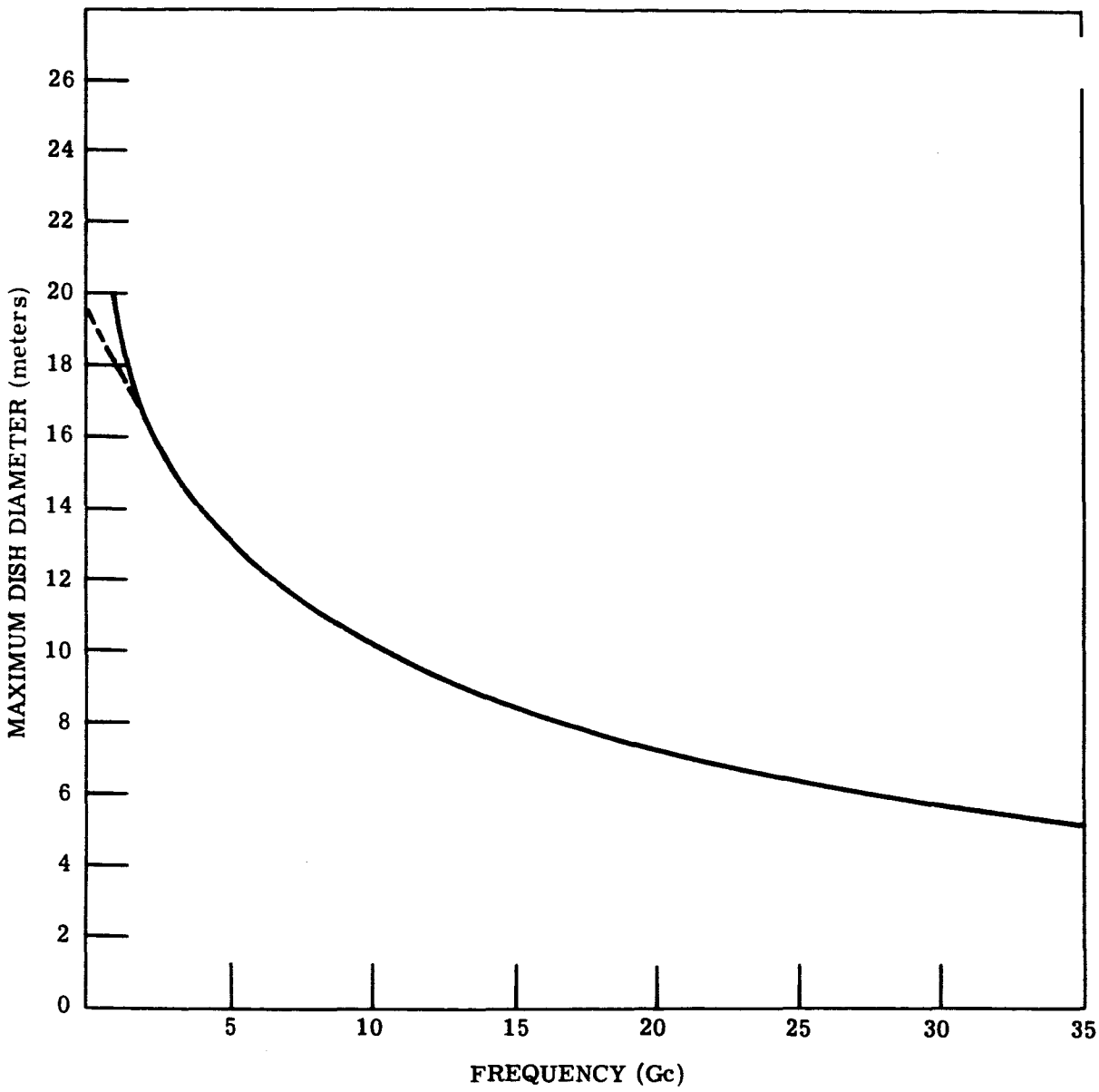

FIGURE 40. ATTAINABLE DISH DIAMETER vs. FREQUENCY. The maximum dish diameter attainable in space with deployable antennas in the 1970 time frame were explored by Hiatt and Larson with these results (Ref. 15).

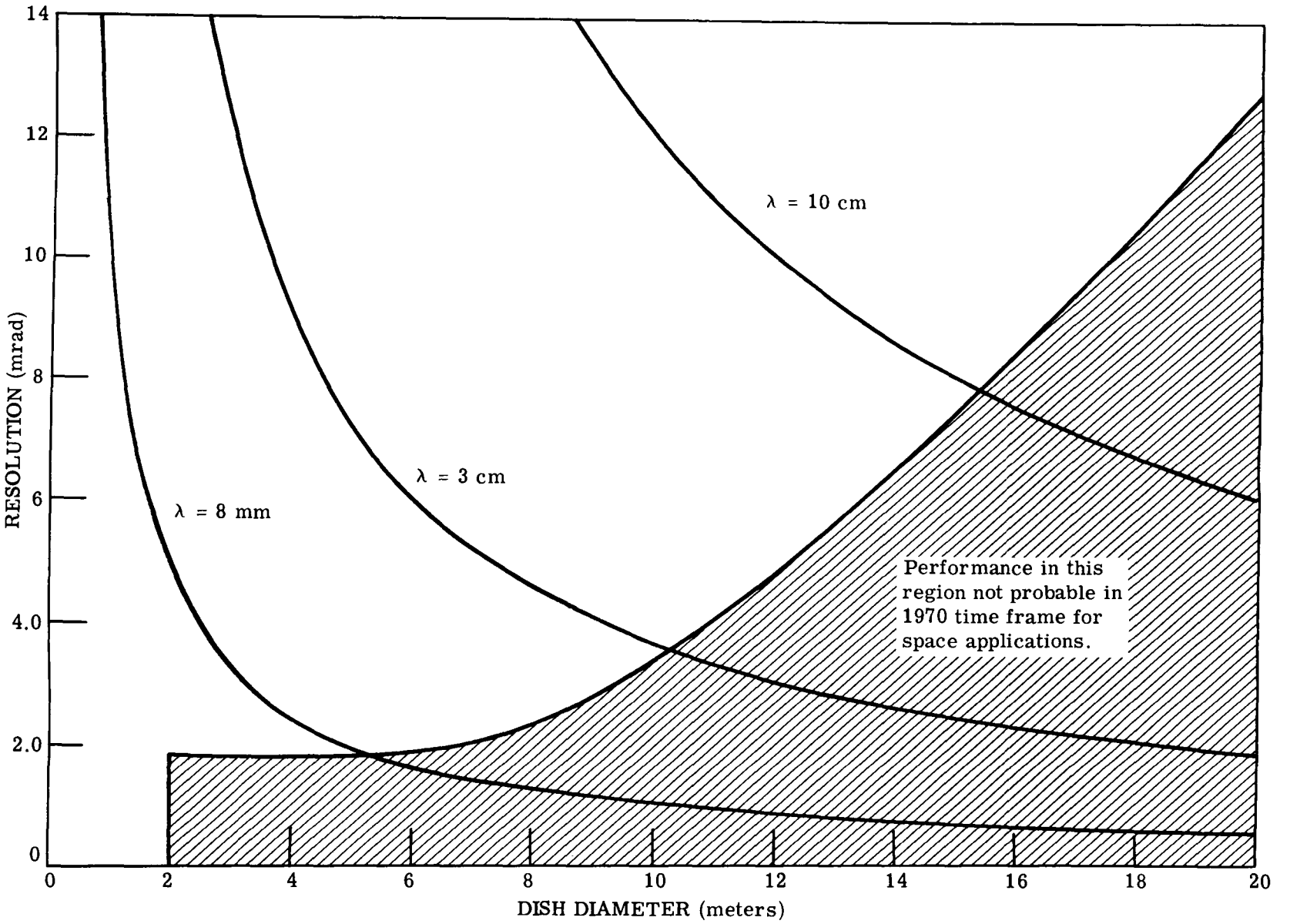

FIGURE 41. RESOLUTION vs. ANTENNA SIZE

and

$$\gamma = 10 \text{ m rad}$$

for the following conditions:

$$D = 1 \text{ m}$$
$$\lambda = 8 \text{ mm}$$
$$C = 5 \times 10^{-2}$$
$$v/h = 0.02$$
$$\alpha = 0.175 \text{ rad}$$

In some cases one may wish to use the scanner as a profiler (i.e., scanning in one dimension only). In Equation 3 the lower limit on the scan angle (α) would then be the resolution limit of the system given by

$$\gamma = \frac{1.2\lambda}{D} \tag{4}$$

Using the previously assumed parameters, the system temperature sensitivity can be obtained. Thus for $\alpha = \gamma$,

$$\Delta T \text{ rms} = 0.10^{\circ}\text{K for a profiler system}$$

C.1.3. SCANNING REQUIREMENTS. Sweeping the antenna for mapping systems presents a very real challenge for the highest resolution systems, particularly when high v/h ratios are encountered. Mechanical sweep techniques have thus far been used in mapping systems. To evaluate the scan rate, it is assumed that the forward velocity and altitude are constant. Thus the scan rate (S) is given by

$$S = \frac{v}{\gamma h} \tag{5}$$

where S is the number of scans/sec. It is assumed that there is no overlap and that the sweep is normal to the flight path about a point normal to the flight path and the earth's surface. Shown in Figure 42 is a plot of the scan rate vs. resolution for various v/h ratios.

C.2. DATA RATES

For any system placed in orbit, the data must be stored and/or telemetered to ground stations. In the following discussion the analog data rates for a passive system will be presented

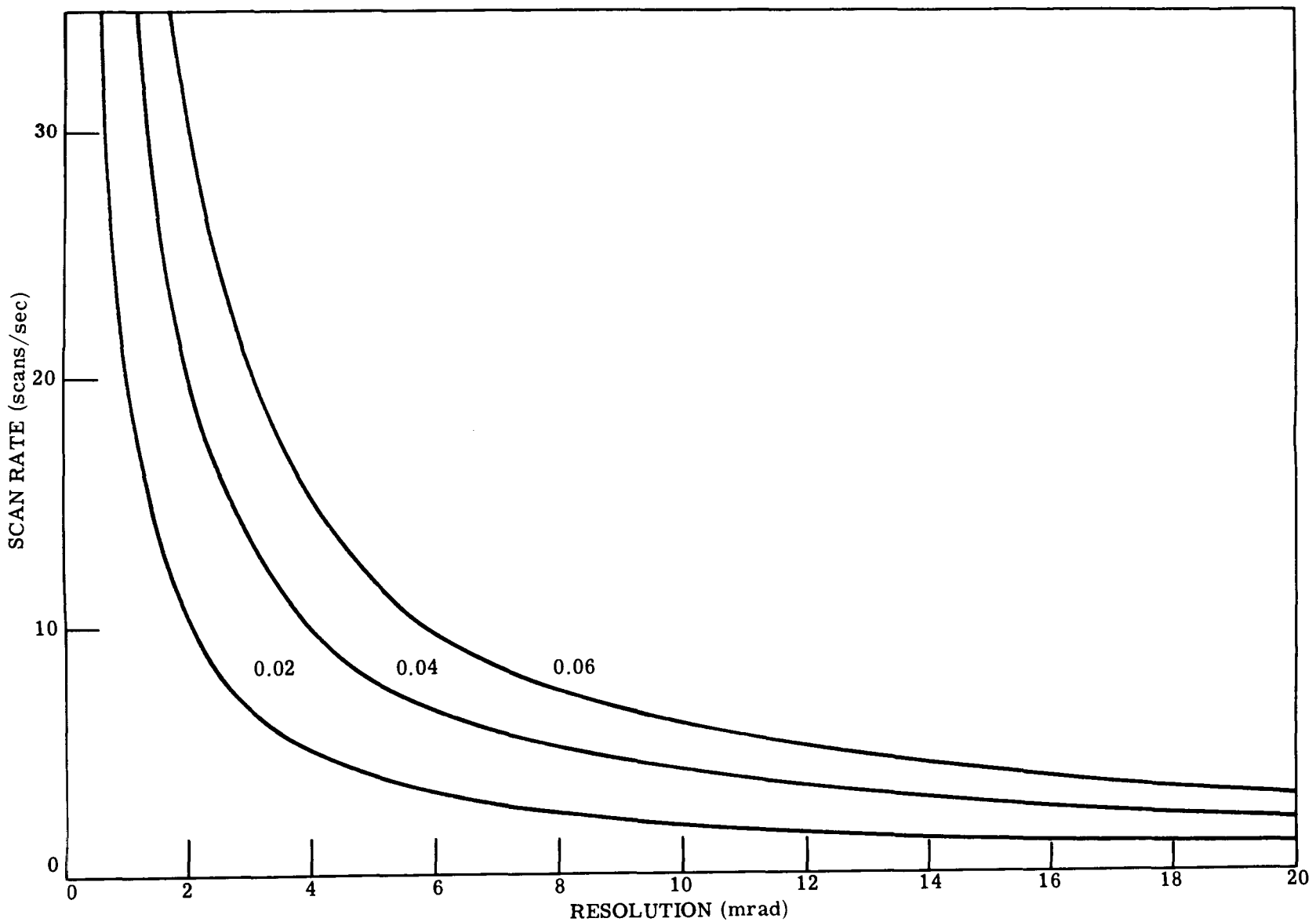

FIGURE 42. SCAN RATE vs. RESOLUTION

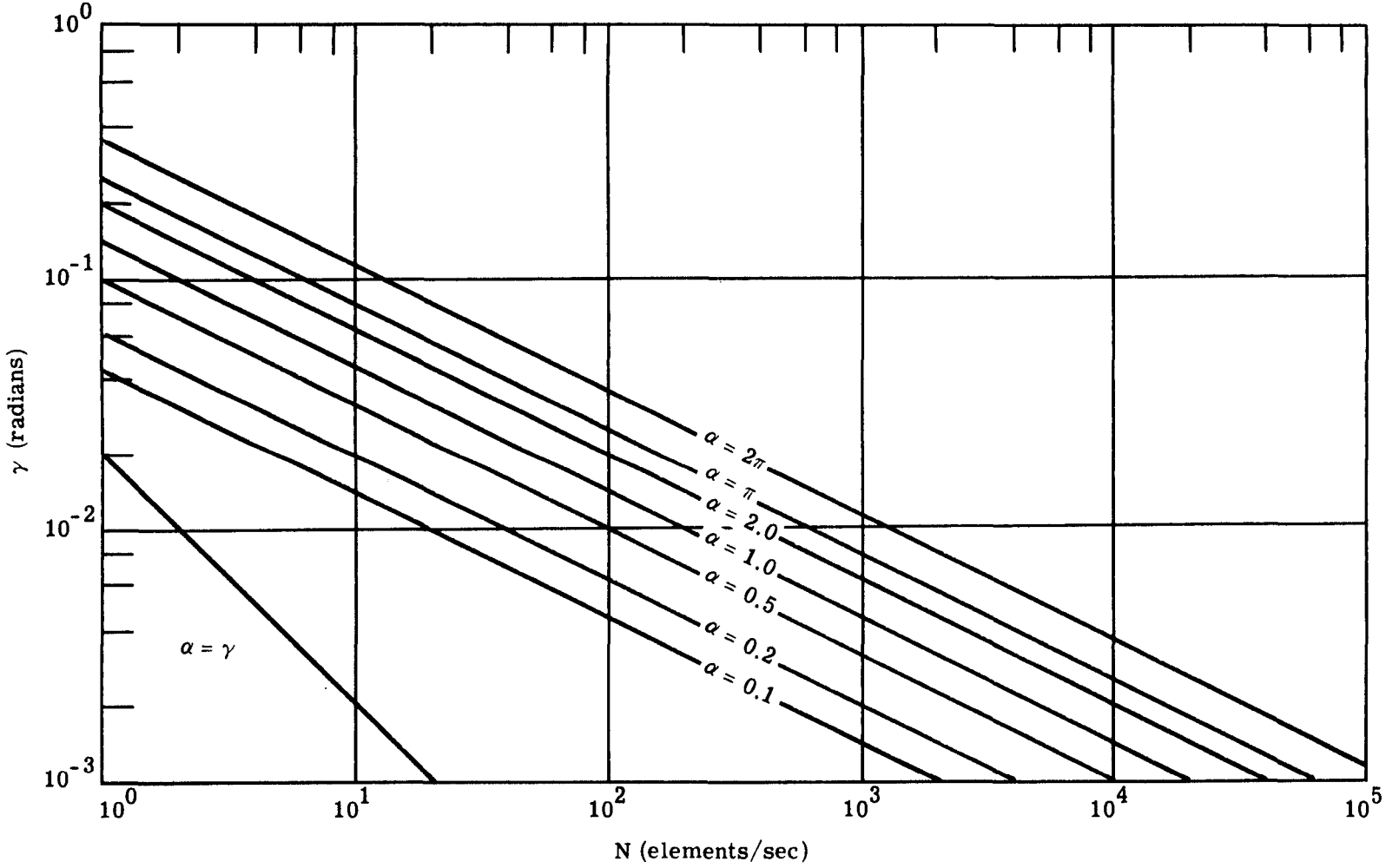

FIGURE 43. ANALOG DATA RATES (N) vs. ANGULAR RESOLUTION (γ) FOR VARIOUS SWEEP ANGLES (α). Assumed v/h = 0.02 sec^{-1}. (Good for any passive system with no overlap.)

for a system in general and given as a function of the variable parameters involved. Those parameters include the scan rate (S), scan width (α), and the instantaneous resolution (γ).

The analog data rate is just the number of resolution elements (N) per unit time and is given in the following expression.

$$N = \frac{\alpha}{\gamma} S \tag{6}$$

where N is given in resolution elements/sec.

By substitution in (6) then

$$N = \frac{\alpha v}{\gamma^2 h} \tag{7}$$

A plot of N vs. γ with α as a parameter is shown in Figure 43. v/h is considered as a constant of 0.02 since the orbit has been previously fixed at 200 nautical miles. Thus for any system the analog data rates can be obtained directly from Figure 43. Again it should be noted that "fly-back" time has not been included and thus the data rates would be effectively greater in all cases except for $\alpha = 2\pi$ radians. This can be corrected for by using an effective scan angle (α_e).

The effective scan angle is given by the following expression:

$$\alpha_e = \frac{\text{data time + "flyback" time}}{\text{data time}} (\alpha) \tag{8}$$

and it is seen that

$$\text{data time + "flyback" time} = 1/S$$

thus

$$\alpha_e = \frac{1}{1 - ST_f} (\alpha) \tag{9}$$

where T_f = "flyback" time. Therefore, when the flyback time has been determined, the effective scan angle (α_e) will be used for determining the data rates.

REFERENCE LIST FOR RADIOMETER vs. FREQUENCY SENSITIVITY

A - Attainable using tunnel Diode Amplifiers

B - Reference 67 Airborne Instrument Laboratories

C - Reference 68 Sperry Systems

D - Reference 69 Wiley Systems

E - Reference 70 Royal Radar Establishment, England

F - Reference 70 Royal Radar Establishment, England

G - Reference 71 Electronic Communications, Inc.

H - Reference 71 Electronic Communications, Inc.

I - Reference 72 General Electric

J - Reference 72 General Electric

K - Reference 72 General Electric

L - Reference 72 General Electric

M - Reference 73 Attainable with University of Michigan Maser

N - Planned University of Michigan Parametric Amp/Tunnel Diode Superheterodyne System

P - Reference 74 Airborne Instrument Laboratories Paramp. in Development

BIBLIOGRAPHY FOR APPENDIX C

"Observation of Satellites for Arms Control Inspection," R. S. Rochlin, General Electric Co., J. of Arms Control, Vol. I, No. 3.

"Ocean Waves," W. J. Pierson, Jr., International Science and Technology, June 1964.

"Satellite Reconnaissance Gains," W. S. Heavner, Aviation Week, 22 May 1961, Vol. 26.

"Infrared-Optical Techniques Applied to Oceanography," E. D. McAlister, Applied Optics, Vol. 3, No. 1.

"Proceedings of the Second Symposium on Remote Sensing of Environment," University of Michigan, 4864-3-X, February 1963.

"Proceedings of the Third Symposium on Remote Sensing of Environment," University of Michigan, 4864-9-X, October 1964.

"Apparent Temperatures of Smooth and Rough Terrain," Sinclair W. C. Cheu, Ohio State University, July 1960, AD 251 436L.

"Study of Thermal Microwave and Radar Reconnaissance Problems and Applications," No. 898-10, Ohio State University Research Foundation, July 1960.

"Study of Thermal Microwave and Radar Reconnaissance Problems and Applications," No. 898-17, Ohio State University Research Foundation, October 1961, AD 271 062.

"Polarization and Other Properties of Radar Echoes," Royal Radar Establishment, Technical Note 628, September 1957.

"Some Measurements of X-band Interference Patterns at Low Altitudes Over the Sea," Royal Radar Establishment, Technical Note 581, October 1959 (SECRET).

Gross, V. E., and A. I. Weinstein, "A Cryogenic-Solid Cooling System," paper presented at 10th National IRIS, October 1963.

"Measurement of the Roughness of the Sea Surface from Photographs of the Sun's Glitter," JOSA, Vol. 14, No. 11, pp. 838-850, 1954.

"Microwave Radiometer Measurements Program," W. H. Conway, et al. paper given at 2nd Remote Sensing Symposia, University of Michigan, 1962.

"Application of Microwave Radiometers to Oceanographic Measurements," A. Mardon, October 1963, Presented at 3rd Symposium on Remote Sensing at University of Michigan.

IDA Report of September 1962, "Starlight Study."

"Reflection Properties of Radar Targets," M. L. Meeks, et al. Georgia Institute of Technology 1954 (CONFIDENTIAL).

"Reflection Properties of Radar Targets" (Secret Supplement), M. L. Meeks, et al. Georgia Institute of Technology, 1954.

"Oceanographic Satellite System Concept and Feasibility Study," Final Report, Vol. I, Summary Rept., August 1963, General Electric Company, AD 436 745.

"Investigations of Specular Reflections from Sea Surface at X-band," Royal Radar Establishment No. 1540 and 1301, respectively, 1959 and 1957 (SECRET).

"The Application of Passive Microwave Technology to Satellite Meteorology: A Symposium," J. H. Katz, Memo. RM-3401-NASA, Rand Corporation, August 1963.

"Fine Structure of Water Waves," A. H. Schooley, Symposium on SESS, U. S. Naval Research Lab., October 1960.

"Foliage Penetration Measurements," R. Graham, Conductron Corp., August 1964, Given at 10th Annual Radar Symposium (CONFIDENTIAL).

"Oceanographic Observations from Manned Satellites for Fishery Research and Commercial Fishery Applications," J. F. T. Saur.

"Microwave Radiometric Measurement of Ice and Water," Pascalar, et al., paper given at 3rd Remote Sensing Symposia, University of Michigan, October 1964.

"A Review of Theories and Measurements of Radar Ground Return," Wolff, Electromagnetics Research Corp., Feb. 1960, AD 316 627L (CONFIDENTIAL).

"Final Summary Report on Studies of Non-Acoustic Detection of Submarines," (Project Genny, Task Report No. 11) K. A. McIntrie, General Electric Rept., December 1961, AD 327 753 (SECRET).

"Orbiting Space Station Study," University of Michigan, subcontract from IBM, 1964, Contract AF 04(695)-560. Unpublished.

"Influence of System Parameters on Airborne Microwave Radiometer Design, McGillem and Seling, IEEE Transactions on Military Electronics, Vol. MIL-7, No. 4, October 1963.

"Survey of High Gain Broadband, Passive Deployable Antennas with Scanning Capabilities for Installation in a Manned Satellite," R. Hiatt and R. W. Larson, University of Michigan, Memo 6734-502-M, August 1964.

"MORL Multispectral Experiment Definition," M. R. Holter, F. C. Polcyn, and M. E. Bair, University of Michigan, Rept. 6688-1-F, August 1964.

"Quarterly Progress Report CRQ61-2," R. K. Moore, University of Kansas, NASA Contract NSR17-004-003, 1 Oct. 1964 to 1 Jan. 1965.

"Development of a Low Noise Millimeter Wave Parametric Amplifiers," TRG Inc., July 1964, AD 450 674.

"Microwave Temperature Mapping with an Airborne Antenna," J. B. Roberts, Naval Ordnance Lab/Corona, AD 424 765.

"Design and Construction of Radiometric Mapping Set, AN/AAR-27 (XH^{-1})," F. Arms, et al., Contract AF 33(600)-41234.

"Investigations of Passive Ranging Techniques for Microwave and Submillimeter Surveillance Radiometers," Sperry Gryoscope Co., Syosset, N. Y., WPAFB Contract AF 33(616)-7518 (SECRET).

Wiley Electronics Co., WPADC, Contract AF 33(600)-39067.

"Superheterodyne Radiometers for Use at 70 Gc and 140 Gc," R. Meredith and F. L. Warner, presented at the Millimeter Conference, Orlando, Florida, January 1963.

"High Sensitivity, 100 and 300 Gc Radiometers," M. Cohn, et al., presented at Millimeter Conference, January 1963.

"Project Genny," General Electric Co., ONR Contract NOWR 2628(00)-1960.

"The Ruby Maser," J. J. Cook, M. E. Bair, and L. Cross, University of Michigan, Project MICHIGAN Rept. 2900-288-T, September 1961.

Electronics News, 14 September 1964.

"Final Report on Microwave Research," Bell Telephone Labs., Rept. 27269-K, Contract AF 19(122)-458, March 1956, AD 101 745 (SECRET).

"Iceberg Detection by Microwave Radiometry," Rept. on Experimental Flight Test Programs, AC Spark Plug Division, General Motors Corporation, U. S. Coast Guard Contract No. TcG-41456, July 1960.

"Domains of the Marine Microbiologists," by C. E. Zobell, Scripps Institute of Oceanography, given at Symposium on Marine Microbiology, 1963.

Appendix D
RADAR SYSTEM CONSIDERATIONS

It is the purpose of this appendix to present the theory and analysis required to compute the radar operating parameters, transmitted peak power, transmitted average power, and system data rate, for a satellite borne surveillance system used for agricultural and oceanographic applications. Both noncoherent radar and coherent, synthetic aperture; radar sensors will be treated.

To facilitate the calculations the flat earth assumption was used. This assumption provide results of high accuracy out to elevation angles on the order of 50^{o} to 60^{o}. Beyond this angle earth curvature effects become of increasing importance. All equations presented here will be derived using this assumption.

All calculations and curves presented in this appendix will assume a satellite altitude of 200 n mi and a satellite velocity of 2.4×10^{4} fps.

Separate discussions and sections will be devoted to noncoherent and coherent radar systems in the remainder of this report. Sample calculations are made to illustrate the use of the results that are derived.

D.1. NONCOHERENT RADAR SYSTEM CONSIDERATIONS

The power requirements are derived for a satellite borne surveillance system using noncoherent radar sensors. It will be shown that both hardware and theoretical constraints have to be considered in the computation of these requirements. Data rates encountered by this type of system are also considered.

D.1.1. PEAK POWER REQUIREMENTS. The reflected target power intercepted by the radar system antenna is given by the familiar expression

$$P_R = \frac{P_T G^2 \lambda^2 \sigma}{(4\pi)^3 R^4} \tag{1}$$

where P_R is the received peak power in watts,

P_T is the transmitted peak power in watts,

G is the antenna gain,

λ is the operating wavelength of the system,

σ is the radar cross section of the target,

R is the range between the target and the antenna.

In terms of the transmitted power this relation can be rewritten in the form

$$P_T = \frac{(4\pi)^3 P_R R^4}{G^2 \lambda^2 \sigma} \tag{2}$$

The detection capability of such a system is limited by the system noise power given by

$$P_n = F_0 kTB \tag{3}$$

where P_n is the noise power,

k is Boltzmann's Constant (1.38×10^{-23} joules - $^oK^{-1}$),

T is the effective system temperature,

F_0 is the system noise figure,

B is the system predetection bandwidth.

The required transmitted power can be expressed in terms of the receiver noise power (for a signal-to-noise ratio of unity) as follows

$$P_T = \frac{(4\pi)^3 F_0 kTBR^4}{G^2 \lambda^2 \sigma} \tag{4}$$

The system antenna gain, G, can be related to the system antenna aperture area by the familiar expression

$$G = \frac{K_1 A}{\lambda^2} \tag{5}$$

where K_1 is a constant (has a value of ~10 for a rectangular aperture), and A is the aperture area (assumed to be rectangular for this analysis and equal to $D_a \times D_R$, where D_a is the azimuth aperture and D_R is the range aperture); therefore,

$$P_T = \frac{(4\pi)^3 F_0 kTBR^4 \lambda^2}{K_1^2 D_a^2 D_R^2 \sigma} \tag{6}$$

The target cross section can be related to the system range resolution, r_R, the system azimuth resolution, r_a, and the target backscatter coefficient, η, by the expression

$$\sigma \doteq \eta r_a r_R \tag{7}$$

For a side looking radar (noncoherent), the azimuth resolution is just equal to the length of ground wetted by the antenna beamwidth in the azimuth direction, i.e.,

$$r_a = K_3 \beta_a R \tag{8}$$

where β_a is the antenna azimuth (3 db) beamwidth,

and K_3 is a constant (has a value ~1.1 to 1.2)

The antenna beamwidth is related to the antenna aperture by the familiar expression

$$\beta_a = \frac{K_2 \lambda}{D_a} \tag{9}$$

where K_2 is a constant (having the value of 1.2 for Rayleigh Limited operation),

thus,

$$r_a = \frac{K_2 K_3 R \lambda}{D_a} \tag{10}$$

If the flat earth assumption is used for range, namely that $R = h\ (\cos\ \theta)^{-1}$, the azimuth resolution becomes

$$r_a = \frac{K_2 K_3 h \lambda}{D_a \cos\ \theta} \tag{11}$$

where θ is the antenna elevation angle,

and h is the antenna altitude.

Figure 44 shows a plot of the product of the azimuth resolution and the cosine of the elevation angle as a function of system operating wavelength for fixed values of azimuth aperture. The range resolution of the system is a function of the system pulse width, γ, and can be expressed in the form

$$r_R = \frac{\gamma c}{2 \sin\ \theta} \tag{12}$$

where c is the velocity of propagation in free space (3×10^8 m $\sec^{-1}$).

This expression says that narrow pulse widths are required to obtain fine range resolution (see Figure 45). From Figure 45, it can be seen that to obtain range resolutions on the order of 10 ft, pulse widths on the order of 3 to 15 nanoseconds are required for reasonable elevation angles ($> 10^o$). However, certain system and hardware constraints have a direct bearing on the narrowness of the obtainable system pulse width. First, the system must be capable of transmitting the pulse. This requires the system bandwidth be sufficient to transmit the frequency information in the pulse, i.e., to a good approximation this implies the pulsewidth-bandwidth product be at least unity. Second the pulse must contain at least one and probably more cycles of the transmitting frequency (it will be assumed here that $\gamma f_c = 10$ is a sufficient criterion, f_c being the transmitter frequency). Third, there is a hardware constraint which must be con-

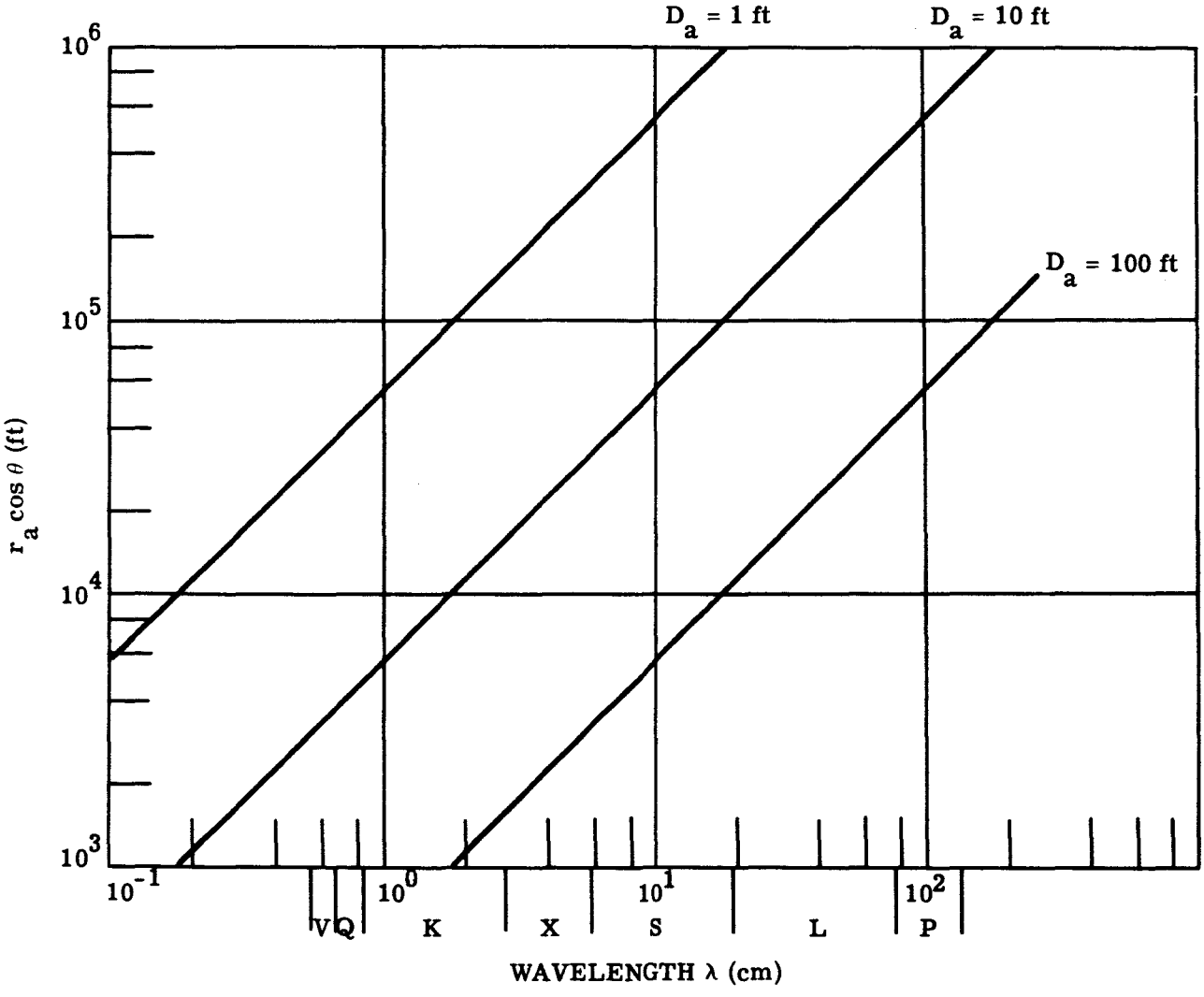

FIGURE 44. AZIMUTH RESOLUTION FOR SATELLITE ORBITING AT 200-n mi ALTITUDE

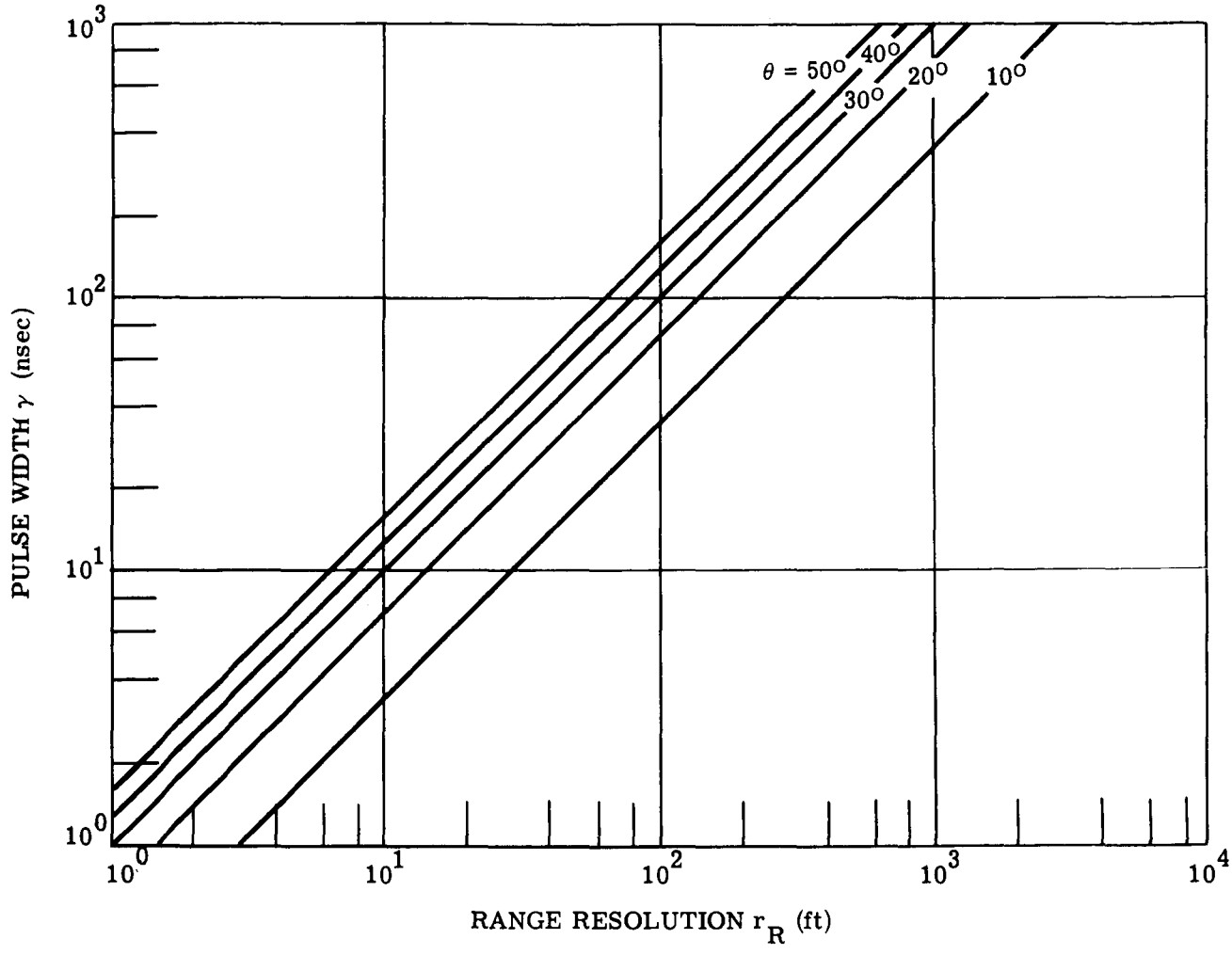

FIGURE 45. PULSE WIDTH DEPENDENCE FOR RANGE RESOLUTION

sidered. Maximum system bandwidths on the order of 10% of the transmitter frequency are obtainable, thus when determining the required pulse width of the system range resolution is not the only constraint or variable involved. What the above discussion implies is that system resolution will be on the order of 10 ft at high operating frequencies (short wavelengths); however, the bandwidth and frequency constraint limits the system range resolution to between 25 to 100 ft at the long wavelength end of P-band (133 cm). For noncoherent radar systems the system azimuth resolution will undoubtedly be larger than the range resolution, and since little is gained by having fine range resolution and coarse azimuth resolution, a square resolution element will be assumed whose dimensions are determined by the system azimuth resolution; therefore the above discussion was of academic interest only when applied to noncoherent radar. The discussion will be more applicable to the coherent radar discussion to follow since these systems have much better azimuth resolution capabilities (on the order of the obtainable range resolution).

Considering the above discussion the system peak power requirement becomes

$$P_T = \frac{(4\pi)^3 F_0 kTBR^2}{K_1^2 K_2^2 K_3^2 D_R^2 \eta} \tag{13}$$

Substituting

$$D_R = \frac{K_2 \lambda}{\beta_R} \text{ (see Figure 46.)} \tag{9}$$

then

$$P_T = \frac{(4\pi)^3 F_0 kTBR^2 \beta_R^2}{K_1^2 K_2^4 K_3^2 \lambda^2 \eta} \tag{14}$$

Now the antenna range beamwidth, β_R, can be related to the illuminated ground swath width, W, by examination of the illumination geometry shown in Fig. 47. It is obvious that

$$R_2^2 = h^2 + (h \tan \theta + W)^2 = h^2 \sec^2 \theta + 2 hW \tan \theta + W^2 \tag{15}$$

$$= h^2 \sec^2 \theta \left[1 + \frac{W}{h} \sin 2\theta + \frac{W}{h} \cos \theta \right]^2 \tag{16}$$

From the Law of Sines it can be seen that

$$\frac{W}{\sin \beta_R} = \frac{R_2}{\sin (90 + \theta)} = \frac{R_2}{\cos \theta} \tag{17}$$

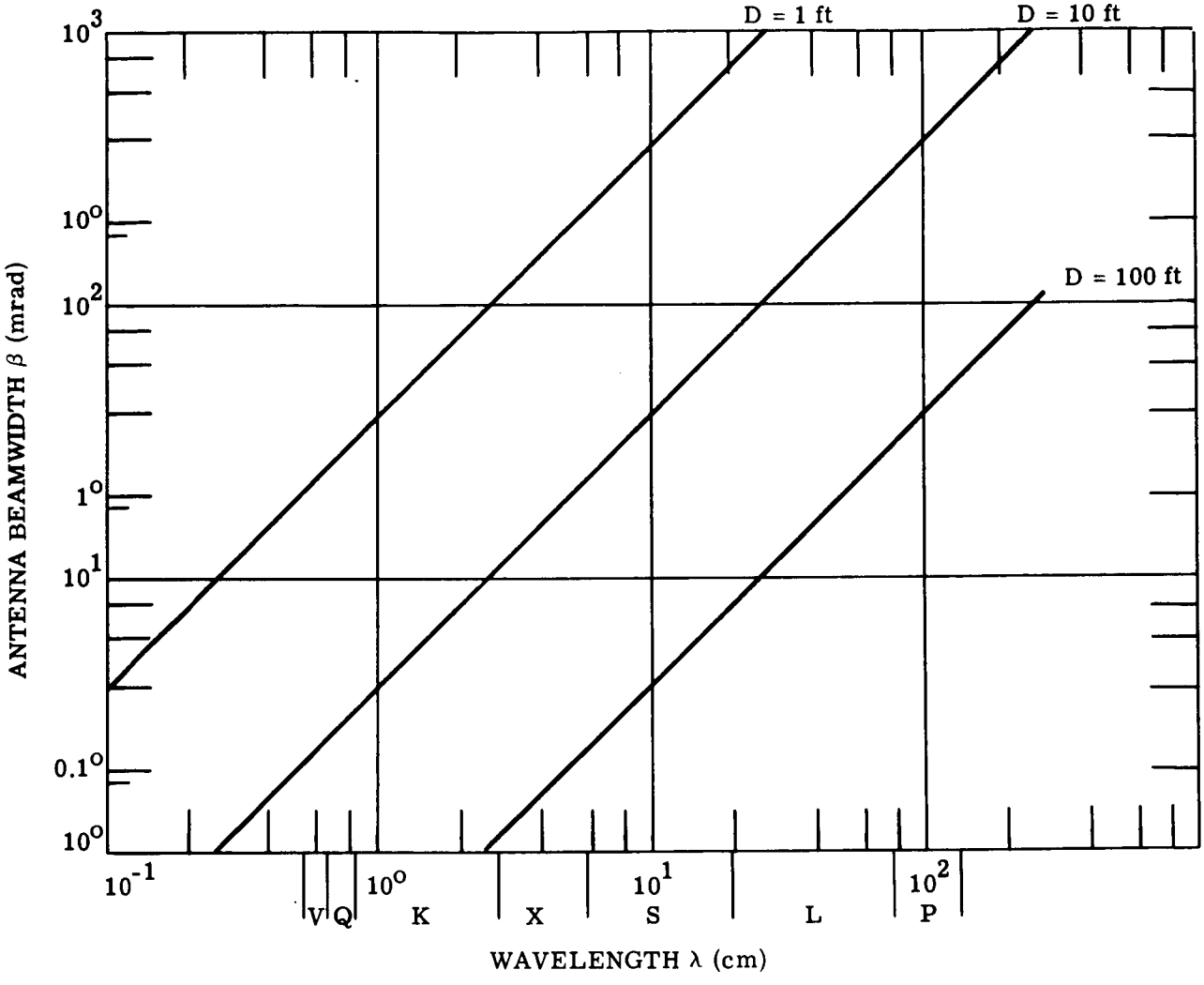

FIGURE 46. ANTENNA BEAMWIDTH

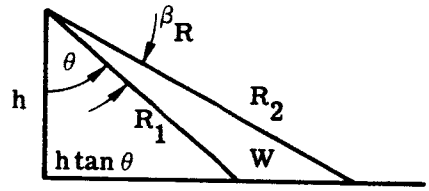

FIGURE 47. ILLUMINATION GEOMETRY

Solving Equation 17 for R_2, substituting into Equation 16 and taking the square root of both sides

$$\frac{W \cos \theta}{\sin \beta_R} = h \sec \theta \left[1 + \frac{W}{h} \sin \theta + \left(\frac{W}{h} \cos \theta\right)^2\right]^{1/2} = Ch \sec \theta \tag{18}$$

or

$$\beta_R = \sin^{-1}\left[\frac{W}{Ch} \cos^2 \theta\right] \tag{19}$$

For illustrative purposes this function is shown plotted in Figure 48 for typical values of β_R. Substituting this value of β_R into Equation 14 and using the flat earth approximation for R

$$P_T = \frac{(4\pi)^3 F_0 kTBh^2 \left\{\sin^{-1}\left[\frac{W}{Ch} \cos^2 \theta\right]\right\}^2}{K_1^2 K_2^4 K_3^2 \lambda^2 \eta \cos^2 \theta} \tag{20}$$

The value of the system noise factor, F_0, is in general a function of system operating wavelength. Attainable system noise figures are shown as a function of wavelength in Figure 49. The dashed lines shows the spread in attained noise figures. It is interesting to note the spread is approximately 3 db at all wavelengths. By using the system bandwidth pulse width constraint, namely that

$$B\gamma \simeq 1 \tag{21}$$

substituting Equations 11 and 12 into 21 and using the equal resolution assumption

$$B \geq \frac{cD_a \cos \theta}{2K_2 K_3 h\lambda \sin \theta} \tag{22}$$

and substituting this into Expression 20 using the minimum bandwidth (minimum system bandwidth is used to minimize the power requirement).

$$P_T = \frac{(4\pi)^3 F_0 kTcD_a h \left\{\sin^{-1}\left[\frac{W}{ch} \cos^2 \theta\right]\right\}^2}{K_1^2 K_2^5 K_3^3 \lambda^3 \eta \sin 2\theta} \tag{23}$$

the system peak power expression can be written in the form

$$P_T = K_0(\lambda) \frac{D_a \left\{\sin^{-1}\left[\frac{W}{ch} \cos^2 \theta\right]\right\}^2}{\eta \sin 2\theta} \tag{24}$$

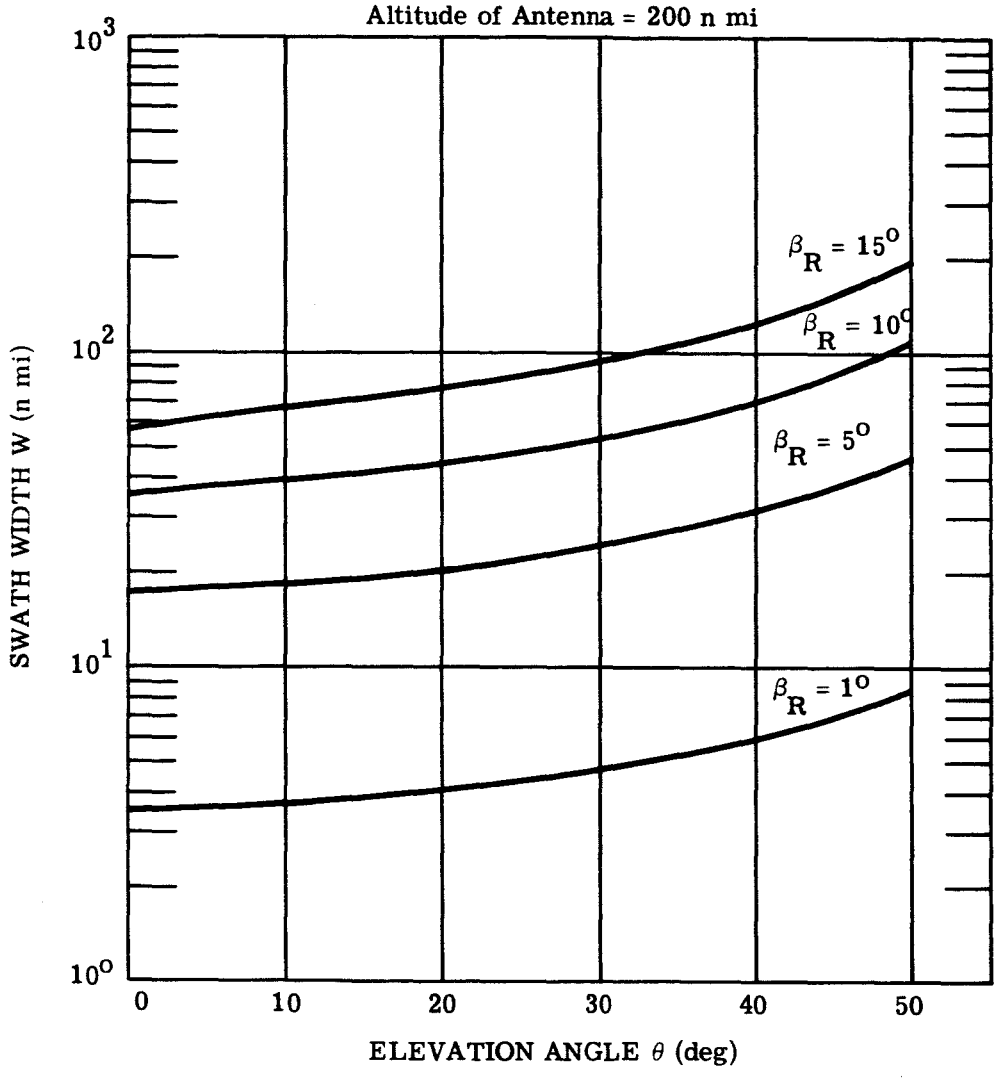

FIGURE 48. ILLUMINATED SWATH WIDTH

UM = Data from University of Michigan reports and radar receiver system

GE = Data from General Electric Project GENNY Report

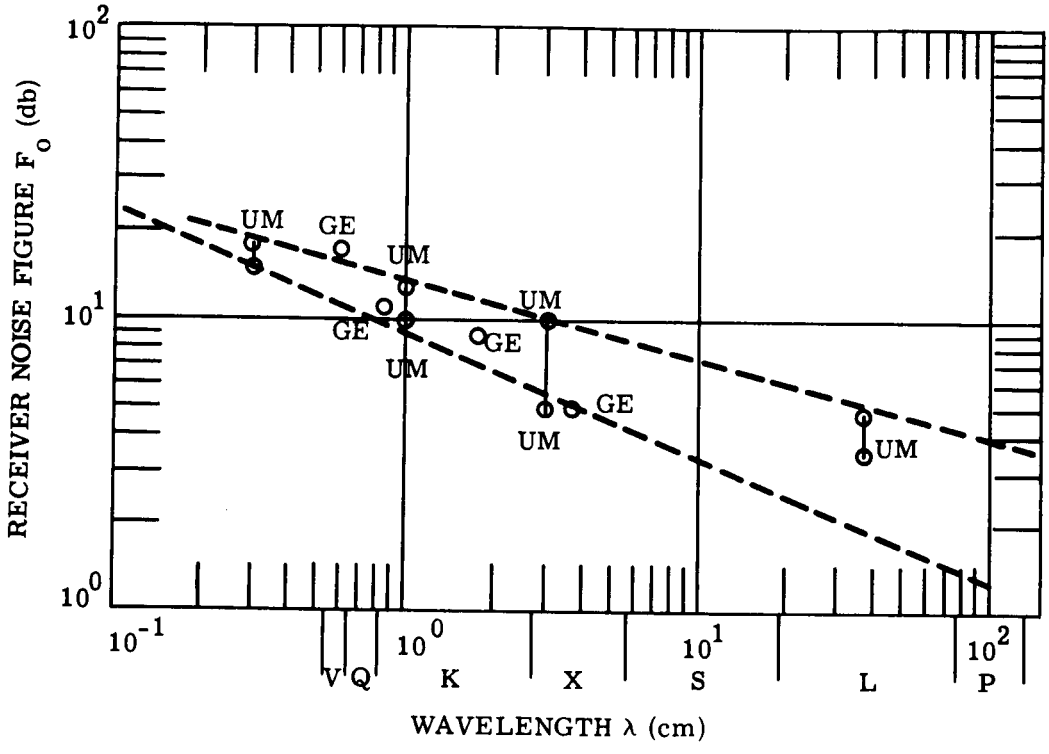

FIGURE 49. ATTAINABLE SYSTEM NOISE FIGURES

where

$$K_0(\lambda) = \frac{(4\pi)^3 F_0 kTch}{K_1^2 K_2^5 K_3^3 \lambda^3} \tag{25}$$

The value of $K_0(\lambda)$ is shown as a function of system wavelength in Figure 50.

D.1.2. AVERAGE POWER REQUIREMENTS. The system average power requirements can be computed knowing the system peak power requirements. The system average power, P_{av}, is

$$P_{av} = P_T \gamma \text{ (prf)} \tag{26}$$

where prf is the system pulse repetition frequency. There is one system constraint which should be mentioned in connection with Equation 24, that is the constraint placed on the system pulse repetition frequency. The system pulse rate should be sufficient to provide at least one pulse return per resolution element. That is to say

$$\text{prf} \geq \frac{V}{\beta_a R K_3} \tag{27}$$

or

$$\text{prf} \geq \frac{V \cos\theta D_a}{K_3 K_2 h \lambda} \tag{28}$$

Actually the pulse rate will have to be set at some multiple, m, of the minimum pulse rate so that there will be sufficient time for the pulse to travel to the target and back to the antenna while the target is in the antenna beam. Therefore the minimum pulse rate that should be used is

$$\text{prf} = \frac{mD_a V \cos\theta}{K_3 K_2 h \lambda} \tag{29}$$

Figure 51 is a plot of the minimum pulse rate as a function of system operating wavelength for various antenna azimuth apertures for a value of m of 5 and an elevation angle of 45^o.

Using the minimum value for system prf and the value of the system pulse as derived in the preceding section

$$P_{av} = K_0' P_T \sin\theta \tag{30}$$

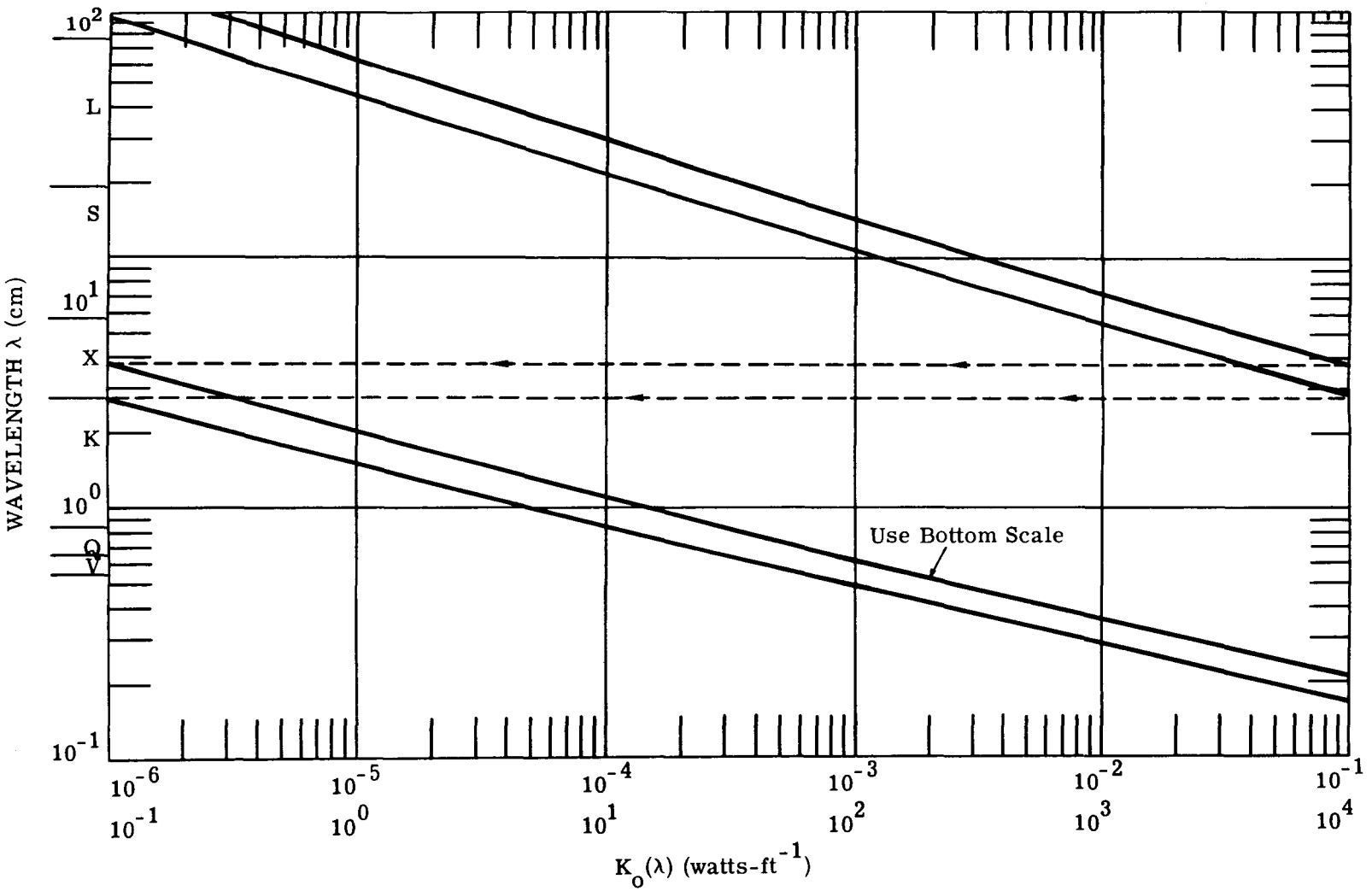

FIGURE 50. $K_o(\lambda)$ vs. WAVELENGTH

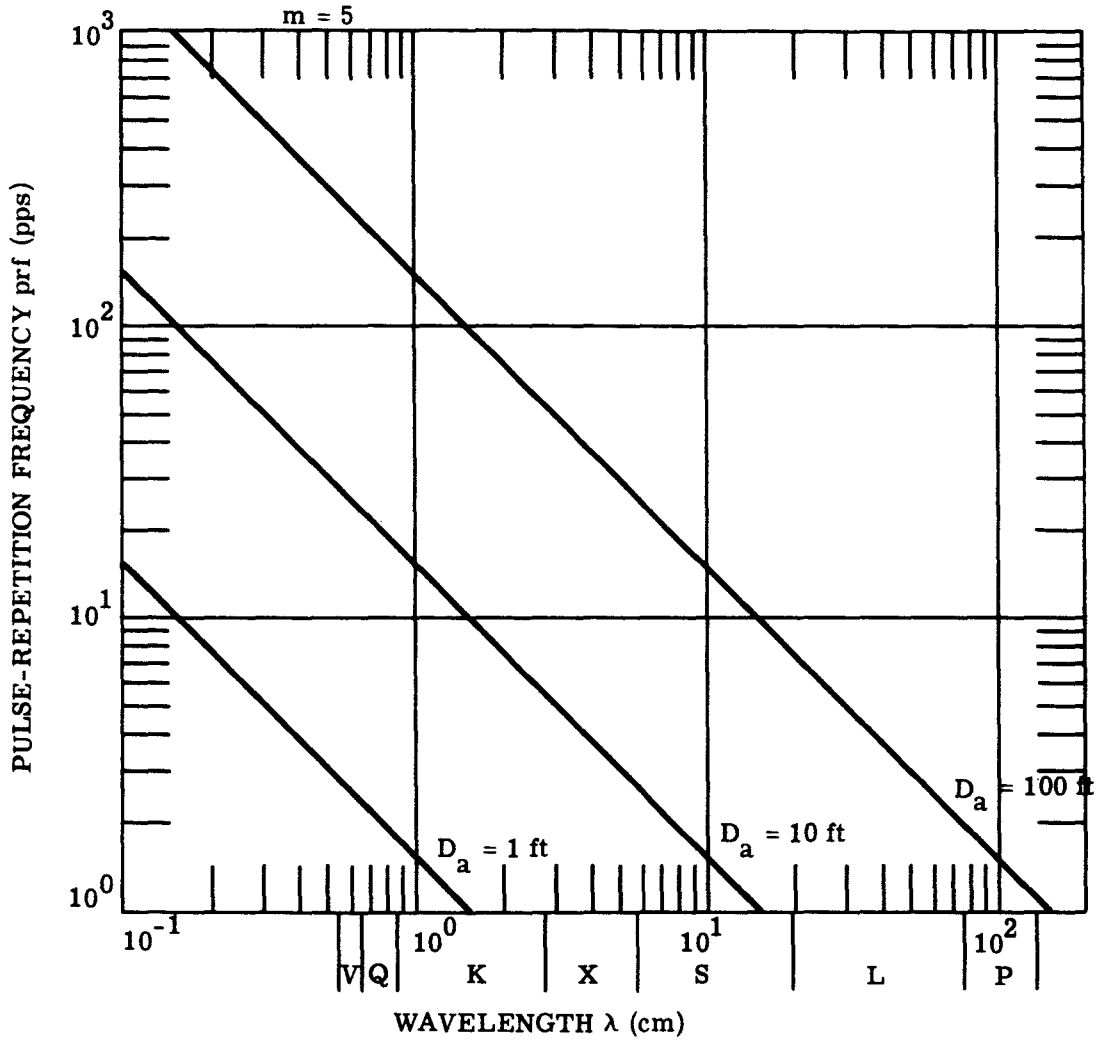

FIGURE 51. NONCOHERENT-RADAR PULSE-RATE REQUIREMENTS

where

$$K_0' = \frac{10V}{c} = 2.5 \times 10^{-4} \tag{31}$$

D.1.3. DATA RATE CONSIDERATIONS. The data rate which must be handled by an orbiting surveillance station equipped with a non-coherent type of radar is a function of several system parameters, namely, the observation geometry, the radar operating parameters, the desired ground resolution, and the number of gray scales required to adequately reproduce the scene being viewed. This section will not consider the gray scale requirement aspect of the data rate problem; however, this can be easily incorporated into the results obtained here since the gray scale consideration introduces only a multiplicative constant (greater than unity) by which the results can be modified.

Excluding the gray scale considerations, the data rate (resolution elements per second) is related to the system observation geometry, the radar operating parameters, and the desired ground resolution area by the expression:

$$DR = A_I A_r^{-1} (prf) \tag{32}$$

where A_I is the ground area illuminated per pulse (see Fig. 52).

A_r is the resolvable ground area

prf is the radar pulse repetition frequency (cps)

DR is the data rate (resolvable ground elements per second)

Each of the area factors on the right side of Equation 32 will be given separate consideration.

D.1.3.1. Computation of Illuminated Ground Area. The flat earth illuminated ground area is shown in Figure 52. The area of the illuminate, being a trapezoid, is equal to the product of the illuminated swath width, W, and average swath length, L. The deviation of relation between swath width, elevation angle, and system range beamwidth, β_R is discussed in Section D.1.1 of this report. This function is shown in a little different format in Figure 53.

The swath length, L, at any given elevation angle can be computed from the expression

$$L = \beta_a R = \frac{\beta_a h}{\cos \theta} \tag{33}$$

However the swath length varies over the illuminated ground area, the limits being

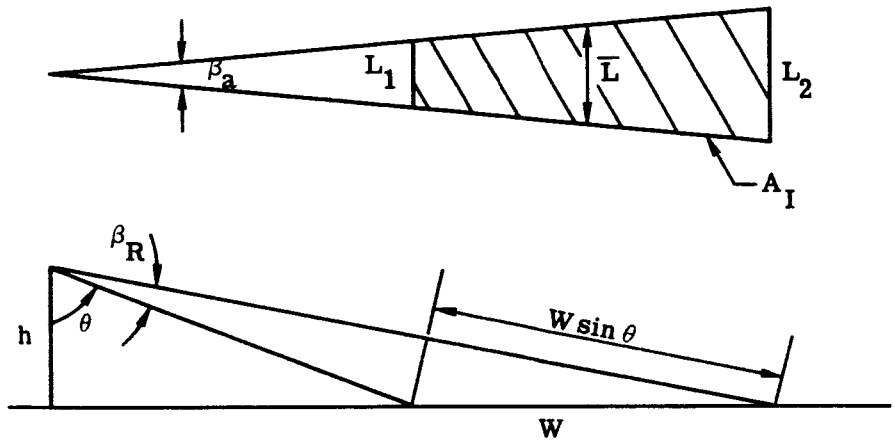

FIGURE 52. ILLUMINATED AREA GEOMETRY

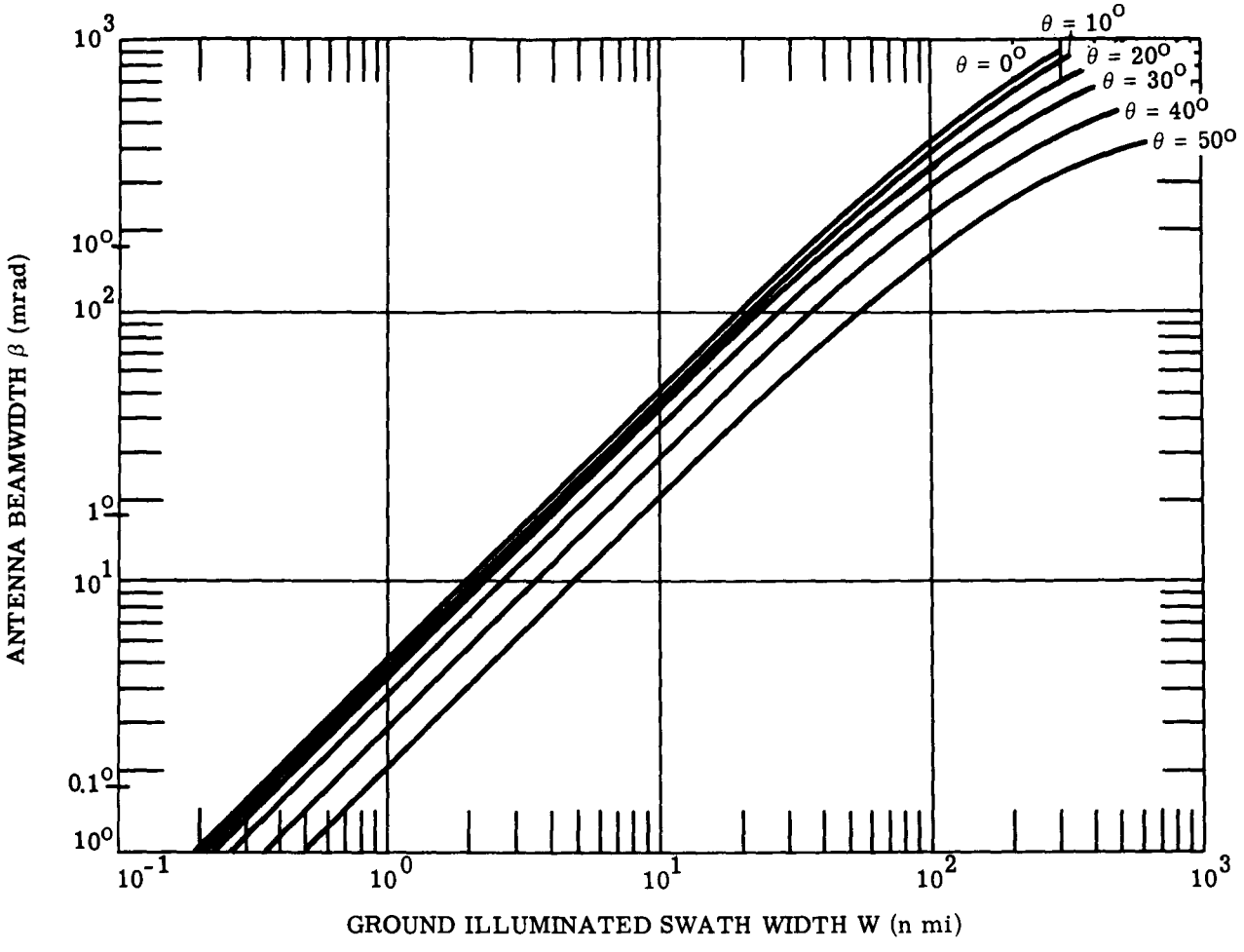

FIGURE 53. GROUND ILLUMINATED SWATH vs. ANTENNA BEAMWIDTH

$$\frac{\beta_a h}{\cos\theta} \leq L \leq \frac{\beta_a h}{\cos(\theta + \beta_R)} \tag{34}$$

However, it can be shown that

$$\overline{L} \simeq \frac{\beta_a h}{\cos(\theta + \beta_R/2)} = \frac{K_2 \lambda h}{D_a \cos(\theta + \beta_R/2)} \tag{35}$$

This function can now be conveniently plotted in a form which will aid in the data rate calculation, thus the illuminated swath area becomes

$$A_I = \frac{WK_2 \lambda h}{D_a \cos(\theta + \beta_R/2)} \tag{36}$$

D.1.3.2. Resolvable Ground Area. The resolvable ground area is given by the product of the system range and azimuth resolution, i.e.,

$$A_r = r_a x r_R \tag{37}$$

or since r_a is assumed to equal r_R

$$A_r = r_a^2 = K_3^2 \beta_a^2 R^2 = \frac{K_3^2 \beta_a^2 h^2}{\cos^2\theta} \tag{38}$$

at any value of elevation angle; however, like the illuminated length r_a is variable over the swath width, therefore it is assumed that

$$\overline{r_a^2} = \frac{K_3^2 \beta_a^2 h^2}{\cos^2(\theta + \beta_R/2)} = \frac{K_2^2 K_3^2 \lambda^2 h^2}{D_a^2 \cos^2(\theta + \beta_R/2)} \tag{39}$$

D.1.3.3. Data Rate Formulation. Substituting Equations 29, 36, and 39 into 32

$$DR = \frac{mVWD_a^2 \cos(\theta + \beta_R/2) \cos\theta}{K_2^2 K_3^2 \lambda^2 h^2} \tag{40}$$

D.1.4. SAMPLE CALCULATION FOR NONCOHERENT RADAR SYSTEM. A noncoherent system operating at 8.6 mm may be useful for the ORL program. This is due to the fact that

short wavelength systems will provide the best system resolution for a given antenna azimuth aperture. Since storage space will be at a premium the maximum azimuth aperture will probably be on the order of 25 to 50 ft and the range aperture will be on the order of 0.5 to 1 ft. These are the system antenna constraints used to compute the system constraints. An elevation angle of 45^{o} is also assumed. These are computed in the following sections.

D.1.4.1. Range Resolution. From Figure 44

$r_a \cos \theta = 10^3$ ft ($D_a = 50$)

$r_a \simeq (1.5 \text{ to } 3) \times 10^3$ ft

for the antenna azimuth aperture of 50 to 25 ft respectively.

D.1.4.2. System Pulse Width

2 to 4 μsec (see Figure 45)

D.1.4.3. System Bandwidth

B = 0.25 to 0.5 mc (see Equation 21)

D.1.4.4. System Pulse Rate

~ 50 to 100 pps (see Figure 51)

D.1.4.5. Transmitted Peak Power. Since Equation 24 is dependent upon the target backscatter coefficient it is important that a value be used which will represent a minimum value so that all elements in the scene will provide sufficient return to be mapped; in actual practice this is not always necessary since the absence of signal can also be used to infer a target's presence in a mapping scheme. Data is sparse for backscatter coefficients at 8.6 mm wavelength, however, some grasses have been measured to have backscatter coefficients on the order of -20 db at 8.6 mm. A value of -40 db will be used in the calculations presented. It is felt by the author that this value is probably a lower bound for targets of interest at this wavelength.

From Figure D.7, $K_0(\lambda)$ has the range of values of 9 to 30. From Equation 24 then

$$(P_T)_{min} = \frac{(9)(25)(2 \times 17.5 \times 10^{-3})^2}{10^{-4}(1)}$$

$$= 2.8 \text{ K watts}$$

however this value is for a signal to noise of unity. For a signal to noise ratio of 10

$$(P_T)_{min} \approx 30 \text{ K watts}$$

$$\therefore (P_T)_{max} \approx 30 \text{ K watts } (4/2)^2 (50/25)(30/9) = 800 \text{ K watts}$$

D.1.4.6. Average Transmitted Power

$$(P_{av})_{min} = (30 \text{ K})(2.5\ 10^{-4})(0.707) \approx 5 \text{ watts (see Equation 31)}$$

$$(P_{av})_{max} \approx 150 \text{ watts}$$

D.1.4.7. Data Rate. Using Equation 40 and Figure 53

$$(DR)_{min} = \frac{(5)(2.4 \times 10^4)(9 \times 10^4)(25)^2(0.707)^2}{(1.2)^5(8.6)^2(3.28 \times 10^{-3})^2(1.22 \times 10^6)^2} \approx 1.2 \times 10^3 \frac{\text{resolution elements}}{\text{sec}}$$

$$(DR)_{max} = (1.5 \times 10^3)(50/25)^2(30/15) = 1 \times 10^4 \frac{\text{resolution elements}}{\text{sec}}$$

D.2. COHERENT (SYNTHETIC APERTURE) RADAR SYSTEM CONSIDERATIONS

In this section the system power, and data rate requirements are considered for the high resolution coherent or synthetic aperture radar operating from a satellite surveillance system. Much of the theory and equations discussed in connection with the noncoherent radar system is also applicable here. The repetition of material will be held to a minimum; however, some repetition is necessary to maintain continuity of the discussion.

D.2.1. PEAK POWER CONSIDERATIONS. As was the case for the noncoherent radar system, the peak transmitted power can be expressed in the form

$$P_T = \frac{(4\pi)^3 F_0 kTBR^4 \lambda^2}{K_1^2 D_a^2 D_R^2 \sigma} \qquad (6)$$

However, a coherent radar system has the advantage of being able to integrate many return signal pulses (signal phase information is used) from a target as the antenna beam passes over the target. For a system integrating n pulses, the signal power increase with n^2 (signal voltage being proportion to the number of integrated pulses). The advantage of this integration technique is the fact that noise power increases linearly with the number of integrated pulses (the noise power resulting from a random noise process); therefore the signal to noise ratio varies directly with the number of integrated pulses (provided sufficient system bandwidth is available), thus the system transmitted power requirements for a coherent radar system using a pulse integration processing becomes

$$P_T = \frac{(4\pi)^3 F_0 kTBR^4 \lambda^2}{nK_1^2 D_a^2 D_B^2 \sigma} \tag{41}$$

The number of pulses, n, which are processed is a function of the system pulse repetition frequency (prf), the system azimuth beamwidth, the range to the target of consideration, and the antenna velocity, V, and can be expressed in the form

$$n = \frac{R\beta_a}{V}(prf) \tag{42}$$

however

$$\beta_a = \frac{K_2 \lambda}{D_a} \tag{9}$$

thus

$$P_T = \frac{(4\pi)^3 F_0 kTBVR^3 \lambda}{K_1^2 K_2 D_a D_R^2 \sigma\,(prf)} \tag{43}$$

In Section D.1.1 it was shown that

$$\beta_R = \sin^{-1}\left[\frac{W}{Ch}\cos^2\theta\right] \tag{19}$$

and since

$$\beta_R = \frac{K_2 \lambda}{D_R} \tag{9}$$

it follows that

$$D_R = K_2 \lambda \left\{ \sin^{-1} \left[\frac{W}{Ch} \cos^2 \theta \right] \right\}^{-1} \tag{44}$$

thus substituting Equation 44 into Equation 43 and using the flat earth assumption for range, the expression for the peak transmitted power becomes

$$P_T = \frac{(4\pi)^3 F_0 kTBVh^3 \left\{ \sin^{-1} \left[\frac{W}{Ch} \cos^2 \theta \right] \right\}^2}{K_1^2 K_2^3 D_a \lambda \sigma (prf) \cos^3 \theta} \tag{45}$$

The target cross section can be related to the system resolution, r, by the expression

$$\sigma = \eta r^2$$

where η is the target backscatter coefficient which in general is an empirical function of radar energy grazing angle

r is the system resolution (the resolvable area is assumed to be square, i.e., the range and azimuth resolution are assumed to be equal)

Substituting Equation 18 into Equation 17

$$P_T = \frac{(4\pi)^3 F_0 kTBVh^3 \left\{ \sin^{-1} \left[\frac{W}{Ch} \cos^2 \theta \right] \right\}^2}{\eta K_1^2 K_2^3 D_a \lambda (prf) r^2 \cos^3 \theta} \tag{47}$$

From coherent radar theory the minimum system resolution (assuming no phase errors are present) is on the order of one half the azimuth aperture; however to achieve this resolution a constraint is placed on the system prf, namely the prf has to be sufficient to sample the doppler information for targets in the azimuth beamwidth, or

$$prf \geq \Delta f_d \tag{48}$$

where Δf_d is the doppler frequency bandwidth of targets in the antenna azimuth beamwidth, β_a. The doppler bandwidth is a function of the antenna velocity (for stationary ground targets) and is easily derived considering the geometry in Figure 54. For a target at angle α with respect to the center of the antenna the doppler frequency shift, f_d, of the return signal will be

$$f_d = \frac{2\mu}{\lambda} \tag{49}$$

from the geometry

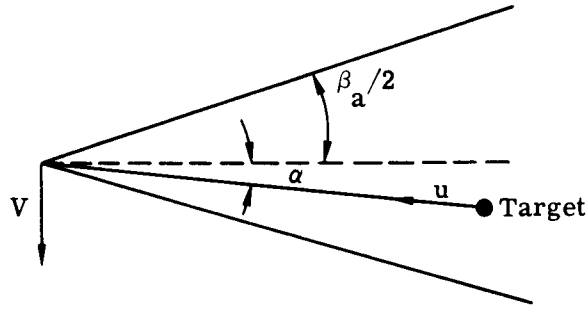

FIGURE 54. TARGET DOPPLER GEOMETRY

$$\mu = V \sin \alpha \tag{50}$$

for small angles (a reasonable assumption)

$$\sin \alpha \simeq \alpha \tag{51}$$

so that

$$f_d = \frac{2V\alpha}{\lambda} \tag{52}$$

therefore the doppler frequency bandwidth, Δf_d, becomes

$$\Delta f_d = \frac{2V}{\lambda}\left[\frac{\beta_a}{2} - \left(-\frac{\beta_a}{2}\right)\right] = \frac{2V\beta_a}{\lambda} \tag{53}$$

remembering that

$$\beta_a = \frac{K_1 \lambda}{D_a} \tag{9}$$

then

$$\Delta f_d = \frac{2K_1 V}{D_a} \tag{54}$$

therefore the doppler prf constraint becomes

$$\text{prf} \geq \frac{2K_1 V}{D_a} \tag{55}$$

In general there is another factor, F (where F has a value of 1 or 2), which enters into the doppler frequency constraint which is dependent upon the type of data processing that is used, thus

$$\text{prf} \geq \frac{2FK_2 V}{D_a} \tag{56}$$

The minimum resolution, $(r)_{min}$ can be related to the minimum antenna displacement between signal pulses as follows

$$(r)_{min} = V\,\Delta t = V\frac{1}{\text{prf}} \tag{57}$$

however

$$= V \cdot \frac{D_a}{2FK_2 V} = \frac{D_a}{2FK_2} \tag{58}$$

The length of the illuminated swath width also places a constraint on system prf. For non-ambiguous range information in the swath width, W, the system prf must be constrained such that (see Figure 52).

$$prf \leq \frac{c}{2W \sin \theta} \tag{59}$$

therefore, combining both prf constraints the system prf is constrained by the inequalities

$$\frac{2FK_2V}{D_a} \leq prf \leq \frac{c}{2W \sin \theta} \tag{60}$$

In theory then for the best system resolution

$$D_a \geq \frac{2FK_2V}{prf} \tag{61}$$

and

$$r \geq \frac{D_a}{2FK_2} \geq \frac{V}{prf} \tag{62}$$

The limiting values of the antenna azimuth aperture, swath angle, and resolution are shown in Figures 55, 56, and 57, respectively as a function of system prf for a surveillance system in a 200 n mi circular orbit.

The swath width constraint must be met to avoid ambiguities in the processing; however, if the antenna aperture constraint is not met system resolution is degraded. The amount of degradation can be approximated by comparing the system resolution under the ideal situation (the minimum value as computed by Equation 62 to that computed from Equation 57). These considerations must be kept in mind when computing the system peak power requirements, of course, the system peak power requirements are also a function of the obtainable system noise powers (Eq. 3), in general this is a function of system wavelength (see Fig. 49).

As was the case with the noncoherent radar system, it is convenient for computational reasons to lump all the system constants and variables into a wavelength dependent constant. To meet this end a system bandwidth constraint must be assumed. As mentioned in Section D.1.1 a bandwidth-pulse width constraint can be employed. Assuming a bandwidth-pulse width product of unity, then the system bandwidth can be expressed in the form

$$B_1 \geq 1/\gamma = \frac{c}{2R \sin \theta} = \frac{2FK_2c}{2D_a \sin \theta} \tag{63}$$

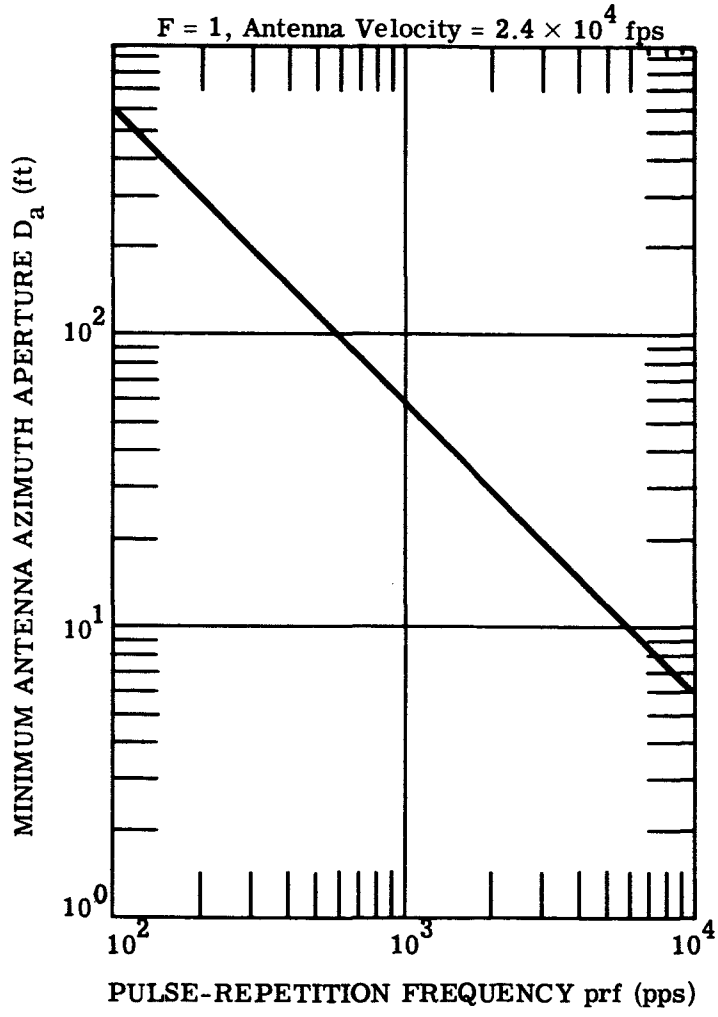

FIGURE 55. MINIMUM ANTENNA APERTURE

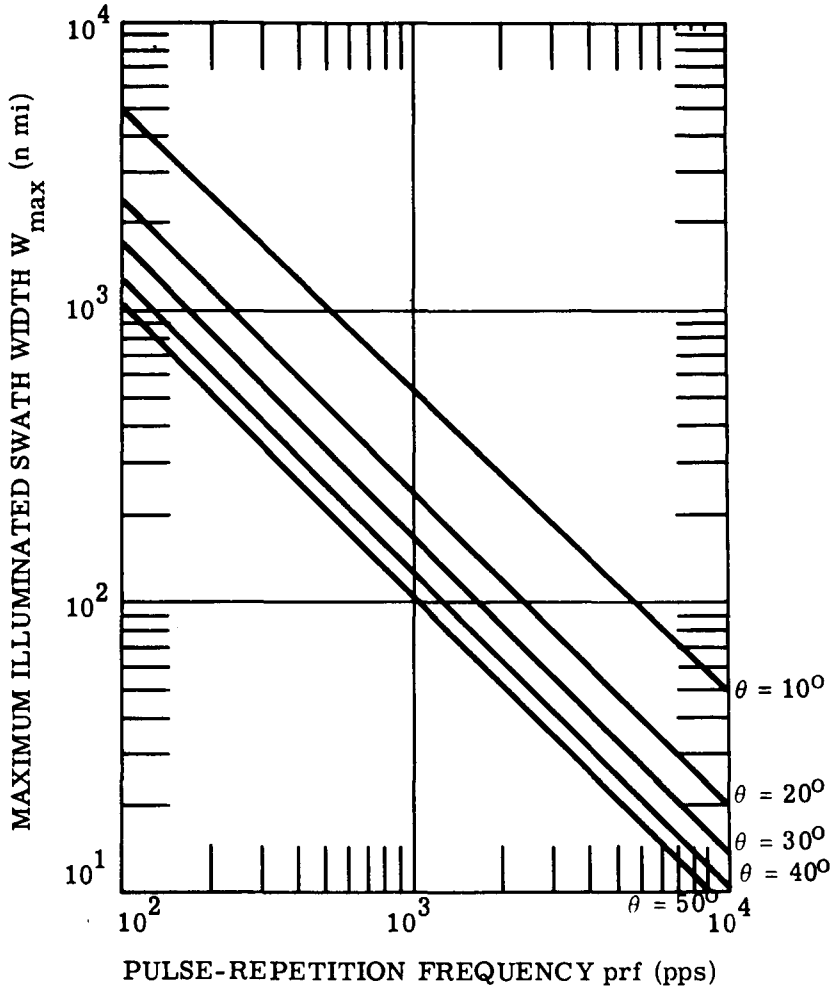

FIGURE 56. MAXIMUM SWATH WIDTH

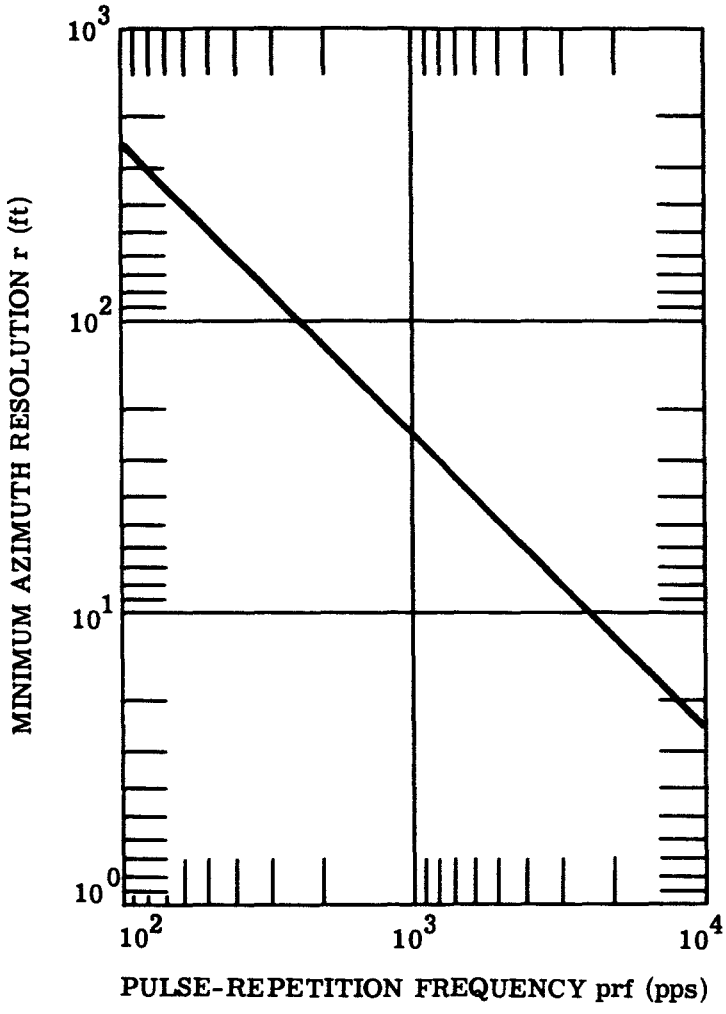

FIGURE 57. AZIMUTH RESOLUTION BASED ON SYSTEM CONSTRAINTS

Substituting Equations 58 and 63 into Equation 47, the transmitted power may be written in the form

$$P_T = K_0''(\lambda) \times \frac{\left\{\sin^{-1}\left[\frac{W}{c\,200}\cos^2\theta\right]\right\}^2}{\eta D_a^4\,(\dot{p}rf)\sin\theta\cos^3\theta} \tag{64}$$

$$= K_0''(\lambda) \times \frac{\beta_R^2}{\eta D_a^4\,(prf)\sin\theta\cos^3\theta} \tag{65}$$

where

$$K_0''(\lambda) = \frac{4(4\pi)^3 F^2 F_0 kTVh^3 c}{K_1^2 \lambda} \tag{66}$$

The value of $K_0''(\lambda)$ as a function of system wavelength is shown in Figure 58.

D.2.2. AVERAGE POWER REQUIREMENTS. As before the average power requirements for the system can be computed from the system peak power requirements. The system average power, P_{av}, is given by

$$P_{av} = P_T \gamma\ (prf) \tag{26}$$

Putting the minimum values of both the pulse width and prf into Expression 26

$$P_{av} = K_0'' P_T \sin\theta \tag{30}$$

where

$$K_0'' = 2V/c = 5 \times 10^{-5}$$

D.2.3. DATA RATE CONSIDERATION. As in the case of the non-coherent radar system the data rate can be computed by determining the values of each term of the right side of Equation 32; however, in the case of the coherent system there are several system constraints which have to be considered. These considerations will be discussed in the following section.

D.2.3.1. Illuminated Ground Area Constraints and Considerations. The size of the illuminated ground area is approximately trapezoidal in shape (see Fig. 52), and its limiting

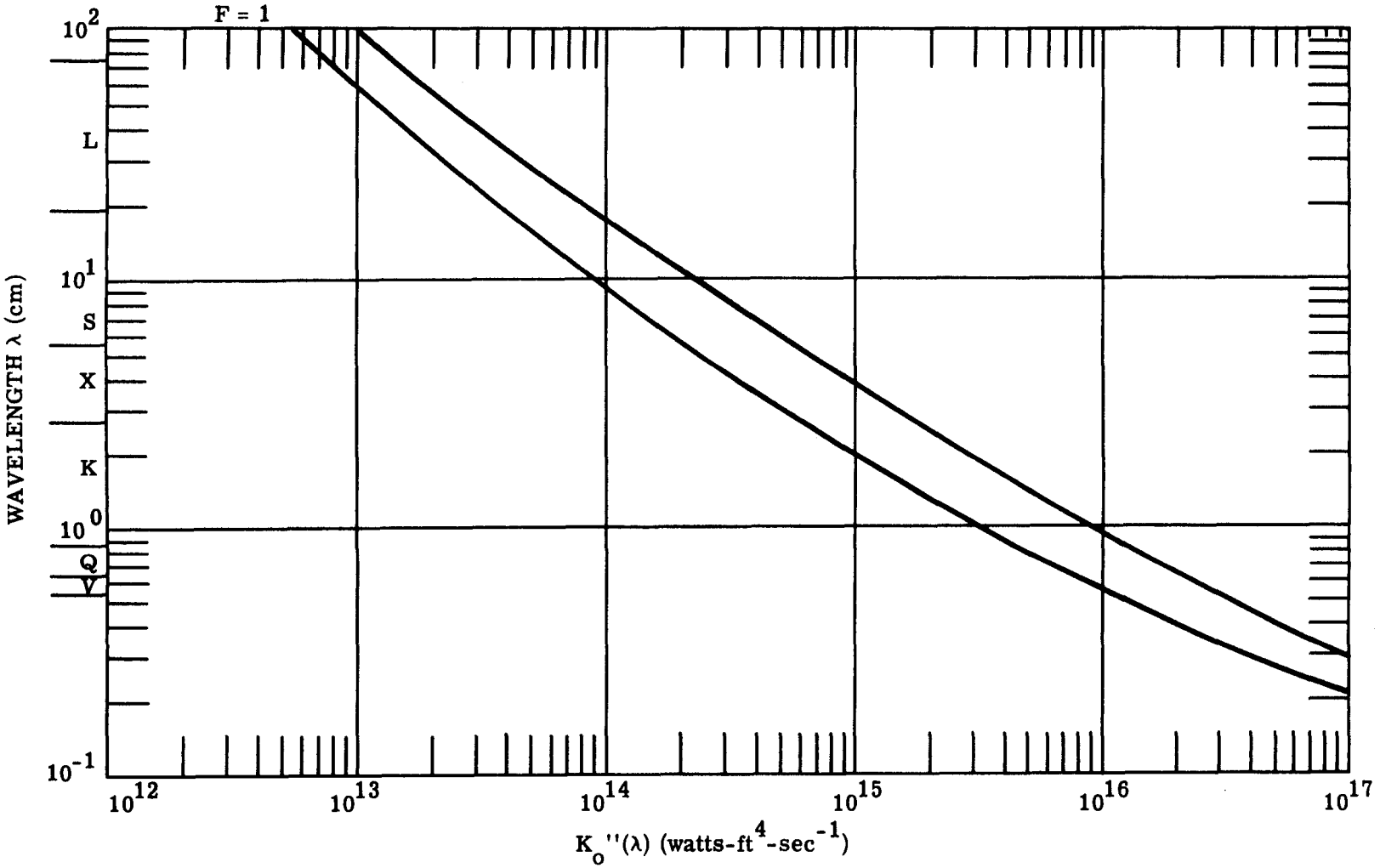

FIGURE 58. $K_o''(\lambda)$ vs. λ

dimensions are a function of the radar system prf. Or looking at it in another way it has been shown that the system prf has two constraints placed on it, one is due to azimuth channel considerations (the lower bound of the prf is that prf which will pass the doppler frequency information of targets between the antenna half power beamwidth and will provide the best resolution) and the other is due to range channel considerations (the upper bound of the prf is that prf which will allow unambiguous range information in the ground swath width; see Fig. 52). The prf constraints can be expressed as the inequality

$$\frac{2FKV}{D_a} \leq \text{prf} \leq \frac{c}{2W \sin \theta} \tag{60}$$

In practice there is an upper limit on the obtainable system prf set by a hardware constraint, so that there is a limiting value of the ground illuminated swath width which can be handled without range ambiguities, this limit is given by

$$W \leq \frac{c}{2(\text{prf}) \sin \theta} \tag{67}$$

The illuminated swath length, L, at a given elevation angle is given by

$$L = \frac{h\beta_a}{\cos \theta} \tag{33}$$

However the half power beamwidth can be related to the antenna aperture as follows

$$\beta_a = \frac{K_2 \lambda}{D_a} \tag{9}$$

The azimuth aperture has a prf constraint on it such that

$$D_a \geq \frac{2FK_2V}{\text{prf}} \tag{68}$$

therefore

$$\beta_a \leq \frac{\lambda(\text{prf})}{2FV} \tag{69}$$

and

$$L \leq \frac{h\lambda\,(\text{prf})}{2FV \cos \theta} \tag{70}$$

The maximum swath length as expressed in Equation 70 is that obtained at any given elevation angle, θ; however, it is obvious that this maximum swath length is variable within the antenna

beamwidth, β_r (see Fig. 52). Also it can be noted that swath area, A_I, being a trapezoid is computed by taking the product of the swath width, W, and the average swath length, $\bar{L}$. The maximum (based on the prf constraint) value for the average swath length can be shown to be given (approximately) by

$$\bar{L} \lesssim \frac{h\lambda\ (prf)}{2FV \cos\ (\theta + \beta_R/2)} \tag{71}$$

The maximum allowable swath area can now be related to the swath width and length by the equation

$$A = W \times \bar{L} \leq \frac{ch\lambda}{4FV \sin\ \theta \cos\ (\theta + \beta_R/2)} \tag{72}$$

It is interesting to note that while both swath width and length have prf constraints the swath area seems to be independent of system prf.

D.2.3.2. Computation of the Resolvable Ground Area. According to theory the minimum resolution element obtainable with a coherent radar is given by the inequality

$$r \geq \frac{D_a}{2FK} \tag{58}$$

Therefore, for a square resolution area the minimum resolvable area is

$$[A_r]_{min} = \frac{D_a^2}{(2FK)^2} \tag{73}$$

or

$$A_r \geq \frac{D_a^2}{(2FK)^2} \tag{74}$$

remembering the prf constraint on the azimuth aperture

$$A_r \geq \frac{V^2}{(prf)^2} \tag{75}$$

D.2.3.3. Computation of the Maximum System Data Rate. Recalling that the data rate is iven by

$$DR = A_I \times A_r^{-1}\ (prf) \tag{32}$$

then substituting Equations 72 and 74 into

$$DR \leq \frac{ch\,\lambda}{4FV^3 \sin\theta \cos(\theta + \beta_R/2)} (prf)^3 \tag{76}$$

or

$$[DR]_{max} = \frac{ch\,\lambda}{4FV^3 \sin\theta \cos(\theta + \beta_R/2)} (prf)^3 \tag{77}$$

Expression 77 states that the maximum data rate is a function of the system geometry, velocity, altitude and elevation angle, and the radar parameters, prf and operating wavelength. The selection of the prf is a question of optimization. The maximum data rate increases rapidly with prf; however, the peak transmitted power of a coherent radar system varies inversely with the prf (average power being unaffected); therefore, equipment limitation will undoubtedly set the requirements on system prf. For this reason the maximum data rate is normalized to remove the prf dependence, i.e.,

$$(DR)_{norm} = [DR]_{max} \times (prf)^{-3} \tag{78}$$

and this expression is plotted in Fig. 59 (for a surveillance system orbiting in a circular orbit at an altitude of 200 n mi for an antenna range beamwidth of 1^o) as a function of the operating wavelength and for different values of elevation angle. Maximum normalized data rates are 5 to 10% larger for an antenna range beamwidth of 10^o. Also for illustrative purposes values of the minimum antenna azimuth aperture and maximum swath width are plotted as a function of system prf (Figs. 55 and 56).

D.2.4. SAMPLE CALCULATIONS FOR ORL PROGRAM. Suppose it is proposed that for the first ORL program a X-band synthetic aperture radar be included. There are three primary reasons for including an X-band system. These are (1) it is desired to map surface phenomena and there is little surface penetration at X-band frequencies, (2) there will be little atmospheric attenuation at these frequencies, and (3) most of the synthetic aperture hardware which has been developed to date operates at these frequencies. The system requirements will be computed for a 8-10 Gc system having a resolution capability of at least 25 ft.

D.2.4.1. System Resolution. 25 ft an arbitrary selection

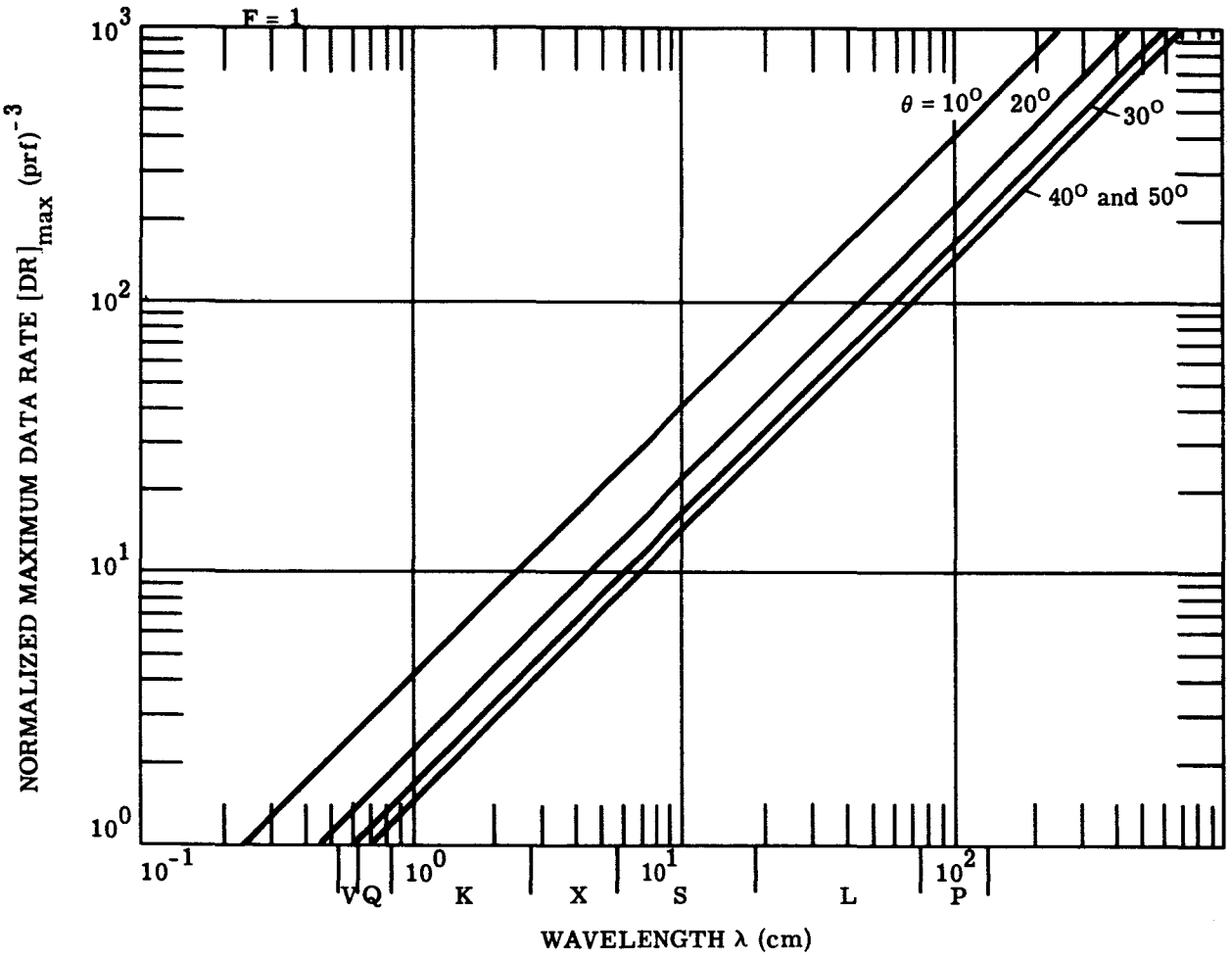

FIGURE 59. MAXIMUM NORMALIZED DATA RATES

D.2.4.2. Require Antenna Azimuth Aperture. ~50 ft (see Eq. 58, F = 1)

D.2.4.3. System Pulse Width Bandwidth and prf Requirements. For a nominal elevation angle of 45^{o} the required system pulse width for a resolution of 25' is

γ = 25 nanoseconds (see Fig. 45

then

$B = 1/\gamma = 10^{9}/25 = 40$ MC

The required pulse rate for a 50 ft antenna aperture is

prf = 1200 pps (see Fig. 55

D.2.4.4. System Peak and Average Power Requirements. As was the case of the noncoherent system, it is important to select a value for the target backscatter coefficient which is representative of the minimum value to be encountered for targets of interest. Considerably more backscatter data were available for X-band frequencies and it appears that a value of -30 db is about minimum. This value was used to compute the transmitted power requirements of the system. From Equation 64 it can be seen that the system peak power is an increasing function of the illuminated swath width. For the selected system prf, the maximum swath width is on the order of 100 n mi; however, if the system is designed to illuminate this swath width the power requirements would be exorbitant: Therefore a swath width of 10 n mi was selected. For such a swath width an antenna range beam width of 25 milliradians is required (1.4^{o}) (see Figure 53) resulting in a range aperture of approximately 5 ft. From Figure 58 the range in the value of $K_0''(\lambda)$ is 4 to 11×10^{14} thus the system peak power becomes (from Equation 65)

$$(P_T)_{min} = \frac{(4 \times 10^{14})(25 \times 10^{-3})^2 (4)}{10^{-3}(50)^4 (1.2 \times 10^{3})} = 130\,\text{K watts}$$

however this value is for a signal-to-noise ratio of unity. For a signal to noise ratio of 10

$(P_T)_{min}$ = 1.3 M watts

and

$(P_T)_{max}$ = 3.5 M watts

From Equation 30

$$(P_{av})_{min} = 1.3 \times 10^{6})(5 \times 10^{-5})(.707) = 45 \text{ watts}$$

$$(P_{av})_{max} = 120 \text{ watts}$$

It must be remembered that these transmitted power requirements, system power require can be 4 to 10 times the transmitted values.

D.2.4.5. Data Rate Calculation. From Figure 59

$$(DR)_{max} (prf)^{-3} = 4$$

$$(DR)_{max} = 4 \times (1.2 \times 10^{3})^{3} = 7 \times 10^{9}$$

however this assumes a swath width of 100 n mi so, the data rate must be modified to account for the fact that only a 10 n mi swath width is illuminated, thus

$$DR = (7 \times 10^{9}) \times (10/100) \simeq 10^{9} \frac{\text{resolution elements}}{\text{second}}$$

D.2.4.6. Special System Considerations. The discussion of the synthetic aperture radar has been conducted assuming a theoretically perfect system, i.e., it was assumed that there was no radial (towards the target) antenna motion and that the antenna and signal processing were perfect. In reality, none of these assumptions is valid and the presence of each system imperfection can introduce phase errors which will degrade the system resolution. The lack of radial movement is probably the best of the three since a satellite system will not incur the turbulence that an aircraft does so a relatively simple motion compensation scheme can be used in space.

BIBLIOGRAPHY LIST FOR APPENDIX D

L. J. Cutrona, E. N. Leith, and G. O. Hall, A High-Resolution Radar Combat-Surveillance System (U).

G. O. Hall, General Theory of Synthetic-Antenna Radars (U), Radar Laboratory, IST, The University of Michigan, November 1963 (CONFIDENTIAL).

J. L. Beard, W. A. Malila, "Description of Microwave Radiometers (U)," appendix to Passive Microwave Detection of Threats to Aircraft (U), Tech. Doc. Rept. ASD-TDR-63-848, Infrared Laboratory, IST, The University of Michigan, October 1963 (SECRET).

G. L. Shelton, Microwave Radar and Radiometer Instrumentation Equipment, Project Genny, Tech. Rept. 7, Advanced Electronics Center, General Electric Company, Ithaca, New York, July 1964 (UNCLASSIFIED).

Flight Tests of Radiometric Mapping Set AN/AAR-24(XH-1)(U), Second Quarterly Rept. Project 4108, Wiley Electronics Company, Phoenix, Arizona, October 1959 (SECRET).

R. K. Moore and J. Butler, Synthetic Aperture Power Requirements, Tech. Memo 61-8, Remote Sensing Laboratory, The University of Kansas, Lawrence, Kansas (UNCLASSIFIED).

R. L. Cosgriff, W. H. Peake, and R. C. Taylor, Terrain Scattering Properties for Sensor System Design (Terrain Handbook II), Engineering Experiment Station, The Ohio State University, Columbus, Ohio, Vol. XXIX, No. 3, May 1960 (UNCLASSIFIED).

Heavner, W. S., "Satellite Reconnaissance Gains," appearing in Aviation Week, 22 May 1961.

APPENDIX E
LASER ALTIMETERS

E.1. GENERAL

The two types of optical radar altimeters are the FM-CW laser altimeter and the pulse laser altimeter. These altimeters, in an orbiting satellite, can be used to accurately measure the relative height of ocean waves and the variation of the height of objects in the earth's land area surface for a very small patch. Since present coherent lasers operate at very high frequencies, $3.5(10^{12})$ to 10^{15} cps; it is possible to construct satellite-borne high resolution altimeters which have transmitting and receiving apertures of reasonable physical size. Laser altimeters are able to measure surface variation only if there are no clouds occluding the beamed electromagnetic energy path. At any one time, 40 to 60 percent of the earth's surface is covered with clouds.

The ocean covers a large part of the earth's surface (71%) and exhibits a complex and thoroughly random surface shape. Irregularities in the vertical direction can span a range as high as 20 meters. However, certain individual elements of the total pattern, individual kinds and groups of waves, do repeat themselves and are periodical with time. Table XIV shows the relationship of the various parameters of wind waves at sea. Thus, from the data of the ocean wind waves, one can estimate wind velocity and possibly other weather conditions. Also, with additional complication in data processing, swell type ocean waves can be detected and measured. There is some possibility that even tsunamis can be detected and measured if the satellite's stability in height, roll and pitch is constant enough and if one were alert to their occurrence via seismics sensing by ground stations.

Land height irregularities are greater than the various ocean wave heights and they have very little, if any, periodicity. Narrow strips of land surface profile can be determined by data processing providing the changes in satellite attitude are slow and sufficiently well known.

The selection of an appropriate system has to be based on many diverse factors. The important considerations are: resolution, power requirements, operational duty cycle, and physical size. A discussion of these factors will now follow.

E.1.1. RESOLUTION USING LASERS. The striking characteristics of coherent electromagnetic radiation of any frequency is that a plane wave front with a uniform time phase will propagate as a parallel beam of radiation spreading only through a diffraction angle which is determined by the wavelength of the radiation and the size of the source of the original plane

TABLE XIV. WIND WAVES AT SEA

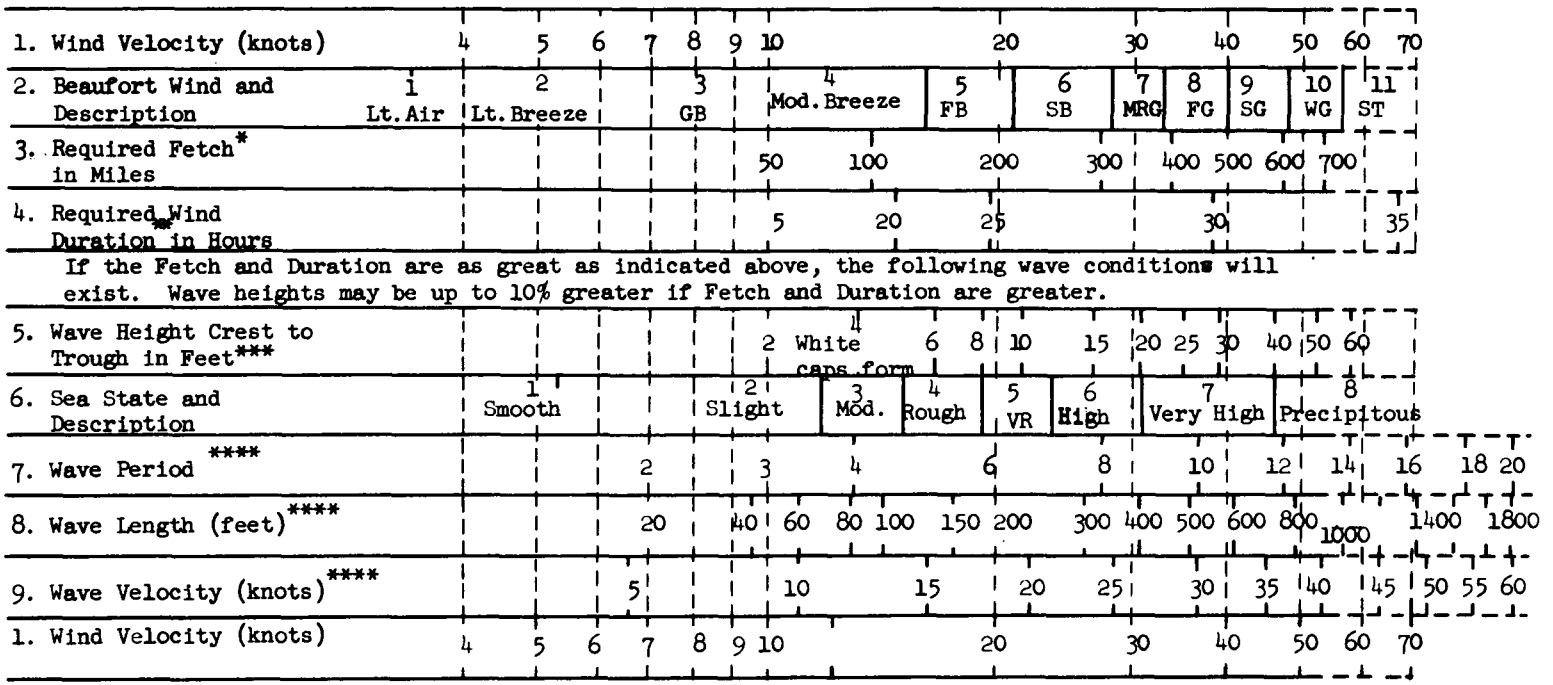

*Fetch is the number of miles a given wind has been blowing over open water.

**Duration is the time a given wind has been blowing over open water.

***The height of waves is arbitrarily chosen as the height of the highest 1/3 of the waves. Occasional waves caused by interference between waves or between waves and swell may be considerably larger.

****Only lines 7, 8 and 9 are applicable to swell as well as waves.

Note: The above values are only approximate due both to lack of precise data and to the difficulty in expressing it in a single easy way.

Key to Abbreviations: Lt. = light GB = gentle breeze Mod. = moderate FB = fresh breeze
SB = strong breeze MRG = mode rate gale FG = fresh gale SG = strong gale
WG = whole gale ST = storm VR = very rough

wave front. A circular source of coherent plane waves of uniform strength produces at great distances, on a plane parallel to the source plane, a symmetrical distribution. This distribution can be given by an analytical expression

$$\frac{I}{I_0} = \left[2 \frac{J_1\left(\frac{\pi\theta}{\theta_0}\right)}{\left(\frac{\pi\theta}{\theta_0}\right)} \right]^2$$

where I_0 is the maximum beam intensity at the center of the pattern, J_1 is the Bessel function of the first kind and the first order, θ is assumed to be small and approximately equal to sin θ, and

$$\theta_0 = \frac{\lambda}{D} \text{ radians}$$

with λ the wavelength and D the source diameter. The full width of the central beam at the first pattern nulls is 2.44 θ_0. According to classical geometrical optical theory, the best angular resolution for a passive viewing system is given by the relation

$$\theta_d = 1.22 \frac{\lambda}{D}$$

A graph of angular resolution versus wavelength for various apertures, ranging from 100 meters to 0.1 cm in diameter is given in Figure 60). It can be seen that for constant aperture angular resolution is best at shorter wavelengths. Superimposed on this figure are four dashed lines indicating the magnitude of the field of view of beamwidth obtainable with the indicated wavelength and aperture sizes. Thus, one can easily obtain a field of view of 10 seconds by employing a 10 centimeters source diameter at a wavelength of one micron.

A transmitter with a 10 second beamwidth mounted on a satellite at a height of 370 km (200 n mi), will intercept an area on earth whose diameter is approximately equal to 17.9 meters. From Table XIV we observe that the beam will cover one wavelength for a moderate breeze on the sea, and only portions of the total wind wave for higher wind velocities. Thus, from the standpoint of resolution, the optical spectrum (0.2 to 100μ) is advantageous. Similar resolutions at microwave frequencies (except using synthetic antennas) are impossible to obtain because of the sizable mechanical tolerances in the manufacture of large antennas. For example, using the highest microwave frequency used by present radar systems, 70 Gcs, requires a theoretical antenna diameter of 58.7 meters for a beamwidth of 10 seconds of arc.

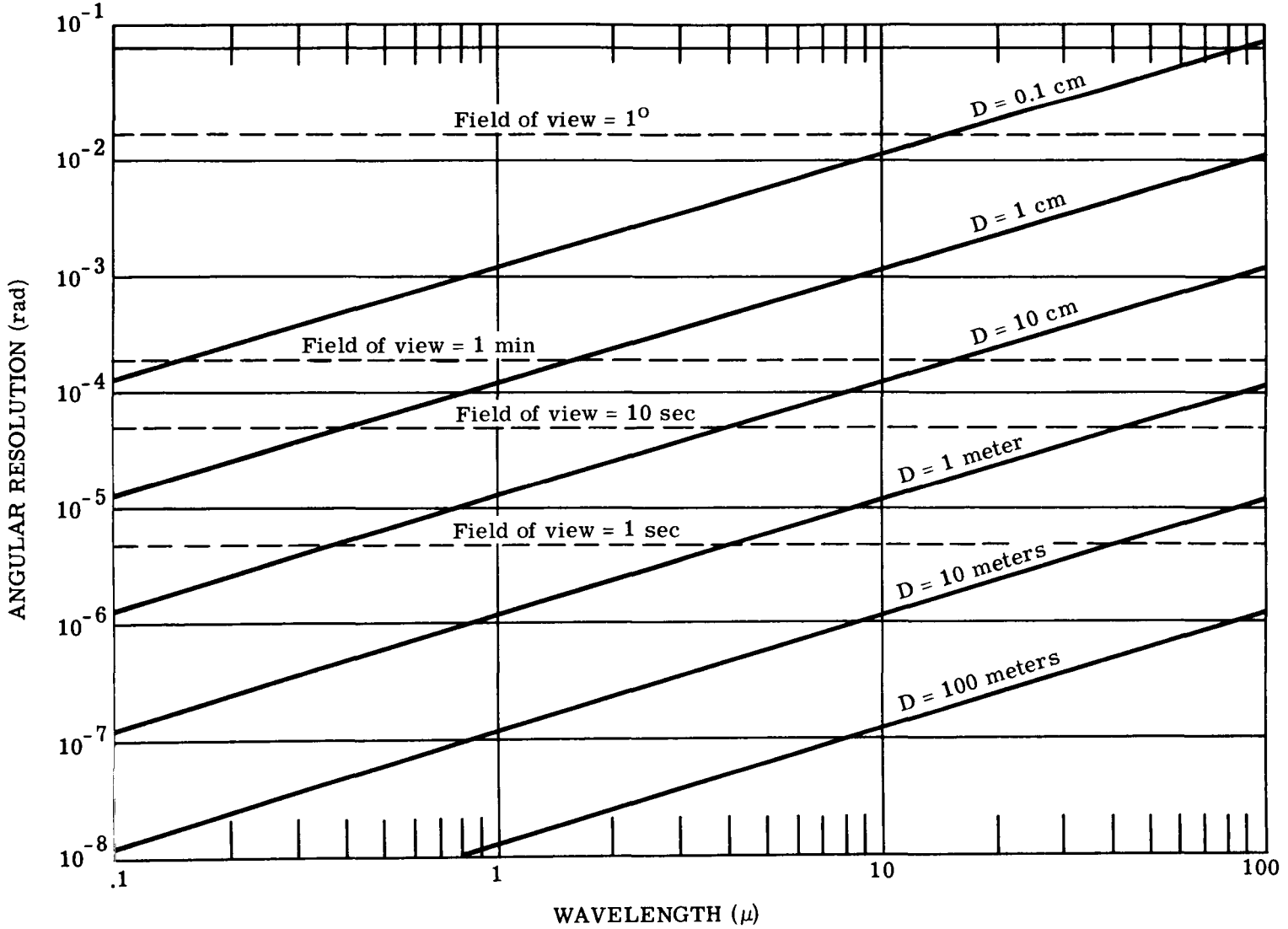

FIGURE 60. RAYLEIGH DIFFRACTION RESOLUTION (APERTURE) vs. WAVELENGTH
(D = diameter of limiting aperture)

E.1.2. POWER CONSIDERATIONS AND OPERATION DUTY CYCLE. The beam solid angle Ω is given by

$$\Omega = \frac{\pi \theta_d^2}{4}$$

For the power within the beam there is an average power gain $\frac{4\pi}{\Omega}$ over an isotropic radiator. For a 10 second beamwidth, Ω is of the order of 10^{-9} steradians giving a power gain of more than 90 dbs. By working in the optical spectrum, one obtains very high directional power gains. Thus for the case where the beamwidth of the optical and microwave systems are limited by Fraunhofer diffraction, the advantage of an optical system as far as power requirements are concerned is unquestionable (Ref. 75).

To counterbalance this advantage, we have the large atmospheric transmission losses in poor weather operability; thus laser altimeters can be used only through good visibility paths as observed from the satellite to the earth's surface.

E.1.3. STEADY STATE TRANSMITTANCE OF THE ATMOSPHERE. Absorption, turbulence and scattering are the three main sources of energy loss encountered in propagation of electromagnetic waves through the atmosphere. A light beam passing through the atmosphere suffers from both absorption and scattering. The attenuation in a pure atmosphere consisting only of the permanent gases is caused by scattering from the gas molecules and is proportional to the inverse fourth power of wavelength (Rayleigh scattering). In the lower atmosphere, Rayleigh scattering is small, because of the absorption and Mie scattering by natural and man-made contamination (water vapor, dust, smoke, etc.). The variety and random density of these materials are such as to make exact predictions of their effects practically impossible. The atmospheric transmittance has been calculated as a function of wavelength and elevation angle for the clear ARDC standard atmosphere and is given in Figure 61 (Ref. 76). These transmittance curves in Figure 61 were calculated by an IBM-7090 computer assuming the clear ARDC atmosphere (ground visibility of 25 km), no clouds in transmission path and for the non-absorption "windows" (no CO_2 or water vapor gas absorptions) and using the USAF Cambridge Research Laboratory tables (Refs. 77 and 78). The absorption of light waves by clouds and thick fogs requires that laser altimeters be used in clear and partially cloudy weather. The total earth's surface has cloud cover of 40% to 60% at all times as viewed from space. The light ray path cannot be occluded by cloud cover of any appreciable thickness. Table XV indicates the calculated spectral transmittance of 100 meters and 1 km cloud from the only Mie

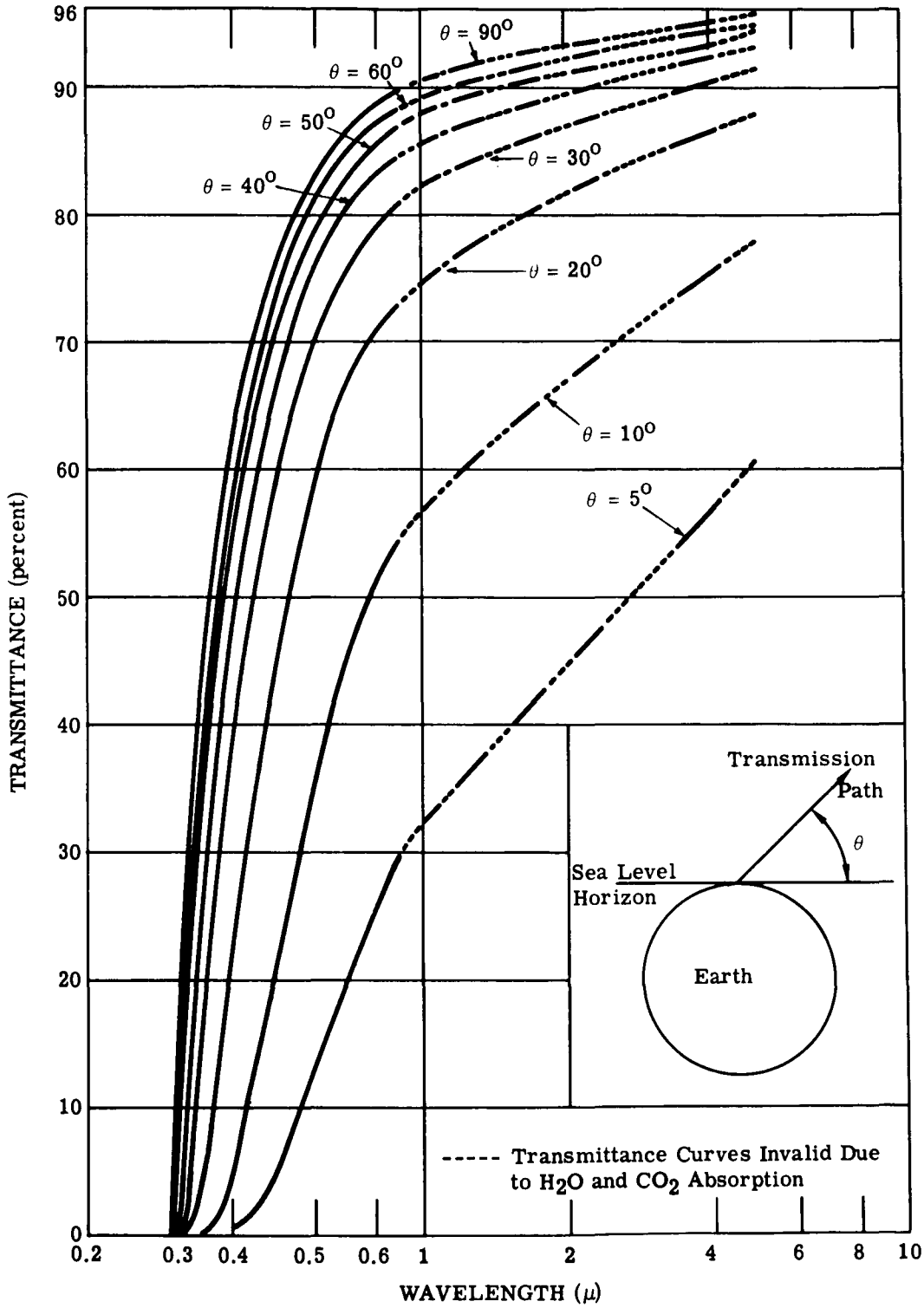

FIGURE 61. TRANSMITTANCE OF THE TOTAL ARDC STANDARD ATMOSPHERE FOR RAYLEIGH AND MIE SCATTERING, AND OZONE ABSORPTION vs. WAVELENGTH AND ELEVATION ANGLE

TABLE XV. TRANSMITTANCE OF 1-KM AND 100 M CLOUD VS. WAVELENGTH
Mie Scattering Coefficients Taken from Ref. 79

Wavelength (μ)	Transmittance of 1 km Cloud	100 m Cloud
0.45	$8.090(10^{-8})$	0.1953
0.70	$5.477(10^{-8})$	0.1878
1.61	$2.317(10^{-8})$	0.1723
2.25	$1.234(10^{-8})$	0.1618
3.07	$8.527(10^{-9})$	0.1559
3.90	$1.076(10^{-9})$	0.1268
5.30	$3.737(10^{-11})$	0.0906
6.05	$2.370(10^{-9})$	0.1372
8.15	$7.194(10^{-9})$	0.1533
10.0	$1.395(^{10-5})$	0.3269
11.5	$4.107(^{10-5})$	0.3642

scattering attenuation coefficient given by Diermendjian (Ref. 79). Note the spectral transmittance of a 1 km cloud is exceedingly small for the optical spectrum.

In addition to the steady state losses, the atmosphere causes short term changes in the apparent characteristics of the source outside the atmosphere. Scintillation can degrade the signal by impressing amplitude modulation on the signal itself analogous to fading in RF systems. In general, scintillation can be decreased by increasing the aperture size. The atmospheric random inhomogeneities will add to the formidable problem of maintaining the relative spatial coherence of the signal and local oscillator in superheterodyne type optical receivers.

E.1.4. REFLECTANCE OF THE EARTH'S SURFACE. The manner in which a particular small area of the earth's surface will reflect, scatter and/or absorb incident electromagnetic waves varies with type of surface and wavelength. Table XVI indicates the visible reflectance of some objects and type of areas on the earth's surface (Ref. 80). Reflectance values of water surfaces, soils, earth areas, and buildings are approximately true (but slightly lower) for the infrared spectrum. Vegetative formation reflectances for the infrared spectrum increase rapidly within a very narrow spectrum (0.68 to 0.70μ) from the given values of 3 to 5% in Table XVI to 30-60%. Using laser altimeters for relative height measurements of small patches of the earth's surface, the reflectance of the ocean water were used for the wave height calculations The reflection of electromagnetic energy from the ocean will be specular, however, for practicability a reflection coefficient of 10%, with a cosine distribution into the outward hemisphere was used for calculation purposes (Refs. 80 and 81).

E.2. FM-CW LASER ALTIMETERS

The system to be considered is shown in Figure 62. It is basically a frequency modulated continuous wave (FM- CW) radar to measure range. The transmitter has a source, a modulator, and an optical system. The modulator is also connected to a local oscillator through a delay line, which feeds into the mixer of the receiver. The receiver has: an optical system, an optical amplifier, a mixer, amplifier, discriminator and an indicator.

In the transmitter, the source generates a light beam with a power of $P_t(\lambda)$ watts, which acts as the carrier for modulation. The modulator imparts to the light beam a variation which contains the information in a bandwidth of Δf cps. The optical system has a transmittance, $\eta_t(\lambda)$, which accounts for the losses of the system, and optical gain, G_t, which normalizes the power in the beam to that from an equivalent isotropic radiator. $G_t = \frac{4\pi}{\Omega}$, where Ω is the solid angle half-power beamwidth of the transmitter beam and given by $\Omega = \frac{\pi}{4}\theta_d^2$.

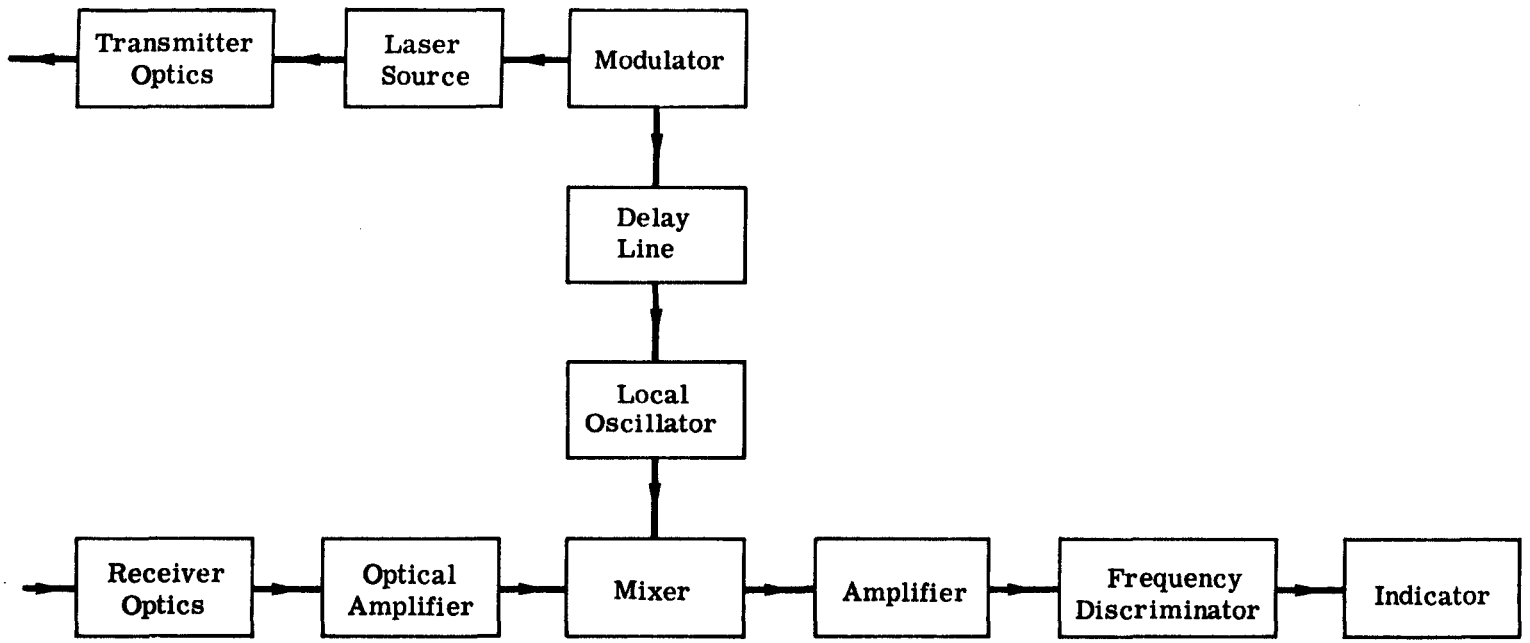

FIGURE 62. BLOCK DIAGRAM OF AN OPTICAL FM-CW RADAR

TABLE XVI. VISIBLE REFLECTANCE OF VARIOUS LARGE AREAS OR OBJECTS ON THE EARTH

Type	Reflectance (%)	Peak Wavelength $\lambda(\mu)$
Water Surfaces		
Inland Waters	3-10	0.4810
Oceans	3-7	0.4810
Bare Areas and Soils		
Snow	70-86	0.4810
Ice	75	0.5795
Limestone	63	0.5790
Calcareous Rocks	30	0.5790
Granite	12	
Mountain Tops (Bare)	24	0.5816
Sand	18-31	0.5616
Clay Soil	1.5-15	0.5828
Ground Bare (Rich Soil)	7.5-20	0.5832
Field (Plowed)	20-25	
Vegetative Formations		
Coniferous Forest	3-10	0.5744-0.5758
Deciduous Forest	10-15	0.5719-0.5858
Meadow (Dry Grass)	3-8	0.5758
Grass (Lush)	15-25	0.5719
Field Crops	7-15	0.5858
Man Made		
Buildings (Cities)	9	0.5828
Concrete	15-35	

The receiver optical system collects and focuses the power to the amplifier which in turn is fed into the mixer. The local oscillator signal is also introduced into the mixer. The local oscillator signal acts as a reference signal required to produce a beat frequency. The beat frequency signal is amplified and fed into a frequency discriminator. This is followed by an indicator to obtain range information.

E.2.1. RANGE MEASUREMENTS. In the frequency-modulated continuous wave optical radar (FM-CW), the transmitter frequency is changed as a function of time in a known manner. Assume that the transmitter frequency to be modulated is a triangular frequency modulation waveform as shown in Figure 63 by the solid line. If there is a reflecting object at a distance, r, a signal will return after a time, $T = \frac{2r}{c}$. The dashed line in Figure 63 represents the turn signal. If the local oscillator signal, which has a time delay T' and is shown in Figure 63 by the dash-dot curve, is heterodyned with the return signal in a mixer, a beat frequency will be produced. If there is no doppler shift, the beat frequency is a measure of the target range. The beat frequency is of constant frequency except at the turn around region. If the frequency is modulated at a rate f_m over a range Δf, the beat frequency is

$$f_b = \left(\frac{2r}{c} - T'\right) 2f_m \Delta f \qquad (1)$$

Thus the measurement of the beat frequency determines the range r.

When more than one target is present within the view of the radar, the mixer output will contain more than one difference frequency. In principle, the range to each target may be determined by measuring the individual frequency components and applying Equation 1 to each. To measure the individual frequencies, they must be separated from one another. This might be accomplished with a bank of narrow band filters, or alternatively, a single frequency corresponding to a single target may be singled out and continuously observed with a narrow band tunable filter.

In this particular case, where we are interested in the height of the ocean waves, it is essential only to obtain the largest and smallest beat frequencies. That is,

$$f_b^t = 2\left(\frac{2r}{c} - T'\right) f_m \Delta f$$

$$f_b^c = 2\left(\frac{2r}{c} + \frac{\Delta r}{c} - T'\right) f_m \Delta f$$

where f_b^t and f_b^c denote the beat frequencies due to the trough and crest respectively (see Fig. 63), and the difference is equal to

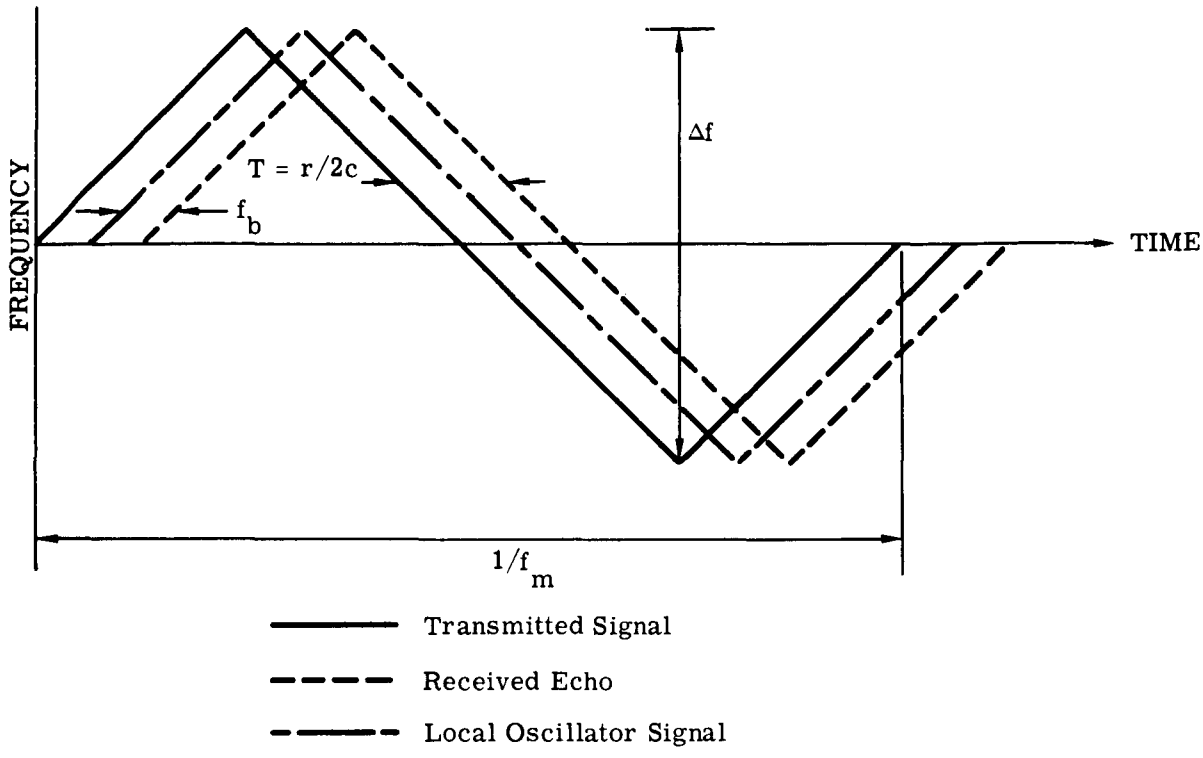

FIGURE 63. FREQUENCY TIME RELATIONSHIP IN FM-CW RADAR

$$f_b^c - f_b^t = 2 \frac{\Delta r}{c} f_m \Delta f$$

where Δr is the distance between trough and crest of the wave. For example, let

$\Delta r = 1$ meter

$f_m = 120$ cps

$\Delta f = 100$ Mc

$c = 3 \times 10^8$ meters/sec

The difference between the two beat frequencies is equal to

$$\Delta f_b = f_b^c - f_b^t = \frac{2}{3 \times 10^8} 120 \times 10^8 = 80 \text{ cps}$$

This difference frequency Δf_b can be increased by increasing the modulation rate f_m and the bandwidth Δf. By tuning the delay line so that f_b^t is equal to 1000 cps, the beat frequency f_b^c will be 1000 cps. Thus, if the discriminator has an accuracy of one cycle in a thousand, one should be able to measure one meter wind wave to an accuracy of 1.25 cm.

E.2.2. MEASUREMENT ERROR

The theoretical accuracy with which absolute distance can be measured depends upon the bandwidth of the transmitted signal and the signal-to-noise ratio. In addition, measurement accuracy might be limited by such practical restrictions as the accuracy of the frequency measuring device, the residual path length error caused by the circuits, errors caused by multiple reflections, and the frequency error due to the turn-around of the frequency modulation.

A common form of frequency measuring device is the cycle counter, which measures the number of cycles or half cycles of the beat frequency during the modulation period. The total cycle count is a discrete number since the counter is unable to measure fractions of a cycle. The discreteness of the frequency measurement gives rise to an error called the "fixed error." The average number of cycles N of the beat frequency f_b in one period of modulation cycle f_m is $\bar{f}_b/f_m$, where the bar over f_b denotes time average. Equation (1) may be rewritten as

$$(2r - cT') = r' = \frac{cN}{2\Delta f}$$

Since the output of the frequency counter is an integer, the range will be an integral multiple of $c/2\Delta f$, and will give rise to a quantization error equal to

or

$$\delta r' \text{ (meters)} = \frac{37.5}{\Delta f(\text{Mc})}$$

Thus, for Δf = 100 Mc, $\delta r'$ = 1.5 meters. Note that the fixed error is independent of range and carrier frequency and is a function of frequency excursion only.

There are several techniques to make the fixed error small. One technique is to make the frequency excursion large, however, this technique reduces the signal-to-noise ratio of the system. For the system proposed by us above, a frequency discriminator was employed. The fixed error is not present in a non-counting (continuous) frequency meter such as a frequency discriminator. The discriminator output is a voltage proportional to frequency and is continuous rather than discrete. The discriminator circuits are not capable of as wide a range of frequency operation as the frequency counter. However, for our application, this will not be problematic since the frequency range of operation is very small. Many of the errors which enter in the measurement of absolute range do not affect this system, since we are primarily interested in measuring the difference of the highest and lowest beat frequencies.

E.2.3. TRANSMITTED POWER REQUIREMENT

E.2.3.1. Derivation of Signal-to-Noise Ratio. Let us derive the signal-to-noise ratio (S/N) expressions for this system operating against a continuous background noise of the earth.

To calculate the signal power available at the mixer, we define the spectral radiance of the source N_λ as the radiant power per unit solid angle per unit wavelength interval omitted from the source. For the laser case

$$N_\lambda = \frac{P_t}{\Delta\lambda_t \Omega_t A_t} \text{ watts-m}^{-2}\text{-sterad}^{-1}\text{-}\mu^{-1} \tag{3}$$

where

$\Delta\lambda_t$ is the laser's transmittance bandwidth in microns

P_t is the power of the transmitting source in watts

A_t is the area of the transmitting source in square meters

Ω_t is the solid angle of the transmitter beam in steradians represented by

$$\Omega_t = \frac{\pi}{4}\theta_d^2$$

in which θ_d is the half power beamwidth.

Consider the wavelength interval λ and $\lambda + d\lambda$. If the emitting aperture has an area A_t, the differential flux density within the beam at a distance r is

$$dP = \eta_t T N_\lambda \frac{A_t}{r^2} d\lambda$$

where the factor η_t accounts for the losses of the transmitter optics at wavelength λ, and T is a factor accounting for the transmittance of the atmosphere.

The power reflected back to the radar by the sea is given by

$$dP = \eta_t T \frac{A_t}{r^2} \frac{\pi}{4} \left(r\theta_d^2\right) \frac{\rho}{\pi} N_\lambda d\lambda$$

where $\frac{\pi}{4}\left(r\theta_d^2\right)$ is the area of the beam intercepted by the ocean, ρ is the reflectivity of the ocean and we assume for the purpose of this calculation to follow the cosine law distribution into the outward hemisphere.

The power input to the mixer is the product of G, A_r/r^2, dP and η_r, where G is the gain of the light amplifier, A_r is the receiving aperture area and η_r is a factor which accounts for losses in the receiver optics at wavelength λ. Thus

$$dP_r = G\eta_t\eta_r T^2 \frac{A_t}{r4} \frac{A_r\eta}{4} \left(r\theta_d^2\right) \frac{\rho}{\pi} N_\lambda d\lambda$$

The total power reaching the mixer is

$$P_r = \frac{GA_tA_r\theta_d^2}{4r^2} \int_{\lambda_1}^{\lambda_2} \eta_t\eta_r T^2 \rho N_\lambda d\lambda \qquad (4)$$

where $\lambda_2 - \lambda_1$ may be the filter or the transmitter modulation bandwidth.

The detector output will be a voltage or current which is proportional to the input flux. For a photoemissive detector we designate this constant or proportionality as $R(\lambda)$; it is called the detector responsivity. For a photoemissive detector, the photocathode current i due to an input dP at wavelength λ is

$$di = R(\lambda) dP_r$$

or

$$i = \int_{\lambda_1}^{\lambda_2} R(\lambda) dP_r$$

Substituting the expression for dP_r in the above equation, one obtains

$$i_{peak} = \frac{GA_t A_r \theta_d^2}{4r^2} \int_{\lambda_1}^{\lambda_2} \eta_t \eta_r T^2 \rho R(\lambda) N_\lambda \, d\lambda \tag{5}$$

No matter which of the modulation techniques one employs, the photocathode current i may be expressed as the sum of the time varying signal $i_r(t)$ and an average (or dc component) I_r:

$$i = i_r(t) + I_r$$

For the purpose of calculating signal-to-noise ratios, it is necessary to determine the root mean square (rms) signal current

$$\left\{\bar{i}_r^{\,2}\right\}^{1/2} = i_{peak}/F_1 \tag{6}$$

where F_1 depends on the type of modulation used, and can be calculated once the modulation is known.

In a similar manner, the average signal current can be evaluated by introducing a factor F_2 which is defined as the ratio of peak to average photocathode current. The average current can be written as

$$I_r = i_{peak}/F_2 \tag{7}$$

The value of F_2 also depends on the type of modulation. Let us now simplify the expression for i_{peak} by substituting the expressing for N_λ

$$i_{peak} = \frac{GA_r}{\pi r^2} \int_{\lambda_1}^{\lambda_2} P_t(\lambda) \eta_t \eta_r T^2 \rho \, d\lambda$$

E.2.3.2. Noise Considerations. There are three important sources of noise in this type of system: background, detector, and photon noise. The background noise arises from the reflection of the suns energy by the earth. Detector noise is caused by various noise sources within the particular detector used. Photon noise is due to the random emission and arrival of photons.

For this type of system it was shown in (Ref. 82) that as long as the photocurrent produced by the local oscillator is larger than the dark current or the photocurrent induced by the background, it is possible to achieve a signal-to-noise ratio determined by the noise in the

signal. Thus for the purpose of this study, we shall assume the system to be photon noise limited.

The statistical emission of electrons at the detectors photocathode gives rise to shot noise. The rms value of this noise current is given by the familiar Schottky formula

$$\bar{i}_n^2 = 2eI\Delta f \tag{9}$$

where I is the average photocathode current. For this study, I will be assumed to be equal to I_r given in Equation (7).

The ratio of the mean square signal current to mean square noise current in the same bandwidth is defined as the signal-to-noise power ratio and is given below:

$$\frac{S}{N} = \frac{\bar{i}^2}{\bar{i}_n^2}$$

The signal-to-noise ratio for the limiting noise is given by

$$\frac{S}{N} = \frac{F_2}{F_1^2}\frac{A_r G}{\pi r^2}\frac{\int_{\lambda_1}^{\lambda_2} P_t(\lambda)\eta_t\eta_r T^2 \rho R(\lambda)\, d\lambda}{2e\Delta f} \tag{10}$$

E.2.3.3. Discussion of Parameters. The parameters employed in the system are state-of-the-art and are immediately realizable. The results obtained do not represent ultimate performance of such a system, but it will serve as an indication of what can be easily accomplished.

E.2.3.4. Assumptions. Source and Transmitting Optics. Using the results of a previous laser systems study for communications through atmosphere to space, the transmitting laser source was determined to be a gas laser operating at a wavelength of 1.0610 μ (Ref. 83) This study concluded that only gas lasers have the necessary spectral coherence for FM techniques. The systems performances were compared by calculations and the best system wavelength was 1.0610μ. Also, the minimum transmitting beamwidth was concluded to be 10 sec. of arc considering tracking servomechanisms state-of-the-art and atmospheric scintillation and dancing of laser beam. Thus we choose a gas laser source operating at 1.0610 μ and a transmitting beamwidth of 10 sec. The transmittance of the transmitting optics will be taken as

$$\eta_t = 0.50$$

because it assumed to use a lens to converge the laser output into 10 sec. beamwidth.

Receiver. The aperture area of the primary collecting parabolidial mirror will be taken to be 1 square meter with hyperbolical secondary mirror forming a pseudo-Cassegrainian reflective optical system. We shall assume this optical system transmittance to be $\eta_r = 0.90$ which also includes the losses in the filter. The system will include 10 Angstrom optical filter to exclude background noise lying outside the spectral region occupied by the returned laser signal.

For the detector-mixer, we choose the photomixer diode or a Riesz photodiode (Ref. 84). Photomixing can only be accomplished by photomultiplier tubes. traveling-wave phototubes and photodiodes. For the 1.0610 μ wavelength, the Riesz photodiode has the highest responsivity of all the photo mixer type detectors. The responsivity for this photodiode is R = 0.426 amps watt and has a response time of 10^{-11} sec with a dark current of 10^{-9} amps.

Modulation Technique. Frequency modulation provides a substantial improvement in S/N at the expense of bandwidth (Ref. 85). In calculating this S/N we shall first calculate it for intensity modulation and then multiply by a factor to obtain the S/N for frequency modulation.

The ratios of peak signal current to the rms and average signal currents are defined by F_1 and F_2, respectively. A 100 percent intensity modulation of light beam by a sine wave would give at the output of the detector a sine wave current whose amplitude varied from zero to some peak value. The rms value of the signal sine wave is its peak to peak value divided by $2\sqrt{2}$; thus $F_1 = 2\sqrt{2}$. The average value of this current is one half the maximum amplitude, so that $F_2 = 2$. For the calculations we will assume

$F_1 = 2\sqrt{2}$

$F_2 = 2.$

E.2.3.5. Calculation of Required Power. Let us calculate the cw power necessary to obtan a signal-to-noise ratio of 10 db for an excursion frequency of 100 Mc. We shall assume that the optical radar source is in a 370 km orbit, with the power radiating perpendicular to a plane tangent to the earth. We shall make use of the following numerical values:

Signal-to-Noise Ratio $\left(\frac{S}{N}\right) = 10$

Receiver Light Amplifier Gain (G) = 10^3

Range (r) = 3.70×10^5 meters

Transmitter Optical Transmittance (η_t) = 0.50

Receiver Optical Transmittance (η_r) = 0.90

Modulation Factor (F_1) = $2\sqrt{2}$

Modulation Factor (F_2) = 2

Receiving Aperture Area (A_r) = 1.0 square meter

Atmospheric Transmittance (T) = 0.90

Ocean Reflectance (ρ) = 0.10

Detector Responsivity (R) = 0.426 amp/watt

Electron Charge (e) = 1.6×10^{-19} coulomb

Bandwidth (Δf) = 100 Mc

For a laser source, Equation (10) can be simplified and written as

$$\frac{S}{N} = \frac{GF_2}{F_1^2}\left(\frac{A_r}{\pi r^2}\right)\left(\frac{\eta_t \eta_r T^2 \rho R}{2e\Delta f}\right)P_t \tag{11}$$

Substituting the above numerical values into this equation we obtain for the power

$$10 = 10^3\left(\frac{2}{2.8}\right)\frac{1}{\pi(3.7 \times 10^5)^2}\left[\frac{(0.5)(0.90)(0.81)(0.1)(0.426)}{2(1.6 \times 10^{-19})10^8}\right] \cdot P_t \tag{12}$$

P_t = 3.550 watts

Thus the CW laser power of 3.55 watts required is well within the present state-of-the-art for laboratory lasers. An argon gas CW laser, operating at 0.5145 μ was reported by Raytheon to produce 14 watts (Ref. 86). It was reported by C. H. Townes during the last American Physical Society meeting that 100 watts of CW power from a laser can be expected by 1970. The neodymium doped glass rod laser amplifier needs further development for continuous wave usage as receiver light amplifier for the FM-CW laser altimeter. This light amplifiers average power output in the pulsed operation presently has enough power gain but needs CW operation. It is highly probable that the required lower power CW laser amplifiers will be developed in the very near future (6 months to 2 years).

By employing frequency modulation, we shall obtain a substantial improvement in $\frac{S}{N}$ of Equation (11) at the expense of increased bandwidth. This is characteristic of all noise improvement systems. This improvement is given in Ref. 85 by the relation

$$\left(\frac{S_0}{N_0}\right)_{FM} = 3\beta^2\left(\frac{S_0}{N_0}\right)_{AM}$$

where $\beta = \frac{\Delta f}{f_m}$. The signal-to-noise ratio of 10 used in equation (11) (which is the AM case) can be increased by 20 to 30 db for wide band FM. However, one cannot increase the output $\frac{S}{N}$ indefinitely by increasing the frequency deviation and hence the bandwidth. This relation fails when β gets very large.

Average Power Reduction Improvements

Employing optical heterodyne detection, the noise limitations due to the detector noise and background interference has been eliminated, leaving the signal noise current the limiting factor. By examining equation (10), we see that the next step is to increase the power at the transmitter. For these type of measurements, we do not require very high information rates, thus by switching from a cw optical radar to a chirped radar, would enable us to employ pulsed light amplifiers and possibly sources of higher output power lasers. A gain of 20 db in light amplifiers stages with 20 db interstage isolation should allow an overall gain of 60 db, thereby improving this system considerably.

E.2.4. FM-CW LASER ALTIMETER ACCURACY. The ultimate accuracy of FM-CW lasers altimeters depends upon the combined error of two factors, the measurement error and the geometrical resolution accuracy. It was shown in Section E.2.2 using Equation (2) that the measurement error for cycle counting (complete cycles only) was determined to be 0.75 meters and was independent of both range and laser carrier frequency. If one uses an FM discriminator as was indicated for the proposed FM-CW optical radar system (FM-CW laser altimeter), the measurement error can be reduced easily by a factor of 1/1000 thus making the measurement error $7.5(10^{-4})$ meters or 0.75 millimeters. The geometrical resolution error for a 10 seconds of arc beamwidth, as shown in Figure 64 is $1.088(10^{-4})$ meters. This resolution accuracy, the difference in range between the center of the beam (h) and the outside of the beam (R), was calculated using the following equation:

$$h - R = R \sec \frac{\theta}{2} - R = R\left(\sec \frac{\theta}{2} - 1\right) \tag{13}$$

where θ is the beamwidth in radians. Using the series expansion for sec θ and reducing equation (13) reduces to

$$h - R = R\left(\frac{1}{2}\theta^2 + \frac{5}{24}\theta^4, \ldots\right)$$

which is plotted in Figure 64.

The resulting accuracy for the FM-CW laser altimeter with a 10 second beamwidth and using an FM discriminator is an rms error of

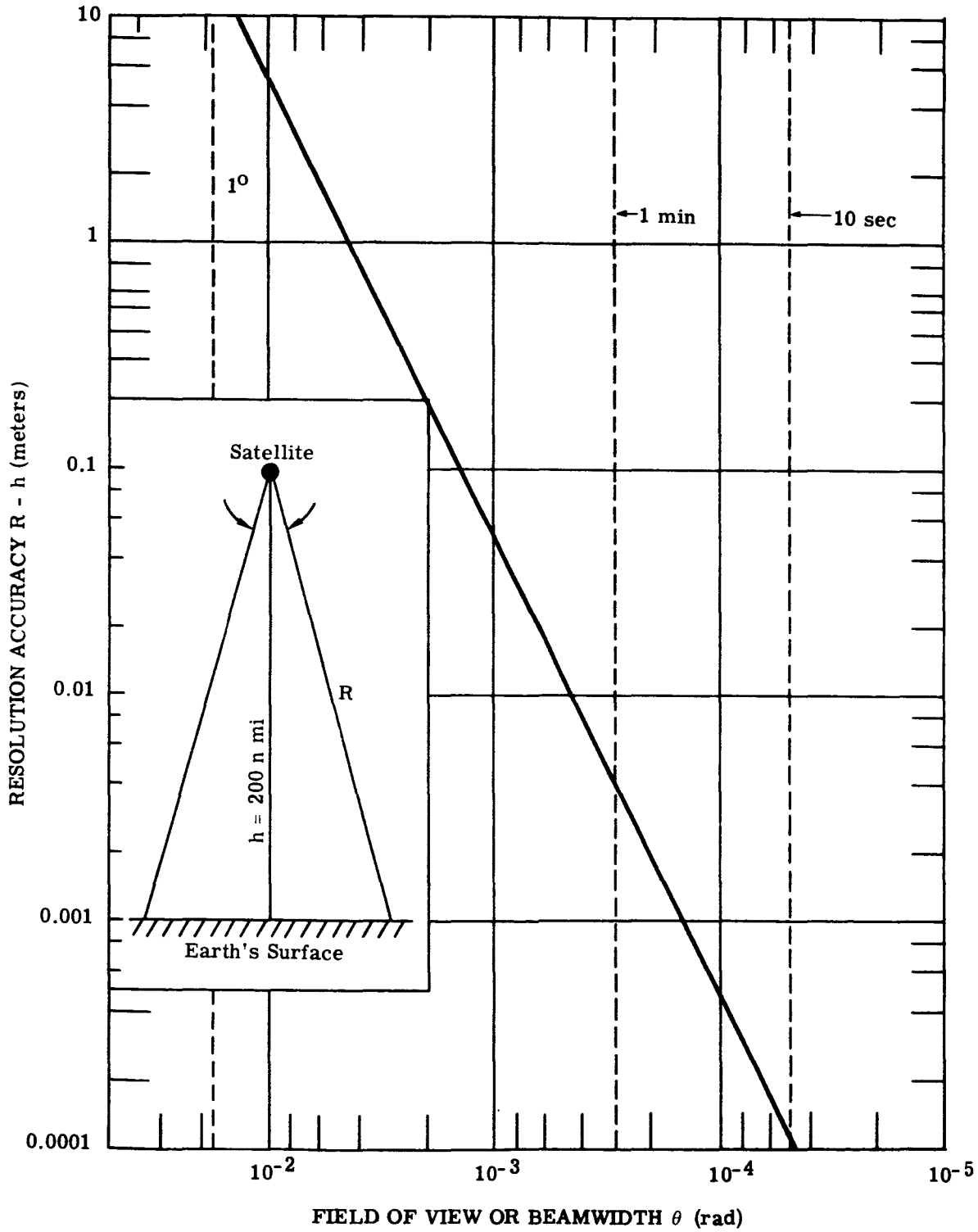

FIGURE 64. GEOMETRICAL RESOLUTION ACCURACY vs. FIELD OF VIEW FROM A 200-n mi SATELLITE

$$\sqrt{[7.5(10^{-4})] + [1.088(10^{-4})]^2} = \pm 7.569(10^{-4}) \text{ meters}$$

E.2.5. FM-CW LASER ALTIMETER CHARACTERISTICS. The estimated characteristics of the proposed 1970 FM-CW laser altimeter considers power input (from an external source), weight and volume (not considering automatic data processing or satellite-to-earth data link) and platofrm (or satellite) stability requirements.

E.2.5.1. Input Power Requirements. The input prime power requirements for the proposed FM-CW laser altimeter are as follows:

Transmitter		
CW Gas Laser	$\frac{3.55 \text{ watts}}{.005 \text{ efficiency}} =$	710 w
Modulator		25 w
Receiver		
CW laser amplifier	$\frac{0.1 \text{ watts}}{.001 \text{ efficiency}} =$	200 w
Optical local oscillator	$\frac{0.01 \text{ watts}}{.001 \text{ efficiency}} =$	110 w
Photomixer, Amplifier, and Discriminator		50 w
Indicator (Spectrum analyzer type with frequency marker generators)		100 w
Servomechanisms (to point combined optical system)		10 w
	Total	1205 watts

It was assumed that receiver electronic circuit components are all solid state.

E.2.5.2. Systems Weight. The weight of the proposed FM-CW laser altimeter is as follows

Transmitter	
Optical System (lens type)	1 lb
CW Gas Laser	50 lbs
Modulator	<1 lb
Receiver	
Pseudo-Cassegranian reflector optical system (an aperature diameter of 1.12 meters and made of coated beryllium metal, parabolidial primary mirror)	20 lbs
CW Laser amplifier	10 lbs
Optical Local Oscillator	10 lbs

Electronics* (photomixer detector, delay line, amplifiers, discriminator)	50 lbs
Indicator* (spectrum analyzer)	50 lbs
Optical System Pointing Servomechanism**	10 lbs
Total	202 lbs

The weight portion of the reactor type prime power source for the 1.005 kilowatts of the FM-CW laser altimeter is between 20 and 35 lbs. This assumes that the total satellite requirements are 35 kw and requires a SNAP 8, 8A or 50 reactor prime power system (see Table XIII, Section 5.5).

E.2.5.3. System Physical Size and Volume. The volume requirements for the proposed FM-CW laser altimeter are as follows:

Transmitter	
Transmitter optics (lens 2 inch diameter and 2 inches long)	6 $in.^3$
CW laser with modulator (10 inch diameter and 3 feet long)	1.6 ft^3
Laser power supply	1.5 ft^3
Receiver	
Pseudo-Cassegrainian Optical System with photomixer (3.2 feet diameter and 3 feet long)	7.7 ft^3
Laser optical amplifier (4 inch diameter and 10 inches long)	125 $in.^3$
Laser local oscillator (4 inch diameter and 10 inches long)	125 $in.^3$
Laser power supplies	2 ft^3
Electronics*** (amplifier, delay line, discrimminator)	1 ft^3
Indicator***	1.5 ft^3
Total	15.3 ft^3

E.2.5.4. Platform Stability Requirements. The transmitter (optical system, CW laser source and modulator) and a portion of the receiver (optical system, laser amplifier, local oscillator and detector) require pointing directly in the nadir direction from the satellite to measure the absolute satellite altitude or relative heights on the earth's surface (i.e., ocean wave

*Receiver electronic and indicator electronics are solid state integrated electronic circuits.

**The spacecraft has an independent stabilizing system and this weight is not included.

***Solid State Integrated Electronics Circuit Packages.

height). Since the data rate can be continuous using this FM-CW altimeter, the platform stability must be within to 1/2 beamwidth of the optical systems. This requires a continuous platform (or satellite) stability of 5 seconds of arc (in roll and pitch) for receiver and transmitter optical and laser components. The yaw stability must be adjustable continuously for the vector ground track on the earth's surface and requires a platform stability of 10 seconds or greater. This depends upon physical distance between transmitter aperature and receiver aperture. The shorter this distance is, the less yaw angular stability is required.

E.2.6. OPERATOR REQUIREMENTS. Since optical laser altimeters cannot be used through clouds, these altimeters need to be turned on only where the satellite is over cloudless or partially cloudy skies. The ground path must be determined manually by a drift sight or orbital path data calculated at ground station. The path angle varies with the satellite yaw axis with changing latitude and therefore must be continuously changed for all orbits except an equitorial orbit. The yaw axis of laser altimeter platform is determined by the line through the centers of the transmitting and receiving optical systems axes.

Because of the round trip propagation time of $2.472(10^{-3})$ seconds for a 200 n mile satellite, the transmitter optical system axis must be pointed as to lead the vertical by 5 seconds of arc and the receiver optical system axis must be pointed as to lag the vertical by 5 seconds of arc. Thus the axes of these two 10 second beamwidths optical systems are required to be displaced by 10.571 seconds of arc which makes it impossible to have coaxial optical systems. The operator must adjust the drift angle to stabilized platform plus it might be desirable to have fine adjustment for the receiver optical pointing axis and tune for maximum signal return by the maximum amplitude on the CRT of the indicator. Since the data is continuous for an FM-CW laser altimeter, the relative ocean or ground profiles must be recorded with a time base so as to determine the data as to position on the earth. This can be done automatically or manually by having the operator record time and relative surface height data.

E.2.7. EXTENSION OF APPLICATIONS OF FM-CW LASER ALTIMETER. To extend this system to other possible uses such as the determination of wavelength, and possibly wind direction of wind waves, would require certain modifications in the system.

To determine the wind direction, one can possibly employ the laser altimeter return characteristics. Since the ocean waves are not sinusoidal, by sweeping the altimeter optics and observing the return characteristics one might be able to determine the wind direction. The

determination of the wind direction would require experimentation and calibrations from high speed aircraft to determine the feasibility of the method.

For the case where the wavelength of the wind waves are larger than the 17 meter diameter of the area subtended by the laser beam, one should be able to measure the wavelength by measuring the time difference between two beat frequencies. That is, by tuning the filter to measure the best frequency of the wave crest one can obtain the time interval between the beat frequencies. By multiplying the time interval by the velocity of the satellite, the approximate wavelength of the wind waves can be obtained.

E.3. PULSED LASER ALTIMETERS

The pulsed laser altimeter to be considered is shown in Figure 65. It is basically a pulsed laser radar rangefinder of the type which have been manufactured and tested by a number of companies. The laser rangefinders are designated by various acronyms such as COLIDAR (coherent light detection and ranging) and OPDAR (optical detection and ranging). Since much of the research effort on laser rangefinders is classified information, we shall discuss the basic system principles and similarities to the FM-CW laser altimeter discussed in Section E.2. The transmitter consists of an optical system, a pulsed laser source and rotating prism Q-spoiler. The receiver has a Cassegrainian optical system, photodiode detector, electronic amplifiers, electronic counter, and indicator. The pulse rate (and data rate) of the system is controlled by the master pulse generator.

In the transmitter pulsed laser source generates a light beam with a peak power of $\hat{P}_t(\lambda)$ watts. The transmitter optical systems is transmission lens type with a transmittance of $\eta_t(\lambda)$ and an optical gain, G_t, which normalizes the power in the beam compared to that from an isotropic radiator. $G_t = \frac{4\pi}{\Omega}$ where Ω is the solid angle half-power beamwidth of the transmitter and is by $\Omega = \frac{\pi}{4}\theta^2$. The power consideration in the beam was discussed in Section E.1.2.

The receiver optical system is a pseudo-Cassegrainian reflection type with optical filtering surfaces plus transmission filters. The transmittance of this optical system is $\eta_t(\lambda)$. This receiver optical collects and focuses the returned received power on the detector. The detector converts the received optical power into electrical voltages which are amplified by the preamplifier and pulse amplifiers. The absolute range is determined by the high speed counter but relative height of surface objects in the beam width is determined by comparing the transmitted pulse with the returned pulse on the CRT display of the indicator. The master oscillator

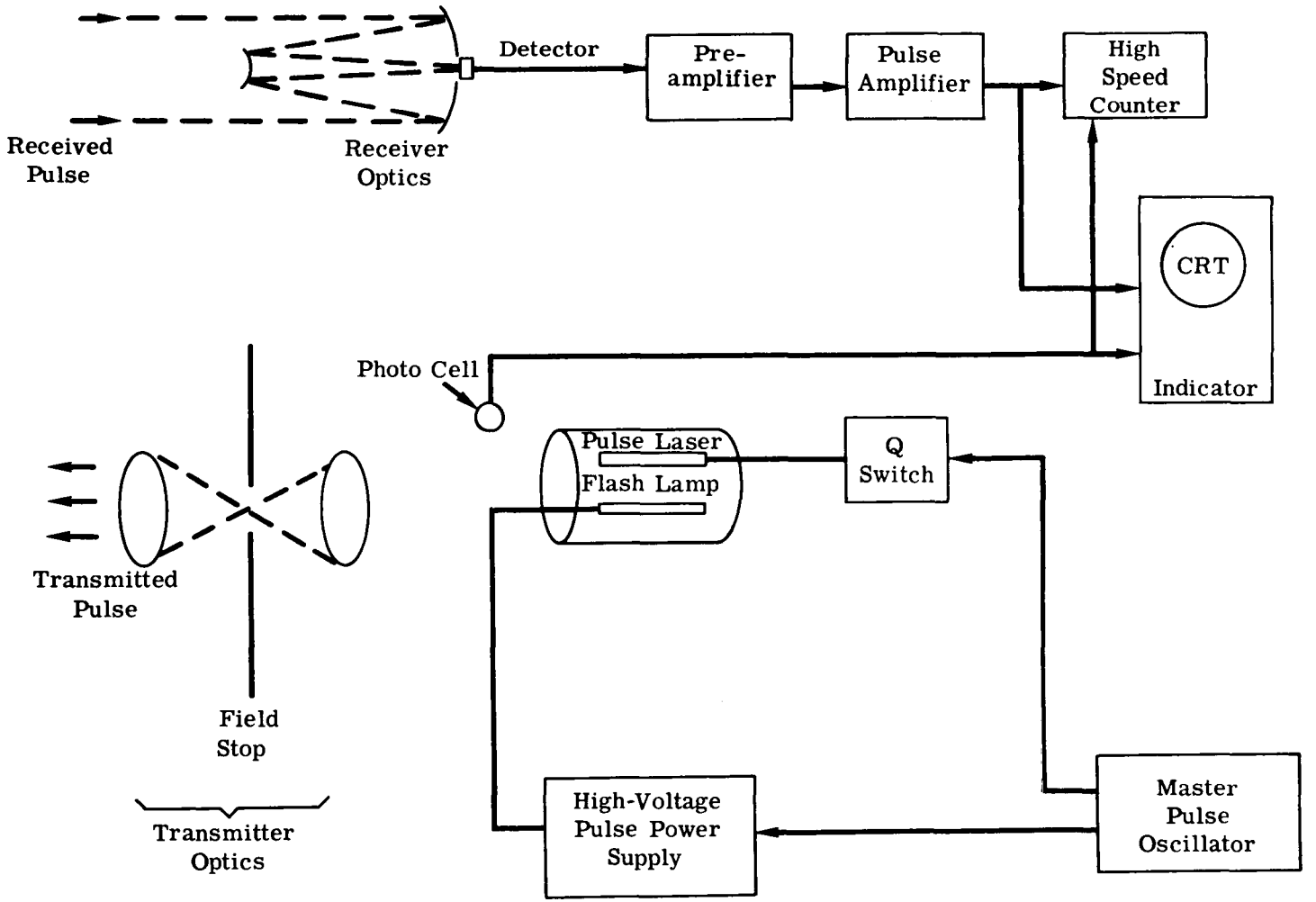

FIGURE 65. A PULSED OPTICAL RADAR BLOCK DIAGRAM

determines the data rate of relative height measurements. Since the output of pulsed laser waveforms are non-repeatable, this type of laser altimeter must take data on each pulse and integrating a number of pulses is very difficult because of the variations in time delays of the pulsed laser when triggered by master oscillator (time jittering). Although the round trip propagation time for a 200 n mile satellite is $2.4723(10^{-3})$ sec (or a prf of 404.5 cycles per second), the maximum prf is limited by the laser to 10 cps.

E.3.1. RANGE MEASUREMENT USING PULSED TECHNIQUES. The absolute range of pulsed altimeters is dependent upon the steepness of transmitted and received pulses and the signal-to-noise of the received pulse. The theories and practices of steep rise time pulse generation is well known and has steadily improved in radar systems since World War II (Ref. 87, 88 89, and 90). The range resolution measurement or the absolute range is normally thought of as the pulse width $(10(10^{-9})$ sec for pulsed best lasers). Absolute range, R, is given by the following well known equation

$$R = \frac{2c}{\delta t}$$

where c is the velocity of light and δt is the time difference transmitted and received pulses. In Figure 66 δt is determined by a high speed counter.

The difference height (range) of objects in the beam (such as ocean waves) can be determined by pulse spreading as shown in Figure 66. Figure 66 shows and compares the transmitted pulse and delay received pulse as would be shown on dual beam oscilloscopes. The pulse spreading or relative height measurement is difficult to measure electrically but with a well-trained operator, it is quite accurately estimated.

E.3.2. SIGNAL-TO-NOISE RATIO FOR PULSED LASERS. The signal-to-noise ratio for laser altimeters was derived in Sections E.2.3.1 through E.2.3.3 and is the same as equation (10) except for peak transmitted power $\hat{P}_t(\lambda)$ is substituted for the average power $P_t(\lambda)$ and since there is no optical amplifier, G = 1. Thus, equation (10) becomes

$$\frac{S}{N} = \frac{F_2}{F_1}\frac{A_r}{\pi r^2}\frac{\int_{\lambda_1}^{\lambda_2} \hat{P}_t(\lambda)\eta_t\eta_r T^2 \rho R(\lambda)\, d\lambda}{2e\Delta f}$$

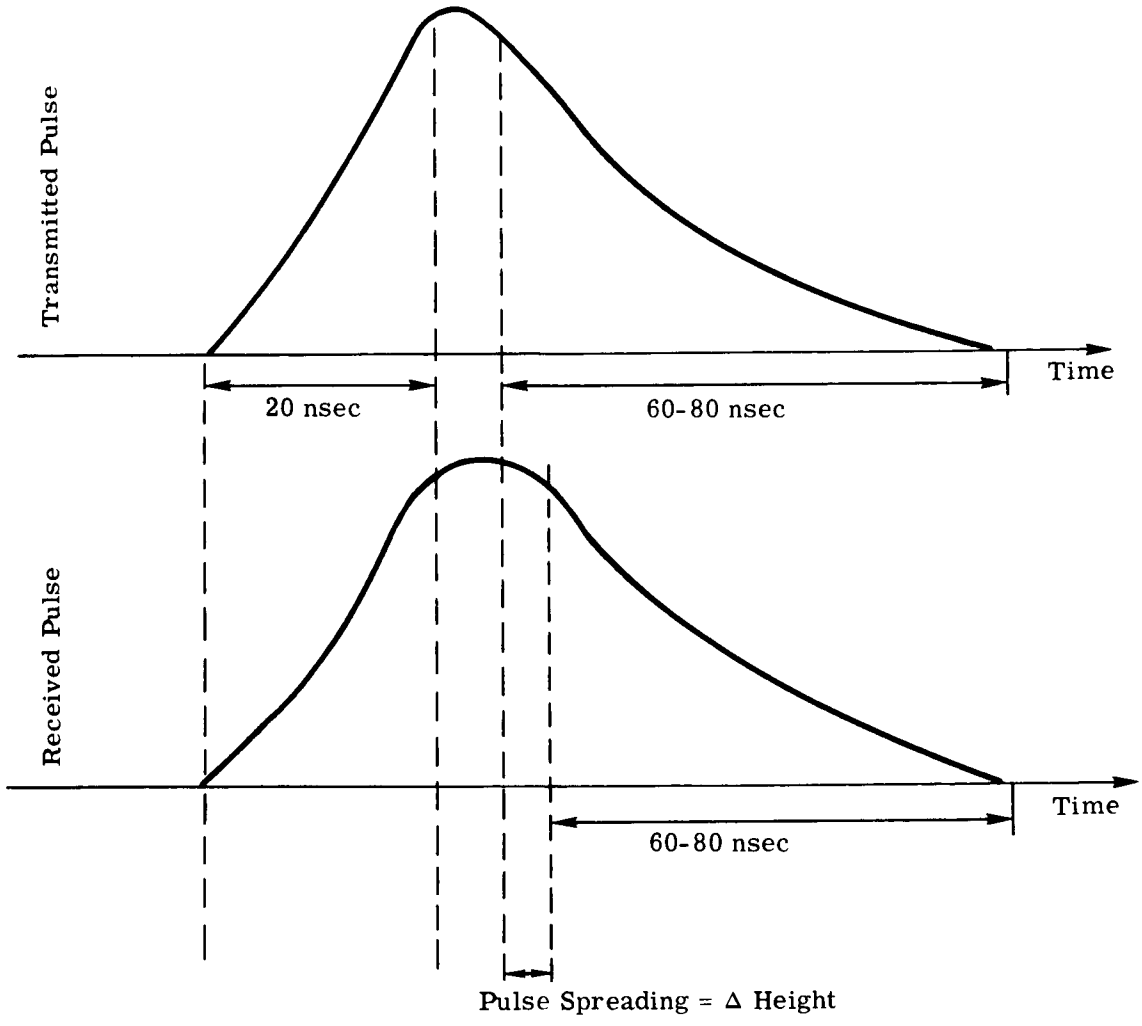

FIGURE 66. TRANSMITTED AND RECEIVED PULSES TO DETERMINE RELATIVE HEIGHT (HEIGHT OF OCEAN WAVES)

Where $\frac{S}{N}$ is the signal-to-noise ratio

F_1 and F_2 are modulation factors

A_r is the area of receiving aperture

$\hat{P}_t(\lambda)$ is the laser peak power

η_t and η_r are the transmittance of transmitter and receiver optical systems, respectively

T is the transmittance of the atmosphere

ρ is the reflectance of target surface

$R(\lambda)$ is responsivity of the detector at wavelength λ

r is the range

e is the electronic charge

Δf is the bandwidth of the receiver

λ_1 and λ_2 are wavelength limits of the system

E.3.3. ASSUMPTIONS

E.3.3.1. Source and Transmitter Optics. The laser source was chosen to be glass doped neodymium laser operating at wavelength of 1.064μ and having a peak power $\hat{P}_t$ of 5 megwatts. The choice was determined from previous study of laser propagation through the atmosphere to space (Ref. 83). The transmitter beamwidth was again chosen to be 10 seconds and the transmittance of its optical system was assumed to be $\eta_t = 0.50$.

E.3.3.2. Receiver. The aperture area of the primary collecting paraboloidal mirror will be taken to be 1 square meter and having hyperboloidal secondary mirror forming a pseudo-Cassegrainian reflective type optical system. We shall assume the transmittance of this optical system with reflective coating filter and transmission filter to be $\eta_r = 0.90$. The total filter pass band will be 10 Angstroms in wavelength to exclude unwanted background radiation.

E.3.3.3. Modulation Techniques. For AM modulation the ratios of peak signal current to the rms and average signal currents are defined by F_1 and F_2, respectively. A 100 percent intensity modulation of light beam by a sine wave would give at the output of the detector a sine wave current whose amplitude varied from zero to some peak value. The rms value of the signal sine wave is its peak to peak value divided by $2\sqrt{2}$; thus F_1 $2\sqrt{2}$. The average value of this current is one half the maximum amplitude, so that $F_2 = 2$. For the calculations we will assume

$F_1 = 2\sqrt{2}$

$F_2 = 2$

E.3.4. CALCULATION OF RECEIVED SIGNAL-TO-NOISE RATIO. The required signal-to-noise ratio can be calculated from the modified equation (11) Section E. 2.3.5. For good puls fidelity, the receiver bandwidth must have a bandwidth of 100 Mc. The calculation will be made considering the pulsed laser altimeter is in a 200 n mile satellite orbiting the earth and the laser power radiates in a perpendicular direction to a plane tangent to the earth (i.e., the nadir) The following numerical values shall be used:

Signal-to-noise (S/N)
Modulation factor for AM (F_1) = $2\sqrt{2}$
Modulation factor for AM (F_2) = 2
Receiver aperture area (A_r) = 1 sq meter
Transmittance of the transmitter optics (η_t) = 0.50
Transmittance of the receiver optics (η_r) = 0.90
Atmospheric transmittance (T) = 0.90
Ocean reflectance (ρ) = 0.10
Detector responsivity (R) = 0.426 amp watt
Peak transmitter power ($\hat{P}_t$) = $5(10^9)$ watts
Range (r) = $3.70(10^5)$ meters
Electronic charge (e) = $1.6(10^{19})$ coulomb
Receiver bandwidth (Δf) = 100 Mc

The modified equation (11) for pulsed laser altimeters is:

$$\frac{S}{N} = \frac{F_2}{F_1}\left(\frac{A_r}{\pi r^2}\right)\left(\frac{\eta_t \eta_r T^2 \rho R}{2e\Delta f}\right)\hat{P}_t$$

Substituting the above numerical values into this equation we obtain for the signal-to-noise ratio

$$\frac{S}{N} = \frac{2}{2.82}\,\frac{1}{\pi[(3.7)(10^5)]^2}\,\frac{(0.5)(0.90)(0.90)^2(0.1)(0.426)}{(2)(1.6)(10^{-19})(10^8)}\,5(10^9)$$

$$\frac{S}{N} = 4.96\,(10^6)$$

Therefore, using 5 megawatts of peak power for the pulsed laser is very adequate for pulse laser altimeters. All the parameters for the above calculation are obtainable by present components and manufacturing techniques.

E.3.5. PULSED LASER SYSTEM ACCURACY. The ultimate accuracy of a pulsed laser altimeter depends upon the error in measuring pulse stretching of the received pulse as compared to transmitted pulse. Using trained A-scope operators and having dual beam presentation, the relative accuracy can be 1/10 of the rise time of 20 nanoseconds can be obtained which equals 2 nanoseconds or ocean wave height accuracy of 0.6 meters. Although it is predicted by Townes that laser pulse power of 10^{12} watts and a pulse width of 10^{-11} seconds is practical, pulse laser altimeters will be limited by the larger electronic amplifier bandwidth and shorter detector response times required (Ref. 91). A pulse width of 10^{-11} sec requires an amplifier bandwidth of 100 Gcs. Also the best detector response times are slightly shorter than 10^{-10} seconds for Reise photodiode detectors.

E.3.6. PULSED LASER ALTIMETER CHARACTERISTICS. The estimated characteristics of the proposed state-of-the-art pulsed laser altimeter considers power input (from an external source), weight and volume (not considering the satellite-to-earth data link) and the platform (or satellite) stability requirements.

E.3.6.1. Input Power Requirements. The input prime power requirements for the proposed pulsed laser altimeter are as follows:

Transmitter		
Pulsed solid state laser (500 pulses)		100 w
Master Oscillator*		10 w
Receiver		
Amplifiers*		50 w
High Speed Counter*		25 w
Indicator*		100 w
	Total	285 w

*All electronic circuits components are solid state.

E.3.6.2. System Weight. The weight of the proposed FM-CW laser altimeter is as follows:

Transmitter		
Optical system (lens type)		2 lbs
Pulsed Neodymium laser (including flash lamp and power supply)		15 lbs
Master Oscillator		1 lb
Receiver		
Pseudo-Cassegrainian reflector optical system (an aperture diameter 1.12 meters with primary and secondary mirrors made of coated beryllium)		20 lbs
Electronics* (preamplifier, pulse amplifier and high speed counter)		30 lbs
Indicator*		50 lbs
Optical Systems Pointing Servomechanism**		10 lbs
	Total	128 lbs

The weight portion of the reactor type prime power source for 285 w of the pulsed laser altimeter is between 5.5 and 4.6 lbs. This assumes that the total satellite requirements are greater than 35 kw and thus requires a SNAP 8, 8A or 50 prime power system (see Table XIII in Section 5.5).

E.3.6.3. System Physical Size and Volume. The volume requirements for the pulsed laser altimeter are as follows:

Transmitter		
Transmitter optical system (lens 2 inch diameter and 4 inches long)		12 $in.^3$
Pulse laser (3 inch diameter, 6 inches long)		.1 ft^3
Laser Power Supply		.5 ft^3
Receiver		
Pseudo-Cassegrainian optical system (3.2 feet diameter and 3 feet long)		7.7 ft^3
Electronics* (preamplifier, pulse amplifier, and high speed counter)		1.0 ft^3
Indicator*		1.5 ft^3
	Total	9.8 ft^3

*Receiver electronics are solid state integrated electronic circuits.

**If the spacecraft has an independent stabilizing system, this weight can be reduced.

E.3.6.4. Platform Stability Requirements. The stability of the platform requirement which points the transmitter laser and optical systems and the receiver optical system and detector are the same as discussed in Section E.2.5.4, because the beamwidths are the same (10 seconds of arc). Section E.2.5.4 concluded that the platform stability required 5 seconds of arc in roll and pitch but a greater tolerance was acceptable in yaw.

E.3.7. OPERATOR REQUIREMENTS. Since optical laser altimeters cannot be used through clouds, these altimeters need to be turned on only where the satellite is over cloudless or partially cloudy skies. The ground path must be determined manually by a drift sight or orbital path data calculated at ground station. The path angle varies with the satellite yaw axis with changing latitude and therefore must be continuously changed for all orbits except an equitorial orbit. The yaw axis of laser altimeter platform is determined by the line through the centers of the transmitting and receiving optical systems axes.

Because of the round trip propagation time of $2.472(10^{-3})$ seconds for a 200 n mile satellite, the transmitter optical system axis must be pointed as to lead the vertical by 5 seconds of arc and the receiver optical system axis must be pointed as to lag the vertical by 5 seconds of arc. Thus the axes of these two 10 second beamwidths optical systems are required to be displaced by 10.571 seconds of arc which makes it impossible to have coaxial optical systems. The operator must adjust the drift angle to stabilized platform plus it might be desirable to have fine adjustment for the receiver optical pointing axis and tune for maximum signal return by the maximum amplitude on the CRT of the indicator.

Since the data is not continuous for a pulsed laser altimeter, but almost continuous (up to 10 pulses per second), the relative ocean height or ground profiles must be recorded with a time base so as to determine the data as to geographical position on the earth. The maximum data rate represents a circular patch of 17.96 meters in diameter every 726.9 meters. (The velocity of the 200 n mile satellites nadir the earths surface is 7269.8 meters/sec for a polar orbit). The profile data every 727 meters is too low for earth land areas but it is sufficient for ocean wave height (Ref. 92).

REFERENCES

1. Ockert, D. L., "Satellite Photography with Strip and Frame Cameras," Photogrammetric Engineering, Vol. 26, No. 4, p. 562-568, September 1960.
2. ITEK Laboratories, "Panoramic Progress, Part I," Photogrammetric Engineering, Vol. 27, No. 5, p. 747-754, December 1961.
3. Leistner, G., and Dieter, P. P., "Some Characteristics of Panoramic Cameras for Aerial Surveillance," Photographic Science and Engineering, Vol. 5, No. 5, p. 257-262.
4. Goldhammer, J. S., and Edwards, R. E., "A Comparison of Panoramic and Serial Frame Camera Systems for High-Speed Low-Altitude Reconnaissance," Photographic Science and Engineering, Vol. 7, No. 1, p. 53-58.
5. Cornell Aeronautical Laboratory, "A Scientific Investigation into Photographic Reconnaissance from Space Vehicles," Final Report, May 10, 1961.
6. Atkinson, J. H., and Jones, R. E., "Atmospheric Limitations on Ground Resolution from Space Photography," S.P.I.E. Journal, Vol. 1, p. 39-42, December 1962-January 1963.
7. Holter, M. R., and Legault, R. R., "Motivation for Simultaneous Multispectral Reconnaissance," Proc. Third Symposium on Remote Sensing of Environment, October 14-16, 1964, The University of Michigan, Ann Arbor, p. 71-78.
8. Colwell, R. N., "Some Practical Applications of Multiband Spectral Reconnaissance," American Scientist, Vol. 49, No. 1.
9. Lowe, D. S., Polcyn, F. C., and Shay, L. R., "Multispectral Data Collection and Analysis," Proc. Third Symposium on Remote Sensing of Environment, October 14-16, 1964, The University of Michigan, p. 667-680.
10. Legault, R. R., and Polcyn, F. C., "Investigations of Multispectral Image Interpretation," Ibid, p. 813-821.
11. Molineaux, C. E., "Aerial Reconnaissance of Surface Features with the Multiband Spectral System," Ibid, p. 399-407.
12. "Microwave Radiometer Measurements Program," W. H. Conway, et al. paper given at 2nd Remote Sensing Symposia, University of Michigan, 1962.
13. "Proceedings of the Second Symposium on Remote Sensing of Environment," University of Michigan, 4864-3-X, February 1963.
14. "Domains of the Marine Microbiologists," by C. E. Zobell, Scripps Institute of Oceanography, given at Symposium on Marine Microbiology, 1963.
15. "Survey of High Gain Broadband, Passive Deployable Antennas with Scanning Capabilities for Installation in a Manned Satellite," R. Hiatt and R. W. Larson, University of Michigan, Memo 6734-502-M, August 1964.
16. Heavner, W. S., "Satellite Reconnaissance Gains," appearing in Aviation Week, 22 May 1961.
17. "Usual Planting and Harvesting Dates by States," United States Department of Agriculture Handbook 283.

18. R. L. Cosgriff, W. H. Peake, and R. C. Taylor, Terrain Scattering Properties for Sensor System Design (Terrain Handbook II), Engineering Experiment Station, The Ohio State University, Columbus, Ohio, Vol. XXIX, No. 3, May 1960 (UNCLASSIFIED).

19. "Quarterly Progress Report CRQ61-2," R. K. Moore, University of Kansas, NASA Contract NSR17-004-003, 1 Oct. 1964 to 1 Jan. 1965.

20. Waite, A. H., and Schmidt, S. J., "Gross Error in Height Indication from Pulse Radar Altimeters Operating over Thick Ice," IRE International Convention Record, Part 5, p. 38-54, 1961.

21. Cummins, W. A., "The Dielectric Properties of Snow and Ice at 3.2 Centimeters," J. Appl. Physics, Vol. 23, No. 7, p. 768.

22. Von Hippel, A. R., Dielectrics and Waves, John Wiley and Son, Inc., (New York, 1954).

23. Von Hippel, A. R., Editor, Dielectric Materials and Applications, The Technology Press of M.I.T. and J. Wiley, Inc., (New York, 1954), p. 301.

24. Private communication with F. Haddock, Radio Astronomy Dept., University of Michigan, 9 April 1965.

25. Chaney, L. W., "Earth Radiation Measurements by Interferometer from a High Altitude Balloon," Proc. Third Symposium on Remote Sensing of Environment, October 14-16, 1964, The University of Michigan, Ann Arbor, p. 225.

26. "Ocean Waves," W. J. Pierson, Jr., International Science and Technology, June 1964.

27. "Measurement of the Roughness of the Sea Surface from Photographs of the Sun's Glitter," JOSA, Vol. 14, No. 11, pp. 838-850, 1954.

28. "The Application of Passive Microwave Technology to Satellite Meteorology: A Symposium," J. H. Katz, Memo. RM-3401-NASA, Rand Corporation, August 1963.

29. "Orbiting Space Station Study," University of Michigan, subcontract from IBM, 1964, Contract AF 04(695)-560. Unpublished.

30. Barringer, A. R., Paper presented to the Third Goddard Memorial Symposium of the American Astronautical Society, Washington, D. C., March 17-19, 1965.

31. "Polarization and Other Properties of Radar Echoes," Royal Radar Establishment, Technical Note 628, September 1957.

32. "Reflection Properties of Radar Targets," M. L. Meeks, et al. Georgia Institute of Technology 1954 (CONFIDENTIAL).

33. "A Review of Theories and Measurements of Radar Ground Return," Wolff, Electromagnetics Research Corp., Feb. 1960, AD 316 627L (CONFIDENTIAL).

34. "Apparent Temperatures of Smooth and Rough Terrain," Sinclair W. C. Cheu, Ohio State University, July 1960, AD 251 436L.

35. "Study of Thermal Microwave and Radar Reconnaissance Problems and Applications," No. 898-10, Ohio State University Research Foundation, July 1960.

36. "Influence of System Parameters on Airborne Microwave Radiometer Design, McGillem and Seling, IEEE Transactions on Military Electronics, Vol. MIL-7, No. 4, October 1963.

37. Swanson, L. W., "Aerial Photography and Photogrammetry in the Coast and Geodetic Survey, Photogrammetric Engineering, Vol. 30, No.5, September 1964.

38. Gross, V. E., and A. J. Weinstein, A Cryogenic Solid Cooling System, Aerojet-General Corp., Azusa, Calif., October 1963.

39. "Operational Experience of Rolling Element Bearings in Vacuum," I.T.I. Tec-Tonic No. 6, Published by Industrial Tectonics, Inc., Compton, California.

40. Bisson, E. E., and Anderson, W. J., "Friction and Bearing Problems in the Vacuum and Radiation Environments of Space," From Advanced Bearing Technology, NASA SP-38 (1964).

41. "Gallium is Useful Bearing Lubricant in High-Vacuum Environment," NASA Tech. Brief 63-10337 (May 1964).

42. Geusic, J., and Scovil, D., "Unidirectional Traveling Wave Optical Maser," Proc. First Conf. on Laser Technology, Vol. II.

43. Kogednik, H., and Yariv, A., "Considerations of Noise and Schemes for its Reduction in Laser Amplifiers," Proc. I.E.E.E., Vol. 52, No. 2, p. 165, Feb. 1964.

44. McGuire, F. G., "AEC Reorganization Debate Deepens," Missiles and Rockets, Vol. 11, No. 23, p. 13, December 3, 1962.

45. "Advanced Research Secondary Power," Space/Aeronautics, Vol. 41, No. 1, p. 173, Jan. 1964.

46. David, Heather M., "Snap 8 Support," Missiles and Rockets, 15 February 1965.

47. Schulman, F., Scott, W. C., and Woodward, W. H., "Power Supplies," Space/Aeronautics Research and Development Handbook, p. 101-105.

48. Osmun, W. G., "Space Nuclear Power: Snap-50/Spur," Space/Aeronautics, p. 38-45, December, 1964.

49. Brock, G. C., Physical Aspects of Air Photography, Longmans, Green & Co., (New York, 1952).

50. Lowman, P. D., "A Review of Photography of the Earth from Sounding Rockets and Satellites," Tech. Note, NASA-TN-1868.

51. Solomon, I., "Estimated Frequencies of Specified Cloud Amounts within Specified Ranges of Altitude," Tech. Report No. 167, Air Weather Service, U. S. A. F., April 1963.

52. Serebreny, S. M., and Blackmer, R. H., "An Investigation to Establish the True Nature of Cloud Cover," Scientific Report No. 2, Stanford Research Institute.

53. Blackmer, R. H., and Alder, J. E., "Statistics of Cumuliform Clouds from U-2 Photographs," Final Report, Stanford Research Institute.

54. Serebreny, S. M., and Blackmer, R. H., "Patterns of Cloud Cover Shown by U-2 Photography," Scientific Report No. 3, Stanford Research Institute.

55. H. F. Nitka, "Sensitivity and Detail Redition in the Recording of Light Images and Electron Beams," Phot. Sci. and Eng., Vol. 7, No. 3, May-June 1963.

56. H. J. Zweig, "The Relation of Quantum Efficiency to Energy and Contrast Detectivity for Photographic Materials," PS and E, Vol. 5, No. 3, May-June 1961.

77. Elterman, L., A Model of a Clear Standard Atmosphere in the Visible Region and Infrared Windows, Report No. AFCRL-63-675, U. S. Air Force Cambridge Research Laboratories, U.S.A.F. Hanscom Field, Mass., July 1963 (UNCLASSIFIED).

78. Elterman, L., Altitude Variation of Rayleigh, Aerosol, and Ozone Attenuating Components in Ultraviolet Region, Report No. AFCRL-64-400, U. S. Air Force Cambridge Research Laboratories, U.S.A.F. Hanscom Field, Mass., May 1964 (UNCLASSIFIED).

79. Diermendjian, D., "Scattering and Polarization Properties of Water, Clouds and Hazes in the Visible and Infrared," Applied Optics, February 1964, Vol. 3, No. 2, p. 117.

80. Handbook of Geophysics for Air Force Designers, U. S. Air Force Cambridge Research Center, U. S. Air Force, 1957, Chapter 7.

81. Hall, F. F., Jr., "The Polarized Emissivity of Water in the Infrared," Applied Optics, June 1964, Vol. 3, No. 6, p. 781.

82. Oliver, B. M., "Signal-to-Noise Ratios in Photoelectric Mixing," Proc. IRE, 1960, Vol. 49.

83. Rollin, R. A., Zwas, F., "Investigation of Space Communications Using Lasers," Report No. 5693-9-T, Optical and Radio Systems Lab., Institute of Science and Technology, The University of Michigan, Ann Arbor, Mich., May 1964 (UNCLASSIFIED).

84. Anderson, L K., "Photodiode Detection," Proc. of the Symp. on Optical Masers, April 1963, Vol. XIII, Polytechnic Press, New York, 1963.

85. Schwartz, M., Information Transmission Modulation and Noise, McGraw-Hill Book Co., 1959.

86. Paananon, R., "Progress in High Power Ionized Argon Lasers," Unclassified paper given during Second Conference on Laser Technology, at the Illinois Institute of Technology, Chicago, Ill., April 6, 7, 8.

87. Collins, G. B., Microwave Magnetrons, MIT Radiation Laboratory Series, Vol. 5, McGraw-Hill, New York, 1948.

88. Hamilton, D. R., J. K. Knapp, J. B. Horner, Klystrons and Microwave Triode, MIT Radiation Laboratories Series, Vol. 6, McGraw-Hill, New York, 1948.

89. Chance, B. et al., Electronic Time Measurements, MIT Radiation Laboratory Series, Vol. 20, McGraw-Hill, New York, 1948.

90. Lewis, I.A.D., F. H. Wells, Millimicrosecond Pulse Techniques, McGraw-Hill, New York, 1954.

91. "Townes Sees Trillion-Watt Laser," Electronic News, November 9, 1964.

92. Private communication, Professor W. J. Pierson, New York University, 22 March 1965.

57. B. A. Bang, "High Sensitivity Television as an Aid to Low Light Level Photographic Recording," J. of the SMPTE, Vol. 70, September 1961.

58. General Electric Tube Data Charts.

59. Gray, S., P. C. Murray, and O. J. Ziemelis, "Improved High Resolution Electron Gun for Television Cameras," Journal of the SMPTE, Vol. 72, October 1963.

60. W. C. Livingston, "Resolution Capability of the Image-Orthicon Camera Tube Under Nonstandard Scan Conditions," Journal of the SMPTE, October 1963, Vol. 72, No. 10.

61. L. L. Pourciau, M. Altman, and C. A. Washburn, "A High-Resolution Television System," Journal of the SMPTE, February 1960, Vol. 69.

62. R. G. Neuhauser, B. H. Vine, J. E. Kuehne, and G. A. Robinson, "The Design and Performance of a High-Resolution Vidicon," Journal of the SMPTE, November 1962, Vol. 71.

63. R. G. Neuhauser, "Sensitivity and Motion Capturing Abilities of Television Camera Tubes," Journal of the SMPTE, July 1959, Vol. 69.

64. J. S. Courtney-Pratt, "Image Converter Tube Photography," Journal of the SMPTE, April 1962, Vol. 71.

65. L. J. Brolak, W. P. Siegmund, and R. G. Neuhauser, "Fiber Optics - A New Tool in Electronics," Journal of the SMPTE, October 1960, Vol. 69.

66. Holter, M. R., et al., Fundamentals of Infrared Technology, The Macmillan Company, (New York, 1962).

67. "Design and Construction of Radiometric Mapping Set, AN/AAR-27 (XH^{-1})," F. Arms, et al., Contract AF 33(600)-41234.

68. "Investigations of Passive Ranging Techniques for Microwave and Submillimeter Surveillance Radiometers," Sperry Gryoscope Co., Syosset, N. Y., WPAFB Contract AF 33(616)-7518 (SECRET).

69. Wiley Electronics Co., WPADC, Contract AF 33(600)-39067.

70. "Superheterodyne Radiometers for Use at 70 Gc and 140 Gc," R. Meredith and F. L. Warner, presented at the Millimeter Conference, Orlando, Florida, January 1963.

71. "High Sensitivity, 100 and 300 Gc Radiometers," M. Cohn, et al., presented at Millimeter Conference, January 1963.

72. "Project Genny," General Electric Co., ONR Contract NOWR 2628(00)-1960.

73. "The Ruby Maser," J. J. Cook, M. E. Bair, and L. Cross, University of Michigan, Project MICHIGAN Rept. 2900-288-T, September 1961.

74. Electronics News, 14 September 1964.

75. Bayley, D S., Technical Note on Optical Communication, I Report Number -2, GPL Division, General Precision Inc., Pleasantville, N. Y., May 1961 (UNCLASSIFIED).

76. Minzer, R. A., K. W. Champion and H. L. Pond, The ARDC Model Atmosphere, 1959, U. S. Air Force Surveys in Geophysics, No. 115, U. S. Air Force Cambridge Research Center, Bedford, Mass., August 1959 (UNCLASSIFIED).